REFERENCE

CRYSTALLISATION AND CHAIN CONFORMATION OF LONG CHAIN N-ALKANES

Jean-Philippe Gorce

A thesis submitted in partial fulfilment of the requirements of
Sheffield Hallam University for the degree of
Doctor of Philosophy

June 2000

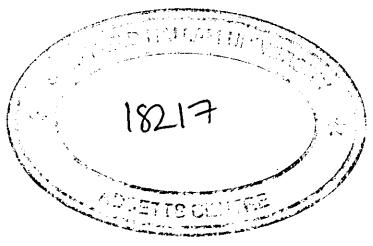
18217

Declaration

The work described in this thesis was carried out by the author in the Materials Research Institute, Sheffield Hallam University, between October 1995 and June 2000. The author declares this work has not been submitted for any other degree. The work is original except where acknowledged by reference.

Author :

(Jean-Philippe Gorce)

Supervisor :

(Doctor Steve Spells)

Acknowledgements

First of all, I would like to thank my supervisor, Doctor Steve Spells from Sheffield Hallam University, for his support and advice throughout this project. Of course, I would like to thank Professor Jack Yarwood from Sheffield Hallam University and Doctor Marcel Besnard from the University of Bordeaux I (France) for the opportunity they gave me to get involved in this research project. I also want to thank Doctor Goran Ungar and Mr Xiangbing Zeng from the University of Sheffield for their helpful discussions and help with setting up the X-ray experiments.

Secondly, I would like to thank all my colleagues at Sheffield Hallam University and specially the ones from the Polymer group : Declan Forde, Stéphane Moyses, Sandry Coutry and Sujeewa De Silva.

Finally, my warmest thanks go to Michèle, Robert and Delphine.

Abstract

Hydrocarbon chains are a basic component in a number of systems as diverse as biological membranes, phospholipids and polymers. A better understanding of the physical properties of n-alkane chains should provide a better understanding of these more complex systems. With this aim, vibrational spectroscopy has been extensively used. This technique, sensitive to molecular details, is the only one able to both identify and quantify conformational disorder present in paraffinic systems. To achieve this, methyl deformations have been widely used as "internal standards" for the normalisation of peak areas. However, in the case of n-alkanes with short chain length, such as n-$C_{44}H_{90}$ for example, the infrared spectra recorded at liquid nitrogen temperature and reported here show the sensitivity of these latter peaks to the various crystal structures formed. Indeed, the main frequencies of the symmetric methyl bending mode were found between 1384 cm^{-1} and 1368 cm^{-1} as a function of the crystal form. Changes in the frequency of the first order of the L.A.M. present in the Raman spectra were also observed. At higher temperatures, non all-trans conformers, inferred from different infrared bands present in the wagging mode region, were found to be essentially placed at the end of the n-alkane chains. At the monoclinic phase transition, the concentration of end-gauche conformers, proportional to the area of the infrared band at 1342 cm^{-1}, increases abruptly. On the contrary, in the spectra recorded at liquid nitrogen temperature no such band is observed.

We also studied the degree of disorder in two purely monodisperse long chain n-alkanes, namely n-$C_{198}H_{398}$ and n-$C_{246}H_{494}$. The chain conformation as well as the tilt angle of the chains from the crystal surfaces were determined by means of low frequency Raman spectroscopy and S.A.X.S. measurements on solution-crystallised samples. The increase in the number of end-gauche conformers which was expected to occur with the increase of the tilt angle as a function of the temperature was not detected due to a perfecting of the crystals. Indeed, due to successive heating and cooling to -173^{0}C, the concentration of non all-trans conformers was found to decrease within the crystals. Their numbers were found to be up to six times higher in n-$C_{198}H_{398}$ crystallised in once folded form than when crystallised in extended form. The C-C stretching mode region of the spectra was used to identify the chain conformation and to estimate the length of the all-trans stem passing through the crystal layers at -173^{0}C. The transition between once folded and extended form crystals was indicated by the presence of additional bands in this region at 1089 cm^{-1}, 1078 cm^{-1} and 1064 cm^{-1}. Some of those bands may be related to the fold itself. At the same time, a strong decrease of the intensity of the infrared bands present in the wagging mode region was observed.

Finally, the triple layered structure proposed on the basis of X-ray measurements obtained from the crystals of a binary mixture of long chain n-alkanes, namely n-$C_{162}H_{326}$ and n-$C_{246}H_{494}$, was confirmed from the study of the C-C stretching mode region of the infrared spectra.

Table of Contents

I INTRODUCTION

I.1 Introduction to Polymers.

Polymers are used in all the area of our life. They have become essential in communication, transportation, textiles, design and medicine. Biological polymers such as DNA and proteins are present in all living beings. The first polymers used and processed by mankind were natural biological ones such as wool and rubber. For example, Charles Goodyear improved the elastic properties of natural rubber in the 1840's. Few years later, polymers such as ebonite were commercialised. In the 1910's, the first synthetic polymers such as bakelite and rubber were produced and commercialised. From then, polymer industry has shown intensive growth and a better understanding of polymer materials has become essential.

Polymer science is divided into the study of synthesis, processing, properties and structure. In the last of these, which will be our main concern in this work, the molecular and crystal structure is studied using techniques such as x-ray scattering, infrared and Raman spectroscopy, differential scanning calorimetry, optical and electron microscopy, electron diffraction, light scattering and density.

I.2 Molecular structures in polymers.

Polymers are macromolecules with a regularly repeating structure. Polymers can be linear or branched. In the latter, side chains are bonded to the main chain at branch points and the polymer is designated a branched polymer. Also, when multiple bonding occurs between the neighbouring chains, the polymer is said to be crosslinked and to have formed a network polymer. Polymers are formed by monomers, which are the repeat units of the chains, linked by primary bonds. When the macromolecules are formed by one species of monomer (...a-a-a-a-a-a-a-a-a... for example) the polymer can be designated by the term homopolymer. When they are formed by more than one monomer (...b-b-b-a-a-b-a-b-b... for example) the polymer can be designated by the term copolymer. Polymers can be synthesised through chemical reactions generally called

polymerisation reactions. Polyethylene, for example, is polymerised from ethylene. It is usually a linear homopolymer, where the repeat unit or monomer is the CH_2 group (see Figure I.1 where the carbon atoms are in black and the hydrogen atoms are in white, from Strobl[1]).

Figure I.1 : Part of a polyethylene chain composed by thirteen monomers.

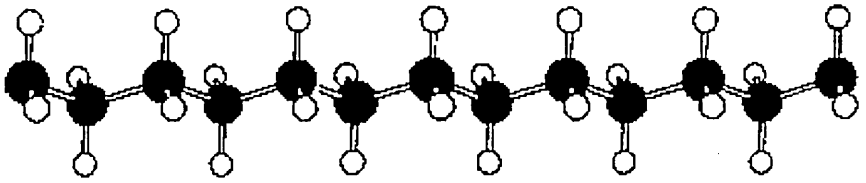

During the polymerisation of polymers from monomers having no centre of symmetry (CH_2=CHX for example), the macromolecules can be synthesised in different configurations : head-to-tail, head-to-head and tail-to-tail. Considering only the more usual configuration, the head-to-tail one, three different stereoregular arrangements can still occur in, for example, a vinyl polymer. Thus, when the substituent groups, X, all lie above (or below) the plane made by the polymeric chain in all-trans conformation, the configuration is called isotactic. When the substituent groups lie alternately above and below the plane made by the macromolecule in the all-trans conformation, the configuration is called syndiotactic. In the case of a random position of the substituent groups, the configuration is called atactic.

The size of a polymer chain can be characterised by its molar mass, *M*. In the case of a homopolymer, the molar mass of the chain is related to the molar mass of the monomer, M_0 through Equation I.1:

Equation I.1

$$M = x \times M_0$$

where x is the degree of polymerisation. One of the characteristics of polymers is the dispersion of chain lengths. Therefore, both the molar mass and the degree of polymerisation follow a statistical distribution. Experimental measurements give only certain average values for these characteristic parameters.

The determination of the conformation of the macromolecule composing a polymeric material is an essential step toward the understanding of the bulk properties.

I.2.1 Rotational Isomeric States.

In the case of a linear flexible polymer molecule (the polyethylene molecule in Figure I.1 for example) changes in the valence angles and bond lengths are very limited but changes in the torsion angles along the backbone of the molecule can occur. In the last case, the overall shape of the molecule is not conserved and can transform the linear molecule into a coil. The simplest case of a butane molecule where similar conformational changes can be observed for the carbon atoms placed in the middle of the chain are represented in Newman projections in Figure I.2.

Figure I.2 : Newman projections of different conformational arrangements in a butane molecule.

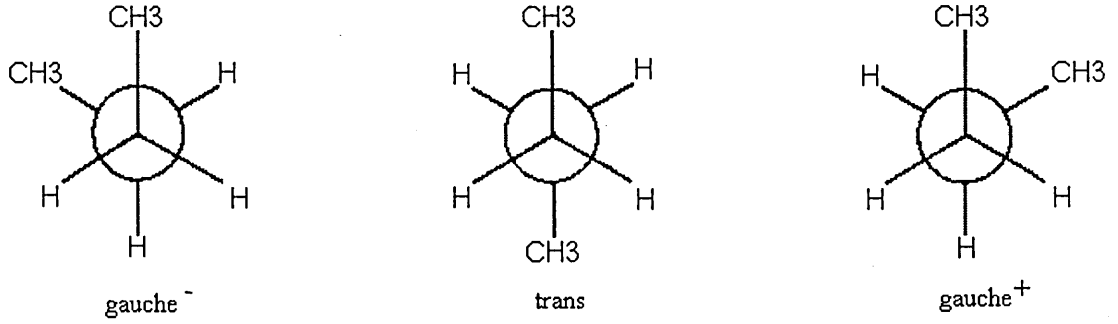

The potential energy associated with such conformational arrangements is shown in Figure I.3.

Figure I.3 : Potential energy of a butane molecule as a function of ϕ, torsional angle.

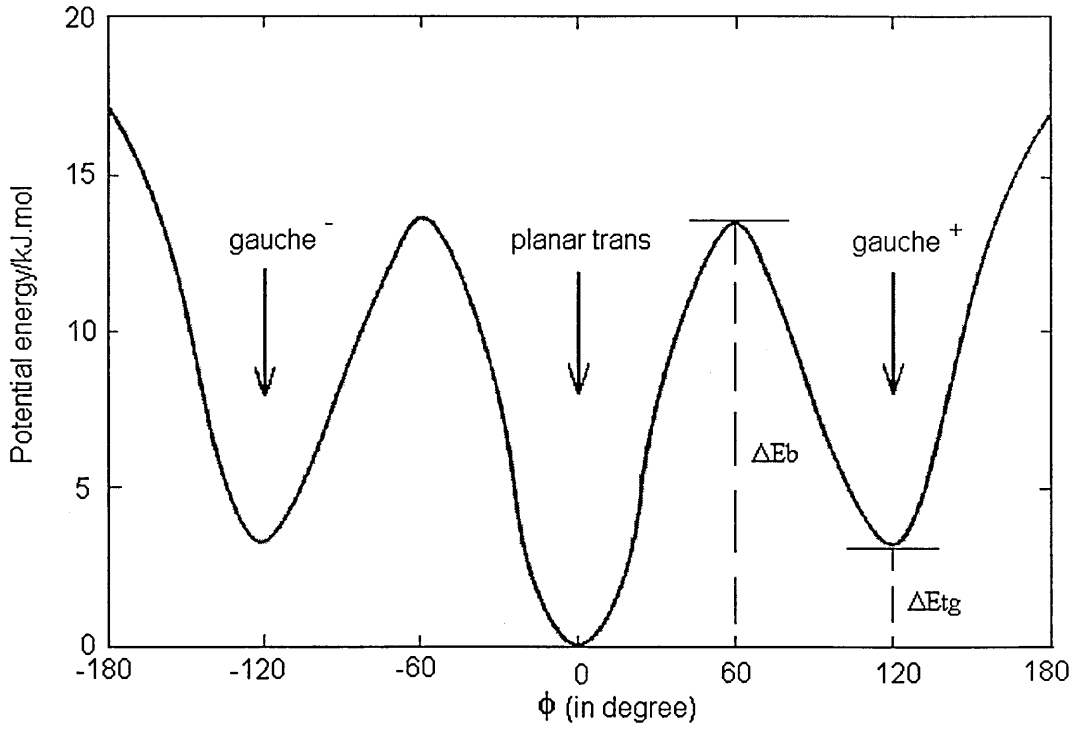

The trans conformation has got the lowest potential energy. It is therefore the most stable conformation for the butane molecule. The energy differences between the trans and gauche conformations, ΔE_{tg}, and the height of the barrier, ΔE_b, can be determined experimentally. Their values were found to be equal to around 3 $kJ.mol^{-1}$ (using different alkanes) and 12 $kJ.mol^{-1}$ (for ethane). Then, from Equation I.2:

Equation I.2

$$\Delta E_b >> RT \approx \Delta E_{tg}$$

we can conclude that the butane molecules can probably be found in any of the three different conformations. Also, for each molecule, the three different rotational isomeric states are accessible and populated in accordance with the thermal energy available.

In the case of a polyethylene chain, we can use the same Newman projections as previously where the methyl end groups of the butane molecule are replaced by bigger groups representing chain sequences. Therefore, the potential energy function associated with the carbon-carbon bond torsional conformation within the polyethylene chain should be similar to the one associated for the butane molecule. Three energy minima

should be present for the three rotational isomeric states, the energy of the trans conformation being the lowest one. Small differences in the values of ΔE_{tg} and ΔE_b found previously are expected. Thus, gauche$^-$, trans and gauche$^+$ bond conformations should be present along the polymeric chain. For each bond, the three rotational isomeric states will be accessible and populated as a function of the thermal energy available. In the case of a polyethylene chain with a degree of polymerisation x, the number of rotational isomeric states accessible is $3^{(x-3)}$. Nevertheless, the most stable conformation for the polyethylene chain is when all the internal carbon-carbon bonds are in the trans conformation. When the chain is in this all-trans conformation, it is also said to be in a planar zigzag conformation (see Figure I.1). This chain structure can be observed within oligomer crystals too, where the chain lengths are monodisperse with up to a few hundred repeat units.

I.2.2 Helices.

In some cases, polymer chains inside crystals adopt helix conformations. Indeed, it is the case of polytetrafluoroethylene for example, where fluorine atoms have replaced the hydrogen atoms present in the polyethylene chain shown in Figure I.1. If the chain stays in an all-trans conformation, there is a strong repulsive force between second nearest CF_2 group neighbours. Therefore, each carbon-carbon bond along the chain twists from the trans conformation by an identical angle to accommodate the bigger CF_2 groups and form a helix. At the same time, this effect increases the rotational energy associated with each carbon-carbon bond. Nevertheless, at a fixed torsional angle of 16.5^0 an energy minimum is found. Polytetrafluoroethylene adopts a 13/6-helix conformation below 19^0C. This notation indicates that 13 CF_2 groups are found along 6 turns of 360^0.

I.2.3 Coils.

In fluid states, each bond within a macromolecule can quite easily reach any of the rotational isomeric states available. Then, instead of the structural properties of polymers on a microscopic level, theories have been developed at lower resolution where any macromolecule can be seen as a random coil-like form without

differentiation of the chemical structure. Parameters related to the chain flexibility and the distribution of chain conformations need to be considered in order to model the global chain properties. In order to achieve this, the chain is divided into n segments of length l, without any restriction of angle between them. This is the so-called freely jointed segment chain. A similar situation is found in the motion of a Brownian particle suspended in a liquid. Therefore, instead of using statistical parameters related to the coil itself, we can determine distribution functions of the segments of the chain which will follow a Gaussian function as in the well known case of the Brownian particle. Nevertheless, contrary to this last case, two different segments along the polymeric chain cannot occupy the same location. Thus, the volume of the segments of the chain need to be considered. This "excluded volume" limitation, which is a long range interaction effect in polymers, made scientists wonder if macromolecules with Gaussian properties exist at all. In two cases, experiments confirmed the existence of Gaussian chains : polymer chains in Theta solvent (where the excluded volume interactions vanished) and in the melt (chains with zero volume). In all the other cases where the volume of the segments of the chain has to be considered, dimensions of the coil are larger than the ones estimated by using Gaussian distribution functions.

Therefore, on a scale where their chemical structure can be ignored, polymer chains with similar behaviour can be divided into two groups : Gaussian or ideal chains and expanded chains.

I.2.3.1 **Ideal chains.**

If we apply the freely jointed segment model to an ideal polymer chain (x segments of length l, without any restriction of angle between them), a distribution function of the end-to-end distance, r, following a Gaussian function can be calculated. From this calculation, Equation I.3 relates r_0, the size of a polymer chain, more exactly the square root of the mean square of the end-to-end distance r, to the number of chain segments, x:

Equation I.3

$$r_0 = \langle r^2 \rangle^{1/2} = lx^{1/2}$$

One can remark that because a Gaussian distribution is asymptotic to the x axis, the distribution of end-to-end distance vectors of an ideal polymeric chain do not reach zero for distance above the chain length. It is why exact distribution functions for finite chain lengths are also available especially in the case of the study of polymer chains submitted to very large deformations.

I.2.3.2 **Expanded chains.**

In the case of expanded chains, the interaction energy is always repulsive between two monomers along the chain. Therefore, the chain becomes expanded and due to the decreasing number of accessible rotational isomeric states, the conformational entropy decreases. Then, a retracting force is produced which will compensate at equilibrium the repulsive force due to the excluded volume interactions.

De Gennes successfully solved the problem of excluded volume in macromolecules in 1972. A general feature for all the expanded chains was revealed : their distribution functions follow simple power laws. r_F, also called the Flory-radius, is related to the diameter of the volume occupied by an expanded polymer chain and is related to the number of monomers per chain, x, and the monomer length, l_F, by Equation I.4:

Equation I.4

$$r_F = \left\langle r_{ex}^2 \right\rangle^{1/2} = l_F x^{3/5}$$

Also, in the case of a polymer chain in a solvent, the size of the expanded chain is related to its unperturbed dimension in Equation I.5 by the coefficient α :

Equation I.5

$$\left\langle r_{ex}^2 \right\rangle^{1/2} = \alpha \left\langle r_{unp}^2 \right\rangle^{1/2}$$

The value of the expansion factor α will depend on the nature of the solvent and will vary as a function of the temperature. For α=1, the chain adopts its unperturbed dimensions. This occurs at the Flory temperature θ and the solvent is called a θ solvent.

I.2.4 The Ising-chain.

The Ising-chain, also known as the Rotational Isomeric State (RIS) model, is based on the one dimensional Ising-model and is well known in statistical mechanics. Each one of the conformational states possible for all the rotational isomeric states accessible to each internal backbone bond represents the particle of the Ising-model and is able to occupy states, interacting only with the nearest pairs. In this model, only the trans, gauche$^-$ and gauche$^+$ conformers are considered. The internal energy or entropy of a polymeric chain can therefore be described by taking in account the short range interactions present in the chain. One of these present in polyethylene chains and called the pentane interaction occurs between the first and fifth carbon atoms of the sequence trans-gauche$^+$-gauche$^-$-trans. The RIS model developed by Flory[2] (1969) successfully took account of this situation and can be used to determine thermodynamic functions and specific structural properties of polymeric chains. Because the RIS-model is based on the microstructure of the polymer chains and short range interactions, it provides a good understanding of ideal chain properties only.

I.3 Crystal structures in polymers.

In the simplest case of monodisperse oligomers the generic name for low molecular weight polymers, crystallisation from solution or melt occurs through the separation of the chains from each other and by their successive attachments in a helical conformation (zigzag chain) onto the growing lateral crystal surface. The crystal layers composed of these chains in helical conformations with their ends at the crystal surfaces forms lamellar shaped crystals, the size of which is of the order of few tens of micrometers laterally and few hundred Angstroms thick (see chapter III, optical photographs III.1 and III.2). These materials are almost purely crystalline.

In the case of polymers with molecular weight distribution, x-ray diffraction and density experiments have shown that many polymers are semi-crystalline. Their x-ray patterns show regular rings superimposed on a diffuse background indicating the presence of both randomly oriented crystalline regions and amorphous materials. The crystalline regions are usually few hundred Angstroms in thickness. The chain length of the

polymers is long enough to go through several crystalline and amorphous regions. For a semi-crystalline polymer, the chains within the crystalline regions preferentially adopt the helical conformations (extended or helix forms). The amorphous regions are composed of the parts of the chains which cannot escape, for kinetic reasons, from the entanglement of the chains present in the fluid state, the chain ends, some branch groups or any local conformations which resist the transition to the helical forms. In fact, the formation and the structure of polymer crystals is strongly dependent upon kinetic considerations rather than by the laws of equilibrium thermodynamics. Indeed, the formation of a crystal structure by a polymer can be allowed for thermodynamic reasons but may not be achieved for kinetic ones. For example, rapidly cooling down a crystalline polymer originally in the melt can, in some cases, produce a fully amorphous material.

Polymer crystals involved the side-by-side packing of the polymeric chains which lie in one specific direction within a regular three dimensional structure. The crystal structure can be identified by its repeating unit, namely the unit cell. This latter corresponds to the minimum number of segments of the polymer chains needed to reconstruct the full crystal structure by its translation. There are seven different shapes of unit cell which characterised seven crystal systems: triclinic, monoclinic, orthorhombic, tetragonal, trigonal and cubic. For each crystal system, the unit cell is identified by the length of three axis (a, b and c) and by the three angles between these axis (α, β, γ). The symmetry of the crystal structure formed by the packing of the segments of the polymeric chains present within the unit cell can be assigned to one of the 230 space groups existing. In the case of polyethylene for example, the most common structure is the one where the chains take the all-trans conformation and lie parallel to each other in the c direction within an orthorhombic crystal structure assigned to the P_{nam} space group. The unit cell is defined by a=7.418 Å, b=4.946 Å and c=2.546 Å and $\alpha=\beta=\gamma=90^0$.

Figure I.4 : Crystal structure of orthorhombic (P_{nam}) polyethylene. (1) side view of the unit cell. (2) Top view along the chain axis (from Young and Lovell[3]).

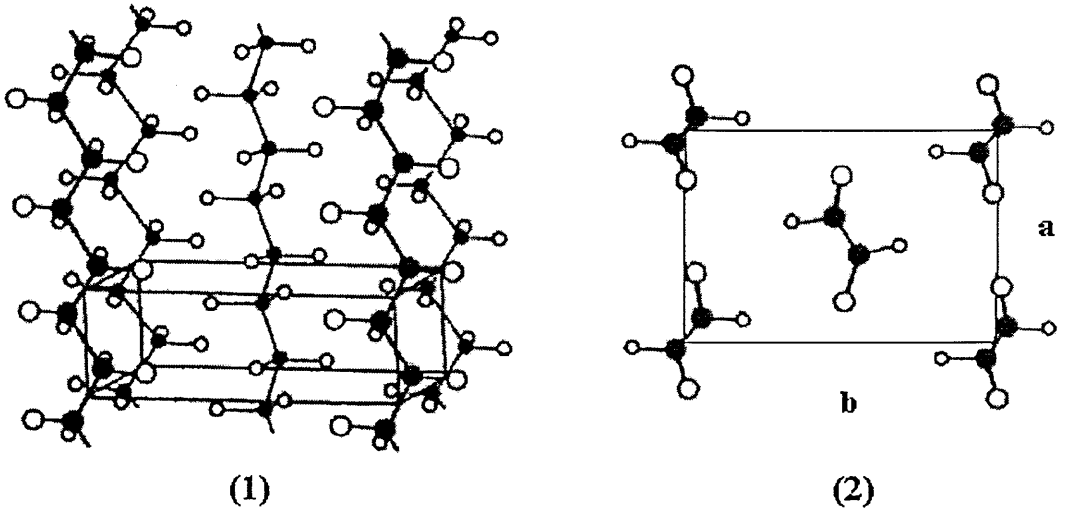

Different crystallisation conditions or mechanical deformation can produce polymer crystals with different structures. This phenomenon is called polymorphism and is well known for polymers and oligomers. In the case of polyethylene for example, a monoclinic crystal form assigned to the space group $C_{2/m}$ can be observed if a mechanical deformation is applied.

I.3.1 Crystallisation from dilute solutions.

Precipitation of polymeric chains from dilute solutions by cooling or by addition of a non-solvent can produce single crystals. In the most widely studied polymer, polyethylene, single crystals usually adopt a lozenge plate-like shape of few micrometers wide and few hundred Angstroms thick. Also, hexagons and curved faces single crystals can be obtained.

The values of the angles within these lozenge shape single crystals are characteristic of the polymer structure. The edges of the single crystals are characteristic of particular crystallographic planes. The most common edges are characteristic of the {110} planes, but truncated lozenge-shaped single crystals can be observed with characteristic {100} edges. Moreover, single crystals possess sectors which can be identified by the edges from which they are built. Also, single crystals can adopt hollow pyramid shapes which collapse on drying. Within all the single crystals, the chains adopt preferentially the all-

trans conformation and are perpendicular (or nearly so) to the crystal surfaces. Because the polymer chain lengths are much more greater than the thickness of the single crystal, the chains must go through the crystal several times with the folding of parts of the chains at the crystal surfaces.

Figure I.5 : Single crystal of linear polyethylene crystallised from perchloroethylene solution (from Statton et al.[4]).

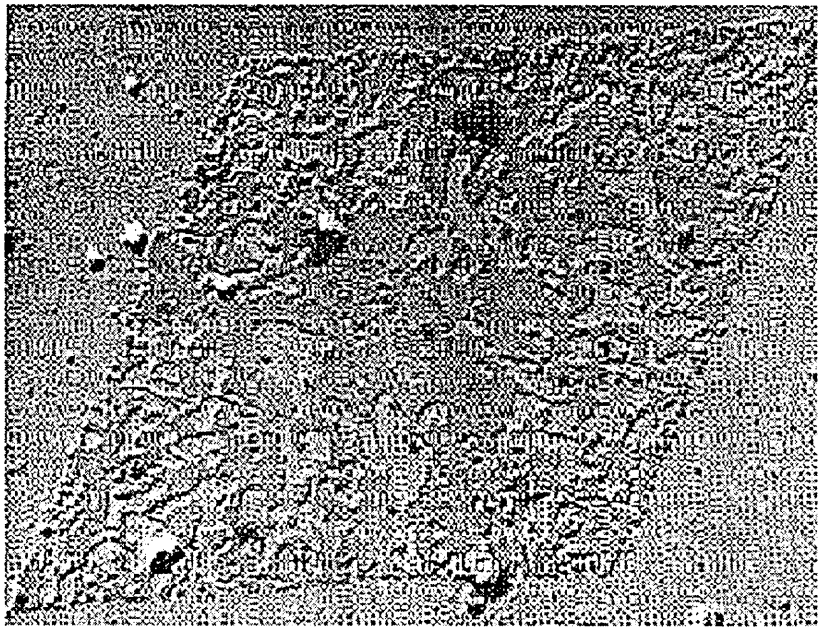

Experiments have shown that single crystals grown from solution are not purely crystalline. The folded parts of the chains, which practically cannot be formed by less than five bonds with three of them in a gauche conformation, are considered to form the non-crystalline region of the single crystals. They are believed to be sharp and to involve a high proportion of adjacent re-entry. Within single crystals, polymeric chains are believed to fold along specific directions parallel to the crystal edges. Therefore, within the common lozenge shape single crystals of polyethylene, the fold planes are parallel to the {110} direction.

Finally, we can note that purely crystalline single crystals can be prepared from solid-state polymerisation. Within these defect-free single crystals, the chains adopt an all-trans conformations and folding does not occur.

I.3.2 Crystallisation from concentrated solutions and from the melt.

When crystallisation occurs at higher concentrations, more complex crystal structures are observed such as twinned crystals, dendritic growths, spiral growths, steps, dislocation networks and Moiré patterns. In the case of crystallisation from the melt, very characteristic spherical objects, the size of which varies from a few micrometers up to millimetres can be observed by optical microscopy. During crystallisation from the melt, nuclei are first observed and these grow in size to form spherulites. Their growth rate is constant until they make contact with their neighbours. It is possible to differentiate adjacent spherulites which have nucleated in the same time from the ones which have not. Indeed, in the first case, linear bondaries are observed where spherulites come into contact. In the second case, curved bondaries are observed. Using polarised light, spherulites show a very characteristic Maltese cross. This is due to an optical anisotropy effect related to the orientation of the polymeric chains found to be perpendicular to the radius of the spherulites. For polyethylene using optical microscopy with polarised light, a regular circular extinction pattern can also be observed. This latter is due to a regular rotation of the chain axis and the layer normal about the radius of the spherulites.

I.3.3 Crystallisation with orientation.

The application of stress on polymeric materials during crystallisation produces specific crystal morphologies with their own physical properties. Inside the crystals, the chains tend to align in the direction of the applied stress. If stirring is applied during crystallisation from a solution of polyethylene for example, a peculiar crystal morphology is obtained consisting of a central backbone used as the nucleus for lamellar overgrowths. This is known as the shish-kebab morphology.

I.3.4 Degree of crystallinity.

The degree of crystallinity affects the physical and mechanical properties of a polymeric material. It is one of the parameters needed to identify a polymer. Several methods can be used to estimate it, none of them giving exactly the same result.

Due to the higher density of the crystalline regions compared to the amorphous ones (a difference of about 20%), the degree of crystallinity can be determined by density measurements using flotation experiments. Wide Angle X-ray Scattering can also be used to determine the degree of crystallinity of a polymer. W.A.X.S. data usually take the form of a spectrum where the intensity of the diffracted x-ray beam is plotted against the diffraction angle 2θ. The area of a broad band proportional to the amount of amorphous material present in the sample can be calculated. The area of sharp peaks proportional to the amount of crystalline material is also needed.

I.4 Polymer crystallisation.

The earlier stage of the study of polymer crystallisation has been developed around the discovery of the structure of polymer single crystals formed from solution, as shown in Figure I.5 and described previously. Then, it was followed by Keller's concept[5] of polymer crystallisation by chain folding. Since the discovery of chain folding in polymer crystals, several crystallisation theories have been developed to explain the growth of these crystals and the subject is still widely debated.

I.4.1 The crystalline model.

The crystal can be schematically represented by a single layer where molecules are parallel to each other and traverse the lamella perpendicular to the crystal surfaces. Any loose parts of the chains, chain ends and folds are outside the crystal layer. The folds are predominantly adjacent and their lengths may vary.

I.4.2 Growth theories

Growth theories can be divided into two main categories based on thermodynamic considerations and kinetics. Among the earlier, Peterlin[6] (1960) assumes that the crystal reaches a minimum free energy state. This model does not take in account the folds formed during polymer crystallisation. Also, Sadler[7] developed a theory which applies to rough and curved single crystals grown from solution or extracted from the melt. He

proposed an entropic barrier model[8] leading to the correct growth laws for these rough crystals. The latter, among which the nucleation theory was developed first by Hoffman and Lauritzen[9] (1960), have received a more general acceptance. They are based on the assumption that free energy barriers are too high for equilibrium and that during crystallisation the preferred crystal thickness is the one which maximises the growth rate of the crystals. In these models, crystallisation of polymers is a two step process. During the first step, also called primary isothermal crystallisation, the temperature of the melt or solution is fixed below the melting point and nucleation followed by the growth of ordered regions occurs. Then, during the second step, called secondary crystallisation, the cooling of the material below its primary temperature of crystallisation forms additional crystallites. Therefore, polymer crystallisation is not instantaneous and in fact, the time to reach its completion can be indefinite.

During the primary isothermal crystallisation, the rate of the crystallisation can be obtained experimentally by determining, for example, the variation of the specific volume of the material as a function of time at a fixed crystallisation temperature. Thus, the rate of crystallisation is defined by the inverse of the time needed to reach one-half of the total volume change.

Figure I.6 : Rate of crystallisation as a function of temperature (from Wood[10]).

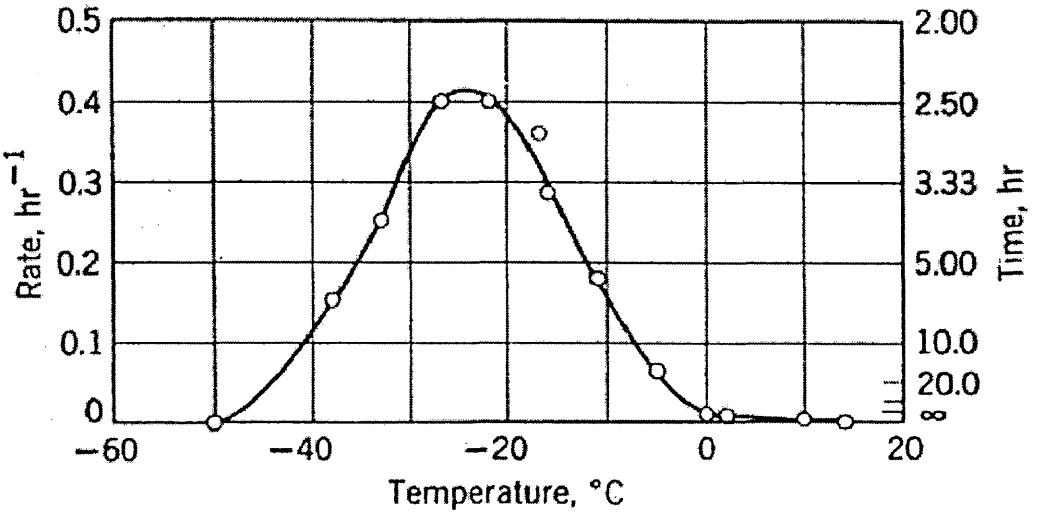

As a function of the temperature, the rate of crystallisation of polymers firstly increases up to a maximum and, then, decreases, as shown in Figure I.6. This variation of the rate of crystallisation can be explained if one considers that the thermodynamic driving force for crystallisation increases with the decrease of the crystallisation temperature. Then, at

a low enough temperature, the viscosity will become sufficiently high to overcome the still increasing driving force allowing the transport of materials at the growth point. From this point, the rate of crystallisation will be progressively reduced with the crystallisation temperature. Also, in the case of a given polymer, the rate of crystallisation of a lower molar mass sample will be higher than its higher molar mass counterpart. If the variation of the specific volume of a polymer is plotted as a function of log time, then the shape of the curves are similar for each different temperature and can be superposed by a translation along the abscissa. These curves follow Equation I.6 known as Avrami's equation :

Equation I.6

$$\ln\left(\frac{V_\infty - V_t}{V_\infty - V_o}\right) = -\frac{1}{W_c} kt^n$$

where V_∞, V_t and V_o are specific volumes at the times indicated by the subscripts, W_c is the weight fraction of crystallised material, k is a constant describing the rate of crystallisation and n known as the Avrami exponent, is characteristic of the nucleation and growth mechanism. The experimental determination of the Avrami exponent and its interpretation may be difficult, specially when secondary crystallisation occurs.

The thickness, d_c, of the crystallites formed during the primary crystallisation of polyethylene from the melt, is inversely proportional to the supercooling determined by the difference of temperature between the melting temperature, T_m and the chosen crystallisation temperature, T, as described by Equation I.7 and as shown by Figure I.7:

Equation I.7

$$d_c(T) = \frac{B_1}{T_m - T} + B_2$$

where B_1 and B_2 are two constants.

Figure I.7 : Thickness of the lamellar crystals of polyethylene, d_c, as a function of the supercooling (from Barham et al.[11]).

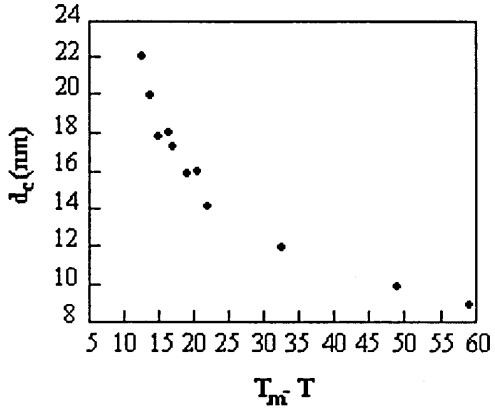

Leung et al[12]. have studied isothermal crystallisation of low molecular weight polyethylene single crystals from solution. The lamellar thickness was found to decrease continuously with the crystallisation temperature. For the higher molecular weight polyethylene samples (M≥11600), a continuous increase of the growth rate as a function of the crystallisation temperature was observed. On the contrary, for the lower molecular weight materials (M=3100 and M=4050), a discontinuity in the growth rate versus the crystallisation temperature was observed. This unusual behaviour is consistent with previous work realised on low molecular weight poly(ethyleneoxide)[13] which has shown several discontinuities in the growth rate of melt-crystallised samples as a function of the crystallisation temperature. As we will see below, these discontinuities correspond to a change in the conformation of the chains deposited on the growth surfaces. Therefore, in the case of PE3100 for example, the discontinuity in the growth rate observed near 74°C is due to the change between once folded and twice folded chain conformations. Reducing the temperature from the melting point, the polymeric chains crystallise in an extended conformation and the rate of crystallisation strongly decreases. Because polymer crystallisation is first controlled by kinetics, the crystallites formed at a fixed temperature are the ones which have the highest growth rate. In the case of poly(ethyleneoxide)[13] with a molecular weight of M=6000, the growth rates of the crystallites formed from the melt were measured by optical microscopy and are plotted as a function of the temperature of crystallisation in Figure I.8. In addition, the chain conformation for different temperature regions is shown. Therefore, near to the melting point, we first observe the increase of the growth rate

with the supercooling for crystallites in extended chain form. This sample can be crystallised in extended chain conformation near to the melting point due to its low molecular weight and, therefore, due to the shortness of its chains. Then, just below 60°C, a discontinuity in the growth rate is observed, characteristic of a change in the crystallite structure. Crystallites in once folded form are the ones which have the highest growth rate from this temperature and they are the ones preferred during the crystallisation process. However, their melting point is lower and they are less thermodynamically stable than the extended form. Then, the growth rate of these crystallites in once folded form increases with the supercooling.

Figure I.8 : Growth rate of poly(ethyleneoxide) (molecular weight equal to 6000) as a function of temperature, with crystals of different chain conformations (respectively extended, once-folded, twice folded) from Kovacs et al.[13].

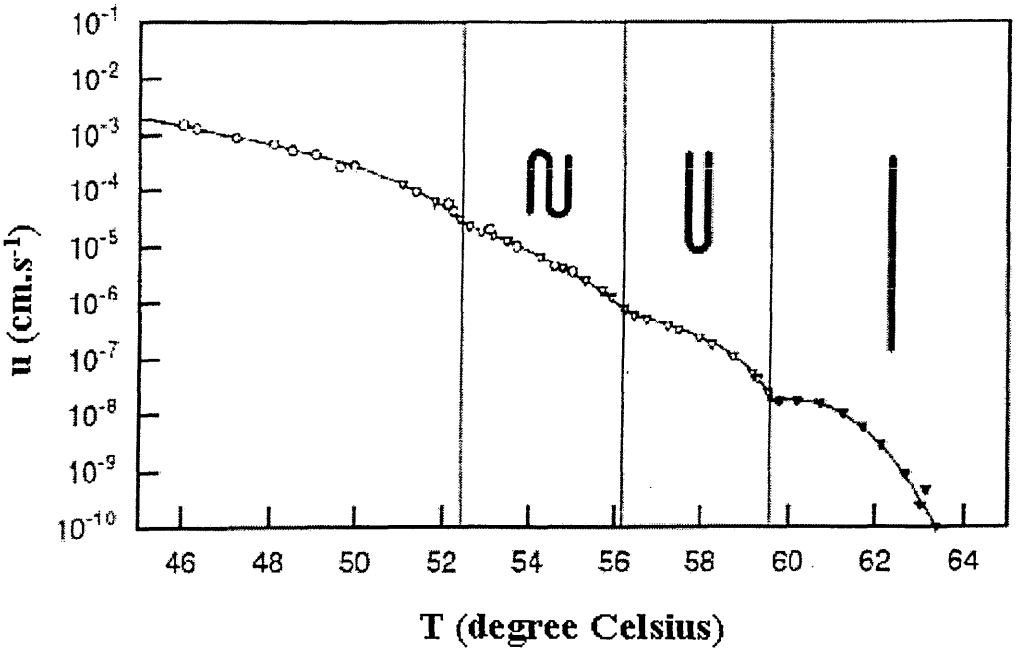

Once again, a discontinuity is found near 56°C. This time, it is due to a transition between the once folded to the kinetically preferred twice folded crystallites. Finally, a third transition is observed between the twice folded and multi-folded crystallites. This last region of the diagram is characteristic of high molecular weight polymer behaviour. Indeed, as observed previously in Figure I.7, the growth rate varies continuously with the supercooling in this last region. Therefore, in the case of low polydispersity and low molecular weight PEO, a discontinuity of the thickness of the crystal layers formed from the melt and equal to integral fractions of the chain length is observed as a function

of the temperature of crystallisation. This polymeric material was the first one to show quantised chain folding during crystallisation from the melt[14].

Within nucleation theories, a barrier is involved and must be overcome in order to deposit an initial nucleus. In these theories, the size of this initial nucleus has to be larger than a critical size to observe the crystal growth. The critical size decreases with the increase of the supercooling and then, leads to the increase in overall growth rate. Lauritzen and Hoffman have developed a well established Nucleation theory which envisages three regimes of crystallisation, giving different temperature dependence of the growth rates. Within the first regime, also known as the mononucleation regime, the growth rate is proportional to the width of the substrate. Within the second regime, also known as the polynucleation regime, several nucleation events give rise to simultaneous growth at different points on the substrate also called patches. Within the third regime, both the additions and subtractions at the end of the patch, also called fluctuations, are so frequent that patches have a low probability to spread before meeting another nucleus.

After the isothermal primary crystallisation, further crystallisation is going on if the material is cooled down below its primary crystallisation temperature. Indeed, after the primary crystallisation, crystallites are separated from each others by amorphous materials. The distance between the crystallites is comprised between a lower and upper limit, the upper one being approximately equal to twice the lower one. Cooling down the material will form new crystallites of lower crystal thickness within the thickest amorphous regions of the sample without additional nucleus formation. Then, on further cooling, the next thinner amorphous regions will be occupied by new crystallites with thinner crystal layers than the previous ones. This process, occurring during the secondary crystallisation and leaving the primary crystallites unchanged, is known as the insertion mode.

Low molecular weight fractions of PEO were the first polymeric materials to provide experimental data related to quantised lamellar thickness during polymer crystallisation from the melt. The transitions between the different quantised lamellar thicknesses as a function of the crystallisation temperature were demonstrated to result from crystal growth kinetics. Experimental determination of the free energy of a once folded chain

within a crystal gave the possibility to determine that only a few monomers were involved in the fold. The fold was expected to linked the nearest or next nearest neighbour chains. The chain ends are at the crystal surfaces. Even if low molecular weight PEO is, at the moment, the only polymer showing such crystal thickness behaviour as a function of the crystallisation temperature, it should not be unique. The other example of low molecular weight polyethylene, where discontinuity in the growth rate as a function of the crystallisation temperature was also observed, indicates that this phenomenon is a general behaviour of flexible, low molecular weight polymeric materials with low polydispersity.

Since long chain n-alkanes, n-C_nH_{2n+2}, with up to n = 390 were synthesised by Bidd and Whiting[15], new purely monodisperse materials have become available to study crystallisation by chain folding. Indeed, materials from 150 up to 390 carbon atoms per chain were found to crystallise by quantised chain folding as a function of the supercooling with up to four folds per chain in the case of the longest n-alkane available[16].

I.5 Long chains of n-alkanes : an ideal model for polymer crystallisation.

I.5.1 Synthesis.

In 1985, Bidd and Whiting synthesised essentially pure n-alkanes following the procedure shown in Figure I.9. They started with 12-Bromododecanal ethylene acetal which gave, after deprotection, an aldehyde (1) while reaction with triphenylphosphine gave the phosphonium bromide (2). The reaction of (1), (2) and potassium carbonate in the presence of 18-crown-6 to generate the ylide in situ in tetrahydrofuran, gave the chain doubled C_{24} bromo acetal (3). The repetition of the reaction sequence with (3) gave the second chain doubled product C_{48} bromo acetal, which was converted to C_{96} bromo acetal, then to C_{192} bromo acetal and finally to C_{384} bromo acetal.

Figure I.9 : Scheme, (a) base, (b) hydrolysis (half material); reaction with Ph_3P (half material); repetition, (c) hydrolysis, reaction with RP^+Ph_3Br and base, $LiBHEt_3$, hydrogenation at 130°C.

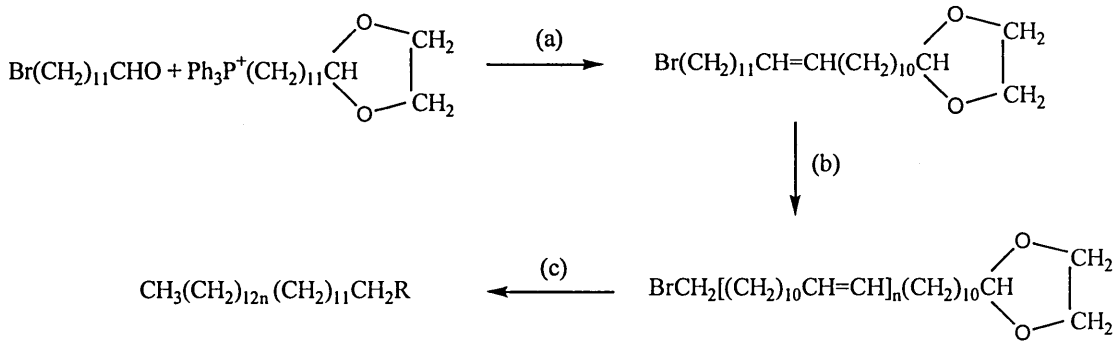

The deprotection of acetals and capping of the resulting aldehydes was followed by the replacement of the bromine by hydrogen and hydrogenation of the polyalkene to gave the n-alkane of desired length.

Further development of this synthesis by Brooke et al.[17] made it possible to obtain these materials in gram amounts. New monodisperse long alkanes were also synthesised with different branched groups in the middle of the chain.

I.5.2 Crystallisation behaviour.

Ungar et al.[16] using differential scanning calorimetry, X-ray scattering and Raman spectroscopy techniques, showed the quantised chain folded behaviour of these purely monodisperse materials. Contrary to the case of the low molecular fractions of PEO, where the crystallisation behaviour at high supercooling was found to be similar to that of polymeric materials, within these monodisperse n-alkanes the crystallisation by chain folding is systematic whatever the supercooling. They determined[18] that the fold in these long chain n-alkanes must be sharp and adjacently re-entrant, the chain ends lying at the crystal surfaces. These materials were expected to give the opportunity to study quantised chain folded crystallisation without the complication of polydispersity present in polymeric materials. Also, the study of these materials confirms that crystallisation by chain folding must be a general behaviour of long flexible chains. Using differential scanning calorimetry, Hobbs et al.[19] have demonstrated from low concentration solutions of monodisperse long chain n-alkanes that two distinct forms of phase diagram (dissolution temperature versus solution concentration) exist. In the case of n-alkanes

with less than 160 carbon atoms per chain, a classical form of the phase diagram is observed when the dissolution temperature increases with the solution concentration. In the case of n-alkanes with more than 200 carbon atoms per chain, a polymeric form of the phase diagram is determined where the dissolution temperature is not affected by the solution concentration. This is expected to be due to locally higher concentrations where molecules are partially attached to a crystal.

I.5.2.1 **Initial stages of crystallisation.**

With the help of real time small angle X-ray scattering techniques using a synchrotron X-ray source, the first stage of crystallisation of a monodisperse long chain n-alkane, n-$C_{246}H_{494}$, from the melt was studied[20]. It was found out that non integer fractions (NIF) of the chain length were initially formed during crystallisation from the melt, and then were transformed to once folded or extended form crystals by respectively thinning or thickening processes (see Figure I.10). The presence of this NIF form in the initial crystallisation from the melt indicates that kinetics favour this structure which is less thermodynamically stable than the extended or once folded crystal forms. It can be remarked that, in the NIF form, a higher degree of disorder is present in the interface layers. Zeng and Ungar[21] determined by inverse Fourier transformation the electron density profiles of the NIF and extended forms formed during the initial stage of the melt-crystallisation of long n-alkanes n-$C_{162}H_{326}$, n-$C_{194}H_{390}$ and n-$C_{246}H_{494}$. They found high and low density regions with sharp boundaries representing respectively the crystalline and interface layers. In the case of the extended form crystals, the density profiles matched the crystal thickness of this structure for the chains tilted by about 35^0 from the crystal surfaces. The value of the tilt angle is characteristic of the n-alkane crystals and is due to the shift of each chain by one CH_2 group along the chain axis. It is believed to create a greater surface area for the disordered chain ends. The electron density determined for the interface layers was estimated to correspond to a truly amorphous phase. In the case of the NIF form crystals, the density profiles indicated a crystal thickness equal to half the value of the extended form crystal structure with the chains tilted by about 35^0 from the crystal surfaces. The thickness of the interface layers was estimated to vary between 1 and 3 nm in the case of the extended form crystals and

between 6 to 8 nm in the case of the NIF form crystals as a function of both the n-alkane chain lengths and crystallisation temperatures. In the latter structure, approximately half the chains are in once folded form within the crystal layers and tilted by 35^0 from the crystal surfaces. The others only traverse the crystal layers once and are also tilted by 35^0 from the crystal surfaces. In the NIF form, the crystallinity is estimated to be less than 66% due to an alternation of truly crystalline and amorphous layers. A model structure was determined for the NIF form and its subsequent transformation to one of the quantised folded forms (once folded or extended) and is shown in Figure I.10.

Figure I.10 : Schematic representation of the different structures obtain from melt-crystallised long chain n-alkanes.

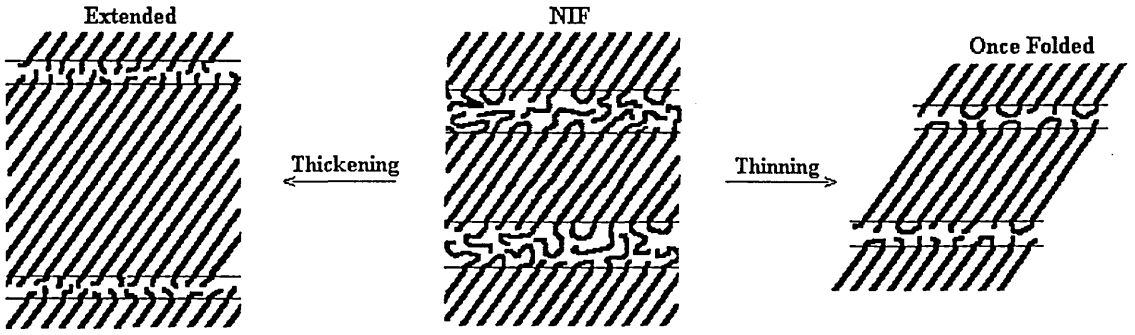

Finally, Zeng and Ungar observed a decrease of the average layer periodicity of the NIF form crystals with decreasing temperature and increasing time. This effect was explained by a thinning of the amorphous layers whereas the thickness of the crystal layers stays constant. It was thought to occur by a progressive migration of the cilia present initially in the interface layers towards the crystal layers. Both real time Raman Longitudinal Acoustic Mode (LAM) spectroscopy and X-ray scattering techniques have confirmed[22] this explanation. Indeed, in the case of isothermally melt crystallised n-$C_{246}H_{494}$, the first order of the LAM, characteristic of the number of carbon atoms present in the all-trans part of the chains traversing the crystal layers was initially observed at 20 cm^{-1}, corresponding to 123 carbon atoms, very nearly exactly half the chain. The intensity of this Raman band increased with time at this constant frequency, indicating an increasing number of crystalline units within the crystal layers in the once folded chain conformation. Nevertheless, in the case of shorter melt-crystallised n-alkanes, such as n-$C_{210}H_{422}$ and n-$C_{198}H_{398}$, a more complex triple layer phase was observed after the formation of the initial NIF structure. It is believed to be formed by a

stacking of extended form chains aligned with once folded ones. This model is supported by small angle X-ray scattering and by the spectrum of n-$C_{210}H_{422}$ obtained by real time Raman LAM spectroscopy in which two bands are observed at 11.7 cm^{-1} and 23.6 cm^{-1}, characteristic respectively of the extended and once folded chains traversing the crystal layers.

I.5.2.2 **Crystallisation rate minima.**

Ungar and Keller[20] noticed that during crystallisation from the melt of n-$C_{246}H_{494}$, the D.S.C. cooling scan showed unusual behaviour within the extended chain crystallisation range. Further investigations[23,24,25] on a full range of monodisperse long chain n-alkanes using D.S.C., S.A.X.S., phase contrast and polarised optical microscopy techniques have shown that both the primary nucleation (see Figure I.11 from reference 23) and crystal growth go through a minimum with increasing supercooling.

Figure I.11 : Isothermal crystallisation from the melt of n-$C_{246}H_{494}$, t_{10} corresponds to the time needed to reach 10% of the crystallisation, $1/t_{10}$ is related essentially to the primary crystallisation process.

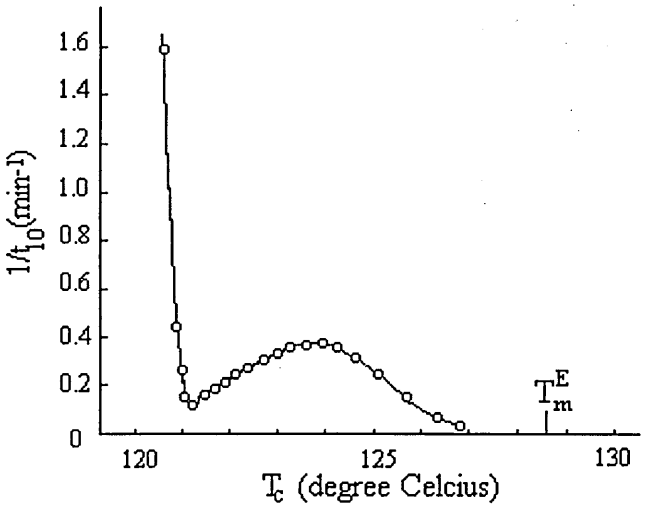

These unexpected minima are believed to be due to competition between extended and once folded chain deposition on the crystal growth area. A few degrees above their melting temperature, the deposition of once folded chains on the growth surface of the stable extended chain crystals leads to a strong inhibition to the crystallisation rates of these latter. This process was called self-poisoning. Further study on solution-crystallised long n-alkanes were carried out by Organ et al.[26,27] on n-$C_{198}H_{398}$ and

confirmed the presence of these crystallisation rate minima. Once folded n-$C_{198}H_{398}$ crystals in solution were found to transform to the extended form by isothermal thickening. Isothermal thickening is well known in the case of polyethylene crystallisation from the melt but does not occur from solution crystallisation. Furthermore, kinetic measurements of the isothermal thickening as a function of the crystallisation temperature shown an unexpected maximum. This effect is believed to be due to an increasing rate of extended chain nucleation with decreasing solution concentration. Therefore, at higher crystallisation temperatures, the concentration of once folded chains in solution is higher, thus, reducing the rate of extended chain nucleation. Finally, models[28] and theoretical revisions[29,30] were proposed for the growth of low molecular weight polymers and monodisperse long chain n-alkane crystals in particular.

I.5.2.3 **Crystal morphologies.**

Very regular polymer crystals can be obtained from solution crystallisation. Organ et al.[27,31] used electron microscopy techniques to study solution-crystallised n-$C_{198}H_{398}$ single crystals prepared from toluene under different experimental conditions. They all gave thin lamellae crystals. Shadowing techniques were used to determine the crystal thickness induced by the different chain conformations. This technique indicated the quantised nature of the crystal thickness as already observed by S.A.X.S. and Raman LAM spectroscopy techniques. Furthermore, isothermal thickening was observed and thickness are again integral fractions of the extended chain length. Different crystal morphologies were obtained as a function of experimental conditions. They were found to be similar to the case of short n-alkanes and polyethylene. Electron diffraction patterns and dark field images were obtained and indicated a similar orthorhombic crystal structure to polyethylene (see Figure I.4). The alkane chains were found to be perpendicular to the crystal surfaces. Crystal decoration with polyethylene revealed particular crystal sectorisations. The fold direction was found to be parallel to the {110} crystal faces.

Using polarised optical microscopy techniques and electron microscopy, Bassett at al.[32,33] studied the relationship between spherulitic growth and chain conformations in

melt-crystallised n-$C_{294}H_{590}$. The presence of spherullites was found to depend on the presence of once-folded chain conformations, the presence of impurities not being a prerequisite. Indeed, in the case of the crystallisation of once folded molecules, half the chains were at one time in the melt and formed a cilium. On the other hand, extended chains are not expected to provide such a cilium during their crystallisation from the melt and therefore do not allow the presence of spherulites. This explanation strongly supports the idea of dependence of spherulitic crystallisation on pressure from molecular cilia. Furthermore, different organisations of the lamellar structure of extended chain crystals and spherulites within once folded chain crystals are observed by electron microscopy. A study of a broader range of monodisperse long chain n-alkanes was realised by Vaughan et al.[34] using transmission optical microscopy with polarised light.

I.5.2.4 **Molecular Folds.**

Over the years, the determination of the structure and orientation of the fold during the crystallisation of flexible polymeric materials, especially polyethylene, has been a central issue in polymer science. A model where the folding parts of the chains are seen as tight and adjacently re-entrant has won broader acceptance, at least in the case of solution crystallised polymers The purely monodisperse long chain n-alkanes were the first materials which give the opportunity to unambiguously verify this model. The combination of D.S.C., X-ray scattering, Raman LAM spectroscopy and electron microscopy techniques[18] definitively demonstrate the existence of sharp chain refolding within monodisperse long chain n-alkanes. The folds must be composed of a minimum number of CH_2 groups and are preferentially oriented along the {110} growth plans. Transmission Electron Microscopy with self-decoration techniques[31] provides evidence of fold regularity and preference for the folds to lie parallel to the particular {110} growth planes of polyethylene crystals. Neutron scattering gives evidence of the stem arrangement in similar samples (not for n-alkanes yet). Among the different techniques available to study the {110} folds in polyethylene and long chain n-alkanes, computer simulations using molecular dynamics have been widely used. (Note that in the following parts of this thesis, the gauche$^+$ conformers will be represented by " g " and

gauche⁻ ones by " g' "). Initial work from Frank showed that the (110) fold cannot be simply composed of g, g' and t bonds, particularly if the number of carbon atoms is small. Indeed, additional stem twists and slight alterations in intersegment distance are required to make this path correspond to a fold along (110) in the polyethylene lattice. The most recent of these works realised by Chum et al.[35] determined five lowest energy {110} fold conformations, the most stable being composed of the following successive chain conformers (g'g'g g t g). Only 1.7 kcal/mol differentiates this last fold conformation from the highest energy one. The two lowest fold conformations are within 1 kcal/mol of each other but one additional carbon atom is present within the fold in the later. This implies that more than one type of fold conformation could be present in polyethylene crystals, and therefore in long chain n-alkanes. One possible {110} fold conformation is shown in Figure I.12.

Figure I.12 : {110} fold conformation in long chain n-alkanes.

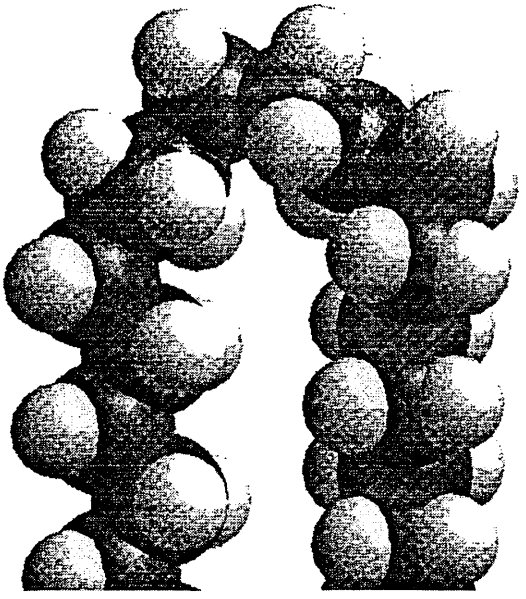

Atomic force microscopy[36] was used to observe directly the arrangements of the folds on the surface of folded chain polyethylene crystals. Local variations in the orientation and shapes of the spots forming the images were interpreted as due to the presence of different fold conformations in these polyethylene crystals.

Finally, vibrational spectroscopy, and in particular infrared spectroscopy, was found to be a powerful tool in the identification of the fold conformations. Indeed, the methylene wagging mode region of the infrared spectra of hydrocarbon compounds contains

information about the non-planar chain conformations including the folds. The identification of infrared bands due to the folds in long chain n-alkanes will be used here to study chain folded crystallisation in general. The identification of conformational isomers in hydrocarbon chain compounds by infrared spectroscopy has been reported by Snyder[37] from the study of the shortest chains of the n-alkane family in the liquid state. He assigned several localised methylene modes of vibration in the limited wagging mode region between 1400 cm^{-1} and 1300 cm^{-1}. He ascribed the bands at 1368 cm^{-1} and 1308 cm^{-1} to methylene sequences involving gtg and gtg' conformations, a band at 1352 cm^{-1} to a methylene sequence involving gg conformations and a band at 1344 cm^{-1} to end gauche conformations. These different conformers are represented in Figure I.13 in the case of a short n-alkane chain (from Maroncelli et al.[38]).

Figure I.13 : Different non-all trans conformers detectable by infrared spectroscopy.

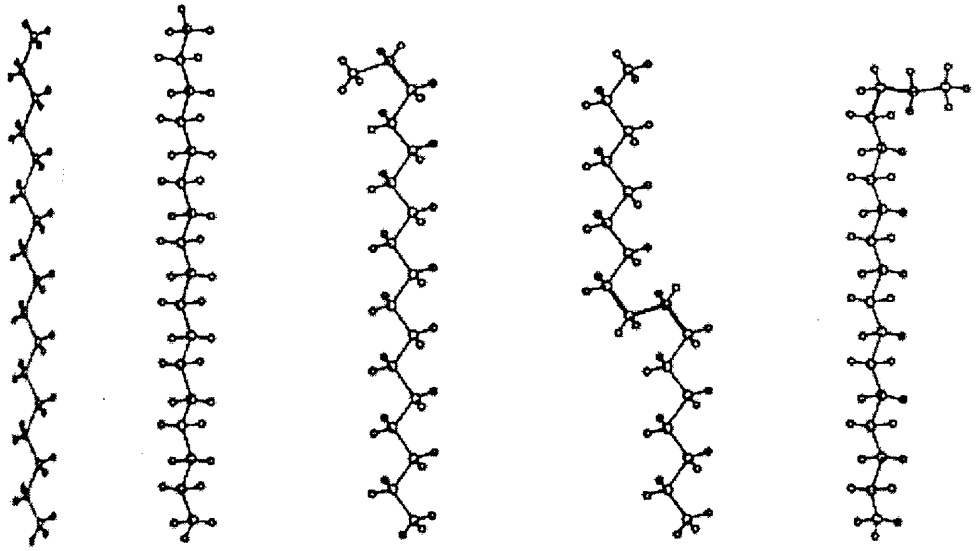

From these assignments, Snyder and Schachtschneider[39,40] also calculated the normal modes of vibration of an infinite hydrocarbon chain using various gauche/trans sequences. On the other hand, Zerbi and co-workers[41,42], using the same force field, calculated the density of states in model systems. The nature of the fold surface in polyethylene and long chain n-alkanes has been subject to numerous infrared spectroscopic studies. Computerised Fourier transform spectrometers allowed the use of spectral subtraction and self-deconvolution techniques with confidence. Thus, Painter

and co-workers[43,44] reported an analysis of methylene wagging and rocking modes of vibration in the infrared spectra of polyethylene single crystals where they discussed the assignment of the band at 1346 cm^{-1} to the regular, tight fold structure. Spells et al.[45] reported a study of polyethylene single crystals obtained at different crystallisation temperatures in the methylene wagging mode region of the infrared spectra. They associated, as Painters and co-workers[43,44], a band at 1346 cm^{-1} with regular tight folding. However, they pointed out that folds along different directions, such as the {200} or {100} ones, are possible in polyethylene crystals in addition to the {110} fold. These could give additional infrared peaks in the region from 1342 cm^{-1} to 1348 cm^{-1}. Ungar and Organ[46], using spectral subtraction and self-deconvolution techniques, reported the infrared spectra of the pure {110} fold itself present in the orthorhombic crystals of the monodisperse long chain n-alkane n-$C_{198}H_{398}$ at room temperature and 110K. They confirmed previous assignments of the 1346 cm^{-1} band to a regular re-entry {110} fold type as well as bands at 1298 cm^{-1} and 1369-1370 cm^{-1}. Moreover, Hägele and co-workers[47] calculated the defect density of states of the tight {110} fold in polyethylene using the Green's function method. They confirmed the assignment of the 1346 cm^{-1} and 1295 cm^{-1} bands to the regular {110} fold. Using the same method, they also calculated[48] the eigenvectors of vibrating polyethylene chains with {200} and {110} folds.

I.6 Aim and objectives.

Our aim is to study, by means of vibrational spectroscopy, disorder in these highly ordered materials which are purely monodisperse long chain n-alkanes. Infrared spectroscopy is the only experimental technique able to characterise specific types of conformational disorder present in paraffinic materials in both qualitative and quantitative ways. It is sensitive to molecular details rather than overall variations such as electron density (S.A.X.S.) or stem length (L.A.M.). For example, infrared spectroscopy[38] has been used to study disorder through premelting phase transitions occurring in odd n-alkanes from n-$C_{17}H_{36}$ to n-$C_{29}H_{60}$. Also, Maroncelli et al.[49] have studied the distribution of non all-trans conformers as a function of position along the hydrocarbon chains.

First, we report D.S.C. and X-ray scattering measurements to determine the phase transition temperatures and to distinguish the different crystal forms present in a short chain n-alkane, namely n-$C_{44}H_{90}$ crystallised from solution. Short chain n-alkanes are known to crystallise only in an extended chain conformation with their methyl end groups at the crystal surfaces. They form very perfect lamellar crystal structures. Then, we show the use of infrared spectroscopy to characterise the amount of disorder within different crystal structures of n-$C_{44}H_{90}$ crystallised form solution under different experimental conditions. The intensity and frequency of different infrared bands present in the wagging mode region of the spectra were studied with reference to this "perfect" crystalline structure. The use of the symmetric methyl deformation band (usually assigned at 1378 cm^{-1} in the infrared spectra of paraffinic materials) for spectral normalisation is discussed. The sensitivity of the infrared bands ascribed to the modes of vibration of the methyl end groups and present outside the wagging mode region of the spectra is analysed as a function of the crystal structures.

Secondly, the study of purely monodisperse long chain n-alkanes, namely n-$C_{198}H_{398}$ and n-$C_{246}H_{494}$, was undertaken taking in consideration the latest results obtained on n-$C_{44}H_{90}$. These long paraffins were crystallised from solution in extended and/or once folded forms. S.A.X.S. measurements, low frequency Raman and infrared spectroscopy were used to investigate the crystal organisation of these long paraffins. Spectral subtractions were used to obtain the spectrum of the pure fold region. The numbers of specific non all-trans conformers present in n-$C_{198}H_{398}$ crystals in both extended and once folded forms were estimated. Differences in the carbon-carbon stretching mode region of extended and once folded forms are analysed. The transition from once folded to extended form crystals was also monitored by infrared spectroscopy. Finally, the tilting of the n-alkane chains within the crystal layers was investigated by means of infrared and low frequency Raman spectroscopy and S.A.X.S. techniques.

Changes in the fold conformation due to the presence of branch groups in the middle of a long chain alkane, namely $C_{96}H_{193}CH(CH_3)C_{94}H_{189}$ and $C_{96}H_{193}CH(CH_2CH_2CH_2CH_3)C_{94}H_{189}$, were analysed by means of infrared and low frequency Raman spectroscopy and S.A.X.S. techniques. The carbon-carbon stretching mode region of their infrared spectra was studied. With the aim of estimating the effect

of polydispersity on the crystal structures of these long chain n-alkanes, an appropriate binary mixture of n-$C_{246}H_{494}$ and n-$C_{162}H_{326}$ was prepared from the melt. The heating of this mixture from room temperature above the melting point using different rates was investigated by infrared spectroscopy and with the help of the results obtained by the S.A.X.S. technique[50].

II TECHNIQUES

II.1 Differential Scanning Calorimetry.

The determination of the enthalpy changes when heating, annealing or crystallising a sample can provide useful information about the actual mechanism occurring during one of such heat treatments. During a D.S.C. experiment, the temperature of a sample and reference holder is controlled and follows a pre-recorded program as a function of time. The temperature of the sample and the reference holders are constantly compared. Heating power is applied to both holders to keep them at the same temperature at all times. When the sample undergoes a phase transition, a difference in the power applied to the sample and reference holders is noticed. Therefore, a D.S.C. trace consists of this difference between the applied power to both holders as a function of time. During a phase transition, a peak is observed in this curve, and its area provides the means of measuring the enthalpy change during this transition. The melting of a sample is characterised by a large endotherm, as are the transitions between different crystal structures within a sample. On the other hand, recrystallisation will be characterised by an exotherm.

II.2 Small and Wide Angle X-ray Scattering techniques.

X-ray diffraction techniques are a powerful tools in the determination of the degree of order within structures the size of which is comparable to the wavelength of the radiation, i.e. one to several hundred Angstroms. In the case of polymer crystals, the distance between the atoms is of the same order than the wavelengths of the X-rays. Strong diffraction patterns are observed in specific directions, and are due to the interferences occurring between the X-rays scattered by each atom. The specific scattering X-ray directions are related to the shape and size of the crystal unit cell of the lattice. The intensity in each scattered direction is dependent upon the atomic arrangement in the lattice. Small scattering angles (below 5^0) are used to get information

from large periodicities such as the average layer periodicity. Indeed, in the case of polymers crystallised form solution, a solid mat can be obtained where crystals have a preferred parallel orientation. This mat is formed by an alternation of lamellar crystals and amorphous materials, each one having its own electron density. In the specific case of isothermal crystallisation from solution, crystals formed have an approximately constant thickness. Therefore, a regular alternation of electron density is observed. The stacks scatter X-rays in a similar way to the atoms in a crystal lattice. Therefore, Bragg's law is obeyed and the value of the average layer periodicity, d, which includes in addition to the crystal thickness, the thickness of any amorphous or void layers that might be present in the sample, can be determined by Equation II.8.

Equation II.8

$$n\lambda=2d\sin\theta$$

where λ is the wavelength of the incident X-ray beam, 2θ, the scattering angle of the peak and n, its order. The experimental set-up we used is schematically represented in Figure II.14, where the sample was positioned in such a way that the mat normal was perpendicular to the incident X-ray beam.

Figure II.14 : Schematic representation of the S.A.X.S. experimental set-up.

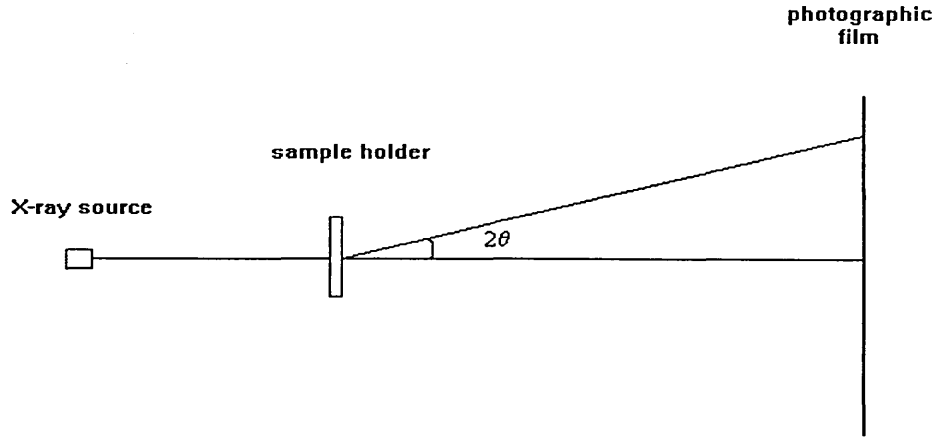

The distance between the sample holder and the photographic film is known. The scattering angle 2θ, is determined from the measurement of the diameter of the rings observed on the photographic film. Then, knowing the wavelength of the X-ray beam λ, the average layer periodicity d can be determined.

For the wider scattering angles, information from the spatial arrangements of the atoms is obtained. In relation to any crystal lattice defined by $\vec{a}$, $\vec{b}$ and $\vec{c}$, a reciprocal lattice present in a reciprocal space is employed to simplify the understanding of X-ray diffraction by single crystals. This reciprocal lattice is defined by $\vec{a}^*$, $\vec{b}^*$ and $\vec{c}^*$ in reciprocal space where $\vec{a}^* = \frac{\vec{b} \wedge \vec{c}}{V}$, $\vec{b}^* = \frac{\vec{c} \wedge \vec{a}}{V}$ and $\vec{c}^* = \frac{\vec{a} \wedge \vec{b}}{V}$ and where V is the volume of the unit cell. A set of (hkl) planes is known as Miller planes and h, k and l as the Miller indices. A given set of (hkl) planes in the direct lattice is represented by a lattice point in the reciprocal lattice. Moreover, in the reciprocal lattice, the vector $\vec{s}(hkl)$ defined from this point lattice to the origin is perpendicular to the set of parallel (hkl) planes in the real space. Its magnitude is equal to the reciprocal of the interplane spacing, $\frac{1}{d_{hkl}}$. The interplanar spacing of a particular set of Miller planes is given by the Bragg's law defined in Equation II.8 where $d=d_{hkl}$. Certain hkl reflection will be absent for which there will be a systematic relationship in the h, k or l indices. These space group extinctions are helpful to deduce a space group symmetry of a structure. Then, the measured d-spacing are compared with those calculated for various set of (hkl) planes of unit cells with different structures and dimensions.

II.3 Vibrational spectroscopy.

Vibrational spectroscopy allows the study of a wide range of chemical and physical behaviour. In a typical spectrum, the intensity is plotted as a function of the frequency of the electromagnetic radiation. The rate at which a molecule makes a transition from one energy level to another is proportional to the intensity. The energy difference between the initial and final energy levels are directly linked to the frequency. In the absence of any incident electromagnetic radiation, molecules possess quantised energy

levels which are the solutions of the time-independent Schrödinger equation shown in Equation II.9

Equation II.9

$$\hat{H}\Psi_n = E_n\Psi_n$$

where n stands for a quantum number or set of quantum numbers, Ψ_n represent the wavefunctions satisfying the equation, E_n represent the energy states of the system and $\hat{H}$ called the Hamiltonian for the system.

The Hamiltonian is equal to the sum of the operators for the kinetic energy $\hat{T}$, and potential energy $\hat{V}$ as shown in Equation II.10

Equation II.10

$$\hat{H} = \hat{T} + \hat{V}$$

The wavefunction Ψ_n characterises the state of the system. When multiplied by its complex conjugate, it (shown in Equation II.11) is known as the probability density.

Equation II.11

$$\Psi_n^*\Psi_n = |\Psi_n|^2$$

In a three dimensional space, the probability to find a particle over all space is unity as shown in Equation II.12

Equation II.12

$$\int \Psi_n^*\Psi_n d\tau = 1$$

Also, if two different states correspond to different energy levels, the eigenfunctions must be orthogonal. This is defined by Equation II.13

Equation II.13

$$\int \Psi_n^*\Psi_m d\tau = 0 \text{ if } E_n \neq E_m$$

Then, if the eigenfunctions of Equation II.9 can be found, other physical properties can be predicted. These physical properties can also be associated with Hermitian operators. Thus, the average value of a physical property A can be estimated when the system is in state n following

Equation II.14

$$\langle A \rangle = \int \Psi_n^* \hat{A} \Psi_n d\tau$$

where $\hat{A}$ is now the operator for the quantity A. Incident electromagnetic radiation can induce the transition between energy levels E_i and E_f characterised by the wavefunctions Ψ_i and Ψ_f with a certain transition probability. The transition probability is proportional to the square of the magnitude of the transition moment, the later being defined by

Equation II.15

$$|T|_{if} = \int \Psi_f^* T \Psi_i dq$$

where T is the operator involved in the interaction phenomenon.

Apart from the few simplest cases such as a particle in a box, the rigid rotator and the harmonic oscillator (which provide the basis for approximating the translational, vibrational and rotational energies of molecules) the exact solutions of the Schrödinger equation can not be determined theoretically. On the other hand, spectroscopy gives access to these energy levels experimentally.

II.3.1 The Born-Oppenheimer approximation.

For a polyatomic molecule, the Hamiltonian $\hat{H}$ is equal to the sum of the kinetic energy operator for the nuclei and electrons and the potential energy operators for the Coulombic interactions electron-electron, electron-nuclear and nuclear-nuclear. The Born-Oppenheimer approximation allows to write the total wavefunction Ψ present in the Schrödinger equation, as a product of the electronic and nuclear wavefunctions due to the much slower nuclear motion than that of the electrons. Furthermore, the nuclear wavefunction can be factorised into vibrational and rotational parts. Therefore, the total wavefunction can be factorised as follows

Equation II.16

$$\Psi = \Psi_e \times \Psi_v \times \Psi_r$$

and the total energy can be treated additively as follows

Equation II.17

$$E = E_e + E_v + E_r$$

This result is the reason for which electronic, vibrational and rotational spectroscopy can be treated separately.

II.3.2 The Quantum Mechanical Harmonic Oscillator.

Let consider a diatomic molecule, the mass of the atoms being m_1 and m_2, where the bond is believed to be equivalent to a Hooke's law spring. At equilibrium, the distance between the atoms is R_e. The displacement of the bond length R from its equilibrium position R_e is chosen to be denoted $x=R-R_e$. Then, the Hamiltonian for this system is defined by Equation II.18 where $\hbar = h/2\pi$, h being the Planck constant, μ is the reduced mass and k a force constant which measures the stiffness of the spring.

Equation II.18

$$\hat{H} = \frac{-\hbar^2}{2\mu}\frac{d^2}{dx^2} + \frac{1}{2}kx^2$$

The eigenvalues of this Hamiltonian are the harmonic oscillator energy levels defined by Equation II.19 and represented in Figure II.15.

Equation II.19

$$E_v = \left(v + \frac{1}{2}\right)h\upsilon_0$$

where v is a quantum number (0, 1, 2,..., ∞) and ν_0 is the frequency defined by Equation II.20.

Equation II.20

$$\nu_0 = \frac{1}{2\pi}\sqrt{\frac{k}{\mu}}$$

We can notice that the lowest energy for the system is equal to $\frac{1}{2}h\upsilon_0$. The nonzero energy of the ground state is required by the uncertainty principle also known as the Heinsenberg uncertainty principle defined by Equation II.21

Equation II.21

$$\Delta x \Delta p_x \geq \frac{\hbar}{2}$$

where the product of the uncertainties in the position and momentum of a particle in a box can not be less than $\frac{\hbar}{2}$. The uncertainty of a quantum mechanical property such as x for example, is defined by the following

Equation II.22

$$\Delta x = \sqrt{\langle x^2 \rangle - \langle x \rangle^2}$$

In Figure II.15 the energy levels determined from Equation II.19 are represented by horizontal lines in front of which the quantum number is shown. Some of the wave functions are shown using the energy lines as the abscissas.

Figure II.15 : Eigenfunctions and energies of a quantum mechanical harmonic oscillator[51].

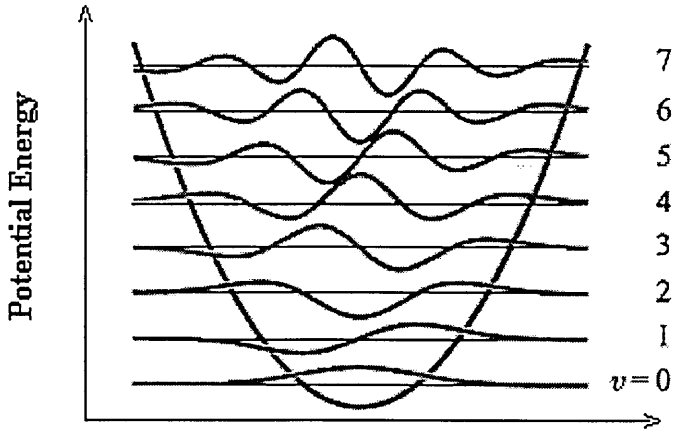

The fact that the tails of the wavefunctions can be found outside the parabolic potential well indicates that quantum mechanics allows the system to be found in regions which are forbidden, as defined by classical mechanics. Also, it indicates that outside the potential well, the potential energy exceeds the total energy of the system.

II.3.3 Absorption and emission of radiation.

Electromagnetic radiation is composed of oscillating electric and magnetic fields. These fields can exert torques on the electric and magnetic multipoles of molecules, causing energy to be absorbed by matter. On the other hand, the oscillation of the charge distribution of a molecule creates emission of electromagnetic radiation.

II.3.3.1 Einstein coefficients.

Three different processes can occur between two stationary states, namely states *1* and *2* *with* $E_2 > E_1$: induced absorption, induced emission and spontaneous emission. The first two processes require the presence of a radiation field of frequency ν, in such way that $\Delta E = E_2 - E_1 = h\nu$. The last, introduced by a quantum mechanical treatment, occurs in the absence of a radiation field. The rate of both absorption and emission are proportional to the energy per unit volume per unit frequency interval as shown in Equation II.23 :

Equation II.23

$$\rho(\upsilon) = \frac{du}{d\upsilon}$$

The rate of an upward transition will be equal to

$$W_{12} = \frac{dN_2}{dt} = N_1 B_{12} \rho(\upsilon)$$

where B_{12} is a first Einstein coefficient and N_1 is the population of state *1.*

Similarly, the rate of an downward transition will be equal to

$$W_{21} = -\frac{dN_2}{dt} = N_2 B_{21} \rho(\upsilon) + N_2 A_{21}$$

where B_{21} is the same Einstein coefficient than B_{12}, A_{21} is the second Einstein coefficient and N_2 is the population of state *2.*

When the populations of both states have reached an equilibrium, N_1 and N_2 are related through the Boltzmann distribution law :

Equation II.24

$$\frac{N_2}{N_1} = \frac{g_2}{g_1} e^{\left(-\frac{\Delta E}{kT}\right)}$$

where g_i is the number of states at the energy level i, also called degeneracy, k is the Boltzmann constant and T is the temperature in Kelvin.

At equilibrium, and in the presence of a radiation of frequency ν,

Equation II.25

$$N_1 B_{12} \rho(\upsilon) = N_2 B_{21} \rho(\upsilon) + N_2 A_{21}$$

Also, the energy density of the radiation is defined by

Equation II.26

$$\rho(\upsilon) = \frac{8\pi h\upsilon^3}{c^3} \frac{1}{e^{h\upsilon/kT} - 1}$$

Therefore, solving Equation II.25 using Equation II.24, we get

Equation II.27

$$\rho(\upsilon) = \frac{A_{21}}{B_{12} \frac{g_1}{g_2} e^{h\upsilon/kT} - B_{21}}$$

Equation II.26 and Equation II.27 are in agreement if

$$g_1 B_{12} = g_2 B_2$$

and

$$\frac{A_{21}}{B_{21}} = \frac{8\pi h\upsilon^3}{c^3}$$

This last equation indicates that spontaneous emission increases rapidly relative to induced emission as the frequency increases.

II.3.4 Vibrational infrared spectroscopy : selection rules.

As mentioned above, to be able to observe any infrared absorption by a material, the incident radiation field of frequency ν must satisfy the equation $h\nu=\Delta E$, where ΔE corresponds to the energy difference between lower (indexed by ν) and upper (indexed by ν') vibrational states characterised by the vibrational wavefunctions Ψ_ν and $\Psi_{\nu'}$. Then, in order for a transition to occur, the transition probability $P_{\nu\nu'}$ defined earlier in Equation II.9 as the square of magnitude of the transition moment, must be different

from zero. In the case of vibrational infrared spectroscopy, the operator involved in the interaction phenomenon is $\hat{\mu}$, the electric dipole moment operator defined by :

$$\hat{\mu} = \sum_i q_i \vec{r}_i$$

where q_i and $\vec{r}_i$ are the charge and the position vector of the i^{th} particle. Therefore, the transition probability is defined in Equation II.28 by :

Equation II.28

$$P_{v'v} = \left|\vec{R}_{v'v}\right|^2 = \left[\int \Psi_{v'}^* \hat{\mu} \Psi_v d\tau\right]^2$$

where $\vec{R}_{v'v}$ is the transition moment vector.

The transition probability is related to the B_{21} Einstein coefficient through :

$$B_{v'v} = \frac{8\pi^3}{(4\pi\varepsilon_0)3h^2} P_{v'v}$$

If we come back to the case of the harmonic oscillator approximation treated in the previous paragraph for a diatomic molecule, then Equation II.28 can be rewritten as

$$P_{v'v} = \left|\vec{R}_{v'v}\right|^2 = \left[\int \Psi_{v'}^* \mu \Psi_v dx\right]^2$$

where x, the displacement of the internuclear distance from equilibrium, is equal to R-R_e. In order for this transition to occur, the transition moment $R_{v'v}$ equal to $\int \Psi_{v'}^* \mu \Psi_v dx$ must be different from zero. If the dipole moment is nil such as in the case of a homonuclear molecule, then the transition moment is nil and all transitions are forbidden. In the case of an heteronuclear diatomic molecule, the dipole moment is non-zero and varies with x. This variation can be expressed in a Taylor series expansion for positions near to the equilibrium position such that

$$\mu = \mu_e + \left(\frac{d\mu}{dx}\right)_e x + \left(\frac{d^2\mu}{dx^2}\right)_e x^2 + \ldots$$

where μ_e is the equilibrium (i.e. static) dipole moment. Therefore, the transition moment can be expressed by

Equation II.29

$$R_{v'v} = \mu_e \int \Psi_{v'}^* \Psi_v dx + \left(\frac{d\mu}{dx}\right)_e \int \Psi_{v'}^* x \Psi_v dx + \ldots$$

Because the two different states specified by Ψ_v and $\Psi_{v'}$ correspond to two different energy levels, then $\int \Psi_{v'}^* \Psi_v dx = 0$ and Equation II.29 can be rewritten as

Equation II.30

$$R_{v'v} = \left(\frac{d\mu}{dx}\right)_e \int \Psi_{v'}^* x \Psi_v dx + \left(\frac{d^2\mu}{dx^2}\right)_e \int \Psi_{v'}^* x^2 \Psi_v dx^2 + \ldots$$

Then, the transition moment $R_{v'v}$ is different from zero for

Equation II.31

$$\left(\frac{d\mu}{dx}\right)_e \neq 0$$

and

Equation II.32

$$\int \Psi_{v'}^* x \Psi_v dx \neq 0$$

Equation II.31 implies a variation of the dipole moment with the normal mode of vibration. Equation II.32 implies the vibrational selection rule $\Delta v = \pm 1$ in the case of the harmonic oscillator. The transition form v = 0 to v = 1 is referred to as the fundamental. When the population of states having $v \neq 0$ is significant, transitions from upper levels can occur and are referred to as hot bands (i.e. v = 2 to v = 3). Also, the higher order terms of Equation II.30 proportional to q^2, q^3... allow the transitions where $\Delta v = \pm 2, \pm 3, \ldots$ These transitions are known as overtones and are due to anharmonicity effects. Mechanical anharmonicity has the effect of decreasing the spacing of adjacent vibrational energies with increasing quantum number v. The intensity of an infrared transition is proportional to $\left|R_{v'v}\right|^2$ and therefore, to $\left(\frac{d\mu}{dx}\right)_e^2$.

II.3.5 Raman scattering.

When a material is irradiated by incident monochromatic electromagnetic radiation with a known direction of propagation and a frequency ν_0 such that no transition between lower and higher energy levels equivalent to $\Delta E = h\nu_0$ exists, then the greater part of the

radiation intensity passes through the sample with the same direction of propagation as the incident radiation with no frequency change : it is called the transmitted radiation. The radiation which is turned back in the opposite direction to the incident radiation with the same frequency is known as the reflected radiation. Finally, a part of the intensity of the incident radiation is scattered in all directions. Lord Rayleigh in 1871 determined that the intensity of the scattered light is proportional to the frequency of the incident radiation (ν_0) to the power four. The frequency of most of the scattered radiation is identical to that of the incident monochromatic radiation. Nevertheless, some of the scattered radiation possesses frequencies ν_s different from ν_0. The frequencies ν_s are dependent on the frequency of the incident radiation ν_0. Therefore, the intensity of a Raman spectrum is dependent on both the incident and scattered radiation frequency. Nevertheless, the frequency shift between the incident and scattered radiation $\Delta\nu = |\nu_s - \nu_o|$ is characteristic of the molecular properties of the material studied. This is why the intensity of the scattered light is usually plotted as a function of the frequency shift between the incident and scattered radiation. The property of the sample which determines the degree of Raman scattering is the polarisability. The polarisability can be defined as a measure of the ability of an electron cloud surrounding nuclei in a molecule to be deformed by an electric field. The polarisability $\underline{\alpha}$ is an anisotropic property of matter and as such is a tensor property. It can be represented by a matrix. Therefore, when monochromatic radiation falls on a material, the oscillating electric field of the radiation $\vec{E}$ induces in the material an electric dipole $\vec{\mu}_{ind}$ which is related to $\vec{E}$ by the polarisability tensor $\underline{\alpha}$ as follows :

$$\vec{\mu}_{ind} = \underline{\alpha}\vec{E}$$

In the case of classical mechanics and considering the vibrational motion of a molecule then

Equation II.33

$$\vec{E} = \vec{E}_0 \cos(2\pi\nu_0 t)$$

and q, the normal co-ordinate of one of the vibration modes, is defined as

Equation II.34

$$q = q_o \cos(2\pi\nu t)$$

We can then expand each of the components of $\underline{\alpha}$ as a Taylor series as follows

$$\underline{\alpha} = \underline{\alpha}_o + q\left(\frac{\partial \underline{\alpha}}{\partial q}\right)_o + \frac{1}{2}q^2\left(\frac{\partial^2 \underline{\alpha}}{\partial q^2}\right)_o + \ldots$$

where $\underline{\alpha}_o$ is the value of $\underline{\alpha}$ at the equilibrium. In the harmonic approximation all but the two first terms can be neglected. Therefore,

$$\vec{\mu}_{ind} = \underline{\alpha}_o \vec{E} + q\left(\frac{\partial \underline{\alpha}}{\partial q}\right)_o \vec{E}$$

Using Equation II.33 and Equation II.34, the induced dipole moment can be written as

$$\vec{\mu}_{ind} = \underline{\alpha}_o \vec{E}_o \cos(2\pi\nu_o t) + \left(\frac{\text{Intensity(Stokes)}}{\left(\partial q\right)_o} = e^{\left(\frac{h\Delta\nu}{kT}\right)}\right]$$

Furthermore,

$$\cos(2\pi\nu t)\cos(2\pi\nu_o t) = \frac{1}{2}\left\{\cos\left[2\pi(\nu_o + \nu)t\right] + \cos\left[2\pi(\nu_o - \nu)t\right]\right\}$$

Therefore, $\cos(2\pi\nu t)\cos(2\pi\nu_o t) = \frac{1}{2}\left\{\cos\left[2\pi(\nu_o + \nu)t\right] + \cos\left[2\pi(\nu_o - \nu)t\right]\right\}$ can be written by the following form :

Equation II.35

$$\vec{\mu}_{ind} = \underline{\alpha}_o \vec{E}_o \cos(2\pi\nu_o t) + \frac{1}{2}\left(\frac{\partial \underline{\alpha}}{\partial q}\right)_o q_o \vec{E}_o \cos\left[2\pi(\nu_o + \nu)t\right] + \frac{1}{2}\left(\frac{\partial \underline{\alpha}}{\partial q}\right)_o q_o \vec{E}_o \cos\left[2\pi(\nu_o - \nu)t\right]$$

Hence, the dipole moment induced by incident monochromatic electromagnetic radiation emits polychromatic electromagnetic radiation. For one normal mode of vibration, three different types of radiations are scattered, characterised by three different frequencies ν_0, $(\nu_0-\nu)$ and $(\nu_0+\nu)$ respectively known as Rayleigh scattering, Stokes Raman scattering and anti-Stokes Raman scattering. In Equation II.36 , the Maxwell-Boltzmann statistics indicate

Equation II.36

$$\frac{\text{Intensity(Stokes)}}{\text{Intensity(anti-Stokes)}} = e^{\left(\frac{h\Delta\nu}{kT}\right)}$$

that the intensity of the anti-Stokes Raman bands will be always less intense than their Stokes counterparts.

As in the previous case of vibrational infrared spectroscopy, quantum mechanics is used to determined the selection rules of the allowed transitions which may occur in Raman spectroscopy. Once again, we have to define a transition probability which is equal to the square of the magnitude of the transition moment. This time, the transition moment will depend on the induced dipole moment operator as shown below

Equation II.37

$$R_{v'v} = \int \Psi^*_{v'} \hat{\mu}_{ind} \Psi_v d\tau$$

Then, in considering the vibrational motion of a molecule with q, the normal co-ordinate of one of the vibrational modes, the transition moment defined in Equation II.37 can be written as

$$R_{v'v} = \left(\frac{d\underline{\underline{\alpha}}}{dq}\right)_o \vec{E} \int \Psi^*_{v'} q \Psi_v dq + \left(\frac{d^2\underline{\underline{\alpha}}}{dq^2}\right)_o \vec{E} \int \Psi^*_{v'} q^2 \Psi_v dq^2 + \ldots$$

Then, the transition moment $R_{v'v}$ is different from zero for

Equation II.38

$$\left(\frac{d\underline{\underline{\alpha}}}{dq}\right)_o \neq 0$$

and

Equation II.39

$$\int \Psi^*_{v'} q \Psi_v dq \neq 0$$

Equation II.38 implies a variation of the polarisability tensor with the normal mode of vibration. Equation II.39 implies the vibrational selection rule $\Delta v = \pm 1$ in the case of the harmonic oscillator. The intensity of a Raman transition is proportional to $(\nu_o - \nu)^4 N_v |R_{v'v}|^2$.

II.3.5.1 Low frequency Raman Longitudinal Acoustic Modes (L.A.M.).

A series of low frequency bands can be observed in the Raman spectra of hydrocarbon chain crystals and other polymers. The Raman frequency shift of these bands $\Delta\bar{\nu}$, was found to vary inversely with the chain length. Mizushima and Shimanouchi[52] have shown using a semi-empirical approach that the Raman frequency shift of these bands $\Delta\bar{\nu}$ was similar to the wavenumber $\bar{\nu}_m$ ($\bar{\nu}_m = \frac{\nu_m}{c}$ where ν_m is the frequency and c the light velocity) found using classical mechanics in the case of a string of spring-coupled masses undertaking small longitudinal displacements and defined by :

Equation II.40

$$\bar{\nu}_m = \frac{m}{2cL_r}\sqrt{\frac{E}{\rho}}$$

where E is the Young's elastic modulus, ρ is the density, m is the vibration order and L_r the length of the chain at equilibrium. Therefore, the Raman frequency shift of the first order of these L.A. modes corresponds to the wavenumber $\bar{\nu}_1$ of the first order of the symmetric, accordion-like motion of the zigzag carbon backbone of hydrocarbon chain crystals as shown in Figure II.16[53].

Figure II.16 : Longitudinal Acoustic accordion mode of an extended normal hydrocarbon chain.

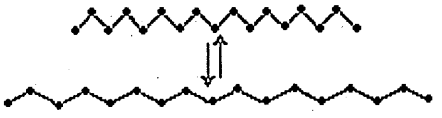

The length of the all-trans hydrocarbon chain L_r, can be determined from the Raman frequency shift of the first order of the L.A. mode present in the low frequency Raman spectra. This length can correspond also to the crystal lamellar thickness of the sample if the chains are perpendicular to the crystal surfaces. Equation II.40 is rewritten[54] in Equation II.41 as follows :

Equation II.41

$$L_r = \frac{3169}{\Delta\bar{\nu}}$$

Furthermore, good agreement was found[54,55] between the values of the lamellar crystal thickness determined by low frequency Raman spectroscopy and the average layer periodicities determined by S.A.X.S. measurements. Therefore, Raman spectroscopy is widely used for lamellar polymer characterisation and has the advantage over the S.A.X.S. technique in not needing highly regular lamellar stacking.

Nevertheless, the frequency of the first order of the L.A.M of a series of short chain n-alkanes was found to be sensitive to their crystal structure and therefore, to the packing of the methyl end groups as shown by Khoury et al.[56]. Furthermore, the frequency shifts between the first, second and higher orders of the L.A.M. were not observed to be a constant as indicated by Equation II.40. The effect of possible interlayer interactions on the L.A.M. was totally neglected in the simple classical model proposed by Mizushima and Shimanouchi[52]. Strobl and Eckel[57] developed Mizushima and Shimanouchi's model in order to include these weak interlamellar forces. They estimated that the Raman frequency shift of the L.A.M. for an hydrocarbon chain behaved as defined in Equation II.42 below :

Equation II.42

$$\bar{\nu}_m = \beta\frac{m\pi}{L} + \beta\frac{2f}{m\pi E}$$

with $\beta = \frac{1}{2\pi c}\sqrt{\frac{E}{\rho}}$ and where f stands for an elastic constant representing the total effect of the intermolecular forces.

Then, Snyder et al.[58] studying n-alkanes with up to 192 carbon atoms per chain determined that the interchain coupling force f, decreases in going to larger chains, contradicting the general view as stated by Strobl and Eckel[57] who considered f as a constant. This decrease in interchain interaction with increasing chain length is attributed to the increase in the layer separation for larger chains. Snyder et al.[57] transformed Equation II.42 in

$$\bar{\nu}_m = \beta\frac{m\pi}{L_r} + \beta\frac{4f_0}{m\pi E}\times\frac{1}{n}$$

assuming $f=f_0/n$ where n is the number of carbon atoms per chain.

II.3.6 Vibrations of polyatomic molecules and polymers.

In the case of a polyatomic molecule composed of N atoms, the 3N-6 vibrational degrees of freedom (3N-5 in the case of a linear molecule) can be represented by a set of collective atomic displacements known as normal modes. A normal mode of vibration is one in which all the atoms undergo harmonic motion, having the same frequency of oscillation and moving in phase. Group Theory is based on the determination of the symmetry operations of the molecule studied from which a punctual group of symmetry can be determined. Then, the number of vibrations of each symmetry species can be determined using the character table of the punctual group. Furthermore, character tables indicate the activity of each vibration in both Raman and Infrared. Because a polymer is formed by a repeat unit which may contain only a few atoms, the number of normal modes of vibration is much lower than the one determined by the formula 3N-5.

II.3.6.1 Calculation of methylene vibrational frequencies.

The determination of the vibrational frequencies of n-paraffins was resolved by Snyder and Schachtschneider[39,40], using normal co-ordinate calculation based on the Wilson G-matrix method from which a secular equation was solved. The accuracy of this method is based on the use of an appropriate force field. In order to assign the bands present in the vibrational spectra of several n-paraffins, Snyder and Schachtschneider[39] used the simple coupled oscillator model which can be used in the case of molecules with periodic structures. This model is based on a linear array of identical coupled oscillators (methylene groups) having one degree of freedom. From this model, they found that the frequency ν_k was a function of φ_k defined in Equation II.43 as the phase difference between adjacent oscillators.

Equation II.43

$$\varphi_k = \frac{k\pi}{m+1}$$

where m is the number of methylene groups in the chain and k=1,2,3...m.

Because all the bands assigned to k odd or k even belong to the same symmetry, selection rules for infrared or Raman activity can be based on the parity of k. The limiting cases where φ is equal to 0 or π defined the in phase or out of phase mode of a

particular vibration. The different methylene modes of vibration for polyethylene are shown in Table II.1 with their frequency and symmetry.

Table II.1 : Limiting methylene modes of vibration in polyethylene.

modes of vibration	φ (rad)	frequencies (cm^{-1})	symmetry species
methylene rocking-twisting	0	722	B_{2u}
	π	1063	A_u
methylene twisting-rocking	0	1295	B_{3g}
	π	1174	B_{1g}
methylene wagging	0	1170	B_{1u}
	π	1415	B_{2g}
C-C stretching	0	1133	A_g
	π	1065	B_{3g}
methylene bending	0	1440	A_g
	π	1475	B_{3u}

II.3.7 Dispersive and Fourier transform spectrometers.

Historically, spectrometers were first equipped with dispersive optical elements such as prisms or gratings. Within these infrared instruments, the incident radiation is split into two beams, the reference and sample beams. Then, the infrared radiation is dispersed and it passes through a slit system which isolates the frequency range falling on the detector. Therefore, the energy transmitted through a sample is obtained as a function of the frequency. Also, only a part of the total energy is falling on the detector at one time and the full frequency range of the spectrum is obtained sequentially. The most accurate low frequency Raman spectrometers are based on the principle of dispersive instruments. But, in order to be able to record spectra of Raman frequency shift down to 5 cm^{-1}, high quality optics including triple monochromators need to be used, preferably with a Charge-Coupled Device (C.C.D.) detector. The major problem is to separate the very intense laser line from the signal. A schematic diagram is shown in Figure II.17.

Figure II.17 : Schematic diagram of a dispersive Raman spectrometer.

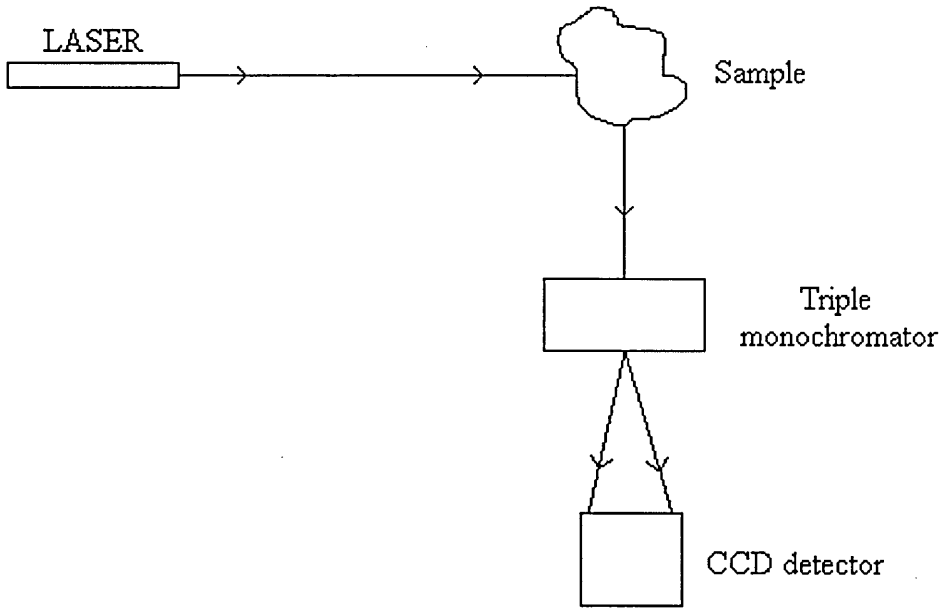

Fourier Transform Infra-Red (F.T.I.R.) spectrometers allow a continuous detection of all the transmitted energy simultaneously. They are based on the Michelson interferometer and became widely used with the discovery of the fast Fourier transform[59] algorithm and the development of powerful microcomputers. Within a Michelson interferometer, the incident infrared beam is first split into two beams. One of these infrared beams reaches a movable mirror. This provide a variable optical path between the two infrared beams. Then, these two beams are recombined so that the energy falling on the detector is obtained as a function of the optical path difference. A Michelson interferometer is schematically represented in Figure II.18.

Figure II.18 : Schematic diagram of a F.T.I.R. spectrometer based on the Michelson interferometer

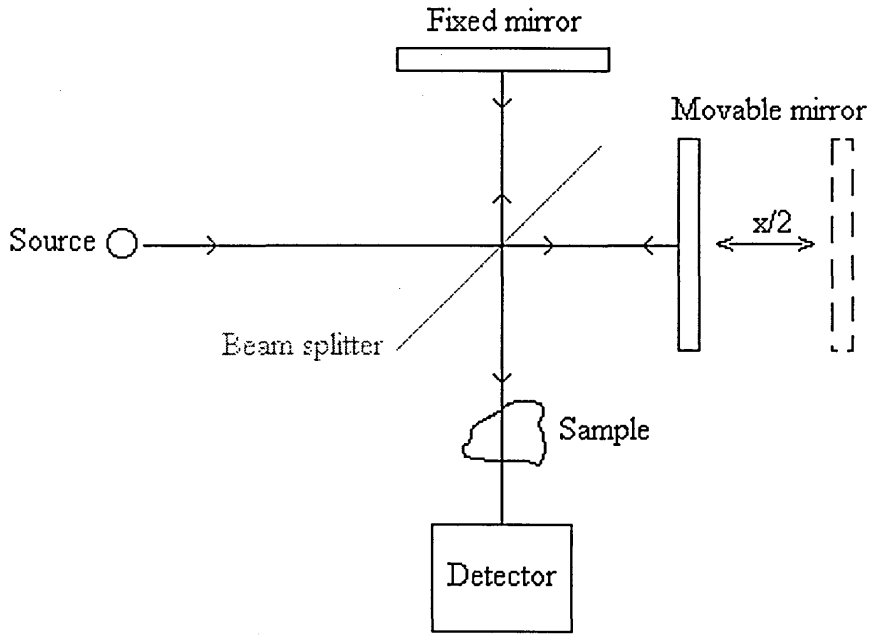

In the simplest case of a monochromatic infrared source of wavelength λ, destructive interferences will occur for path differences x, equal to an odd integral multiple of λ/2, and therefore the measured intensity of the recombined beams will be zero. On the other hand, maximum intensity will be detected in the case of path differences equal to integer multiple of λ. The intensity of the transmitted beam is defined as a function of the optical path difference x by

Equation II.44

$$I(x) = \frac{1}{2} I(\bar{\nu})\left[1 + \cos\left(2\pi\bar{\nu}x\right)\right]$$

where $\frac{1}{2}$ arises from the fact that half the radiation is assumed to be reflected back to the source by the beam splitter and $I(\bar{\nu})$ is the intensity of the monochromatic source.

In the case of a continuous polychromatic source, the intensity of the transmitted beam is defined by the following integral :

Equation II.45

$$I(x) = \frac{1}{2}\int_{-\infty}^{+\infty} I(\bar{\nu})\exp\left(i2\pi\bar{\nu}x\right)d\bar{\nu} = \frac{1}{2}\int_{-\infty}^{+\infty} I(\bar{\nu})\left[\cos\left(2\pi\bar{\nu}x\right) + i\sin\left(2\pi\bar{\nu}x\right)\right]d\bar{\nu} = F\left\{I(\bar{\nu})\right\}$$

where F{ } stands for "Fourier transform of".

The real part of Equation II.45 is referred as the interferogram. Additional factors such as detector response or beam splitter efficiency affect the amplitude of the interferogram. For this reason, the interferogram is defined as

$$I(x) = \int_{-\infty}^{+\infty} B(\bar{\nu}) \cos(2\pi \bar{\nu} x) d\bar{\nu}$$

where $B(\bar{\nu})$, the spectral density amplitude, takes into account the characteristics of the instrument. Also, the spectral density amplitude (i.e. the infrared spectrum) is determined by the inverse Fourier transform of the interferogram and, neglecting the imaginary part :

$$B(\bar{\nu}) = \int_{-\infty}^{+\infty} I(x) \cos(2\pi \bar{\nu} x) dx$$

Practically, the resolution of this last equation requires the digitalisation of the collected interferograms. The sampling interval is controlled using a second interferogram of a monochromatic source (He-Ne laser, λ=632.8nm). A third interferogram produced by a white light source allows the determination of the first collection point of the main interferogram. The sampling interval Δx, defines the highest wavenumber which may be studied following

$$\bar{\nu}_{max} = \frac{1}{2\Delta x}$$

In the case of He-Ne laser with a sampling every 632.8 nm, $\bar{\nu}_{max}$=7960 cm^{-1}. This maximum frequency is well above the frequency range used in our experiments. In order to calculate the Fourier transform, the interferogram must be integrated for minus to plus infinity. Because the data are collected only over the optical retardation of the mirror, the interferogram is truncated abruptly. Therefore, the interferogram is multiplied by an apodization function (triangular, Bessels or sinc functions) which reduces gradually to zero the wings of the interferogram.

In order to identify the position and area of infrared bands which may be overlapped in a spectrum, curve fitting and peak-narrowing methods can be used. Infrared and Raman peaks are known to be closely similar to Lorentzian line shape such as :

$$L(\bar{\nu}) = \frac{I_0\left(\frac{w}{2}\right)^2}{(\bar{\nu}-\bar{\nu}_0)^2+\left(\frac{w}{2}\right)^2}$$

where $\bar{\nu}_0$ is the wavenumber at the line centre, w is the width at half height and I_0 the peak maximum. If a region of an infrared or Raman spectrum corresponds to the overlapping of a known number of Lorentzian bands, then computer programs can be used to fit the spectrum in order to find the values of the centre, width at half heights and heights of these bands. Also, other lineshape bands can be used in a curve-fitting procedure such as the Gaussian form defined by :

$$G(\bar{\nu}) = I_0 \exp\left[\frac{-4(\bar{\nu}-\bar{\nu}_0)^2 \ln 2}{w^2}\right]$$

or combinations of Lorentzian and Gaussian lineshapes.

The number of peaks present in a spectrum can be estimated using the derivative technique and by deconvolution methods. An estimate can be made from the second derivative of the spectrum. The peaks present in the derivative spectrum are narrower than in the original one and therefore overlapping bands may be separated. The second method called deconvolution is a technique to narrow the peaks by determining their real lineshape. Fourier self-deconvolution is used to remove a contributing lineshape from a band profile which produces an apparent improvement of the resolution. It can be written mathematically as $E(\nu)=E'(\nu)*E_0(\nu)$

where $E(\nu)$ is the observed spectrum, $E_0(\nu)$ is the lineshape to be removed and $E'(\nu)$ is $I(x)=I'(x)*I_0(x)$ se Fourier transform of $E(\nu)$, we get

where I stands for interferogram. Therefore,

where I stands for interferogram. Therefore,

Equation II.46

$$I'(x) = \frac{I(x)}{I_0(x)}$$

where $I'(x)$ is the inverse Fourier transform of $E'(\nu)$. Due to an amplification of the noise in the desired spectrum $E'(\nu)$, an apodization function, $D(x)$ has to be used and Equation II.46 is rewritten as

$$I'(x) = \frac{I(x)D(x)}{I_o(x)} = \frac{I(x)D(x)}{F^{-1}\{E_o(\nu)\}}$$

and $E'(\nu)=F\{I'(x)\}$.

Finally, several advantages make the choice of an F.T.I.R. spectrometer preferable over the use of a dispersive instrument. The first advantage is known as Fellgett's advantage. All the spectral elements defined in Equation II.47 are measured simultaneously.

Equation II.47

$$N = \frac{\bar{\nu}_H - \bar{\nu}_L}{\Delta\bar{\nu}_R}$$

where N is the number of spectral elements, $\bar{\nu}_H$ and $\bar{\nu}_L$ are respectively the highest and lowest wavenumbers of the spectrum and $\Delta\bar{\nu}_R$ is the resolution.

The second advantage is known as the Jacquinot advantage and is related to the fact that the full energy throughput reaches the detector without attenuation due to slits or dispersive optical elements.

A third advantage of F.T.I.R. spectrometers over dispersive instruments is the Conne's advantage. It is related to the high accuracy of frequency measurement of the F.T.I.R. spectrometers due to the use of a laser frequency as internal standard.

Finally, within F.T.I.R. spectrometers the spectral resolution is constant as a function of the frequency.

III SHORT CHAIN N-ALKANE CRYSTALS : N-$C_{44}H_{90}$

III.1 Introduction.

Hydrocarbon chains are a basic component in a number of systems as diverse as polymers, biological membranes, fuels or lipids. The conformation of the hydrocarbon chain components is believed to play a leading part in most of the physical behaviour characterising these systems. A better understanding of the physical properties of n-alkane chains should provide a better understanding of these more complex systems. Furthermore, the shorter members of the n-alkane family which do not have the additional complication of chain folds should be the best starting point of such a study.

Short chain n-alkanes crystallise in thin lozenge shapes. Their most stable chain conformation is the all-trans conformation. The ends of the chains (methyl groups) are at the crystal surfaces. The chain axes are parallel to each other inside the same crystal layer. Their crystal structure depends on the number and on the odd or even number of carbon atoms per chain as well as the temperature. At low temperature, the subcell of the stable crystal structure for n-alkane chains with an odd number of carbon atoms is orthorhombic. In the case of n-alkane chains with an even number of carbon atoms lower than 26, the crystal subcell is triclinic. Above 26 carbon atoms, the crystal subcell is monoclinic[60].

The number of pre-melting phase transitions undergone by n-alkane crystals has been found to depend on this odd-even effect and on the chain length. Different kinds of rotational isomers identifiable by infrared spectroscopy can be used to follow these solid-solid phase transitions.

In this chapter, we report changes occurring in the infrared spectra of n-$C_{44}H_{90}$ crystals as functions of the temperature, pressure and crystallisation parameters. The crystal structures and the layer spacing have been determined by the means of Wide Angle X-ray Scattering and Small Angle X-ray Scattering measurements.

III.2 Background.

III.2.1 Methyl deformation modes in the infrared spectra of n-paraffins : H-C-H bending (symmetric U, asymmetric α), C-H stretching (symmetric r^+, asymmetric r^-) and rocking (β) modes.

With the aim of interpreting the infrared spectrum of polyethylene, Krimm et al.[61] used group theory in analysing the infrared spectra of several crystalline n-alkanes in different states. Also, they gave a review of the divergent assignments of the methylene wagging modes and, particularly, of the 1375 cm^{-1} band. They ascribed the 1375 cm^{-1} band present in the spectra of crystalline n-paraffins to the symmetric methyl bending mode. Nevertheless, an additional band at 1369 cm^{-1} (polarised in the a direction), more intense than the band at 1375 cm^{-1} (polarised in the b direction), is observed in the spectrum of a single crystal of n-$C_{36}H_{74}$ in monoclinic form. Moreover, no band was detected at 1375 cm^{-1} in the spectra of a series of even n-alkanes (n-$C_{18}H_{38}$, n-$C_{28}H_{58}$ and n-$C_{30}H_{62}$) but a single band was observed at 1369 cm^{-1}. In these spectra, they ascribed the band at 1369 cm^{-1} to a methylene wagging mode and try to correlate changes in the intensity of the 1375 cm^{-1} band with changes in crystal structure. They also reported the decrease of the intensity of the symmetric methyl bending mode on melting in the case of polyethylene[62]. Finally, they reported the seven fundamental modes of vibration assigned to the methyl groups : the symmetric and asymmetric C-H stretching modes were found at respectively 2872 cm^{-1} and 2962 cm^{-1}, the symmetric and asymmetric bending modes were found at respectively 1375 cm^{-1} and 1460 cm^{-1}, the out of plane rocking mode at 890 cm^{-1} and the in plane wagging mode at 1128 cm^{-1}. The methyl twisting mode was expected to be too weak to observed if not infrared inactive.

Novak and Solovev[63] reported the temperature dependence of the 1352 cm^{-1} and 1341 cm^{-1} infrared band intensities as related to the presence of rotational isomers in short chain n-alkanes. They determined differences in the energies of rotational isomers. Importantly, they pointed out the possible displacement of the methyl deformation band to the higher frequencies, from 1370 cm^{-1} to 1378 cm^{-1}, when going from crystalline to liquid short chain n-alkanes. They suggested that this may be explained by a change in the methyl environment.

Oetjen et al.[64] have determined the infrared spectra of n-octane in liquid and gas phases. From their work, the methyl deformation band may be assigned respectively at 1381

cm^{-1} and 1385 cm^{-1}. Hence, a progression appears with frequency increasing from solid to liquid and finally to gas phase.

Nielsen and Holland[65] ascribed, by means of a polarised infrared beam and a reflecting microscope, the symmetrical methyl deformation band at 1368 cm^{-1} and 1370 cm^{-1} (as well as the bands already known at 1378 cm^{-1} and 1374 cm^{-1}) respectively in the spectra of the crystalline n-$C_{36}H_{74}$ and n-$C_{46}H_{94}$ in monoclinic structures at room temperature. The two lowest frequency bands were found to be polarised perpendicular to the chain axis even though the two highest ones were found to be polarised partly perpendicular and partly parallel to the chain axis. They differentiated the infrared band at 1369 cm^{-1} in liquid short chain n-alkanes ascribed to a methylene wagging mode from the one in solid short chain n-alkanes ascribed to the symmetrical methyl deformation.

At the same time, Snyder[66] reported a list of absorption band frequencies for crystalline n-alkanes from the infrared spectra recorded at -180°C (from n-$C_{20}H_{42}$ to n-$C_{30}H_{62}$) mixed in potassium bromide pressed disks.

In the case of the n-alkanes with an even number of carbon atoms per chain, Snyder assigned the band between 1365 cm^{-1} and 1368 cm^{-1} to the symmetric methyl bending mode. Two additional bands near 1373 cm^{-1} and 1385 cm^{-1} are present in all their spectra. In the spectra of the triclinic crystal structure, the out of plane methyl rocking mode is assigned to a single band near 893 cm^{-1}. In the monoclinic crystal structure, this mode is ascribed to a doublet at 889 cm^{-1} and 893 cm^{-1}.

In the case of the n-alkanes with an odd number of carbon atoms per chain and, therefore, in an orthorhombic crystal structure, the author ascribed the band found between 1373 cm^{-1} and 1376 cm^{-1} to the symmetric methyl bending mode. Two additional bands near 1367 cm^{-1} and 1385 cm^{-1} are present in all their spectra. A doublet at 891 cm^{-1} and 894 cm^{-1} is ascribed to the out of plane methyl rocking mode. In all the n-alkane spectra, from n-$C_{20}H_{42}$ to n-$C_{30}H_{62}$, the asymmetric methyl bending mode is assigned at 1465 cm^{-1}.

In the second part of this paper published in 1961, Snyder[67] studied the splitting of infrared bands caused by intermolecular interactions in the orthorhombic, monoclinic and triclinic n-alkane crystal structures.

In a following paper Snyder and Schachtschneider[39] extended their work by an infrared study of shorter chain n-alkanes, from n-C_3H_8 to n-$C_{19}H_{40}$ (n-alkane vapour deposited on a cooled CsBr window and warmed up). For n-alkanes with a chain length down to 11 carbon atoms, the assignment of the out of plane methyl rocking mode is identical to the one of the earlier paper[67]. On the other hand, the authors reported their difficulty in assigning a " characteristic frequency" for the methyl symmetric mode usually ascribed at 1375 cm^{-1}. They proposed a frequency range between 1360 cm^{-1} and 1380 cm^{-1} where the methyl symmetric bending mode and the methylene wagging mode are coupled. Furthermore, they no longer assign the asymmetric methyl bending mode to a single band at 1465 cm^{-1}, but proposed a spectral range between 1440 cm^{-1} and 1468 cm^{-1} where this mode is coupled with the methylene bending mode.

Using a polarised infrared beam and a reflecting microscope, Holland and Nielsen[68] revealed or confirmed the assignment of different infrared bands present in the spectra of even n-alkanes in different crystal structures. For any even or odd n-alkane crystals in an orthorhombic structure, they assigned the single band at 1378 cm^{-1} to the symmetric methyl deformation mode. Furthermore, in the case of n-$C_{24}H_{50}$ in the orthorhombic crystal structure, they assigned the band at 887 cm^{-1} to the in-plane methyl rocking mode.

In the spectra of n-$C_{36}H_{74}$ in a monoclinic crystal structure, they ascribed the bands at 1368 and 1378 cm^{-1} to the in- and out-of-phase symmetrical deformation mode of adjacent methyl groups. A band at 890 cm^{-1} was ascribed to the in-plane rocking methyl mode. Two bands at 1447 cm^{-1} and 1457 cm^{-1} were ascribed with uncertainty to the asymmetric methyl deformation mode. Because the infrared spectra had been recorded at room temperature, the splitting of the methyl rocking mode was too small to be observed.

Finally, in the spectra of n-$C_{18}H_{38}$ in a triclinic crystal structure, a single band at 1368 cm^{-1} was assigned to the symmetrical methyl deformation. A band at 890 cm^{-1} was ascribed to the in-plane rocking methyl mode. Two bands at 1453 cm^{-1} and 1466 cm^{-1} were ascribed respectively to the out-of-plane and in-plane asymmetric methyl deformation mode.

Kobayashi et al.[69] identified a different orthorhombic form in n-$C_{36}H_{74}$ crystals, which they called orthorhombic II. This form was differentiated from the usual orthorhombic form (called orthorhombic I) and the monoclinic form by means of vibrational spectroscopy and X-ray diffraction. Indeed, they reported differences in the band frequencies characteristic of the methyl group vibration modes in the infrared spectra and of the longitudinal acoustic (L.A.) mode in the low frequency Raman spectra. These differences characterise the non equivalence of the interlayer stacking in all these structures.

In a monoclinic crystal structure, two bands at 1374 cm^{-1} and 1372 cm^{-1} were ascribed to the methyl symmetric bending modes respectively polarised in the a and b directions. In an orthorhombic II crystal structure, two bands at 1382 cm^{-1} and 1370 cm^{-1} were ascribed to the methyl deformation modes respectively polarised in the a and b directions. In the orthorhombic I form , a single band at 1376 cm^{-1} was ascribed to the overlapped a and b polarised bands.

The methyl C-H stretching region of infrared spectra of crystalline n-alkanes has been studied by MacPhail et al.[70,71] in the early eighties. They reported splittings and frequency changes in the infrared spectra due to temperature effects, methyl environments or phase transitions. They ascribed the in-plane and out-of-plane asymmetric stretching modes to respectively the 2962 cm^{-1} and 2952 cm^{-1} bands and the methyl symmetric stretching mode to 2870 cm^{-1}.

III.2.2 Carbon-carbon stretching modes and methylene deformation modes (rocking-twisting, twisting-rocking, wagging, bending and C-H stretching modes) in the infrared spectra of n-paraffins.

In crystalline n-paraffins, the frequencies at which the C-C stretching and the methylene rocking, twisting, wagging and bending modes occur are confined to quite well defined regions of the infrared spectra : respectively between 950 cm^{-1} and 1150 cm^{-1}, 720 cm^{-1} and 1050 cm^{-1}, 1170 cm^{-1} and 1300 cm^{-1}, 1175 cm^{-1} and 1415 cm^{-1} and finally around 1470 cm^{-1}. Most of these modes are non-localised and give rise to band progressions. Each mode of these progressions is characterised by a relative phase difference between the motion of adjacent methylene groups composing the n-alkane molecule. This phase difference is proportional to an integer, k. In the case of the methylene rocking mode for

example, and considering an n-alkane chain in an all-trans conformation, the infrared active vibrations are ascribed to any members of this mode characterised by an odd integer k. The strongest infrared band of the methylene rocking mode is the one near 725 cm^{-1} characterised by k=1, and where the adjacent methylene groups vibrate all approximately in phase. The frequencies of these progression bands are also related to the number of methylene groups composing the n-alkane molecules. Therefore, the length of the chains in the all-trans conformation within an n-alkane crystal can be estimated knowing the frequency of each progression band and the integer, k, characteristic of each one of these bands. Of particular interest over the years has been the study of the splitting of the 725 cm^{-1} band and other members of the progression which have been found to be sensitive to intermolecular effects and crystal structures[66,72]. Thus, among a series of n-alkanes from n-C_3H_8 to n-$C_{30}H_{62}$, Snyder[72] studied with more attention the behaviour of the splitting of these band progressions in the case of samples in monoclinic, orthorhombic and triclinic crystal structures. Apart from the triclinic form, splitting was observed. Also, in a series from n-$C_{20}H_{42}$ to n-$C_{30}H_{62}$ in orthorhombic form, a decrease of the splitting of these bands occurs from the doublet k=1 toward higher frequencies, up to a limit after which this splitting finally increases towards higher frequencies. Differences in the splitting behaviour of these rocking modes have also been noticed in n-alkanes in orthorhombic and monoclinic forms[39]. Thus, the study of these band progressions could be useful in identifying the structure of crystalline n-paraffins. Moreover, the study of the methylene mode region can be helpful for the detection of gauche conformers within the n-alkane chains. Indeed, the presence of the even members of the band progressions in the infrared spectra of n-alkanes has been associated with gauche conformers, more probably concentrated at the end of the chains.

The behaviour of the splitting of the band progressions related to the methylene twisting modes present between 1170 cm^{-1} and 1300 cm^{-1} has been analysed too[40]. But, due to the weaker intensity of these bands, their study is more difficult.

The methylene bending modes have been ascribed to two components at around 1475 cm^{-1} and 1462 cm^{-1} for n-$C_{23}H_{48}$ and n-$C_{29}H_{60}$ in the orthorhombic form and n-$C_{28}H_{58}$ in the monoclinic form[40]. Instead of these, a single band at 1474 cm^{-1} was observed in the

infrared spectrum of n-$C_{24}H_{50}$ in triclinic form[67]. These values are in good agreement with the ones found by Holland and Nielsen[68].

Snyder[37] wrote in 1967 a fundamental publication on which most of the conformational studies using infrared spectroscopy on hydrocarbon chain compounds are based. He reported a full interpretation of most of the infrared bands present in the spectra of n-paraffins between 700 cm^{-1} to 1500 cm^{-1}. This interpretation is based on the identification of localised modes of vibration in the shortest chains of the n-alkane family in the liquid state linked with some specific conformations of these chains. The presence of these localised modes of vibration in the spectra of the longest chains of n-alkanes allows one to determine the conformation of some segments of these chains. In particular, Snyder ascribed in the limited wagging mode region between 1400 cm^{-1} and 1300 cm^{-1} the bands at 1368 cm^{-1} and 1308 cm^{-1} to sequences involving gtg and gtg' conformations, a band at 1352 cm^{-1} to a sequence involving gg conformations and a band at 1344 cm^{-1} to end gauche conformations. These will be used intensively in future chapters of this thesis.

Also, in the rocking-twisting mode region of the infrared spectra, bands at around 878 cm^{-1} and 960 cm^{-1} were assigned to vibrations involving -CH_2-CH_3 groups in a -t-g conformation. Additional bands at around 1078 cm^{-1} and 1164 cm^{-1} were ascribed to end gauche conformers[38].

Finally, in a study on crystalline n-paraffins from n-$C_{16}H_{34}$ to n-$C_{22}H_{26}$ in the all trans chain conformation Snyder et al.[71] ascribed the anti-symmetric, symmetric fundamental and symmetric Fermi resonance methylene C-H stretching modes for the planar carbon skeleton to the bands at 2915 cm^{-1}, 2846 cm^{-1} and 2890 cm^{-1} respectively. The symmetric C-H stretching mode involving the terminal methylene group has been ascribed to a band at 2859 cm^{-1}. The anti-symmetric and symmetric Fermi resonance methylene C-H stretching modes have been found to be sensitive to crystal structure. Indeed, these two bands have shifted towards higher frequencies, respectively by 1 cm^{-1} and 4 cm^{-1}, from the spectrum of n-$C_{20}H_{42}$ in triclinic form to the spectrum of n-$C_{21}H_{44}$ in orthorhombic form. Unfortunately, the saturation of the intensity of these infrared bands in the spectra shown in this work did not allow us to study with confidence this methylene stretching region.

III.2.3 Structural studies.

Rånby et al.[73] used electron microscopy and small angle X-ray scattering to study n-$C_{44}H_{90}$, n-$C_{82}H_{166}$ and polyethylene crystallised from solution in different solvents and at different crystallisation temperatures. They reported the long spacing of n-$C_{44}H_{90}$ crystallised from C_2Cl_4 and n-butyl acetate respectively at 18°C and 35°C to be equal to 58.3 Å. The calculated chain length for n-$C_{44}H_{90}$ was 58.13 Å. The crystal structure was considered to be the $Pca2_1$ orthorhombic form.

Later, Nyburg and Potworowski[74] reported the four "key" crystal structures based on the triclinic n-$C_{18}H_{38}$, monoclinic n-$C_{36}H_{74}$, orthorhombic n-$C_{36}H_{74}$ and orthorhombic n-$C_{23}H_{48}$ which can be used as structural patterns to predict the crystal structure of any n-alkanes.

Boistelle et al.[75] reported a new orthorhombic crystal structure, space group Pbca with Z=4, being a polytypic modification of the monoclinic structure of n-$C_{28}H_{58}$ and n-$C_{36}H_{74}$ crystallised at room temperature from light petroleum solutions. This new orthorhombic structure was reported to be a stacking of monoclinic layers, each following one being the image of the other through a rotation about a twofold axis perpendicular to the (001) plane. In each layer, n-alkane chains are inclined from the normal to (001) plane with an angle of nearly 30°. In the monoclinic and new orthorhombic crystal structures, the stacking of the terminal CH_2 and CH_3 groups were reported to be closely similar.

Craig et al.[76] have used high resolution synchrotron X-ray powder diffraction on the series $C_{13}H_{28}$-$C_{60}H_{122}$. Of particular interest here, they reported the unit-cell parameters for n-$C_{44}H_{90}$ in the orthorhombic Pbca structure, which involves two layers in monoclinic $P2_1/a$ form related by a twofold rotation about their c-axis. This structure is differentiable from the orthorhombic $Pca2_1$ form by its shorter c-axis length due to the tilting of the chains.

Ishikawa et al.[77] studied the structure of n-$C_{19}H_{40}$, n-$C_{24}H_{50}$, n-$C_{32}H_{66}$ and n-$C_{44}H_{90}$ crystals by means of variable temperature solid-state high resolution ^{13}C NMR spectroscopy. They reported the ^{13}C chemical shift values of the internal CH_2 groups and terminal CH_2 and CH_3 groups for these n-alkanes as functions of the temperature and

crystal structures. In particular, they found a gradual decrease towards the chain ends of the ^{13}C chemical shift differences between the internal CH_2, terminal CH_2 and CH_3 group peaks of the orthorhombic and triclinic n-alkane forms. In the case of n-$C_{44}H_{90}$, a transition to an "intermediate" phase was found at 70^0C, the sample being originally in an orthorhombic crystal structure. This transition was characterised by a shift upfield of the terminal CH_2 and CH_3 group peaks. By contrast, the ^{13}C chemical shift of the internal CH_2 group is unchanged.

III.3 Experimental section.

III.3.1 X-ray Scattering.

Small and wide angle x-ray scattering (S.A.X.S. and W.A.X.S.) patterns from powder samples were recorded with an image plate area detector (MarResearch) using graphite-monochromatised CuKα radiation. Dr Goran Ungar and Mr Xiangbing Zeng did the measurements at Sheffield University. Samples in capillaries were held in a custom-built temperature cell controlled to within 0.1^0C. The beampath up to the beamstop was flushed with N_2.

III.3.2 Differential Scanning Calorimetry.

We used a Mettler Differential Scanning Calorimeter 30 equipped with a low temperature cell and coupled to a Mettler-Toledo TA8000 thermal analysis system. We used 40 µl aluminium crucibles (ME-27331) to carry out the experiments. The heating rate used during the experiment was 2^0C per minute.

III.3.3 F.T.I.R.

Transmission infrared spectra were recorded between 700 cm^{-1} and 4000 cm^{-1} with 1 cm^{-1} resolution and typically 200 scans using a Mattson instrument 6020 F.T.I.R. spectrometer based on a Michelson interferometer equipped with a cooled pyroelectric detector doped with mercury cadmium telluride. One of the advantages of Fourier Transform spectrometers over dispersive instruments is the accuracy of the control of

the wavelength. Thus, confident subtractions between spectra can be performed using Fourier Transform spectrometers.

Samples held between two potassium bromide plates were installed in a Graseby/Specac cryostat P/N21500 equipped with a heating cell, a temperature controller P/N20120 and a vacuum pump to evacuate the cryostat allowing us to work in a temperature range between -173^{0}C and 90^{0}C at $^+/_-$ 1^{0}C. We had to calibrate the Graseby/Specac temperature controller P/N20120 of the heating cell. This calibration was done in the real experimental conditions. The cell was cooled down to -173^{0}C and heated successively from this temperature to four higher ones at 120^{0}C, 126^{0}C, 135^{0}C and 144^{0}C. To verify the accuracy of the temperature controller P/N20120, a thermocouple was placed between the KBr plates, at the sample position, with a thermally conducting gel to improve the contact with the thermocouple. We used a nickel-chromium and nickel-aluminium thermocouple. This thermocouple was plugged into a temperature controller Fluka 51. We were able to determine from the temperature calibration that ninety minutes were needed in such a process to reach an equilibrium temperature. The graphs below show the temperature at the sample position determined by the temperature controller Fluka 51 as a function of time for the different temperatures given by the temperature controller P/N20120.

Figure III.19 : Temperature at the sample position as a function of time for a chosen temperature fixed at 120°C on the temperature controller P/N20120.

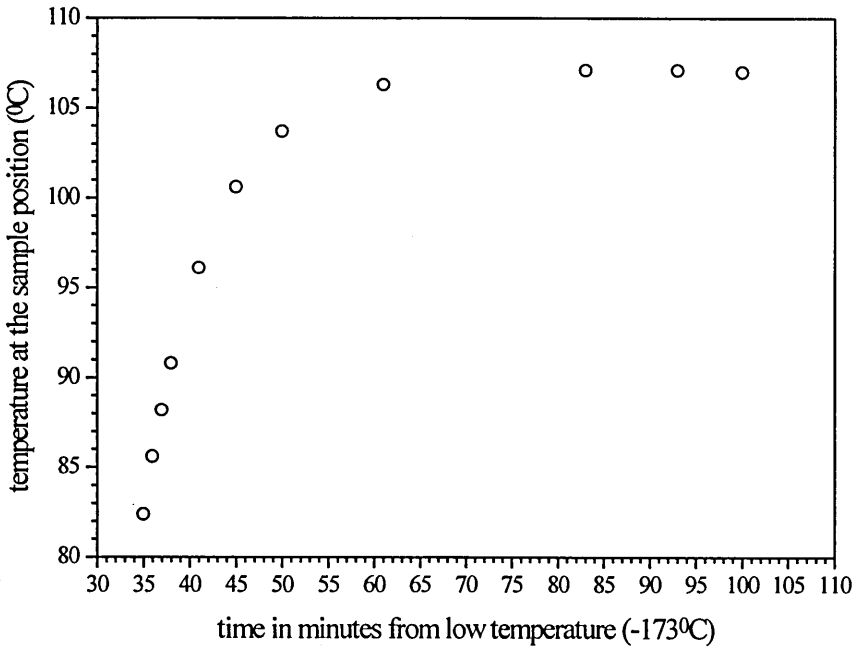

Figure III.20 : Temperature at the sample position as a function of time for a chosen temperature fixed at 126°C on the temperature controller P/N20120.

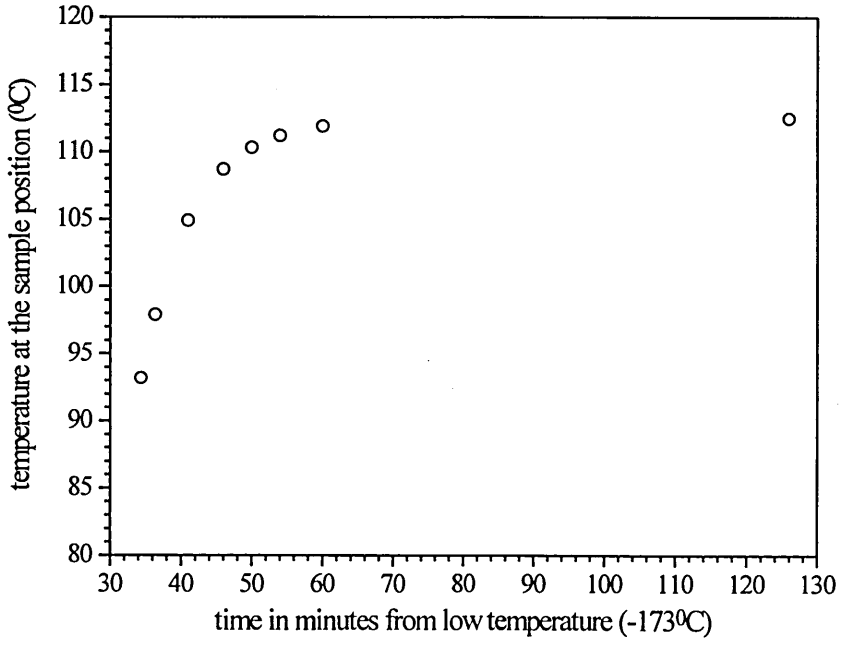

Figure III.21 : Temperature at the sample position as a function of time for a chosen temperature fixed at 135^{0}C on the temperature controller P/N20120.

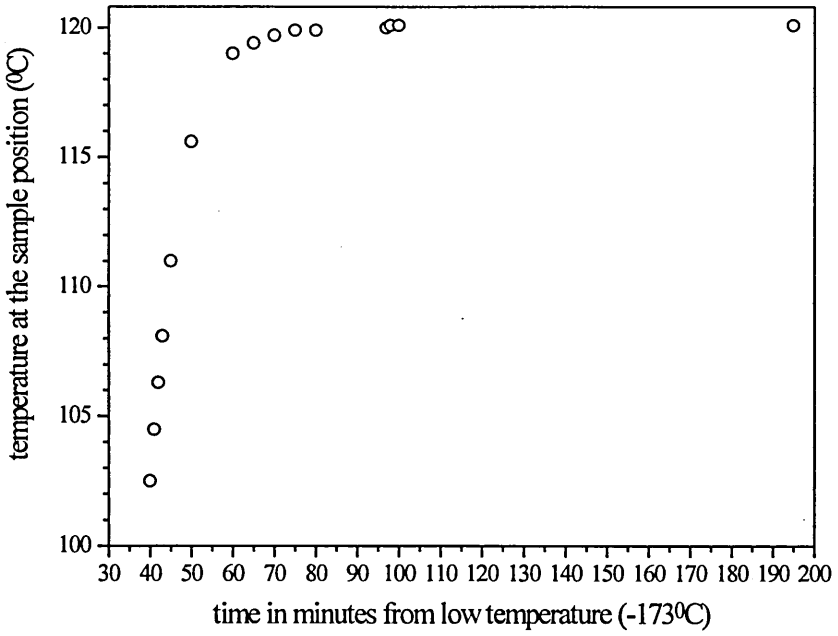

Figure III.22 : Temperature at the sample position as a function of time for a chosen temperature fixed at 144^{0}C on the temperature controller P/N20120.

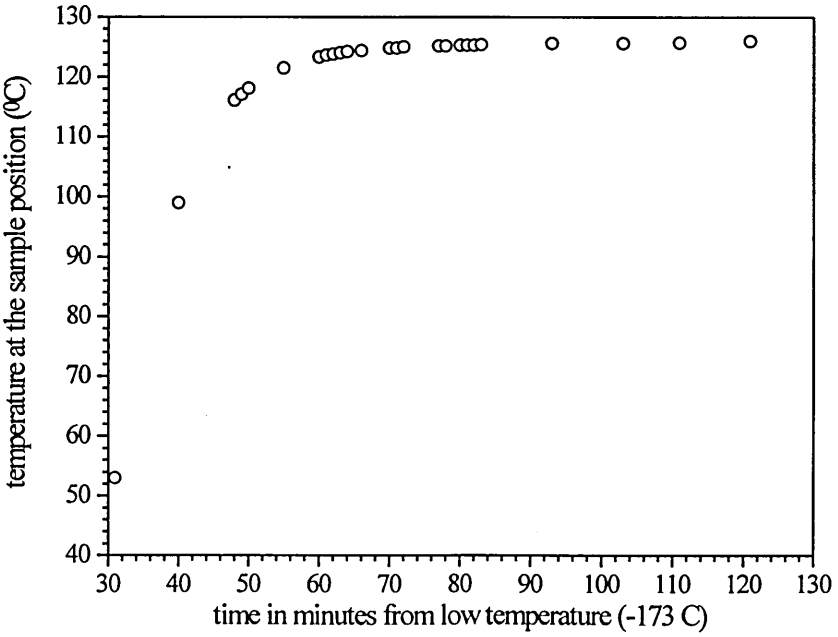

We used these four curves to plot in Figure III.23 the temperature reached at the sample position ninety minutes after the beginning of the heating as a function of the temperatures given by the temperature controller P/N20120.

Figure III.23 : Temperature at the sample position as a function of the temperature given by the temperature controller P/N20120.

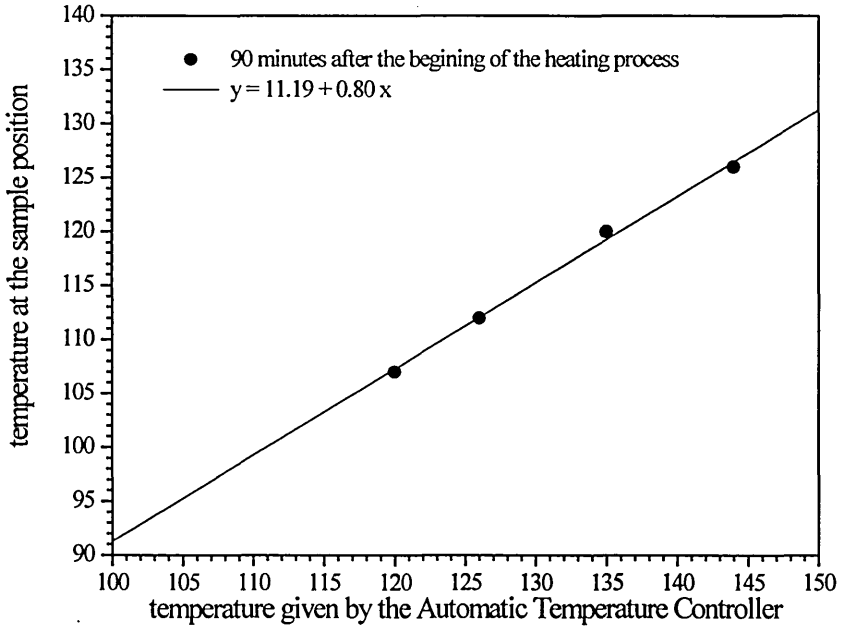

In this thesis, this calibration curve has been used to estimate the temperature reached by the samples for the different temperatures chosen on the temperature controller P/N20120.

By increasing the annealing temperature, we should be able to observe the different phase transitions occurring inside n-$C_{44}H_{90}$ crystals. Then, by cooling them down to -173°C between each elevated temperature, we minimise the thermal population of non all-trans conformers contributing to the methylene wagging modes. The cooling and heating rate were fixed at 10°C/minute. By increasing the temperature, it is possible to observe, by means of infrared spectroscopy, changes in the kind and in the concentration of rotational isomers which accompany phase transitions and changes in the thermal population of crystallographic defects present in the n-$C_{44}H_{90}$ crystals. Theoretically, for samples at the same low temperature, a similar crystallographic defect concentration is expected. So, we can consider differences in the infrared spectra

recorded at -173^{0}C as due almost exclusively to changes in structure rather than the thermal population of rotational isomers present in the crystals. Finally, in this study the infrared spectra are shown without normalisation. In all the cases, the thickness of the compared samples was believed to be a constant through the experiments performed. Indeed, the temperature range used here to observe the phase transitions occurring in n-$C_{44}H_{90}$ crystals is believed to be narrow enough to prevent any major changes in the volume of the sample holders (KBr plates and metal cylinder) and in the density of the samples.

III.3.4 Low frequency Raman Spectrometer.

Raman measurements on a Jobin-Yvon T6400 spectrometer were made by Dr. N. A. Tuan (Jobin-Yvon, Paris). The spectrometer was equipped with a CCD detector. Low frequency Raman spectra were recorded using 2 cm^{-1} resolution.

III.3.5 Samples.

The n-tetratetracontane, n-$C_{44}H_{90}$, sample was purchased from the Aldrich Chemical company. Its purity was 99%. Toluene Aristar quality grade was used for crystallisation. Samples were prepared by crystallisation in solution following four different procedures.

Samples A were prepared by crystallisation of n-$C_{44}H_{90}$ in toluene using different cooling rates and concentrations. The solution and the suspension obtained were filtered at room temperature and the solid was allowed to sediment to form a mat. This mat was left to dry at room temperature and atmospheric pressure for at least 48 hours. The sample was used as it was, lightly pressed (pressure applied over the sample surface lower than 0.4 ton per cm^2) or heavily pressed (pressure applied over the sample surface between 0.8 and 1.2 ton per cm^2) as necessary and installed between two KBr plates inside the sample holder.

Samples B were prepared by crystallisation of n-$C_{44}H_{90}$ in toluene using different cooling rates. Crystals in suspension were dropped onto a KBr plate using a pipette.

After the evaporation of the toluene, a second KBr plate was deposited on the first one and the assembly was installed inside the sample holder.

Samples C were prepared by dissolving n-$C_{44}H_{90}$ in toluene and by depositing a droplet of this clear solution onto a KBr plate at room temperature. After evaporation of the toluene, a second KBr plate was deposited on the first one and the assembly was installed inside the sample holder.

Samples D were prepared by dissolving n-$C_{44}H_{90}$ in toluene and by dropping this clear solution on a filter paper at room temperature. After crystallisation on the filter paper the solid was allowed to sediment to form a mat. This mat was left to dry at room temperature and atmospheric pressure for at least 48 hours. This mat was lightly pressed (pressure applied over the sample surface lower than 0.4 ton per cm^2) and installed between two KBr plates inside the sample holder.

III.4 Results.

III.4.1 X-ray scattering results.

All the x-ray scattering measurements have been done in the Department of Engineering Materials, University of Sheffield by Mr X. Zeng. The same samples were used to carry out the infrared experiments.

III.4.1.1 **Sample A1 : 1.3% solution, crystallised at 25°C, lightly pressed.**

This sample was studied by S.A.X.S. at several elevated temperatures : 25°C, 47°C, 63°C, 71°C, 79°C and 83°C. Up to 71°C, a strong diffraction pattern peak was found corresponding to a long spacing of 52.0 Å and a weak one corresponding to a long spacing of 58.0 Å. Crystals are essentially in a monoclinic {011} structure with some trace of orthorhombic I form. After heating up to 79°C or higher, the long spacing was 55.0 Å, which indicated a pure monoclinic {101} structure.

III.4.1.2 Sample A2 : 1.3% solution, crystallised at 25°C, heavily pressed.

Measurements were done at room temperature. At low angles, the diffraction pattern peak was very weak. At wide angles, the diffraction pattern was found similar to a triclinic form structure with some trace of monoclinic {011} form.

III.4.1.3 Sample A1 cooled down from the melt at 2°C per hour.

This sample was studied by S.A.X.S. at several elevated temperatures : 48°C, 71°C and 79°C. Up to 71°C, the diffraction pattern peak was found to correspond to a long spacing of 57-58 Å. Crystals are essentially in orthorhombic I form. Heating up to 79°C, corresponding long spacing was 56.0 Å. This value is believed to be characteristic of a tilted orthorhombic I form. After 30 minutes at 79°C, the long spacing was 55.0 Å which indicated a pure monoclinic {101} structure.

III.4.1.4 Sample A3 : 0.45% in solution, crystallised at 25°C, mat not pressed at all.

Measurements were done at room temperature. Two diffraction pattern peaks were found corresponding to long spacings of 51.5 Å and of 58.0 Å. Crystals are in the monoclinic {011} and orthorhombic I forms.

III.4.1.5 Sample A3 : 0.45% in solution, crystallised at 25°C, mat lightly pressed.

Measurements were done at room temperature. At low angles, two diffraction peaks were found corresponding to long spacing of 52.0 Å and of 58.0 Å. Crystals are in monoclinic {011} and orthorhombic I forms. But, at wide angles, the diffraction pattern was found to correspond approximately to a triclinic structure.

III.4.2 D.S.C. results.

III.4.2.1 Sample A1 : 1.3% solution, crystallised at 25°C, lightly pressed.

A phase transition was observed from S.A.X.S. measurements between 71°C and 79°C on sample (A1). This transition occurs between the monoclinic {011} form (long

spacing 52.8Å) and the monoclinic {101} form (long spacing 55Å). A D.S.C. experiment was carried out on a sample originally in a monoclinic {011} form.

Figure III.24 : Thermogram of sample A1, heating rate used $2^0C.min^{-1}$

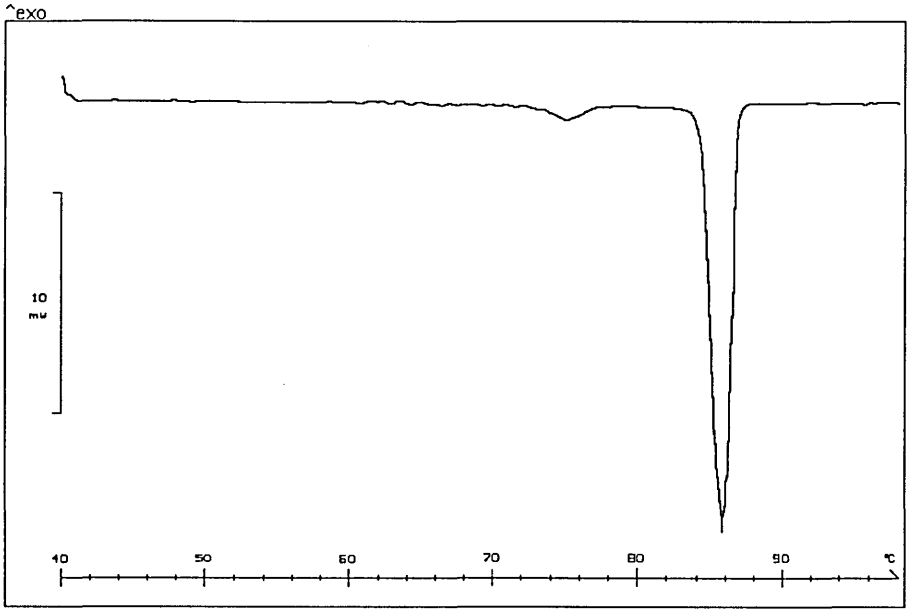

The thermogram of this experiment is shown in Figure III.24. An endotherm is observed at 75^0C which is believed to be the temperature at which the phase transition between {011} and {101} monoclinic crystal forms occurs. A larger endotherm follows at 85^0C which is the melting temperature of the {101} monoclinic crystal form.

III.4.2.2 **Sample D : 1.3% solution, lightly pressed.**

Figure III.25 : Thermogram of sample D, heating rate used $2^0C.min^{-1}$

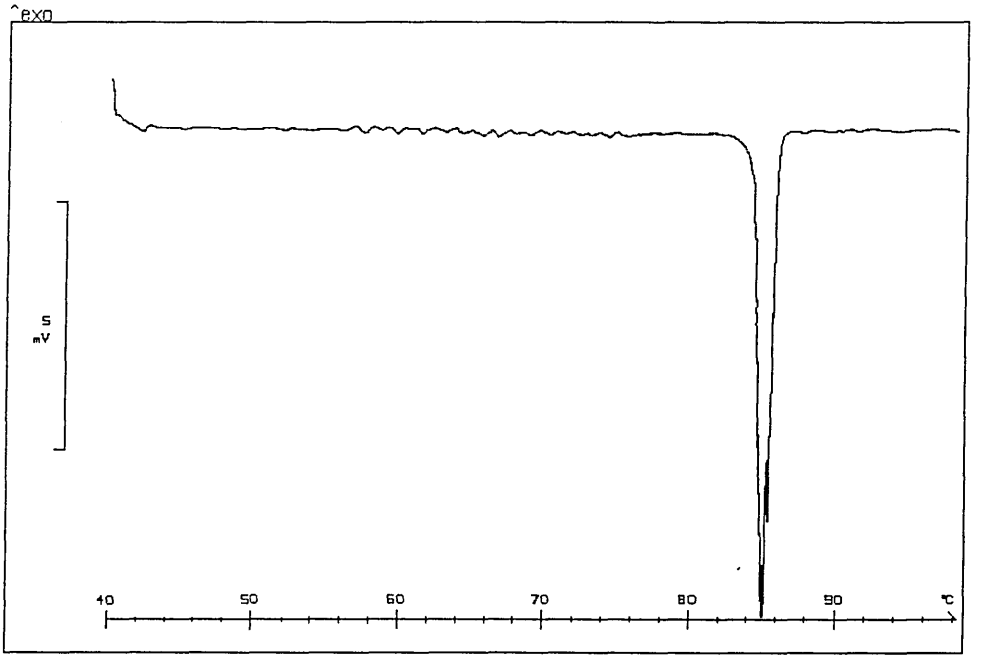

In the thermogram shown in Figure III.25, no endotherm is detected below 80^0C. Nevertheless, a strong endotherm with two maxima at 84.5^0C and 85^0C is observed. From these observations, we can conclude that sample D was not originally in a monoclinic {011} crystal form. Nevertheless, the presence of the two maxima in the thermogram indicates the melting temperatures of crystals in two different structures.

III.4.3 Infrared and Raman Spectroscopy results.

III.4.3.1 Sample A1 : 1.3% solution, crystallised at 25°C, lightly pressed.

III.4.3.1.a High temperature infrared spectra.

III.4.3.1.a.1 Wagging mode region.

Figure III.26 : F.T.I.R. spectra of sample A1 as a function of the temperature, after baseline subtraction

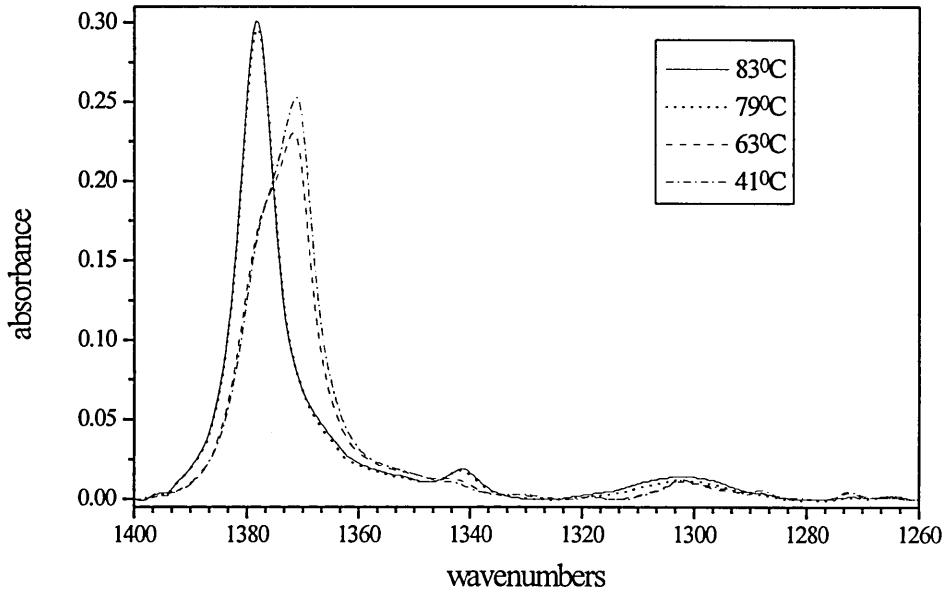

Figure III.26 shows the wagging mode region of the infrared spectra recorded at 41°C, 63°C, 79°C and 83°C. This region of the infrared spectrum is the fingerprint of specific nonplanar alkane chain conformations. It is remarkable to see how low the absorbance is in this region. It is characteristic of a primarily all-trans chain conformation.

Increasing the temperature from 63°C to 79°C, the strongest band, ascribed to the methyl symmetric bending mode, is shifted to higher frequencies, from 1372 cm^{-1} to 1378 cm^{-1}. Also, it is important to notice the increase of the intensity of the 1342 cm^{-1} band assigned to the end gauche defect modes. In the spectra recorded at the two lowest temperatures, a shoulder at 1378 cm^{-1} is present.

Second derivatives, deconvolutions and curve fitting procedures have been used to determine more accurately the frequencies and areas of the different bands present in the spectra. In all the cases, we tried to use the minimum number of bands to perform the curve fitting procedures. The result of this work is shown in Table III.2.

Table III.2 : Curve fitting results obtained from the infrared spectra of sample A1 recorded at elevated temperatures

T=41°C		T=63°C		T=79°C		T=83°C	
cm^{-1}	area	cm^{-1}	area	cm^{-1}	area	cm^{-1}	area
1384.8	0.22	1384.3	0.25666	1386.1	0.30461	1386.1	0.305
1377.5	**1.269**	**1377.5**	**1.312**	**1378.2**	**2.267**	**1378.2**	**2.300**
1371.2	**1.431**	**1371.3**	**1.201**	**1370.7**	**0.347**	**1370.6**	**0.324**
1365.4	**0.570**	**1365.4**	**0.536**	**1365.4**	**0.209**	**1365.4**	**0.243**
1355.5	0.121	1355.5	0.116	1358.8	0.144	1358.8	0.151
1349.2	0.080	1349.2	0.084	1351.3	0.083	1351.3	0.090
1342.6	**0.049**	**1342.6**	**0.070**	**1341.7**	**0.150**	**1341.6**	**0.163**

In Figure III.27, the scaled areas of the major bands (maximum value arbitrarily fixed to one) are drawn versus the temperature. The lines connecting the points are drawn only for clarification of the trends.

Figure III.27 : Scaled areas of the major infrared bands as a function of the temperature

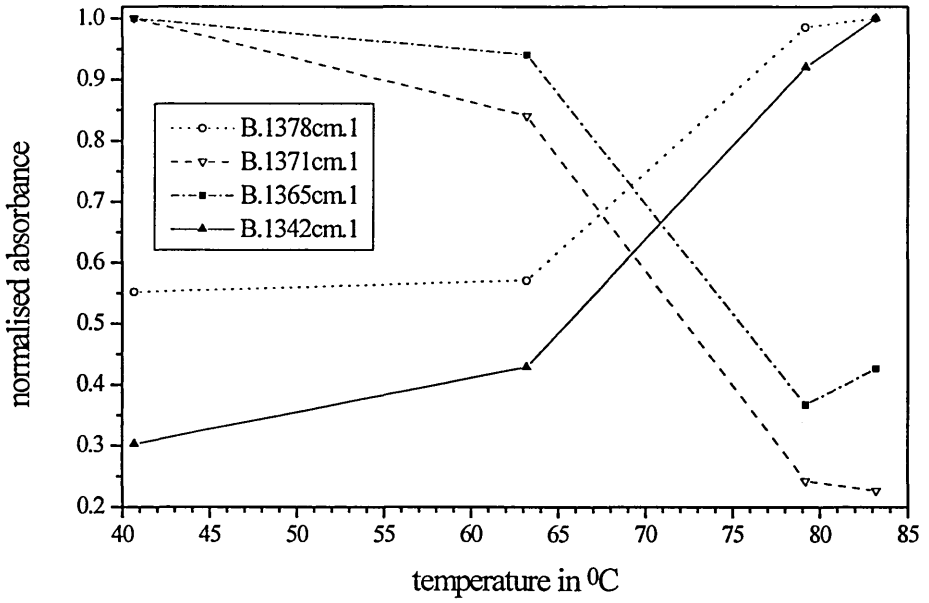

The absorbance of the 1378 cm^{-1} band has increased by a factor of two while the absorbances of the 1365 cm^{-1} and 1371 cm^{-1} bands have decreased by more than a factor of three.

From Small Angle X-ray scattering measurements made at room temperature on the sample heated first to 63°C and then to 79°C, we determined the average layer periodicity of the crystals. For the first sample, a strong diffraction pattern peak was found corresponding to a long spacing of 52.0 Å and a weak one corresponding to a long spacing of 58.0 Å. So, the crystals are essentially in a monoclinic {011} structure with some trace of orthorhombic I form. For the second sample, previously heated up to 79°C, the long spacing was 55.0 Å, which indicated a pure monoclinic {101} structure.

The observed frequency shift of the band assigned to the methyl symmetric bending mode from 1371 cm^{-1} to 1378 cm^{-1} for the sample annealed from 63°C to 79°C is the fingerprint of a premelting phase transition occurring between the two different monoclinic forms. This phase transition involves a change in the direction of the alkane chain axes and thus, in the direction of the dipole moment variation characteristic of the methyl deformation. The low frequency band at 1371 cm^{-1} was found to be mostly

polarised in the b direction. The high frequency band at 1378 cm^{-1} was found to be mostly polarised in the a direction[69].

A band is already present at 1378 cm^{-1} in the spectra recorded at the two lowest temperatures for crystals in monoclinic {011} structure. The increase of its absorbance compared with the 1365 cm^{-1} and 1371 cm^{-1} bands may support the assignment of this band to a symmetric methyl deformation mode polarised in a different direction than the one at 1371 cm^{-1} but still in crystals with a monoclinic {011} structure. Alternatively, the band at 1378 cm^{-1} may be the signature of a small proportion of crystals with an orthorhombic structure

The increase by a factor of 2.1 of the absorption of the band ascribed to the end-gauche defect mode at 1342 cm^{-1} is an additional sign of the premelting phase transition occurring between 63°C and 79°C. Therefore, we do not expect to find more than around one end gauche conformer per chain within crystals in the monoclinic {011} form at this first temperature, since the maximum value obtainable is two such defects per molecule.

III.4.3.1.a.2 Methylene rocking mode region.

The methylene rocking mode region of the high temperature spectra is shown in Figure III.28 (spectra have been translated upwards for a more convenient presentation) :

Figure III.28 : Methylene rocking mode region of the infrared spectra of sample A1 as a function of temperature

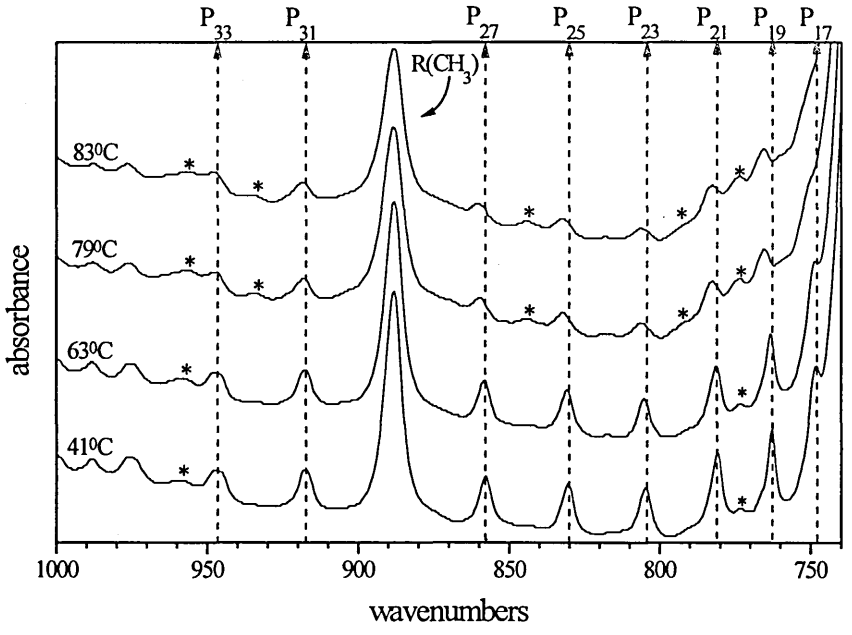

Each one of the progression bands present in this region (marked by a vertical dashed line and indexed by P_k) is ascribed to a non-localised mode of vibration involving the motion of adjacent methylene groups with the same phase difference along the n-alkane chain. This phase difference is proportional to an integer k, which can be used to identify each one of these progression bands. For an n-alkane chain in an all trans conformation, only the odd members of the progression bands (k odd) are infrared active [66,67]. In Figure III.28, the infrared bands marked by a vertical dashed line are the odd members. The most intense band at around 888 cm^{-1} is ascribed to the methyl symmetric rocking mode. The 29th member of the methylene rocking modes is believed to be covered by this last band. Finally, additional bands, centred nearly midway between the odd members of the band progression, the intensities of which increase with temperature, are indicated by an asterisk. These bands are believed to be the even members, due to gauche conformers probably placed at the end of the n-alkane chains.

Up to 63^{0}C only small changes of the odd bands are observed. The alkane chains are expected to be essentially in all trans conformations even if the band at around 772 cm^{-1} indicates the presence of some gauche conformers in the chains. Above this

temperature, a shift of the odd bands towards higher wavenumbers occurs with a clear decrease in intensity. This shift in frequency could be indicative of a change in the crystal structure.

III.4.3.1.b Low temperature infrared spectra.

III.4.3.1.b.1 Wagging mode region.

Figure III.29 : Low temperature F.T.I.R. spectra of sample A1 as a function of the annealing temperature, after baseline subtraction

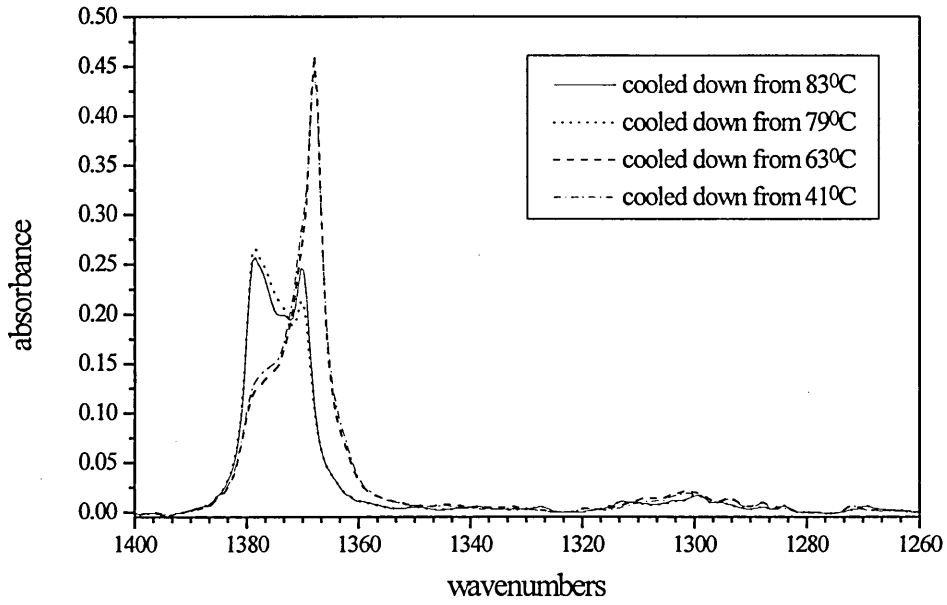

Figure III.29 shows the wagging mode region of the infrared spectra recorded at -173°C, the sample successively cooled down between annealing at each higher temperature. None of the characteristic wagging bands of any rotational isomers has a strong enough intensity to be detectable. In particular, the 1341 cm^{-1} band, characteristic of the presence of the end gauche defect conformations, is not detected in any of these last spectra. By comparison, its intensity had increased with temperature in the spectra recorded from 41°C to 83°C. However, a strong band at 1368 cm^{-1} with a shoulder at 1371 cm^{-1} and a weaker one at 1379 cm-1 are present in the two spectra recorded at -173°C, after the sample had been cooled down from the first two lower temperatures

(41°C and 63°C). A medium band at 1370 cm^{-1}, an unresolved one at 1374 cm^{-1} and a medium one at 1379 cm^{-1} are characteristic of the two spectra recorded at -173°C, after cooling the sample from 79°C and 83°C.

Second derivatives, deconvolutions and curve fitting procedures have been used to determine with accuracy the frequency and area of the different bands present in the spectra. The result of this work is shown in Table III.3.

Table III.3 : Curve fitting results obtained from the infrared spectra of sample A1 recorded at -173°C

cooled down from 41°C		cooled down from 63°C		cooled down from 79°C		cooled down from 83°C	
cm^{-1}	area	cm^{-1}	area	cm^{-1}	area	cm^{-1}	area
1378.9	**0.458**	**1379**	**0.438**	**1379**	**1.144**	**1379**	**1.096**
1376.2	**0.281**	**1376.3**	**0.285**	**1376.7**	**0.451**	**1376.8**	**0.416**
1373.3	**0.213**	**1373.4**	**0.241**	**1373.6**	**0.612**	**1373.6**	**0.566**
1371	**0.960**	**1371.1**	**0.595**	**1369.9**	**1.112**	**1369.9**	**1.297**
1368	**2.133**	**1367.9**	**2.283**				
1363.9	0.118	1364	0.062	1365	0.052	1365	0.023
1362	0.046	1362	0.058				

In Figure III.30 the scaled areas of the major bands (maximum value arbitrarily fixed to one) are drawn versus the temperature. The lines connecting the points are drawn only for clarification of the trends. We consider that the bands at 1371 cm^{-1} in the spectra of the sample cooled down from 41°C and 63°C and at 1370 cm^{-1} in the spectra of the sample cooled down from 79°C and 83°C are the same.

Figure III.30 : Scaled areas of the major bands present in the low temperature infrared spectra of sample A1 as a function of the annealing temperature

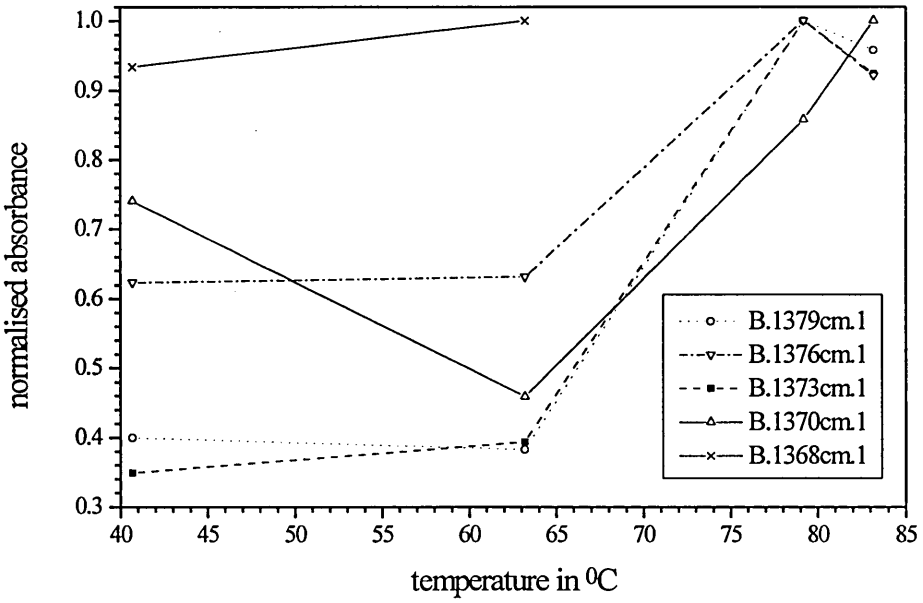

No S.A.X.S. measurements were done at low temperature. But, from the above observations, it is clear that the alkane chains are, inside the different crystal structures, in a rigorously all-trans conformation. No changes in the normalised absorbance of the band ascribed to the end gauche conformers are detected at this low temperature as a function of the crystal structure. The phase transition strongly affects the intensity and the frequency at which the band ascribed to the methyl symmetric bending mode occurs in the infrared spectra. Figure III.30 shows that the major changes occur between 63°C and 79°C. Indeed, the band at 1368 cm^{-1} which is the strongest one in the spectra of sample A1 disappears through the monoclinic phase transition. This band may be a fingerprint of the monoclinic {011} crystal structure at low temperature. A band of constant integrated absorbance is present at around 1379 cm^{-1} in the spectra of sample A1 cooled down from 41°C and 63°C. This weak band may be assigned to the orthorhombic I crystal form present in the sample at -173°C. After annealing at 79°C, the intensities of the bands at 1379 cm^{-1} and 1373 cm^{-1} increase by a factor of respectively 2.5 and 2. The higher frequency band at 1379 cm^{-1} and with less certainty the one at 1373 cm^{-1} may be fingerprints of the monoclinic {101} crystal structure at

low temperature. The intensity of the 1371 cm^{-1} band decreases when the temperature is increased between 41°C to 63°C. This is followed by an increase of the intensity above 64°C with a small shift towards lower frequency : this band at 1370 cm^{-1} may also be a fingerprint of the monoclinic {101} crystal structure at low temperature. Again, a change in the direction of the variation of the dipole moment induced by the methyl vibration mode through the monoclinic phase transition may explain some of the changes observed in the infrared spectra.

III.4.3.1.b.2 Methylene rocking mode region.

The methylene rocking mode region of the low temperature spectra is shown in Figure III.31 (spectra have been translated upwards for a more convenient presentation) :

Figure III.31 : Methylene rocking mode region of the low temperature infrared spectra of sample A1 as a function of the annealing temperature

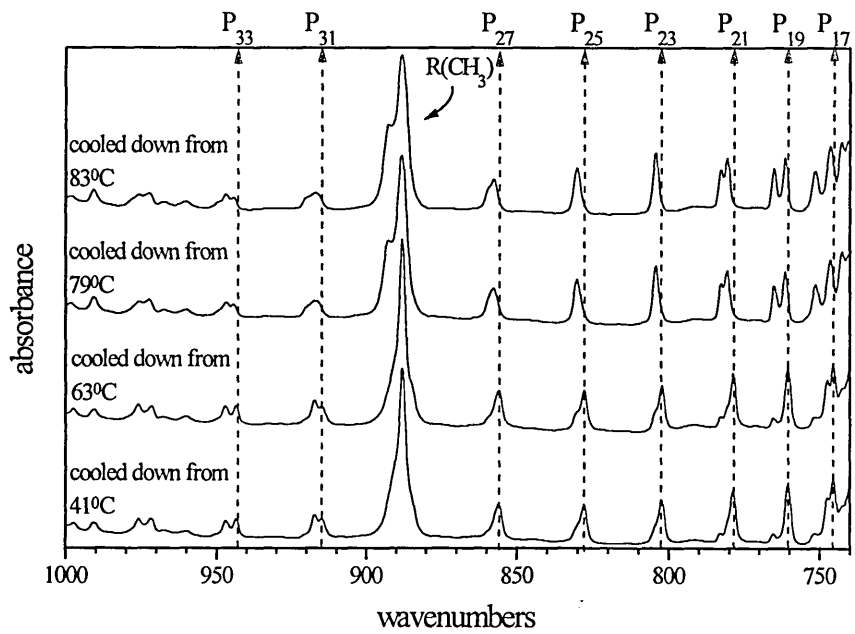

In the spectra recorded at -173°C shown in Figure III.31, only the odd members of the band progression are present. These bands are marked by a vertical dashed line and are labelled by P_k. The lowest frequency component of each band progression has been chosen to identify each member of the progression. At -173°C, none of the characteristic

bands assigned to gauche conformers is present in the spectra. Thus, the n-alkane chains are in a pure extended form whatever the crystal structure. Also, at this low temperature, the splitting of the progression bands can be observed. The splitting of these infrared bands is a characteristic of the monoclinic and orthorhombic crystal structures. The splitting of these bands decreases first, going from the 17th member of the progression to a frequency limit at around 815 cm^{-1}, and then, increases again, going from this frequency limit to the higher members of the progression. Also, the relative intensities of band progression components differ from one to the other. Going to the {101} monoclinic phase, the relative intensity of the component centred at the higher wavenumber increases compared to the lower one. The position of these maxima could be used to identify the crystal structure of this n-alkane sample. Also, it can be noticed that in some cases more than two components can be observed.

Within the methylene rocking mode region of the infrared spectra shown above, a band at around 888 cm^{-1} is ascribed to the methyl rocking mode.

III.4.3.1.b.3 Methyl rocking mode region.

Figure III.32 : Methyl rocking mode region of the low temperature infrared spectra of sample A1 as a function of the annealing temperature

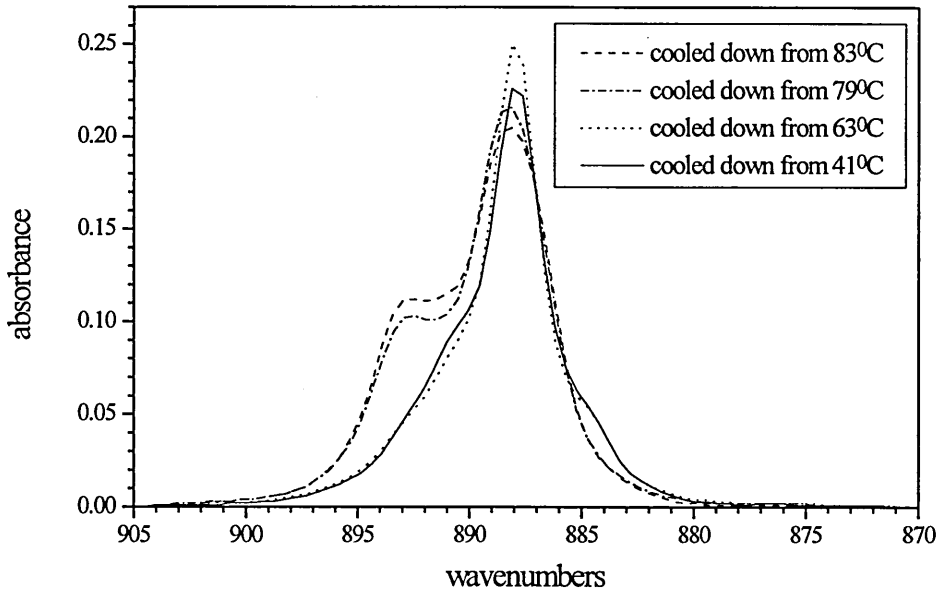

Figure III.32 shows the methyl rocking mode region recorded at -173°C, the sample being cooled down between annealing at each higher temperatures. All the spectra are characterised by a strong band at 888 cm^{-1}. Nevertheless, at this low temperature, additional features are observed. Some of them must be due to changes in the 29th member of the progression bands which is mostly covered by the band assigned to the methyl rocking mode. In the two spectra of the sample cooled down from 41°C and 63°C, two shoulders are found at 885 cm^{-1} and 891 cm^{-1}. A small increase of the intensity of the band at 888 cm^{-1} occurs after annealing to 63°C.

In the two spectra of the sample cooled down from 79°C and 83°C, a medium band at 893 cm^{-1} appears. A small decrease of the intensity of the band at 888 cm^{-1} occurs. At the same time, the intensity of the shoulder at 885 cm^{-1} decreases.

A strong band at 888 cm^{-1} is characteristic of all the infrared spectra. This band does not seem to be sensitive to either the annealing or the monoclinic phase transition occurring

between 63°C and 79°C. Nevertheless, the infrared spectra of the sample cooled down from 63°C and 79°C can be easily differentiated by a medium band at 893 cm^{-1} which may be characteristic of the final monoclinic {101} form.

The shoulder at 885 cm^{-1} may be a fingerprint of the small quantity of orthorhombic I crystals present in the sample as found by S.A.X.S. measurements. Crystals in an orthorhombic I structure are transformed to a monoclinic {101} structure by annealing.

III.4.3.2 **Sample A2 : 1.3% solution, crystallised at 25°C, heavily pressed.**

III.4.3.2.a High temperature infrared spectra

III.4.3.2.a.1 Wagging mode region.

Figure III.33 : F.T.I.R. spectra of sample A2 as a function of temperature, after baseline subtraction

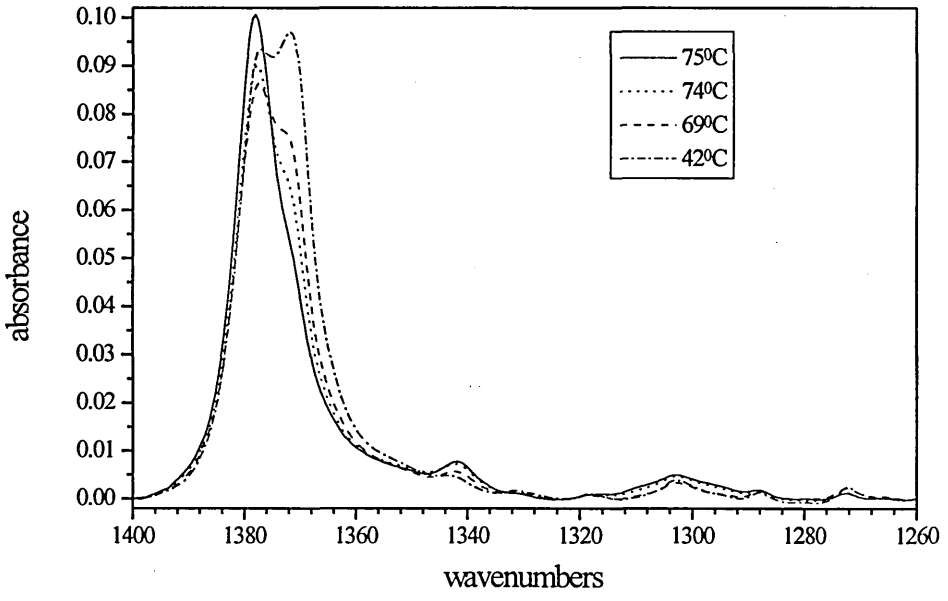

Figure III.33 shows the wagging mode region of the infrared spectra recorded at 42°C, 69°C, 74°C and 75°C. Again, the most intense bands and the most sensitive to temperature changes are ascribed to the methyl deformation modes. Nevertheless, a small increase in the intensity of the 1341 cm^{-1} band occurs with the increase in temperature.

Contrary to the spectrum of sample A1 recorded at the first elevated temperature, the spectrum of sample A2 recorded at 42°C is characterised by two just resolved bands of nearly equal intensities at 1371 cm^{-1} and 1378 cm^{-1}. The increase in temperature is accompanied by a decrease of the intensity of the 1371 cm^{-1} band followed, from 74°C, by an increase of the 1378 cm^{-1} band intensity. It should be noted that the highest temperature at which the sample was annealed is 75°C. In the case of sample A1, the phase transition between the two monoclinic forms was found to occur at around 75°C. Second derivatives, deconvolutions and curve fitting procedures have been used to determine with accuracy the frequency and area of the different bands present in the spectra. The result of this work is shown in Table III.4.

Table III.4 : Curve fitting results obtained from the infrared spectra of sample A2 recorded at elevated temperatures

T=42°C		T=69°C		T=74°C		T=75°C	
cm^{-1}	area	cm^{-1}	area	cm^{-1}	area	cm^{-1}	area
1386	0.081	1386.4	0.079	1386.6	0.085	1386.2	0.111
1377.9	**0.716**	**1377.7**	**0.757**	**1377.9**	**0.774**	**1378.1**	**0.810**
1371.2	**0.543**	**1371.3**	**0.263**	**1371.1**	**0.255**	**1371.2**	**0.200**
1365	0.247	1366.3	0.244	1365.3	0.184	1365.3	0.187
1353.5	0.092	1354.6	0.077	1354	0.082	1354	0.070
1342.2	**0.038**	**1342.2**	**0.059**	**1342.2**	**0.070**	**1342.2**	**0.077**
1331.1	0.012	1331.1	0.006	1331.1	0.008	1331.1	0.006

In Figure III.34 the scaled areas of the major bands are drawn versus the temperature.

Figure III.34 : scaled areas of the major infrared bands as a function of temperature

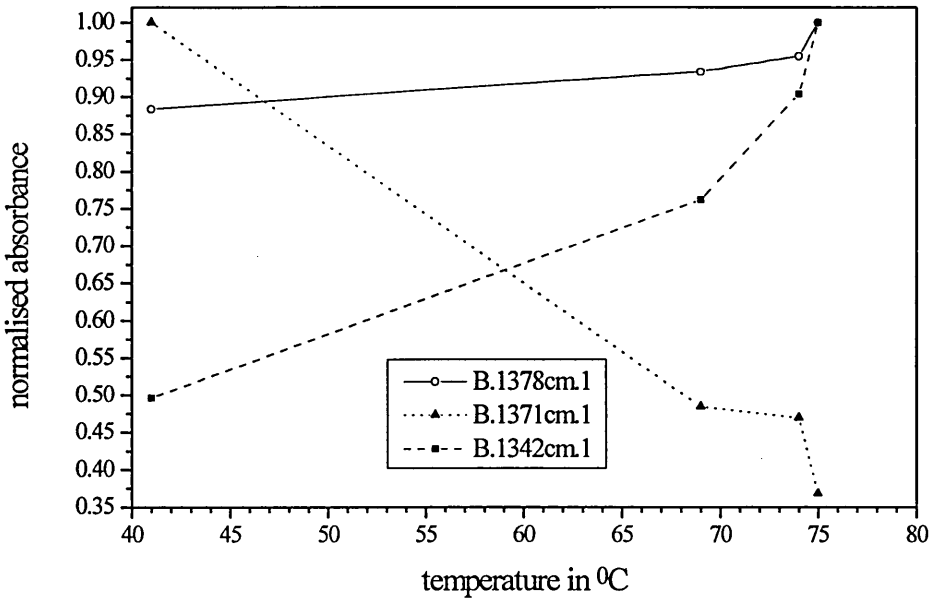

From S.A.X.S. measurements on sample A2 crystals before heating, we were able to determine the average layer periodicity of the crystals and so, to determine the crystal subcell. These data showed both triclinic and monoclinic {011} forms.

By applying pressure to the sample, we partially transformed the n-$C_{44}H_{90}$ crystal structure to a triclinic form. The strong band at 1378 cm^{-1}, in addition to the one at 1371 cm^{-1} found in the spectrum recorded at the lowest temperature, can be considered as characteristic of this last crystal structure.

Nevertheless, a phase transition can still be observed when increasing the temperature. A similar dependence of the infrared band behaviour with temperature seems to occur as in the case of sample A1. In particular, the increase of the 1341 cm^{-1} band intensity with temperature tends to show again an increase in the number of gauche conformations at the end of the alkane chains.

III.4.3.2.a.2 Methylene rocking mode region.

The methylene rocking mode region of the high temperature spectra is shown in Figure III.35 (spectra have been translated upwards for a more convenient presentation) :

Figure III.35 : Methylene rocking mode region of the infrared spectra of sample A2 as a function of temperature

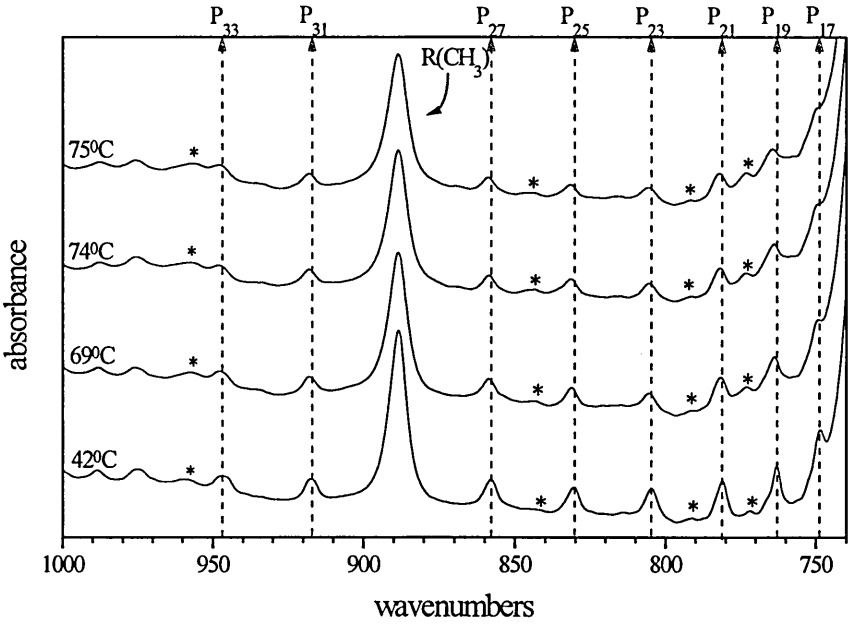

In Figure III.35, the infrared bands marked by a vertical dashed line are assigned to the odd band progression. They are labelled by P_k. The strongest band of this region labelled by $R(CH_3)$, is ascribed to the methyl rocking mode and is centred at 888 cm^{-1}. The bands marked with an asterisk are ascribed to non all-trans chain conformations. They are observed in the spectrum recorded at 42°C and, thus, indicate the presence of gauche conformers before any annealing, most probably positioned at the end of the chains. The band at around 955 cm^{-1} is a localised band and is assigned to the specific end gauche conformers. Through the annealing process, an increase in the intensity of the bands assigned to the gauche conformers is observed. At the same time, a decrease in absorbance and a broadening of the odd bands occurs. Nevertheless, no clear shift in

the position of the odd bands is detected. This is further evidence of a partial phase transition to the monoclinic {101} form.

III.4.3.2.b Low temperature infrared spectra.

III.4.3.2.b.1 Wagging mode region.

Figure III.36 : Low temperature F.T.I.R. spectra of sample A2 as a function of the annealing temperature, after baseline subtraction

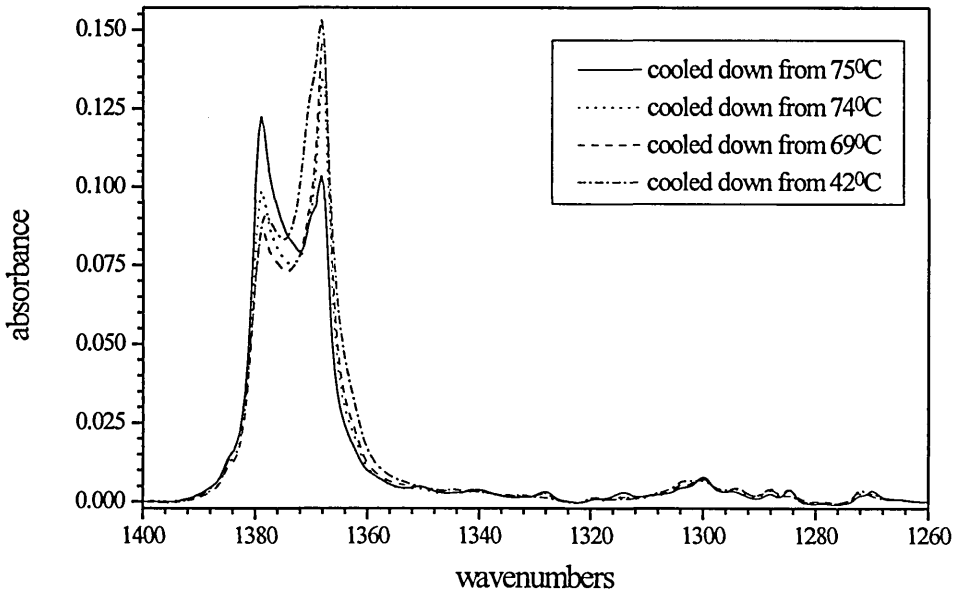

Figure III.36 shows the wagging mode region of the infrared spectra recorded at -173°C, the sample being cooled down between each of the higher temperatures. No band ascribed to any rotational isomer was detectable.

Up to 74°C, the predominant band of the spectra is the one at 1368 cm^{-1} with a shoulder at 1371 cm^{-1}. A less intense but well resolved band is at 1378 cm^{-1}. Compared to the spectrum of the sample A1, this last band is more intense. Above 74°C, a reversal in the intensity of the bands at 1368 cm^{-1} and 1378 cm^{-1} occurs. A clear shoulder is still present at 1371 cm^{-1}.

Second derivatives, deconvolutions and curve fitting procedures have been used to determine with accuracy the frequency and area of the different bands present in the spectra. The result of this work is shown in Table III.5.

Table III.5 : Curve fitting results obtained from the infrared spectra of sample A2 recorded at -173°C

cooled down from 42°C		cooled down from 69°C		cooled down from 74°C		cooled down from 75°C	
cm^{-1}	area	cm^{-1}	area	cm^{-1}	area	cm^{-1}	area
1384.4	0.027	1384.7	0.032	1384.3	0.036	1384	0.047
1379	**0.322**	**1379**	**0.334**	**1379**	**0.375**	**1379**	**0.454**
1376.1	0.205	1375.9	0.129	1375.8	0.140	1375.8	0.174
1373.4	0.130	1373.4	0.136	1373.4	0.133	1373.4	0.158
1370.9	**0.339**	**1370.9**	**0.250**	**1370.9**	**0.290**	**1370.5**	**0.346**
1368.3	**0.754**	**1368**	**0.694**	**1368**	**0.613**	**1368.1**	**0.406**
1365	0.072	1365	0.009	1365	0.001	1365	0.003
1362.5	0.027	1362.6	0.036	1362.5	0.036	1362.5	0.029

In Figure III.37 the scaled areas of the major bands are drawn versus the temperature.

Figure III.37 : Scaled areas of the major bands present in the low temperature infrared spectra of sample A2 as a function of the annealing temperature

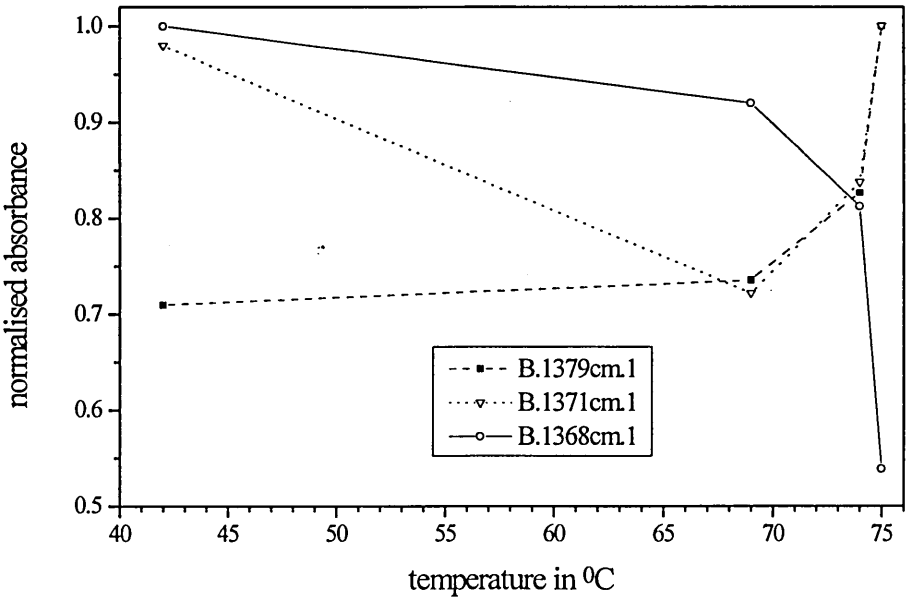

Once again, at low temperature the alkane chains seem to adopt a purely all-trans chain conformation whatever the crystal structure.

By increasing the temperature, the intensity of the 1368 cm^{-1} band decreases. This band is still remaining in the spectrum up to the highest temperatures from which the sample was cooled down. It may be explained by the fact we did not heat the sample at a high enough temperature to complete the phase transition which occurs between monoclinic structures at around 75°C. The clear shoulder at 1371 cm^{-1}, in addition to the band at 1379 cm^{-1}, may be seen as a fingerprint of the triclinic crystal structure.

III.4.3.2.b.2 Methylene rocking mode region.

The methylene rocking mode region of the low temperature spectrum is shown in Figure III.38 (spectra have been translated upwards for a more convenient presentation) :

Figure III.38 : Methylene rocking mode region of the low temperature infrared spectra of sample A2 as a function of the annealing temperature

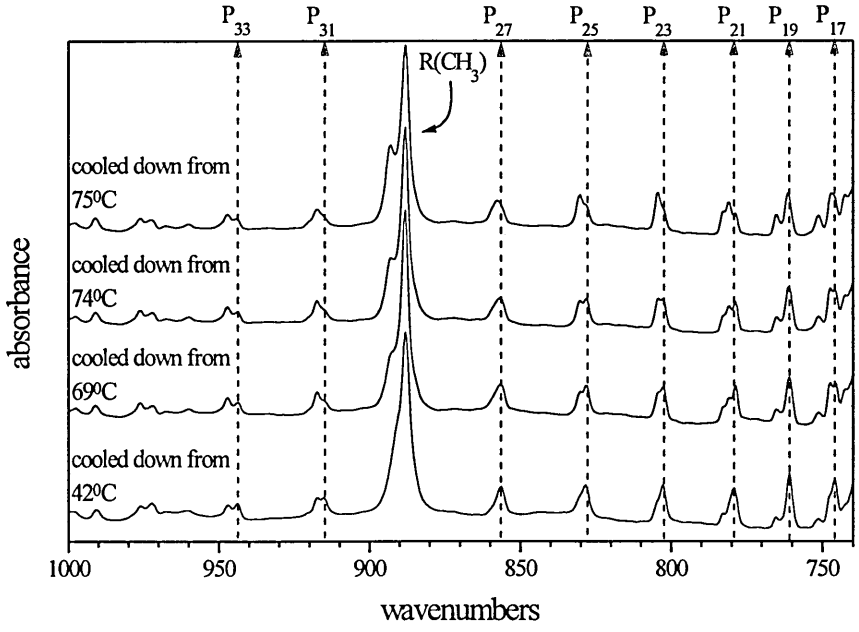

In the spectra recorded at -173°C shown in Figure III.38, apart from the methyl rocking mode labelled by $R(CH_3)$ and centred at 888 cm^{-1}, only the k-odd members of the progression bands are present. None of the bands ascribed to any gauche conformers

was detected. Hence, at -173^{0}C, the n-alkane chains are in a pure extended form whatever the crystal structure. Again, the splitting of some infrared bands is observed. This splitting increases when going from around 850 cm^{-1} towards higher and lower frequencies. This splitting is characteristic of the monoclinic and orthorhombic crystal structures. In crystalline n-alkanes in the triclinic form, there is only one molecule per unit cell and, therefore, no splitting of infrared bands can be observed. Thus here, the sample is not in a pure triclinic form as suggested by the S.A.X.S. measurements. Also, the relative intensity of the components of the band progression differs from one band to the other. But, for each band, the different components are present in the spectrum of the sample annealed up to 75^{0}C. This strongly suggests that up to 75^{0}C the sample is composed of several crystal forms.

III.4.3.2.b.3 Methyl rocking mode region.

Figure III.39 : Methyl rocking mode region of the low temperature infrared spectra of sample A2 as a function of the annealing temperature

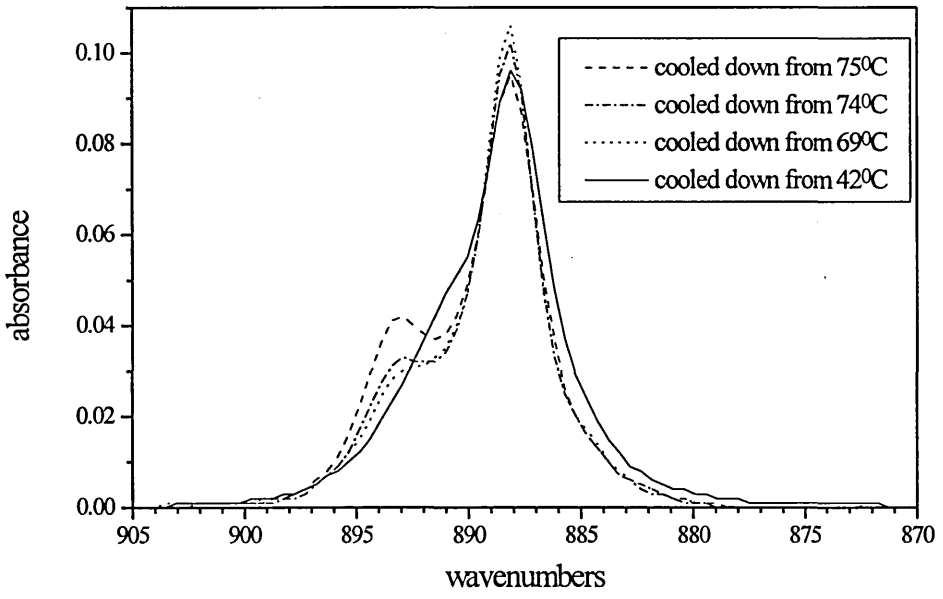

Figure III.39 shows the rocking methyl mode region of the infrared spectra recorded at low temperature, -173°C, for the sample cooled down successively from 42°C, 69°C, 74°C and 75°C. A strong band at 888 cm^{-1} is present in all these spectra.

The spectrum of the sample cooled down from 42°C can be easily differentiated from the others by a broad unresolved component at around 885 cm^{-1} and by a clear shoulder present at 891 cm^{-1}. Indeed, in the three other spectra the components at 885 cm^{-1} and 891 cm^{-1} are very much reduced and a well resolved band at 893 cm^{-1} is present. The intensity of this last band increases with the temperature at which the sample has been heated.

From S.A.X.S. measurements, we have determined the original crystal structures as being triclinic and monoclinic {011}. By annealing, a phase transition should occur to the monoclinic {101} crystal form.

Again, the band at 888 cm^{-1} does not appear to be sensitive to the annealing process. On the contrary, the presence of the 891 cm^{-1} shoulder in the spectrum of the sample cooled down from 42°C may be a fingerprint of the monoclinic {011} subcell structure.

Changes in the infrared spectra recorded at -173°C, the sample being cooled down from higher temperatures, may indicate a phase transition occurring between 42°C and 69°C. This phase transition may be characterised by the decrease in intensity of the bands near 885 cm^{-1} and at 891 cm^{-1} and the increase of the intensity of the band at 893 cm^{-1}. In the infrared spectrum of the sample cooled down from 42°C, the broader component at around 885 cm^{-1} may be a fingerprint of the triclinic structure. On the other hand, the presence of the 893 cm^{-1} band may be ascribed to the monoclinic {101} subcell structure.

III.4.3.3 **Samples A3.**

A3 : 0.45% in solution, crystallised at 25°C, mat not pressed at all.

A3' : 0.45% in solution, crystallised at 25°C, mat lightly pressed (pressure applied over the sample surface lower than 0.4 ton per cm^2).

In Figure III.40, spectra of sample A3 and A3' recorded at respectively -102°C and -173°C are shown.

Figure III.40 : Low temperature F.T.I.R. spectra of sample A3 and A3'

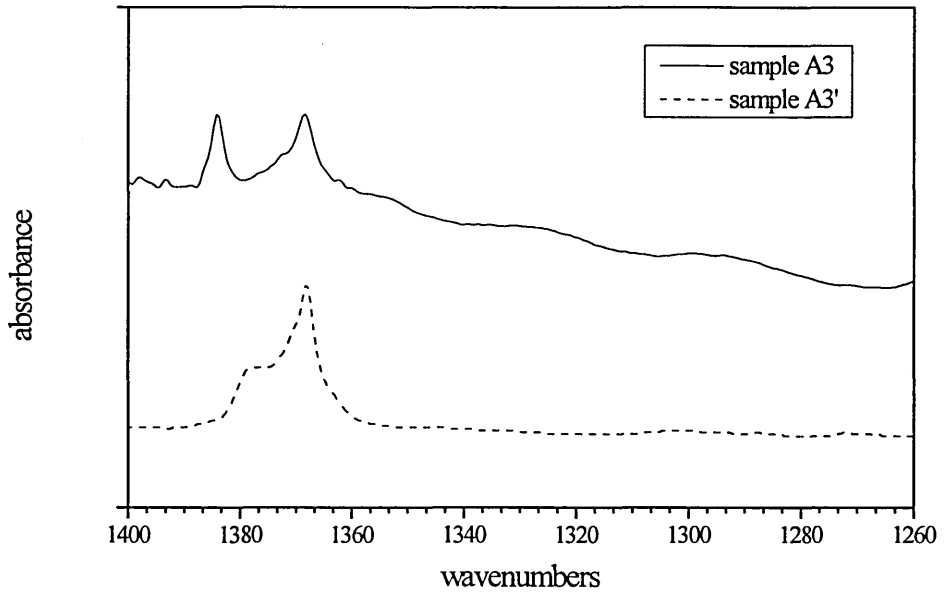

Figure III.40 shows the low temperature infrared spectra of samples A3 and A3' recorded in the wagging mode region. Because sample A3 has not been pressed at all, the thickness and the effect of scattering from the surface caused a poor quality spectrum. Nevertheless, we can easily notice the principal difference between the two spectra with the presence of the strong single band at 1384 cm^{-1}. The bands ascribed to the non all-trans chain conformation show a very low absorbance.

Kobayashi et al. ascribed two bands at 1382 cm^{-1} and 1370 cm^{-1} in the infrared spectra of n-$C_{36}H_{74}$ crystals in the orthorhombic II form to the methyl symmetric bending modes. By the mean of S.A.X.S. measurements, it was found that sample A3 was formed of at least two types of crystals : orthorhombic I and monoclinic {011} structures. Kobayashi et al report that the S.A.X.S. technique is unable to detect the presence of crystals in orthorhombic II form. The 1384 cm^{-1} band in the spectra of sample A3 may be a finger print of crystals in an orthorhombic II structure.

By pressing the sample, S.A.X.S. measurements on A3' indicated the presence of crystals in the triclinic structure in addition to the monoclinic and orthorhombic I forms. On the other hand, the absence of the 1384 cm^{-1} band in the spectrum of sample A3' may indicate the disappearance of crystals in orthorhombic II form under pressure.

Again, due to the low intensity of the bands assigned to gauche conformers, the alkane chains seem to be in a predominantly extended form at low temperature whatever the crystal structure. The behaviour of the 1384 cm^{-1} band with applied pressure may be interpreted in terms of changes in the packing of the crystal layers, causing changes in the arrangement of the methyl groups at the interfaces of these crystal layers.

I.1.1.1 Sample B : 0.265% in solution, cooling rate of 0.3^{0}C/minute, n-$C_{44}H_{90}$ crystals are deposited on a KBr plate.

Photograph III.1 :

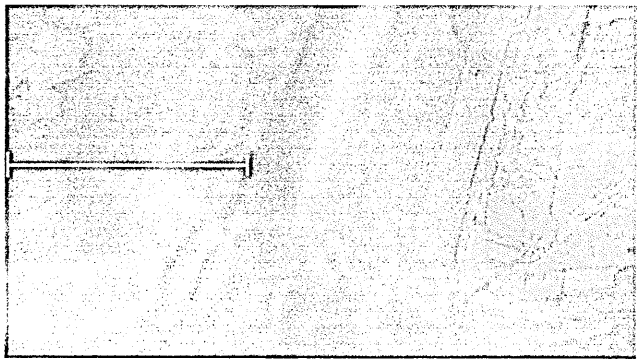

The study of sample B under an optical microscope using white light and a magnification of 500 gave us additional information on the macroscopic structure of this sample. In photograph III.1, the white horizontal line corresponds roughly to 50 μm. Photograph III.1 shows a part of a lozenge-shaped crystal multilayer. Several photographs were taken with the microscope focused on different layers of this large structure. The picture shows that each layer is characterised by a different colour (different greyscale in this black and white reproduction). A periodic succession of colours was followed through successive crystal layers.

In the bottom right side of the picture, small lozenge shaped crystals are seen. A fracture is visible along the long diagonal of the lozenges.

III.4.3.4.a.1 Wagging mode region.

Figure III.41 : Low temperature F.T.I.R. spectra of sample B as a function of the annealing temperature, after baseline subtraction

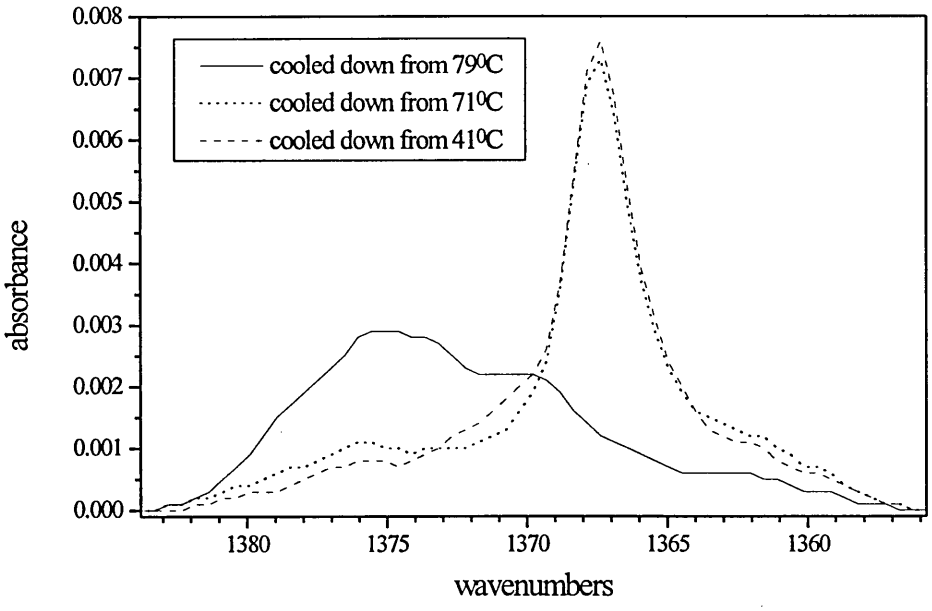

Figure III.41 shows the low temperature spectra of sample B cooled down from 41°C, 71°C and 79°C. A strong single band at 1368 cm^{-1} is characteristic of the two first spectra. The intensity of this band is strongly affected by the increase of the temperature above 71°C. The spectrum of the sample cooled down from 79°C shows a broad band with three maxima at around 1379 cm^{-1}, 1376 cm^{-1} and 1370 cm^{-1}, which are not fully resolved.

Additional S.A.X.S. measurements made on a sample originally in an orthorhombic I crystal form (long spacing 58.0Å) showed a phase transition at around 79°C. At this temperature, tilting of the n-alkane chains is first observed (long spacing 56.0Å) followed, if annealed for a long enough time, by a transition to the monoclinic {101} form (long spacing 55.0Å). With the help of photograph 1 (multilayer structure) and with the observations made on the infrared spectra recorded at low temperature (a strong band at 1368 cm^{-1} which disappears above 79°C) we may conclude that the initial crystal

structure of sample B is mostly monoclinic {011}. Also, the small band at around 1376 cm^{-1} may be indicative of the presence of the orthorhombic I crystal form. The phase transition occurring between 71°C and 79°C should involve the transition from the monoclinic {011} to the monoclinic {101} forms. Nevertheless, the clear band at 1376 cm^{-1} in the spectrum of the sample cooled down from the highest temperature indicates the presence of some crystals remaining in orthorhombic I form.

III.4.3.4.a.2 Methyl rocking mode region.

Figure III.42 : Methyl rocking mode region of the low temperature infrared spectra of sample B as a function of the annealing temperature, after baseline subtraction

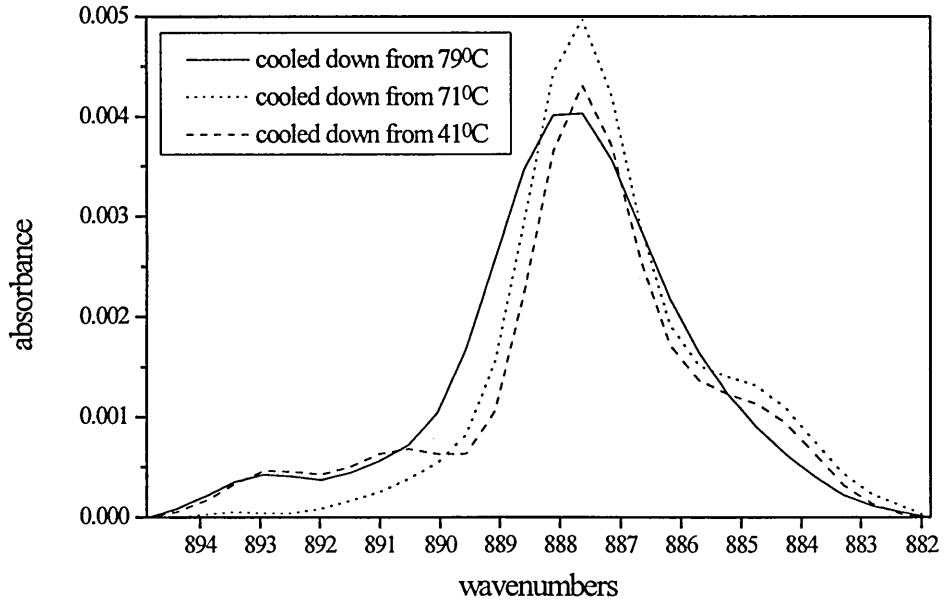

Figure III.42 shows the methyl rocking mode region of the infrared spectra recorded at -173°C of sample B cooled down from 41°C, 71°C and 79°C. The intensity of these spectra in this region is very low. The three spectra are characterised by a band at 888 cm^{-1}. Small changes in the shape of this band can be observed with the increase in temperature. Firstly, by increasing the temperature up to 71°C, a small increase in the intensity of this band is observed. Secondly, after annealing to 79°C, the width of this band increases. In this last spectrum, no shoulder was found at 884 cm^{-1}.

Two other shoulders could be observed at 893 cm^{-1} and 891 cm^{-1} in the spectrum of the sample cooled down from 41°C. After annealing up to 71°C, these two shoulders seem to have disappeared. Finally, the shoulder at 893 cm^{-1} appears again in the spectrum of the sample being annealed to 79°C.

We supposed that the initial crystal structure of sample B was essentially a monoclinic {011} form. The band at 888 cm^{-1} with the shoulder at 891 cm^{-1} may be ascribed to the methyl rocking mode deformation in this crystal structure. But, the very low intensity of the two additional shoulders at 884 cm^{-1} and 893 cm^{-1} may indicate the presence of some trace of additional crystal forms (triclinic, orthorhombic...) which may disappear after annealing up to 71°C.

The band at 888 cm^{-1} with the weak one at 893 cm^{-1} may be a fingerprint of the monoclinic {101} crystal structure.

III.4.3.4.a.3 Methyl C-H stretching mode region.

Figure III.43 : Methyl C-H stretching mode region of the low temperature infrared spectra of sample B as a function of the annealing temperature, after baseline subtraction

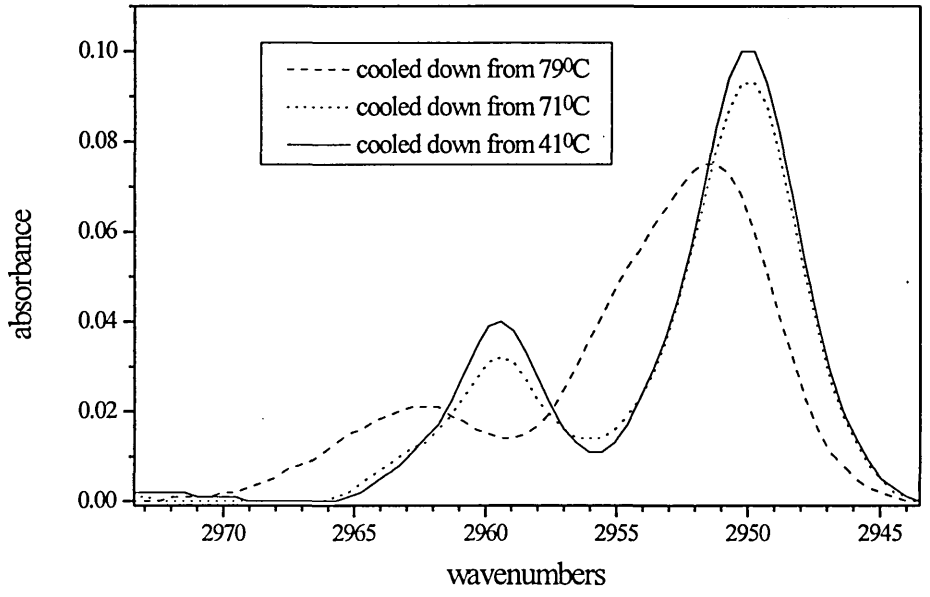

Figure III.43 shows the methyl C-H stretching region of the infrared spectra of sample B recorded at -173C, the sample successively cooled down between annealing at each higher temperature. In the spectra of sample B cooled down from 41°C and 71°C, two bands at 2959 cm^{-1} and 2950 cm^{-1} are found. A small decrease in the intensity occurs after annealing to 71°C. After annealing to 79°C, a shift of these two bands is observed towards higher frequencies. These two major bands are now centred at 2962 cm^{-1} and 2951 cm^{-1}. A shoulder is found on this last band at 2955 cm^{-1}. The splitting of the two major bands increases from 9 cm^{-1} to 11 cm^{-1} in the spectra of the sample cooled down respectively from 71°C and 79°C.

The two major bands centred around 2962 cm^{-1} and 2952 cm^{-1} were ascribed by MacPhail et al.[71] to respectively the in-plane and out-of-plane methyl asymmetric stretching modes. They reported that the frequencies and the splitting of these two bands can change due to temperature effects, methyl environments or phase transitions. All the infrared spectra were recorded at the same temperature, -173°C, so changes occurring in the infrared spectra cannot be due to temperature effects. The shift to the higher frequencies as well as the increase of the splitting of the two bands ascribed to the methyl C-H stretching modes may be explained by the phase transition occurring between the two monoclinic forms between 71°C and 79°C. The phase transition may also induce changes in the methyl environment.

III.4.3.4.a.4 Raman spectroscopy.

Figure III.44 : Low frequency Raman spectrum of sample B recorded at room temperature

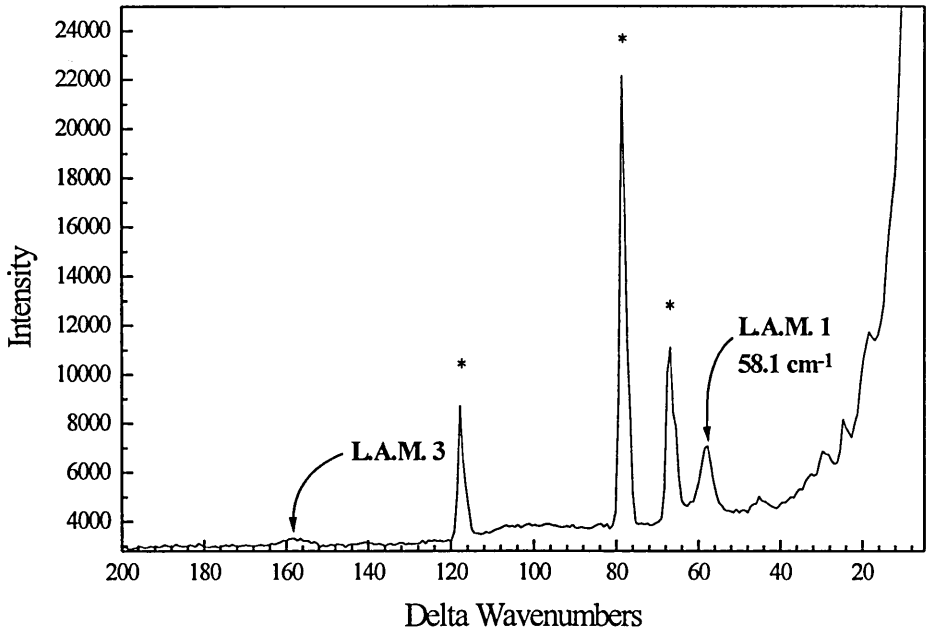

Khoury et al.[56] reported the effects of polymorphism on the L.A.M. frequencies of two short n-alkanes n-$C_{36}H_{74}$ and n-$C_{94}H_{190}$. Depending on crystallisation conditions, these n-alkanes can crystallise in orthorhombic form, in monoclinic {011} form or, in the case of n-$C_{94}H_{190}$, in monoclinic {201} form.

The low frequency Raman spectra of n-$C_{94}H_{190}$ recorded at 297K show bands at 26.2 cm^{-1}, 26.2 cm^{-1} and 27.7 cm^{-1} ascribed to the first order of the L.A.M., respectively for the sample in orthorhombic I, monoclinic {011} and monoclinic {201} forms. Hence, first order of the L.A.M. is shifted to higher frequency by 1.5 cm^{-1} when going from orthorhombic I to monoclinic {201} form.

The low frequency Raman spectra of n-$C_{36}H_{74}$ recorded at 297K show bands at 66.1 cm^{-1} and 68.8 cm^{-1} ascribed to the first order of the L.A.M., respectively for the sample in orthorhombic I and monoclinic {011} forms. The first order of the L.A.M. is shifted to

higher frequency by 2.7 cm^{-1} when going from orthorhombic I to monoclinic {011} form.

Strobl and Eckel[57] reported the frequency of the first order of the L.A.M. for n-$C_{44}H_{90}$ crystals in orthorhombic I form at 55.7 cm^{-1}.

Figure III.44 shows the low frequency Raman spectrum of sample B recorded at room temperature. In the spectrum, the bands indicated by an asterisk are assigned to cosmic ray spikes. The first order of the L.A.M. is observed at 58.1 cm^{-1}. A shift to higher frequency of 2.4 cm^{-1} is found, comparing our result with that of Strobl and Eckel. This shift is comparable with the one found by Khoury et al. for n-$C_{36}H_{74}$ crystals in orthorhombic I and monoclinic {011} forms.

III.4.3.5 **Sample C : 0.325% in solution, crystallised at 25^{0}C directly on the KBr plate.**

Photogragh III.2 :

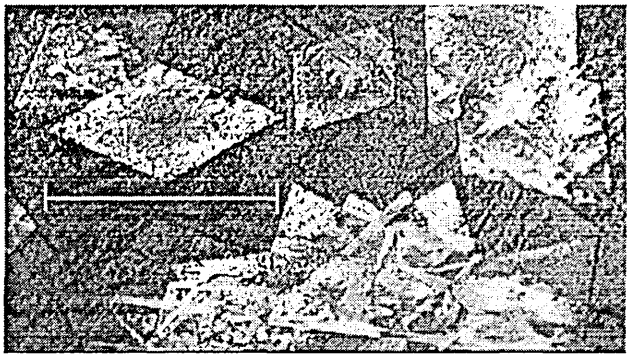

The study of sample C under an optical microscope using white light and a magnification of 500 gave us additional information on the macroscopic structure of this sample. In photograph III.2, the white horizontal line corresponds roughly to 50 μm. Photograph III.2 shows some lozenge shaped crystals formed by monolayers (by monolayers we mean only that the thickness is uniform all over the crystal surface, although the crystals are not necessarily one molecule thick). This structure is believed to be adopted by crystals in orthorhombic II form. Also, aggregates of crystals are seen at the bottom of photograph III.2.

III.4.3.5.a Wagging mode region.

Figure III.45 : F.T.I.R. spectra of sample C as a function of temperature, after baseline subtraction

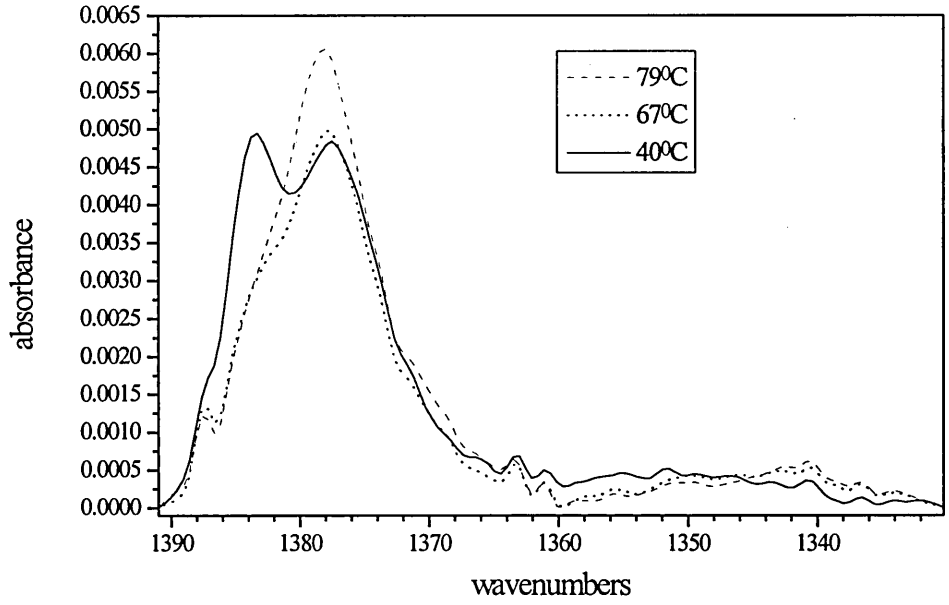

As can be seen from the photograph III.2, sample C is not homogeneous. Crystals were not covering all the area of the incident infrared beam. Also, the thickness of this sample was small. These points explain the poor quality of these spectra. Nevertheless, it can be remarked that none of the bands related to any rotational isomers are intense enough to be clearly distinguished in these spectra recorded at higher temperatures. The alkane chains seem to be in an all-trans conformation.

Figure III.45 shows a clear decrease of the intensity of the band at 1384 cm^{-1} between 40^0C and 67^0C. Above 67^0C, the intensity of the band at 1378 cm^{-1} increases.

Second derivatives, deconvolutions and curve fitting procedures have been used to determine with accuracy the frequency and area of the different bands present in the spectra. The result of this work is shown in Table III.6.

Table III.6 : Curve fitting results obtained from the infrared spectra of sample C recorded at elevated temperatures

T=40°C		T=67°C		T=79°C	
cm^{-1}	area	cm^{-1}	area	cm^{-1}	area
1387.6	0.002	1387.6	0.002	1387.6	0.002
1383.7	**0.023**	**1383.3**	**0.013**	**1383.3**	**0.011**
1377.3	**0.037**	**1377.5**	**0.035**	**1377.9**	**0.042**
1370.7	0.007	1370.7	0.006	1370.7	0.009

In Figure III.46 the scaled areas of the major bands are drawn versus the temperature, confirming the observations reported above.

Figure III.46 : Scaled areas of the major infrared bands as a function of temperature

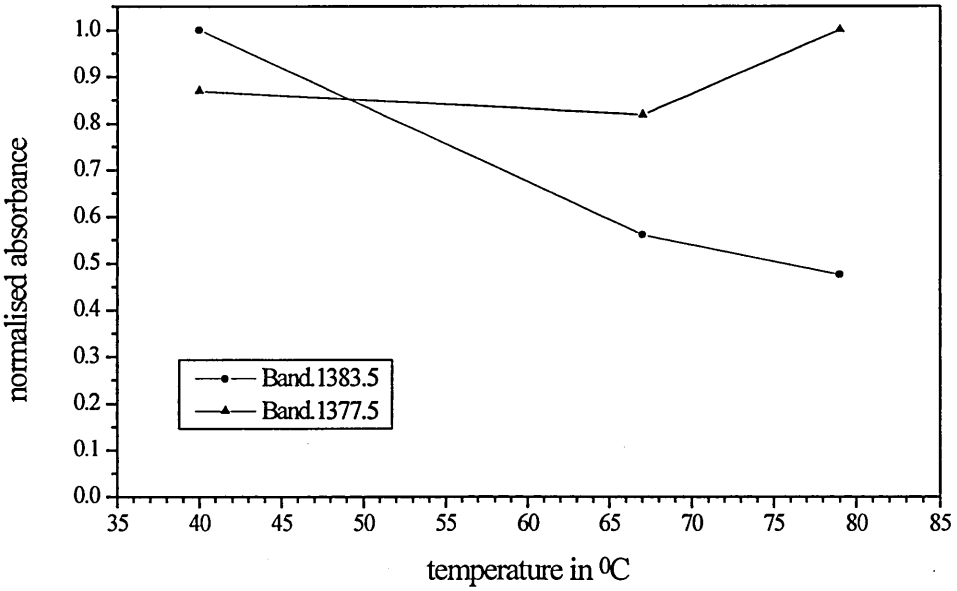

Figure III.47 : Low temperature F.T.I.R. spectra of sample C as a function of the annealing temperature, after baseline subtraction

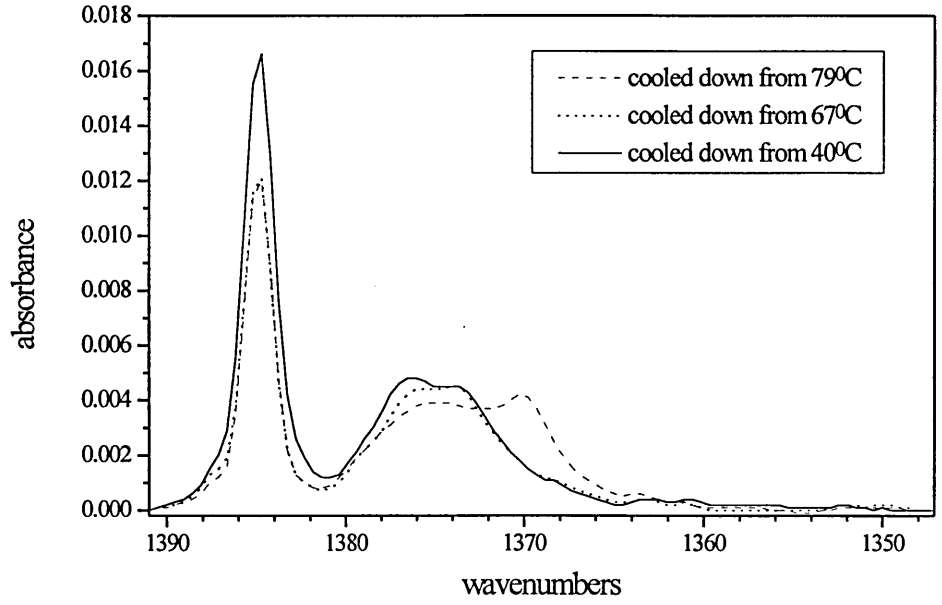

Figure III.47 shows the infrared spectra recorded at -173°C of sample C cooled down respectively from 40°C, 67°C and 79°C. A very strong band with a small width at half height is present at 1385 cm^{-1} in all the spectra. This band is the same as the one found in the spectrum of sample A3. A clear decrease of the intensity of this band occurs after heating the sample up to 67°C. But, contrary to the case of spectra recorded at the highest temperatures, this band is still well resolved even in the spectrum of the sample cooled down from 79°C.

The intensity of the band at 1373 cm^{-1} is not affected by the increase of the temperature up to 67°C. But, after annealing to 79°C, its intensity decreases slightly. On the other hand, the intensity of the band at 1376 cm^{-1} is decreasing progressively with the increase of the temperature. The major change which occurs after heating to 79°C is the increase in intensity of the band at 1370 cm^{-1}.

Second derivatives, deconvolutions and curve fitting procedures have been used to determine with accuracy the frequency and area of the different bands present in the spectra. The result of this work is shown in Table III.7.

Table III.7 : curve fitting results obtained from the infrared spectra of sample C recorded at -173°C

cooled down from 40°C		cooled down from 67°C		cooled down from 79°C	
cm^{-1}	area	cm^{-1}	area	cm^{-1}	area
1384.9	**0.051**	**1384.9**	**0.034**	**1384.9**	**0.034**
1378.8	**0.004**	**1378.9**	**0.003**	**1379**	**0.004**
1376.6	**0.013**	**1376.5**	**0.011**	**1376.6**	**0.010**
1373.4	**0.017**	**1373.5**	**0.016**	**1373.5**	**0.014**
1369.2	**0.006**	**1369.3**	**0.006**	**1369.9**	**0.014**
1363.1	0.001	1366	0.001	1366.4	0.002
1360.3	0.001	1363.5	0.001	1363.5	0.001
		1361	0.001	1361	0.001

Figure III.48 shows the scaled area of the major bands drawn versus the temperature.

Figure III.48 : Scaled area of the major bands present in the low temperature infrared spectra of sample C as a function of the annealing temperature

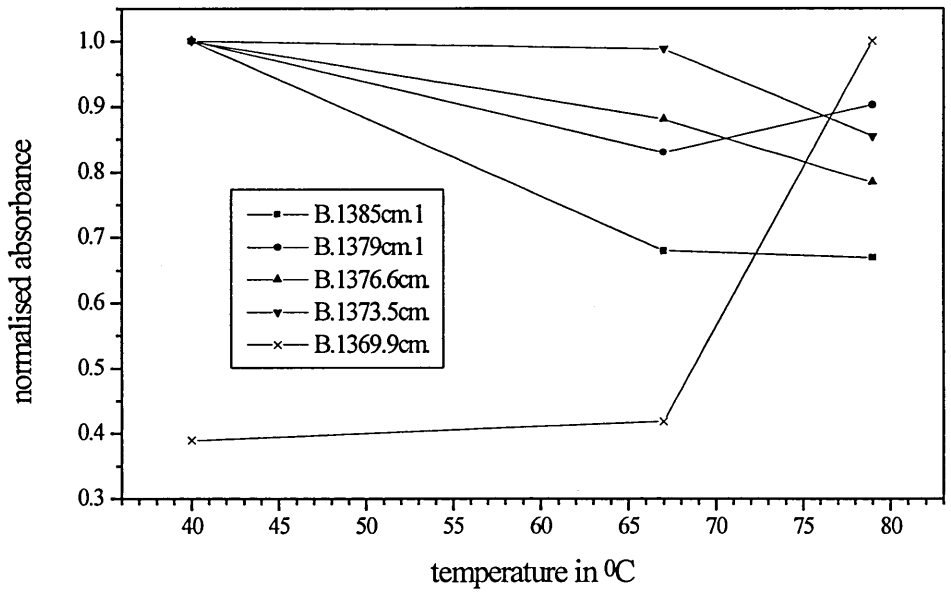

No S.A.X.S. measurements were performed on this sample either at high or low temperatures, but, we can assume that sample C is a mixture of crystals in orthorhombic I, II and monoclinic {011} forms at 40°C. As in the case of the spectrum of sample A3, the band at 1385 cm^{-1} in the spectra of Figure III.48 is ascribed to the symmetric methyl

bending mode, the sample being in an orthorhombic II crystal form. This band is polarised in the a direction. The 1373 cm^{-1} peak is the second component of this mode for an orthorhombic II structure and is expected to be polarised in the b direction. A third band at around 1376 cm^{-1} is believed to be due to crystals in orthorhombic I form. However, as this sample was not submitted to any pressure, crystals in triclinic form are not expected.

From the above observations, we can conclude that the 1385 cm^{-1} band is not sensitive to the monoclinic phase transition occurring near 75^0C. Nevertheless, the intensity of this band dropped when the temperature was increased from 40^0C to 67^0C. We believe that this effect is a consequence of a change in the orientation of the chain axis occurring from an orthorhombic II crystal structure to a tilted orthorhombic II crystal structure. At the same time, no change in the intensity of the band at 1373 cm^{-1}, polarised in the b direction, was detected. The tilt is believed to occur along the a direction[69].

As explained earlier, a S.A.X.S. experiment was carried out on a sample originally in an orthorhombic I crystal form (long spacing 58Å) and a phase transition was observed at around 79^0C. At this temperature, tilting of the n-alkane chains was first observed (long spacing 56Å) followed, if annealed for a long enough time, by a transition to the monoclinic {101} form (long spacing 55Å). In the case of sample C cooled down from 79^0C, the transition from the orthorhombic I to monoclinic {101} forms seems to have partially occurred. Indeed, the intensity of the band at 1376 cm^{-1} assigned to the orthorhombic I form decreases when the intensity of the band at 1370 cm^{-1} ascribed to the monoclinic {101} form increases. At the same time, we observe a decrease of the intensity of the 1373 cm^{-1} band polarised in the b direction and ascribed to the orthorhombic II form.

III.4.3.5.b Methyl rocking mode region.

Figure III.49 : Methyl rocking mode region of the low temperature infrared spectra of sample C as a function of the annealing temperature, after baseline subtraction

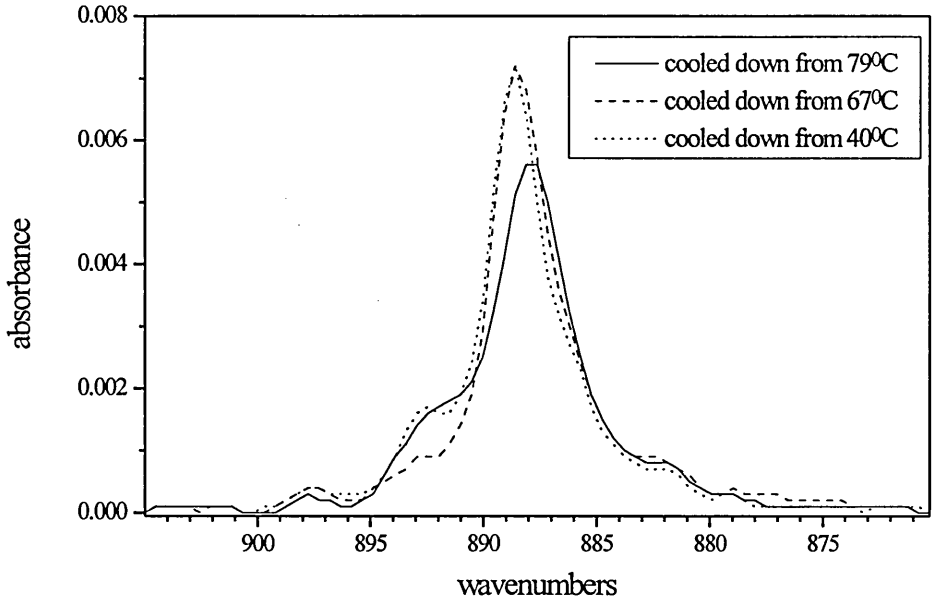

Figure III.49 shows the methyl rocking mode region of the infrared spectra recorded at -173°C of sample C cooled down from 40°C, 67°C and 79°C. The major band of this region is the one at 889 cm^{-1} in the spectrum of sample C cooled down from 40°C and 67°C. A very small shift of this band towards lower frequencies (888 cm^{-1}) is accompanied by a small decrease of its intensity after cooling down from 79°C. In the spectrum of sample C cooled down from 40°C, a clear shoulder at 893 cm^{-1} is present. Its intensity first drops by around half its value after heating up to 67°C and then, increases again after heating up to 79°C.

From the above observations, we ascribed the band at 889 cm^{-1} to the orthorhombic II crystal structure. This band is believed to be polarised in the b direction. We ascribed the band at 893 cm^{-1} present in the spectra of sample C cooled down from 40°C and 67°C to the second component of the methyl rocking mode in the orthorhombic II crystal structure. This band is believed to be polarised in the a direction.

In the spectrum of sample C cooled down from 79°C, we ascribed the strong band at 888 cm^{-1} with the shoulder at 893 cm^{-1} to the crystals in monoclinic {101} form.

III.4.3.5.c Methyl C-H stretching mode region.

Figure III.50 : Methyl C-H stretching mode region of the low temperature infrared spectra of sample C as a function of the annealing temperature, after baseline subtraction

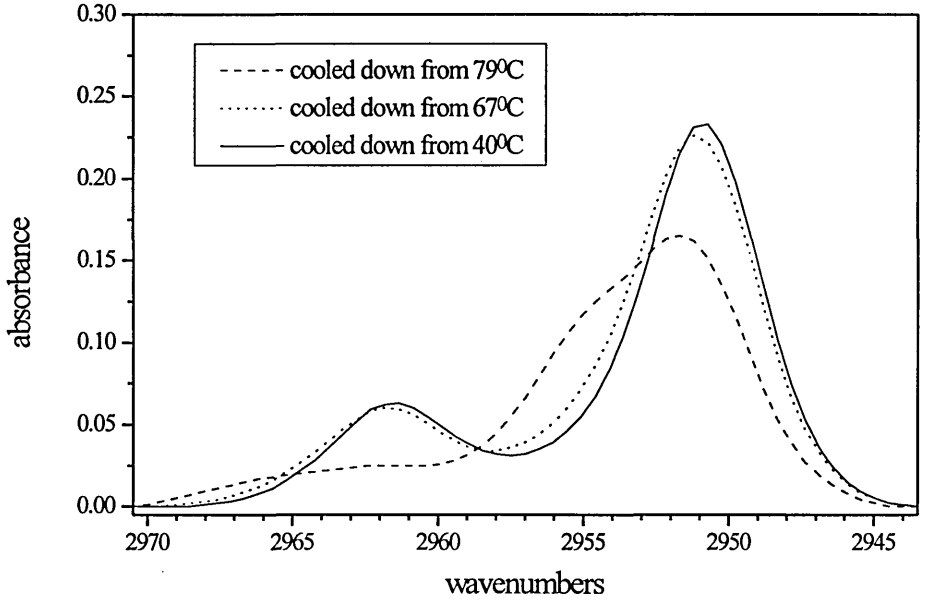

Second derivatives, deconvolutions and curve fitting procedures have been used to determine with accuracy the frequencies and areas of the different bands present in the spectra. The result of this work is shown in Table III.8.

Table III.8 : Curve fitting results obtained form the methyl C-H stretching mode region of the infrared spectra of sample C recorded at -173°C

cooled down from 40°C		cooled down from 67°C		cooled down from 79°C	
cm^{-1}	area	cm^{-1}	area	cm^{-1}	area
				2967	**0.035**
2961.5	**0.350**	**2961.7**	**0.354**	**2962**	**0.178**
2955.7	**0.122**	**2955.5**	**0.173**	**2955.3**	**0.438**
2950.9	**1.170**	**2951**	**1.161**	**2951.3**	**0.774**

Figure III.51 shows the scaled areas of the major bands plotted versus the temperature.

Figure III.51 : Scaled areas of the major bands present in the methyl C-H stretching mode region of low temperature infrared spectra of sample C as a function of the annealing temperature

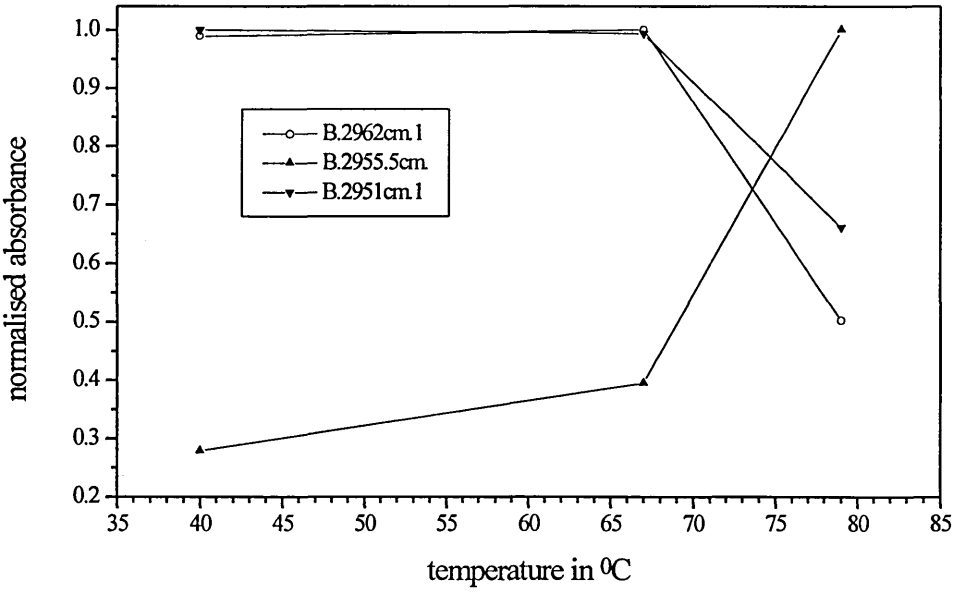

Figure III.50 shows the methyl C-H stretching region of the infrared spectra of sample C recorded at -173°C, the sample successively cooled down between annealing at each higher temperature.

The infrared spectra of sample C cooled down from 40°C and 67°C look very similar. Two bands are centred at 2962 cm^{-1} and 2951 cm^{-1}, the intensity of the first one being around three times larger than the intensity of the second one. After annealing at 79°C, a strong shoulder appears in the spectrum at 2955 cm^{-1} with a smaller one around 2967 cm^{-1}. No shifts were observed for the two major bands which stay at 2962 cm^{-1} and 2951 cm^{-1}. Nevertheless, their intensities clearly decreased (Figure III.51).

The two bands centred at 2962 cm^{-1} and 2951 cm^{-1} are ascribed to the in-plane and out-of-plane asymmetric methyl C-H stretching modes. The major changes occurring in the spectra of sample C are the clear appearance of a shoulder at 2955 cm^{-1} with another small one at 2967 cm^{-1}. These bands may be characteristic of the monoclinic {101} crystal form.

III.4.3.5.d Raman spectroscopy.

Figure III.52 : Low frequency Raman spectrum of sample C recorded at room temperature

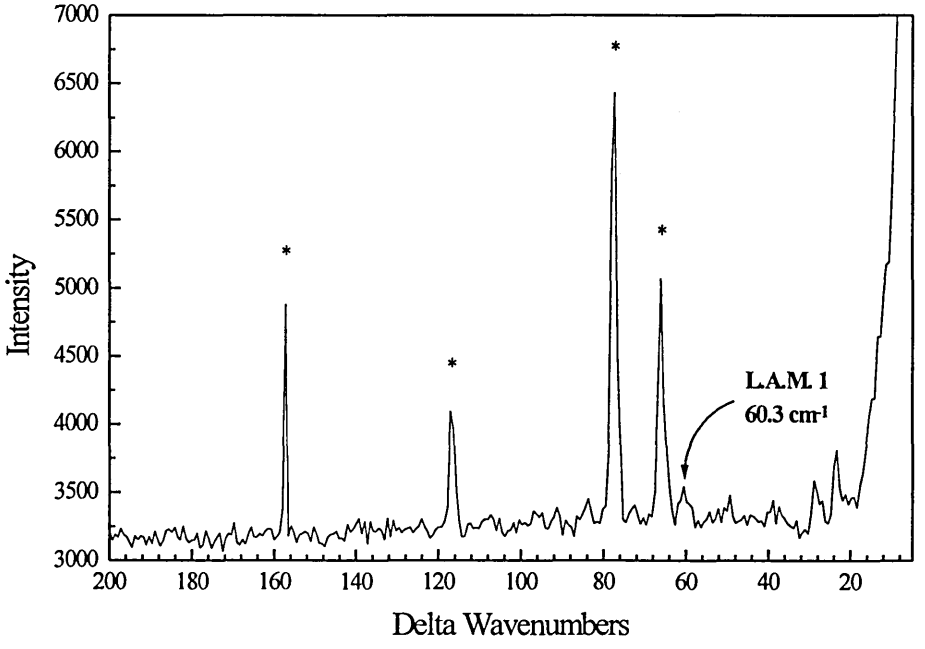

Figure III.52 shows the low frequency Raman spectrum of a single n-$C_{44}H_{90}$ crystal recorded at room temperature. In the spectrum, the bands indicated by an asterisk are assigned to cosmic ray spikes. The frequency of the first order of the L.A.M. is found at 60.3 cm^{-1}. Due to the poor quality of this spectrum, this last value should be taken with some care. Nevertheless, compared to Strobl and Eckel's value for a sample in the orthorhombic form, a shift to higher frequencies of 4.6 cm^{-1} is observed. So, the crystal structure of sample C is unlikely to be orthorhombic. Moreover, this frequency is 2.2 cm^{-1} higher than the one found for sample B, which is supposed to be in a monoclinic {011} form. Also, splitting of the L.A.M. has been reported[69] in the case of crystalline n-alkanes in orthorhombic II form. Again, the poor quality of the spectrum may not allow its detection here.

III.4.3.6 **n-$C_{44}H_{90}$ in liquid state.**

Crystals of n-$C_{44}H_{90}$ were annealed to 87°C. At this temperature, this n-alkane is in the liquid state. An infrared spectrum was recorded at 87°C and the wagging mode region, characteristic of specific gauche conformers, is shown in Figure III.53.

Figure III.53 : F.T.I.R. spectrum of liquid n-$C_{44}H_{90}$ recorded at 87°C

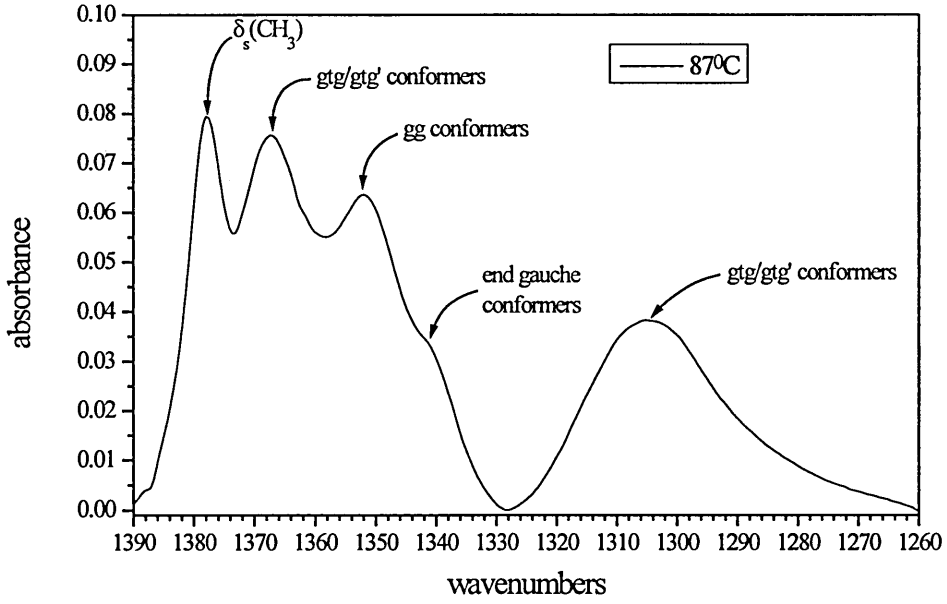

Second derivatives, deconvolutions and curve fitting procedures have been used to determine with accuracy the frequency and area of the different bands present in the spectra. The result of this work is shown in Table III.9 where it is compared with the result obtained from the spectrum of sample A1 recorded at 83°C.

Table III.9 : Curve fitting result obtained from the infrared spectrum of n-$C_{44}H_{90}$ recorded at 87°C compared with the result obtained from the spectrum of sample A1 recorded at 83°C.

83°C		87°C	
cm^{-1}	area	cm^{-1}	area
1386.1	0.305	1385	0.033
1378.2	**2.300**	**1377.9**	**0.606**
1370.6	0.324	1367.9	0.725
1365.4	0.243	1361	0.238
1358.8	0.151		
1351.3	0.090	1352.1	0.782
1341.6	**0.163**	**1340.9**	**0.314**

In the two cases, the sample areas, the thicknesses, the temperature at which the spectra were recorded and the physical states were different. We can observe that the integrated absorbance of the bands at around 1378 cm^{-1}, assigned to the methyl symmetric bending mode, is approximately four times greater in the spectrum of n-$C_{44}H_{90}$ recorded at 83°C than in the spectrum recorded at 87°C. In order to compare the two spectra, we chose to use the methyl symmetric bending band as an internal standard. Then, we can ratio its integrated absorbance against that of the band at 1341 cm^{-1}. This ratio is respectively equal to 1.93 and 14.13 in the case of n-$C_{44}H_{90}$ annealed at 83°C and 87°C. From this result, we can conclude that there are approximately 7 times more end-gauche conformers in the liquid state than at 83°C, where the sample A1 was found to be in a monoclinic {101} crystal form.

III.5 Summary and conclusions.

Table III.10 : Frequency of different infrared modes of vibration as a function of the sample phase.

PHASE	Methylene Wagging for End-*gauche* / cm^{-1}	Methyl Symmetric Deformation / cm^{-1}	Methyl Rocking /cm^{-1} ‡	Methyl C-H Stretching / cm^{-1} ‡
Monoclinic (011)	-	1371 (1368‡)	888 891	2950 2959
Monoclinic (101)	1341†	1370 1373/4 1378/9	888 893	2955* 2962*
Triclinic	-	1371 1379	888 885	
Orthorhombic I		1376	888 ?	?
Orthorhombic II	? †	1373 1384/5	889 893	2951* 2962*
Liquid	1341	1378	889	

* Bands which show asymmetric broadening, probably attributable to factor group splitting. † measurements at higher temperatures. ‡ measurements at -173^{0}C.

Short chain n-alkanes are known to crystallise in various structures depending on the number of carbon atoms per chain and on crystallisation conditions. At the lowest temperature the alkane chains are in the all-trans conformation. By increasing the temperature, the n-alkanes have been found to undergo several solid-solid phase transitions. At these transitions, the concentration of non all trans conformers increases by discontinuous jumps[38].

Using X-ray scattering measurements, we have been able to identify four different crystal structures in n-$C_{44}H_{90}$ samples : monoclinic {011}, monoclinic {101}, orthorhombic I and triclinic forms. Using differential scanning calorimetry we have

determined the temperature at which the solid-solid phase transition between the monoclinic {011} and the monoclinic {101} forms occurs. We have also shown that different crystal forms present in the same sample could be differentiated in a thermogram by the difference of their melting temperatures.

Thus, knowing the crystal structures of some of our n-$C_{44}H_{90}$ samples, we have undertaken the study of n-$C_{44}H_{90}$ by the means of infrared and Raman spectroscopy. The different infrared active modes of vibration involving the methyl groups have shown a strong sensitivity to the n-alkane crystal structure (see Table III.10). Measurements made at the lowest temperature (-173^{0}C) have uncovered the multi-component character of most of these modes[66,67,39] , polarised along the different axes of the crystal unit cell. Splittings of the band progressions assigned to different methylene modes of vibration has been observed too. The changes observed in the relative intensities of band components gives a tool to study the processes involved in the solid-solid phase transitions in crystalline n-alkanes. For example, tilting of the n-alkane chains inside crystals in the orthorhombic II form has been suggested responsible for the observed changes in intensity of the a and b polarised bands at 1385 cm^{-1} and 1373 cm^{-1}, ascribed to the methyl symmetric bending mode. Thus, this study shows that phase transitions occurring in n-$C_{44}H_{90}$ can be identified using infrared spectroscopy. Moreover, we can observe changes outside the transition regions and monitor the presence of gauche conformers at particular positions along the molecules. Also, these results confirm in the case of short chain crystalline n-alkanes, the close relationship between the packing of the methyl end groups and the crystal structure. Methyl end group vibrations can be considered as a powerful conformational probe in the structural study of hydrocarbon chain compounds.

Low frequency Raman spectra of n-$C_{44}H_{90}$ in monoclinic {101} and orthorhombic II crystal structures have been recorded. Differences in the position of the first order of the Longitudinal Acoustic Mode have been observed. The frequency at which the L.A.M. occurs is also sensitive to the n-alkane crystal structure.

We have taken a particular interest in the wagging mode region of the infrared spectra. At the lowest temperature, the symmetric methyl bending mode was found in the region between 1385 cm^{-1} and 1368 cm^{-1}. Snyder[39] reports frequencies ranging between 1380

cm^{-1} and 1360 cm^{-1}. This region overlaps the band at 1369 cm^{-1} ascribed to the wagging mode of methylene groups involved in gtg and gtg' conformers. This is relevant to studies where the aim is the estimation of disorder in hydrocarbon chain compounds. Also, the band progressions assigned to the different methylene modes of vibrations,[66,67,39] and observed in the infrared spectra of crystalline n-$C_{44}H_{90}$, may be used to determine the number of methylene groups, and therefore, the number of carbon atoms involved in this co-operative motion characteristic of n-alkane chains in an all trans conformation. This additional information could be compared to the value of the average layer periodicity determined by S.A.X.S. experiments and to the number of carbon atoms ascribed to the Longitudinal Acoustic Modes determined by low frequency Raman spectroscopy.

On the other hand, at the highest temperatures, the methyl and methylene modes present in the infrared spectra of n-$C_{44}H_{90}$ shown non-resolved and broader components. At the same time, additional bands ascribed to gauche conformers are observed. In the solid state, the gauche conformers observed are situated at the ends of the n-alkane chains[38]. At the phase transition between the two monoclinic forms, the concentration of end gauche conformers, proportional to the area of the infrared band at 1342 cm^{-1}, increases abruptly. The chain end disorder is an essential characteristic of the solid-solid phase transition process.

Finally, in the liquid state, gtg and gtg' conformers, ascribed to the infrared band at 1369 cm^{-1}, are observed in addition to the end-gauche conformers. The number of end-gauche conformers present in liquid state at 87^{0}C is found to be approximately 7 times greater than in crystals in a monoclinic {101} form at 83^{0}C. This ratio was determined using the integrated absorbance of the band present at 1378 cm^{-1} assigned to the methyl symmetric bending mode and used as an internal standard. In the infrared spectra recorded at high temperature, the 1378 cm^{-1} band is at a high enough frequency to differentiate it from any methylene wagging modes.

IV PURE LONG CHAIN N-ALKANES : N-$C_{198}H_{398}$ AND N-$C_{246}H_{494}$

IV.1 Background.

Polymers usually crystallise from either melt or solution in thin and lamellar-shaped crystals with their long chains passing several times through the crystal layers by means of chain folding. In the case of polyethylene for example, inside each crystal layer, the polymer chains are parallel to each other and preferentially adopt an all-trans conformation. The lamellar thickness is typically between 100 and 200 carbon atoms. On the contrary, short molecules do not crystallise by chain folding.

Fifteen years ago, purely uniform long chain n-alkanes having 102, 150, 198, 246 and 390 carbon atoms were synthesised by Bidd and Whiting[78] and became available in small quantities (hundreds of mg). Among these materials, the n-alkane with the shortest chain length was found to crystallise only in extended form. On the contrary, materials from 150 up to 390 carbon atoms per chain were found to crystallise by chain folding with up to four folds per chain in the case of the longest n-alkane available[16]. The thickness of the n-alkane crystal layers was found to depend on the crystallisation temperature as in the case of polymers. However, the thickness was found to take some discrete values equal to the extended chain length of the molecule divided by an integer n, with $n \leq 5$. Thus, in the case of long chain n-alkanes crystallised from solution, the crystallisation temperature, the concentration of the solution and the solvent used are three parameters which are used to control the alkane chain conformation[46,79].

Using two complementary techniques, low frequency Raman spectroscopy and Small Angle X-ray Scattering, it was shown that the fold is sharp and thus, adjacently re-entrant with the end groups at the crystal surface[16,18,54]. The crystals preferentially adopt an orthorhombic subcell structure with the chains in an all-trans conformation. These materials were found to be nearly totally crystallised. Also Organ and Keller[31], using electron microscopy on n-$C_{198}H_{398}$ crystallised from solution in once folded form, reported that crystals preferentially adopted a lozenge shaped morphology with the folds along the {110} direction.

These long chain n-alkanes are a link between short molecules and polymers. They are an ideal model to study polymer crystallisation and, more generally, any complex system containing hydrocarbon chains such as biological membranes, phospholipids or fatty acids.

In this work, our aim was to study, by means of vibrational spectroscopy, disorder in these highly ordered materials which are purely monodisperse long chain n-alkanes. Infrared spectroscopy has been intensively used elsewhere to identify and quantify conformational disorder present in paraffinic materials. For example, infrared spectroscopy has been used to study changes in disorder through premelting phase transitions occurring in odd n-alkanes from n-$C_{17}H_{36}$ through to n-$C_{29}H_{60}$[38]. Also, the distribution of defects along the hydrocarbon chains can be studied. Thus, Maroncelli, Strauss and Snyder[49] reported the non-uniform distribution of defects along the chains of n-$C_{21}H_{44}$ and n-$C_{29}H_{60}$ crystals. They showed that the number of gauche conformations increases exponentially toward the chain ends. Using Molecular Dynamics simulations, Wunderlich et al.[80] reported especially the positional disorder and the distribution of end gauche defects within crystals of long methylene sequences under different experimental conditions. They related the higher concentration of gauche defects at the chain ends to the diffusion of the chains along their long axes.

A recent computer modelling study of the {110} adjacent re-entry fold in polyethylene molecules has been done by Chum et al.[37]. They reported five lowest energy fold conformations within a range of just 1.7 kcal/mol. The second lowest energy fold conformation, within 1 kcal/mol of the lowest one (approximately ggg'g'tg'), had the same number of gauche conformations but in different positions. These results show that more than one {110} fold type may be present in polyethylene crystals and, thus, in long chain n-alkane crystals. Using atomic force microscopy, Patil and Reneker[36] examined folded chain lamellar crystals of polyethylene. Folds with different orientations and structures were detected. In earlier works by Frank[81], Flory[82] or Bassett[83] discussions about the different arrangements of folds within polymer crystals were made without direct experimental evidence about the folds. In particular, Frank demonstrated the impossibility of a fold involving solely trans and gauche bonds.

In this chapter, we report studies of the degree of disorder in different uniform long chain n-alkanes crystallised from solution by means of vibrational spectroscopy. The wagging mode region between 1260 cm^{-1} and 1400 cm^{-1}, well known to contain localised modes of vibrations ascribed to methylene groups involved in non all-trans planar zigzag chain conformations, was investigated. In order to minimise the thermal population of defects within n-alkane crystals, FTIR measurements were done at the same low temperature, -173^{0}C, using a cryostat cooled down with liquid nitrogen. Infrared spectra of n-$C_{198}H_{398}$ crystallised in once folded and extended forms were analysed after annealing at different higher temperatures. The tilting of the once folded n-$C_{198}H_{398}$ alkane chains from the crystal surfaces was determined using both S.A.X.S. and low frequency Raman spectroscopy. The identification of the progression bands assigned to the C-C stretching modes of vibration and observed between 1133 cm^{-1} and 1050 cm^{-1} in the low temperature infrared spectra of these long chain n-alkanes is used to estimate the number of carbon atoms involved in this co-operative motion characteristic of n-alkane chains in all-trans conformation. In chapter III, we have shown that most of the infrared bands present in the spectrum of n-$C_{44}H_{90}$ and assigned to vibrations involving methyl end groups were sensitive (in terms of both frequency and intensity) to crystal structures and tilting of the alkane chains. In particular, the methyl symmetric bending mode was found in a frequency range between 1384 cm^{-1} and 1368 cm^{-1}. This band is found at 1377 cm^{-1} in the infrared spectra of crystals in an orthorhombic structure. Therefore, the consideration of this methyl mode of vibration for spectral normalisation must involve an awareness of its conformational sensitivity to chain end environments. In this chapter, exclusively dedicated to long chain n-alkanes in an orthorhombic subcell structure, the methyl symmetric bending mode is found at 1377 cm^{-1}. Nevertheless, tilting of the alkane chains and the transition from once folded to extended forms may affect the chain ends environment or the crystal surfaces and, therefore, affect the absorbance of this last band. When normalisation was not needed, we tried to find the infrared band which was least affected by structural changes. Among these bands, the one present at 2670 cm^{-1} has been chosen. When normalisation was needed and when low temperature (-173^{0}C) infrared spectra were available, we used the integrated area of the band present at 2670 cm^{-1} in these spectra as an internal standard.

Its integrated area was also used to normalise the spectra recorded at the highest temperatures. When low temperature spectra were not available, we used the methyl symmetric bending mode as an internal standard. Also, in this chapter, spectral subtraction was used to obtain a " fold " spectrum. This lead to an evaluation of the different conformations composing the fold. Moreover, an estimate of the number of specific conformations per molecule is presented in the case of n-$C_{198}H_{398}$ crystallised in once folded and extended forms. Finally, the transformation to the extended form of n-$C_{246}H_{494}$ originally crystallised in once folded form is reported.

IV.2 Experimental section.

IV.2.1 F.T.I.R.

Transmission infrared spectra were recorded between 700 cm^{-1} and 4000 cm^{-1} with 1 cm^{-1} resolution and 200 scans using a computerised (First version 1.70 software) Mattson Galaxy 6020 F.T.I.R. spectrometer based on a Michelson interferometer equipped with a cooled pyroelectric detector doped with mercury cadmium telluride.
Samples held between two potassium bromide plates were installed in a Graseby/Specac cryostat P/N21500 equipped with a heating cell and a temperature controller P/N20120. A vacuum pump allowed the cryostat to be evacuated, enabling us to work in a temperature range between -173°C and 140°C at $^{+}/_{-}$ 1°C.
Infrared spectra were recorded for samples successively annealed at higher temperatures and then cooled down to -173°C. In this process, the cooling rate was 10°C/minute.

IV.2.2 Raman spectroscopy.

Low frequency Raman spectra were recorded at room temperature between 550 cm^{-1} and 5 cm^{-1} on a Dilor XY triple monochromater spectrometer equipped with a 514.5 nm Laser source, a variable slit aperture and a CCD detector. These measurements were done at the Technical University of Warsaw (measurements by Dr S. J. Spells and Dr W. Gembicki).

Also, Raman spectra between 3790 cm^{-1} and 400 cm^{-1} using 4 cm^{-1} resolution were recorded at room temperature on a Renishaw Ramanscope 2000 spectrometer equipped with a 514.5 nm Laser source, a microscope sample stage with a magnification of 200 and a CCD detector.

IV.2.3 Small Angle X-ray Scattering.

We used a Rigaku-Denki instrument with a copper K_α X-ray tube, a sample holder, pinhole collimation (diameter 0.3mm) and a camera. The camera was under vacuum and comprised a photographic film holder in front of which was fixed a beam stop. The distance between the sample and the photographic films was measured. These measurements were done in the Department of Engineering Materials, University of Sheffield (courtesy of Dr. G. Ungar).

IV.2.4 Sample preparation.

Samples were synthesised by Brooke et al.[17] We crystallised them from solution in Aristar grade toluene and prepared them as follows:

(1) n-$C_{198}H_{398}$ crystallised from 1.4% $^{w}/_{v}$ solution in toluene at 73.2 $^{+}/_{-}$ 0.4 ^{0}C for 90 minutes to obtain crystals in the once folded chain conformation, and then filtered. The resulting mat was allowed to dry before pressing (pressure applied over the sample surface lower than 0.4 ton per cm^2).

(2) n-$C_{198}H_{398}$ crystallised from 0.8% $^{w}/_{v}$ solution in toluene at 81.5 $^{+}/_{-}$ 0.4 ^{0}C for 6 hours to obtain crystals in the extended chain conformation, and then filtered. The resulting mat was allowed to dry before pressing (pressure applied over the sample surface lower than 0.4 ton per cm^2).

(3) n-$C_{246}H_{494}$ crystallised from 1.35% $^{w}/_{v}$ solution in toluene at 81.6 $^{+}/_{-}$ 0.4 ^{0}C for 90 minutes to obtain crystals in the once folded chain conformation, and then filtered. The resulting mat was allowed to dry before pressing (pressure applied over the sample surface lower than 0.4 ton per cm^2).

Using Small Angle X-ray Scattering, we determined the average layer periodicity of the different crystals, and so, the nature of their chain conformations. In addition to the

crystal thickness, the average layer periodicity includes the thickness due to the fold or due to any amorphous layers which may be present in the sample. Using the relationship between carbon number and chain length reported by Broadhurst[60], values of the crystal thickness for n-$C_{198}H_{398}$ in once folded and extended chain conformations were calculated and found to be equal respectively to 127 Å and 254 Å. The S.A.X.S. layer periodicities corresponding respectively to samples (1) and (2) were found to be 124.7 $^{+}/_{-}$ 1.1 Å and 253.3 $^{+}/_{-}$ 1.3 Å. These values are in good agreement with the calculated ones.

The calculated values of the crystal thickness for n-$C_{246}H_{494}$ in once folded and extended chain conformations are respectively 158 Å and 314 Å. The layer periodicity corresponding to sample (3) was found to be 158.6 $^{+}/_{-}$ 1.7 Å, in good agreement with the calculated value for the once folded form.

IV.3 RESULTS.

IV.3.1 Sample (1) : n-$C_{198}H_{398}$ crystallised in once folded form.

IV.3.1.1 S.A.X.S. measurements.

As noted above, the experimental layer periodicity was found to be in good agreement with the calculated one. Therefore, within each crystal layer of sample (1), the alkane chains are in the once folded form with the chain axis perpendicular to the crystal surfaces.

IV.3.1.2 Raman spectroscopy

Figure IV.54 shows the Raman spectrum of sample (1) recorded at room temperature between 1650 cm^{-1} and 850 cm^{-1}.

Figure IV.54 : Raman spectrum of sample (1) recorded at room temperature between 1650 cm^{-1} and 850 cm^{-1}

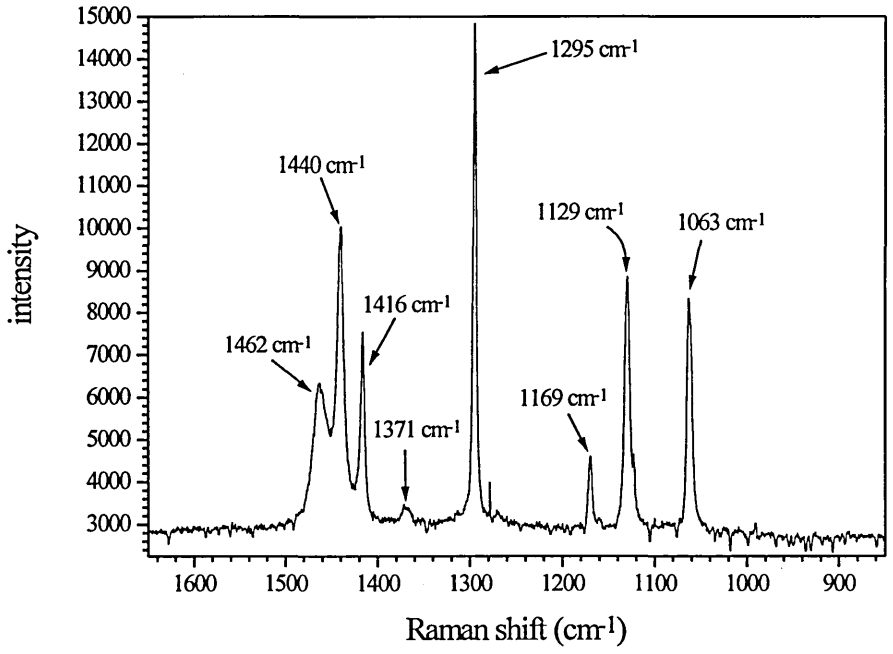

The Raman bands present in the spectrum of sample (1) shown in Figure IV.54 are assigned in Table IV.11 :

Table IV.11 : Assignment of the Raman bands present in the spectrum of sample (1)

Raman shift (cm^{-1})	assignment
1462	methylene bending mode[84]
1440	methylene bending mode[84]
1416	methylene bending mode[84], characteristic of the orthorhombic subcell packing[85]
1371	methylene wagging mode[85]
1295	in-phase methylene twisting mode [40]
1169	out-of-phase methylene rocking mode[40]
1129	in-phase C-C stretching mode[40]
1063	out-of-phase C-C stretching mode [85]

Additional bands at 1082 cm^{-1} and 1305 cm^{-1} (not detected here) present in the Raman spectra of polyethylene were ascribed[85] respectively to the out-of-phase C-C stretching mode and in-phase methylene twisting mode involved in the non all-trans part of the polymer chains.

In Figure IV.55, the C-H stretching region of the Raman spectrum of sample (1) is shown.

Figure IV.55 : Raman spectrum of sample (1) recorded at room temperature between 3100 cm^{-1} and 2500 cm^{-1}

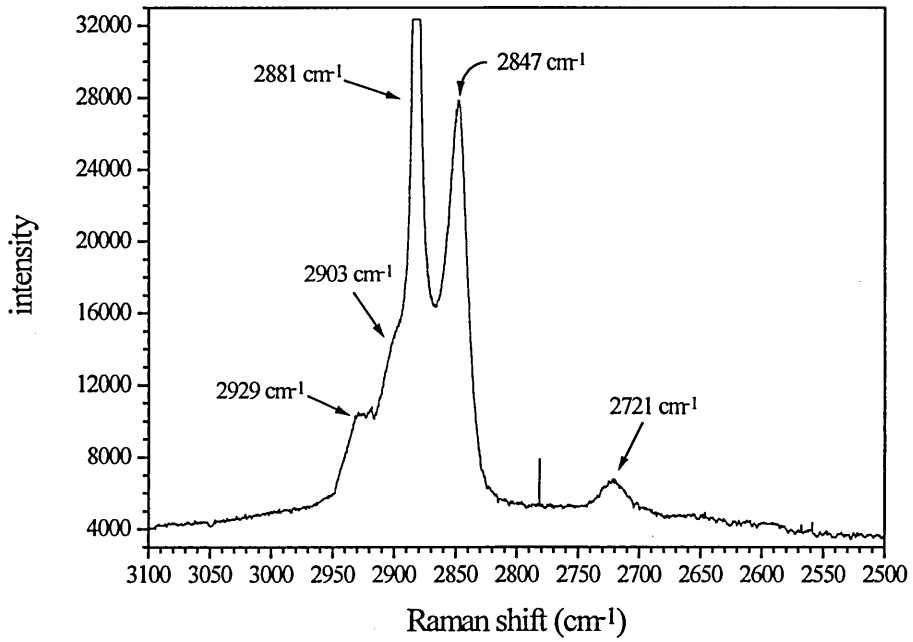

The Raman active bands at 2847 cm^{-1} and 2881 cm^{-1} are ascribed[86,87] respectively to the symmetric and antisymmetric methylene C-H stretching modes. In this spectrum, the intensity of the band at 2881 cm^{-1} is saturated. The bands present in the Raman spectrum at 2903 cm^{-1} and 2929 cm^{-1} are also associated with the symmetric and antisymmetric methylene C-H stretching modes but, in this case, are the result of Fermi resonance[86,87]. A weak band at around 2721 cm^{-1} has not been assigned previously. In the C-H stretching region, the ratio of the intensities of some of these bands (e.g. $\frac{I_{2850}}{I_{2930}}$ or $\frac{I_{2890}}{I_{2850}}$) have been used to study structure and conformational changes in hydrocarbon chain systems such as polyethylene[88] and biological membranes[89].

Also, no bands at around 1030 cm^{-1}, 1604 cm^{-1} and 3056 cm^{-1}, ascribed[90] to fundamental modes of vibration of toluene, were detected in these Raman spectra. This result strongly suggests the absence of any trace of remaining solvent in the n-alkane samples.

IV.3.1.2.a Low frequency Raman spectrum.

In Figure IV.56, the low frequency Raman spectrum of sample (1) recorded at room temperature is shown.

Figure IV.56 : Low frequency Raman spectrum of sample (1) recorded at room temperature, shown after baseline subtraction

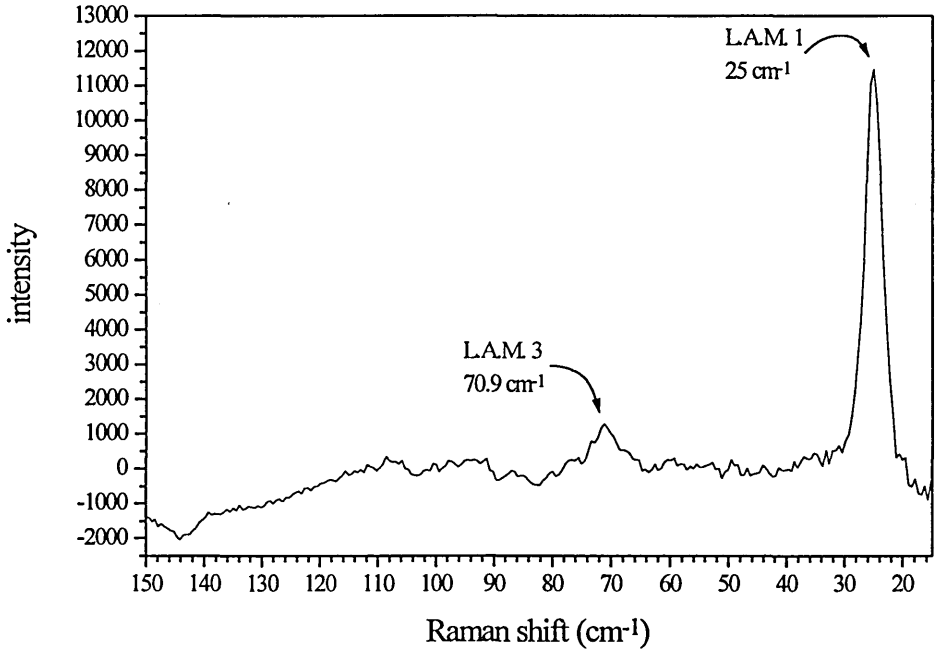

The first and third orders of the Longitudinal Acoustic modes of vibration are present at respectively 25 cm^{-1} and 70.9 cm^{-1}. These "accordion-like" modes of vibration were discovered by Mizushima and Shimanouchi[52]. Since then, they have been used as a complementary technique with S.A.X.S. measurements to determine the length of the part of the n-alkane chain in an all trans conformation (called the stem) inside the crystals of paraffinic compounds[54,57]. Using $\Delta\bar{\nu}$ (in cm^{-1}), the Raman shift of the first order of the L.A. mode, the length of the all-trans stem L_R (in Å), characteristic of the lamellar crystals can be determined using Equation IV.48[54] :

Equation IV.48

$$L_R = \frac{3169}{\Delta\bar{\nu}}$$

The number of carbon atoms present in the all trans stem of length L_R can be determined using Equation IV.49[60] :

Equation IV.49

$$n_C = \frac{L_R - 2}{1.27}$$

Thus, the number of carbon atoms involved in the all-trans stem characteristic of the lamellar crystals of sample (1) was found to be equal to 98. The number of carbon atoms within the n-$C_{198}H_{398}$ chain involved in this L.A. mode therefore corresponds to almost exactly a half of the chain. Hence, inside the crystals of sample (1), the n-alkane chains are in the once folded conformation.

IV.3.1.3 **Conclusion.**

From the values of the average layer periodicity of the crystal layers determined by S.A.X.S. and the number of carbon atoms involved in the extended part of the n-alkane chains present in sample (1) determined by low frequency Raman spectroscopy, we conclude that inside sample (1), the n-alkane chains are in the once folded conformation with the chain axis perpendicular to the crystal surfaces and the folds exactly in the middle of the chains.

IV.3.1.4 **Tilting of the n-alkane chains.**

IV.3.1.4.a Tilting as a function of the annealing temperature.

By increasing the temperature above 90°C, the n-alkane chains present in the crystal layers of sample (1) were expected to tilt from the crystal surfaces. Also, the tilt angle was expected to increase with increasing temperature[79]. We used S.A.X.S. measurements to determine the average layer periodicities of the sample (1) crystals after annealing at each elevated temperature. We used low frequency Raman spectroscopy to determine the frequency of the longitudinal acoustic mode, from which the number of carbon atoms involved in this mode of vibration can be estimated[22,54,57].

Once the infrared spectra of sample (1) successively annealed at higher temperatures and then cooled down to -173^{0}C were all recorded, we used this final sample to perform S.A.X.S. experiments and record the low frequency Raman spectrum. A different sample was used to determine by S.A.X.S. measurements the layer periodicity of sample (1) annealed at 95^{0}C.

IV.3.1.4.a.1 S.A.X.S. measurements.

Sample (1) was annealed to 95^{0}C and 110^{0}C. At these temperatures the layer periodicities were found to be equal respectively to 120.8 $^+/_-$ 0.8 Å and 120.6 $^+/_-$ 0.7 Å. These values were determined using a densitometer to plot the intensity of the scattered X-rays versus the distance from the centre of the photographic film. Then, we digitised these plots (see Figure IV.57). Baselines were subtracted to remove the scattering background and curve fitting procedures were used to determine with accuracy the position of the maximum intensity of the peaks of diffraction (see Figure IV.57 for example where the black curve represents the Lorentzian function used for the curve fitting procedure). The distance between these peaks is directly related to the average layer periodicity of the crystals which can be determined using the Bragg's equation.

Figure IV.57 : Intensity of the scattered X-rays versus position on the photographic film for sample (1) annealed at 95°C, after baseline subtraction.

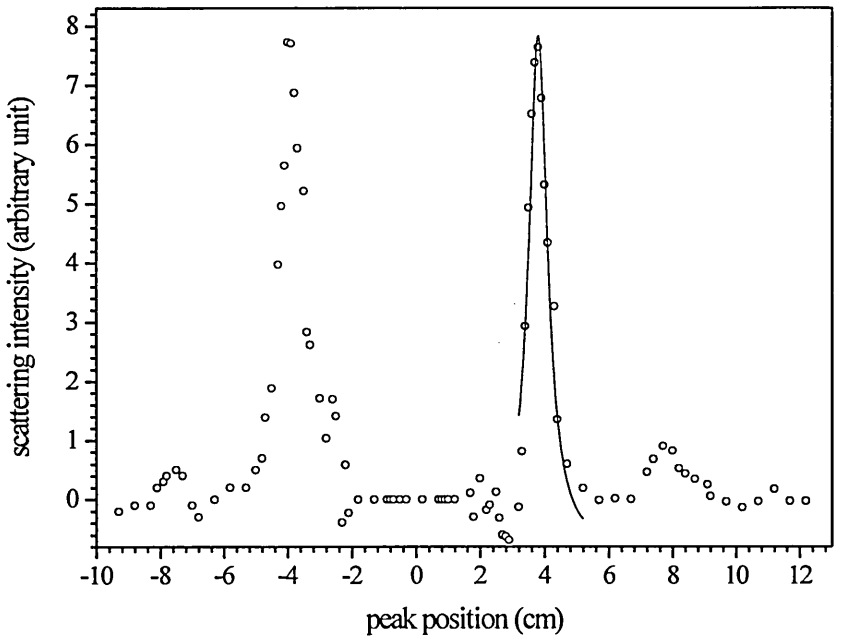

By comparison with the S.A.X.S. periodicity of the unannealed sample, for annealing to 95°C, the alkane chains are estimated to be tilted from the crystal surfaces at an angle of 15 +/- 3 °. Once the n-alkane chains are tilted, no increase in the value of the tilt angle was observed with the increase of annealing temperature.

IV.3.1.4.a.2 Low frequency Raman spectrum.

The low frequency Raman spectrum recorded at room temperature of sample (1) after being annealed at 110°C is shown in Figure IV.58 after baseline subtraction.

Figure IV.58 : Low frequency Raman spectrum recorded at room temperature of sample (1) after annealing at 110°C, after baseline subtraction

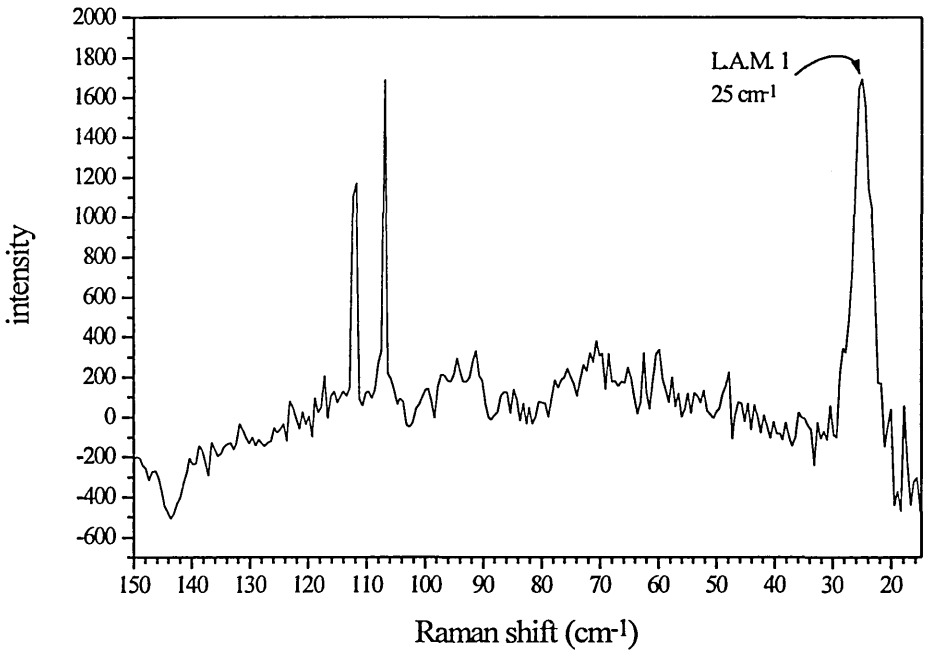

The signal to noise ratio is low in this spectrum and does not allow us to detect the higher orders of the Longitudinal Acoustic mode. Only the first order is visible at 25 cm^{-1}. Nevertheless, the value of this frequency is identical to the one found in the low frequency Raman spectrum of sample (1) before any annealing and shown in Figure IV.56. Thus, the number of carbon atoms involved in the all-trans stems characteristic of the lamellar crystals is identical to this previous case. After annealing to 110°C, the n-alkane chains present in the crystals of sample (1) are still in the once folded conformation.

IV.3.1.4.a.3 Summary.

After annealing sample (1) at 95°C and 110°C, the values of the average layer periodicity of the crystal layers determined by S.A.X.S. measurements and the number of carbon atoms involved in the extended part of the n-alkane chains present in sample (1) determined by low frequency Raman spectroscopy indicate that, inside sample (1), the n-alkane chains are in the once folded conformation with the folds exactly in the middle of the chains and the chain axis tilted from the crystal surfaces by around 15°.

IV.3.1.4.a.4 Infrared Spectroscopy.

Sample (1), originally crystallised in the once folded form with the all-trans chains perpendicular to the surface of the crystal layers, was annealed at successively higher temperatures from 51°C to 95°C and 110°C, and then cooled down to -173°C. As noted above, after annealing at 95°C, the alkane chains were found to be tilted from the crystal surfaces at an angle of 15 +/- 3 °. The presence of tilted chains inside the n-alkane crystals of sample (1) was expected to lead to an increase of the number of crystal defects placed at the end of the chains. Investigations were carried out using F.T.I.R. spectroscopy.

IV.3.1.4.a.4.1 Highest temperature spectra.

Figure IV.59 shows the methylene wagging mode region of the infrared spectra of sample (1) recorded at 51°C, 95°C and 110°C. Between each one of these temperatures, the sample was cooled down to -173°C. Linear baselines have been used with reference points of 1391 cm^{-1}, 1324.9 cm^{-1} and 1280.1 cm^{-1}.

Figure IV.59 : F.T.I.R. spectra of sample (1) as a function of temperature

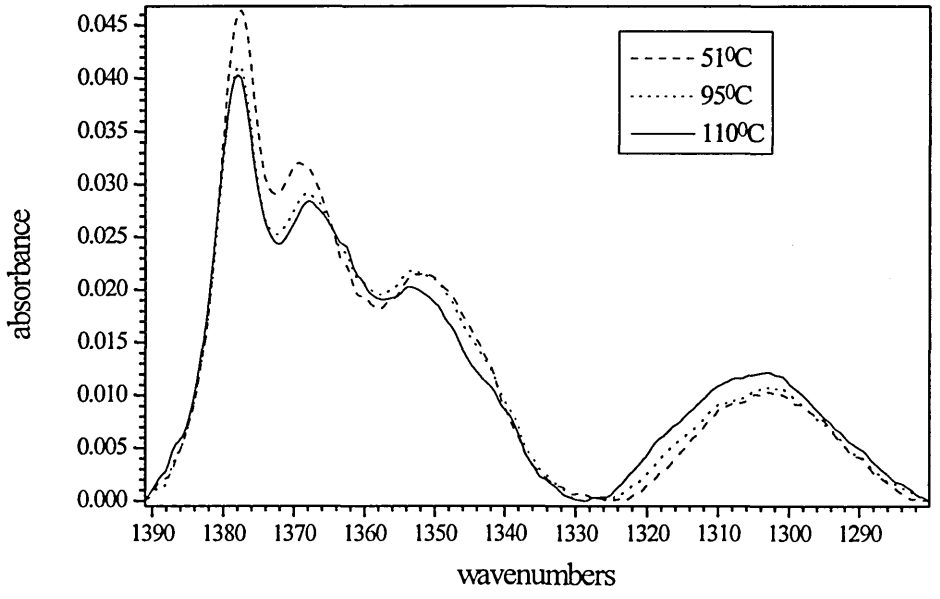

The most intense band at 1377 cm^{-1} is ascribed to the symmetric methyl bending mode of vibration. Most of the other bands are ascribed to localised methylene modes. Indeed, the band at 1354 cm^{-1} is ascribed to gg conformers, the shoulder at 1341 cm^{-1} is assigned to end gauche conformers and the bands at 1369 cm^{-1} and 1307 cm^{-1} are ascribed to gtg/gtg' conformers. Increasing the temperature from 51°C to 110°C is followed by a decrease of the absorbance of some of the infrared bands assigned to non all-trans conformers. This unexpected effect may indicate that the concentration of non all-trans conformers present in the sample is not only temperature dependent but also time dependent. This is the first sign of perfecting of the n-alkane crystals.

Second derivatives, deconvolutions and curve fitting procedures were used for the region between 1391 cm^{-1} and 1328.8 cm^{-1} (Table IV.12) and from 1328.8 cm^{-1} to 1280.1 cm^{-1} (Table IV.13) to determine with accuracy the frequencies and areas of these different bands. The minimum number of components within the infrared spectra to provide a satisfactory fit has been used for these procedures.

Table IV.12 : Curve fitting results performed on the higher frequency part of the infrared spectra of sample (1) recorded at elevated temperatures

	area		
wavenumbers cm^{-1}	T=51°C	T=95°C	T=110°C
1386	0.0173	0.0179	0.0248
1378	**0.3399**	**0.3049**	**0.3015**
1369.9	**0.2052**	**0.1773**	**0.1667**
1363.5	**0.1892**	**0.2020**	**0.2110**
1353.8	**0.1876**	**0.1940**	**0.1811**
1347.2	**0.1036**	**0.0938**	**0.0684**
1341.1	**0.0728**	**0.0776**	**0.0829**
1333.4	0.0073	0.0083	0.0008

Table IV.13 : Curve fitting results performed on the lower frequency part of the infrared spectra of sample (1) recorded at elevated temperatures

	area		
wavenumbers cm^{-1}	T=51°C	T=95°C	T=110°C
1316	0.02814	0.03614	0.05145
1310	0.05608	0.06171	0.07380
1302	0.07947	0.08740	0.1078
1295.4	0.04978	0.04519	0.04417
1289.7	0.01958	0.02446	0.03196

Some of the bands present in Table IV.12 (bold type) and Table IV.13 are shown respectively in Figure IV.60 and Figure IV.61 where their integrated absorbance (maximum value arbitrarily fixed to one) is plotted against the temperature at which the sample was annealed. The lines connecting the points are drawn only for clarification of the trends.

Figure IV.60 : Scaled area of the major infrared bands present in the higher frequency part of the spectra as a function of the temperature

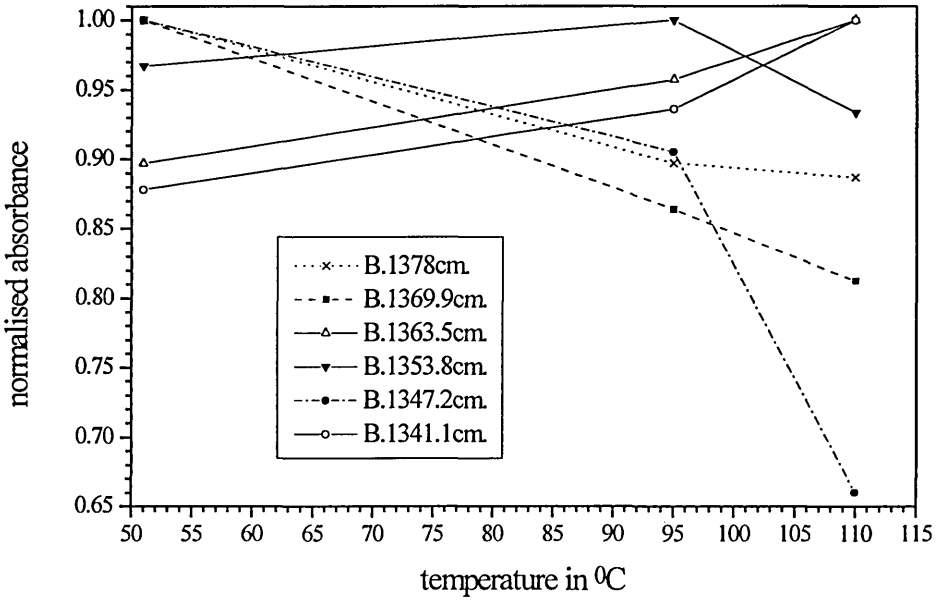

In Figure IV.60, the variation as a function of the annealing temperature of the normalised integrated absorbance of the bands at 1341.1 cm^{-1}, 1363.5 cm^{-1} and 1378 cm^{-1} is limited to around 10% of their maximum values. The normalised absorbance of the two bands at 1341.1 cm^{-1} (ascribed to the end gauche conformers) and 1363.5 cm^{-1} increases progressively with the increase of the temperature. At the same time, the normalised absorbance of the band at 1378 cm^{-1} assigned to the symmetric methyl bending mode decreases. This last band, which has been used in the past as a reference band, shows here a sensitivity to the annealing temperature. The band which is the least sensitive to the annealing process is the one at 1353.8 cm^{-1} ascribed to gg conformers. Its normalised absorbance varies within 7% of its maximum value.

On the other hand, the normalised absorbance of the two bands at 1347.2 cm^{-1} and 1369.9 cm^{-1} decreases more significantly with the increase of the temperature, respectively by around 35% and 20% of their maximum values. These bands are ascribed respectively to the fold itself and to the gtg/gtg' conformers. So, by increasing the temperature up to 110^0C, we observe a decrease in the number of gtg/gtg' conformers present originally within the n-alkane chains. Also, it seems that the number of folded chains present originally in the crystal layers decreases even though the temperature at which melting of the folded chain conformation occurs has not been reached. Changes in the conformation of the fold, due perhaps to the presence of tilted chains inside the crystal layers, may also involve a decrease in the intensity of this band at 1347.2 cm^{-1}.

Figure IV.61: Scaled area of the major infrared bands present in the lower frequency part of the spectra as a function of the temperature

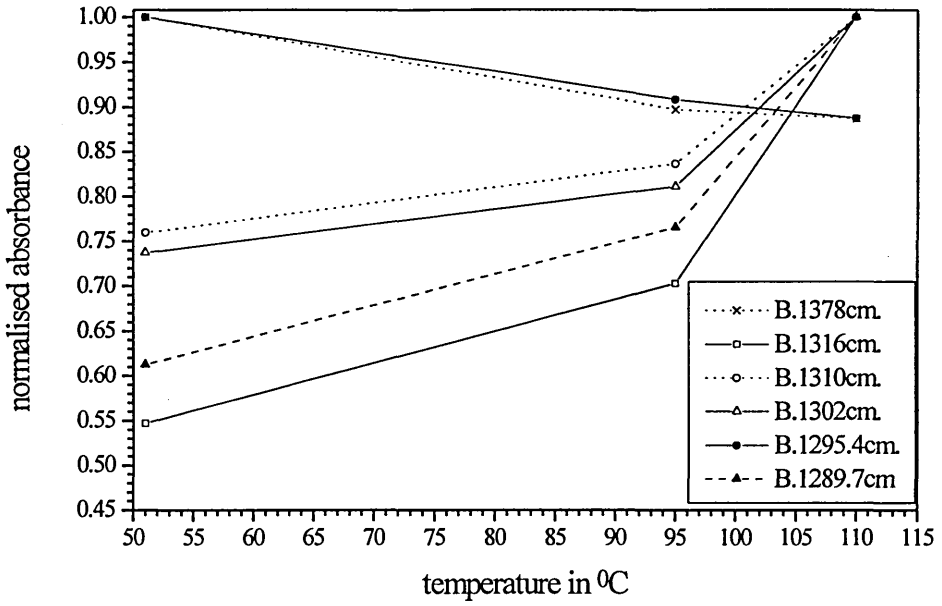

In Figure IV.61, the variation as a function of the temperature of the normalised integrated absorbance of the infrared bands present in the lower frequency part of the wagging mode region is shown. The normalised absorbance of all the bands but the one at 1295.4 cm^{-1} ascribed to the slightly off zone centre methylene wagging mode[46], increases by up to 45% of their maximum values with the increase of the temperature. A strong increase is observed after heating to 110^{0}C. Moreover, the normalised absorbance of the bands at 1302 cm^{-1} and 1310 cm^{-1}, components of the broader band at 1306 cm^{-1} usually ascribed to the gtg/gtg' conformers, increases by around 20%. This variation is in contradiction with the observation made at higher frequency where the normalised absorbance of the band at 1369.9 cm^{-1}, also ascribed to gtg/gtg' conformers, was decreasing. This experiment may point out the non-equivalence of the bands at 1369.9 cm^{-1} and at 1306 cm^{-1}. Different proportions of gtg and gtg' giving rise to these two bands may explain this effect.

IV.3.1.4.a.4.2 Low temperature spectra.

Figure IV.62 shows the wagging mode region of the infrared spectra of sample (1) recorded at -173°C, the sample being successively cooled down following annealing at each higher temperature.

Figure IV.62 : Low temperature F.T.I.R. spectra of sample (1) as a function of annealing temperature

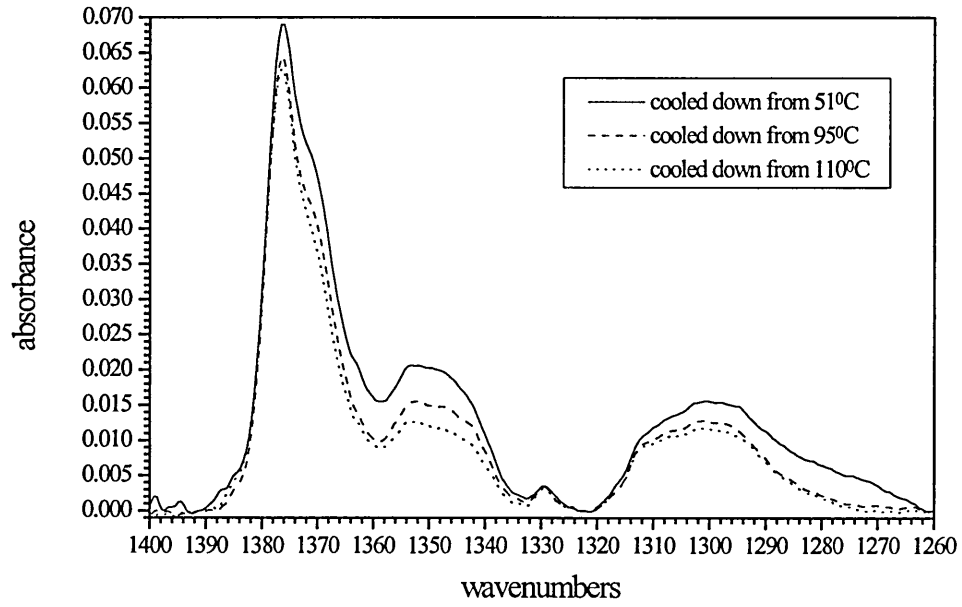

A decrease of the total absorbance of the spectra with the increase of the temperature at which the sample was annealed is observed. Again, this result is contrary to expectations for thermally activated crystal defects. Nevertheless, it may be explained by a perfecting of the crystals through annealing. The major band of this region at 1376.8 cm^{-1} is ascribed to the symmetric methyl bending mode of vibration. Most of the other infrared bands are assigned to specific conformational defects present in the non all-trans n-alkane chains.

Second derivatives (Figure IV.63), deconvolutions (Figure IV.64) and curve fitting procedures (Figure IV.65) were used in the region 1391 cm^{-1} to 1322 cm^{-1} (Table IV.14)

and from 1322 cm^{-1} to 1260.3 cm^{-1} (Table IV.15) to determine with accuracy the frequency and area of these different bands.

Figure IV.63 : Second derivative of the higher frequency part of the methylene wagging mode region of the infrared spectrum of sample (1) cooled down from 110°C.

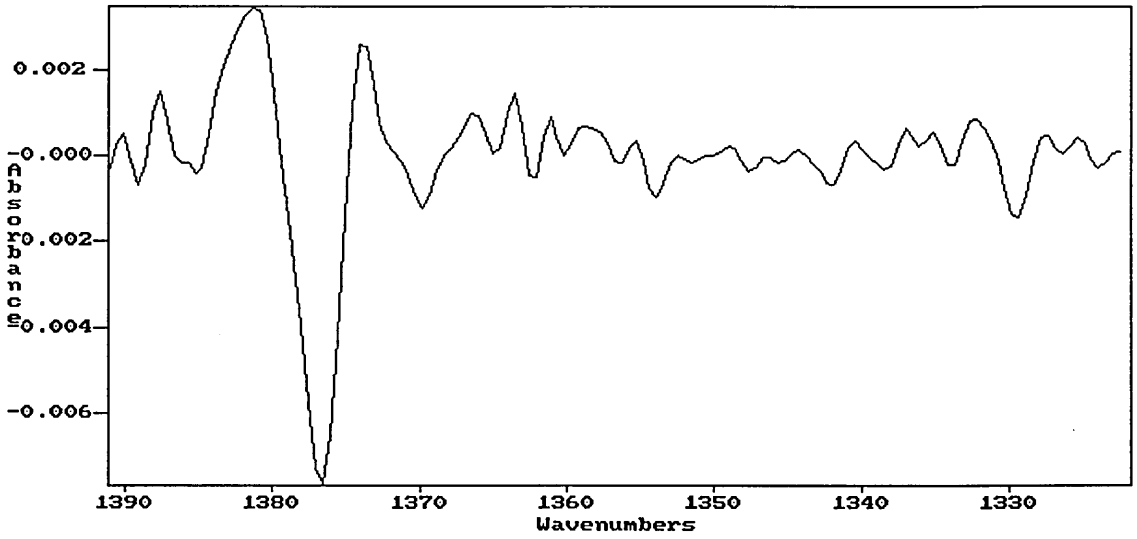

The major bands present in Figure IV.63 (second derivative of the infrared spectrum of sample (1) cooled down form 110°C) are observed at 1376.5 cm^{-1}, 1370 cm^{-1}, 1363 cm^{-1}, 1354 cm^{-1}, 1347 cm^{-1}, 1342 cm^{-1} and 1329 cm^{-1}.

Figure IV.64 : Deconvolution results for the higher frequency part of the methylene wagging mode region of the infrared spectrum of sample (1) cooled down from 110°C.

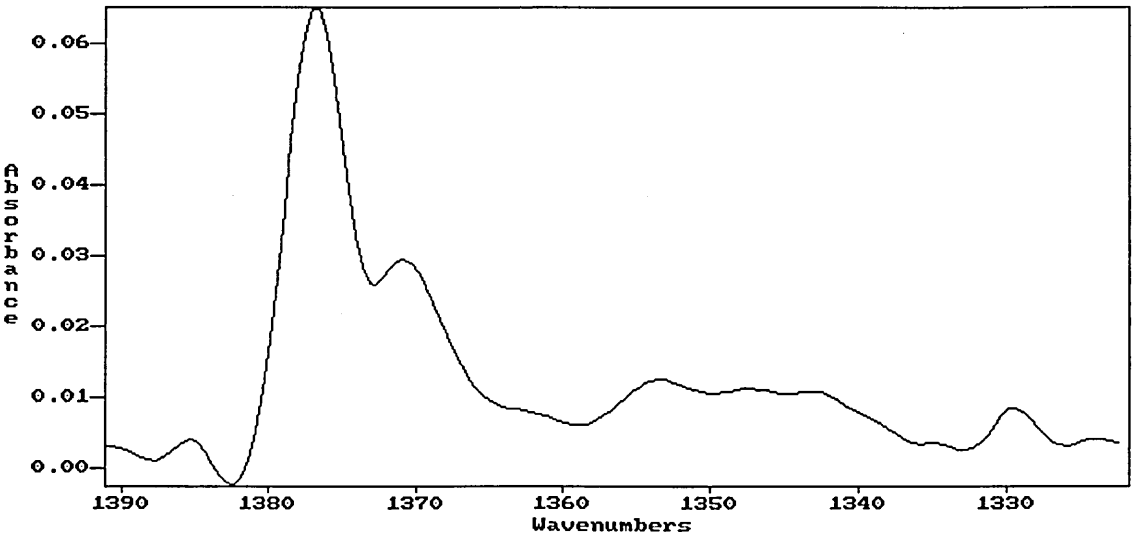

From the deconvolution of the infrared spectrum of sample (1) cooled down from 110°C, we observe in Figure IV.64 bands at 1385 cm^{-1}, 1377 cm^{-1}, 1371 cm^{-1}, 1363 cm^{-1},

1354 cm^{-1}, 1347 cm^{-1}, 1342 cm^{-1} and 1329 cm^{-1}. For the deconvolution, we chose to use for each band a Lorentzien function with full width at half height of 5.2 cm^{-1}, a Bessel apodization function and a enhancement factor of 1.6.

Figure IV.65 : Curve fitting obtained from the higher frequency part of the methylene wagging mode region of the infrared spectrum of sample (1) cooled down from 110°C.

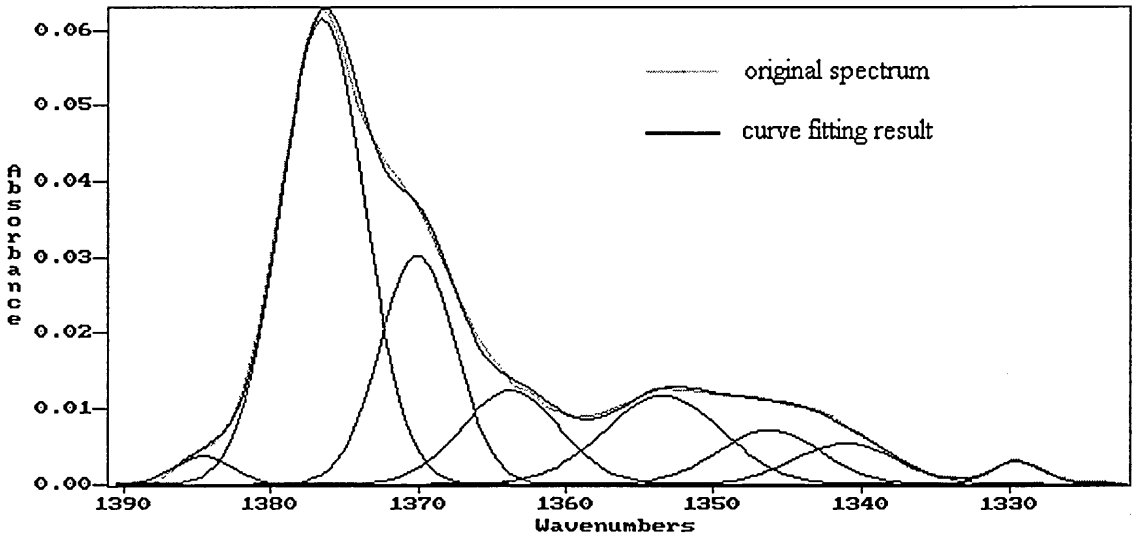

The result of the curve fitting procedure carried out on the infrared spectrum of sample (1) cooled down from 110°C is shown in Figure IV.65. The use of Gaussian functions in this procedure has been found to give better results than the use of Lorentzian functions.

Table IV.14 : Curve fitting results performed on the higher frequency part of the infrared spectra of sample (1) recorded at -173°C

	area		
wavenumbers cm^{-1}	cooled down from T=51°C	cooled down from T=95°C	cooled down from T=110°C
1384.6	0.02553	0.00776	0.01799
1376.5	**0.47213**	**0.43657**	**0.43905**
1370.1	**0.26374**	**0.2284**	**0.19424**
1363.8	**0.15762**	**0.11091**	**0.10269**
1353.4	**0.2073**	**0.13555**	**0.11603**
1346.4	**0.09256**	**0.08358**	**0.06191**
1341	**0.08268**	**0.05863**	**0.04618**
1329.2	**0.0186**	**0.01559**	**0.01314**

Table IV.15 : Curve fitting results performed on the lower frequency part of the infrared spectra of sample (1) recorded at -173°C

	area		
wavenumbers cm^{-1}	cooled down from T=51°C	cooled down from T=95°C	cooled down from T=110°C
1312.2	**0.06343**	**0.05607**	**0.05604**
1306.3	**0.08367**	**0.07098**	**0.06287**
1301	**0.07230**	**0.05797**	**0.05453**
1295.5	**0.08454**	**0.07333**	**0.06898**
1289.2	0.1007	0.05861	0.05306
1280.4	0.04485	0.01199	0.01005
1272.4	0.03816	0.00529	0.00004
1265.5	0.00531	0.00314	0.00009

Most of the bands present in Table IV.14 (bold type) are shown in Figure IV.66 where their integrated absorbance (maximum value arbitrarily fixed to one) is plotted against the temperature from which the sample was cooled down.

Figure IV.66 : Scaled area of the major infrared bands present in the higher frequency part of the low temperature spectra as a function of annealing temperature

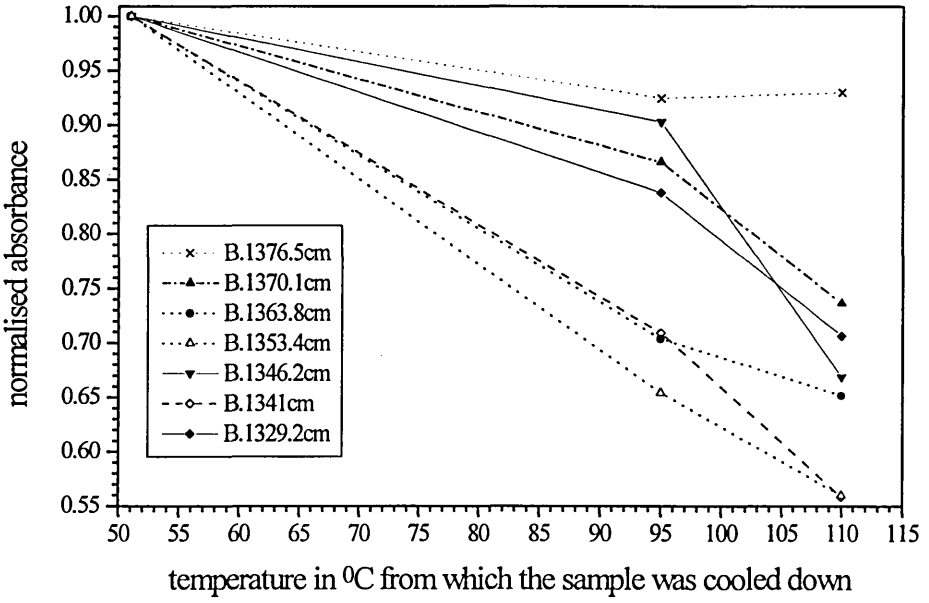

Methylene groups involved in end-gauche, double gauche (gg) or gtg/gtg' conformers are detected in the infrared spectra at respectively 1341 cm^{-1}, 1353.4 cm^{-1} and 1370.1 cm^{-1} (with another band around 1306 cm^{-1}). Two bands at 1363.8 cm^{-1} and 1329.2 cm^{-1} present in these spectra have not been previously ascribed to any specific conformations. A band present in the spectra at 1346.2 cm^{-1} has been ascribed to the tight {110} fold itself.

In Figure IV.66, we can observe each band area decreasing with the increase of the temperature at which the sample was annealed. The infrared band which seems to be the least sensitive to the annealing temperature is the one ascribed to the methyl symmetric bending mode. Its normalised absorbance decreases by 8% of its maximum value, for the sample annealed at 95°C. No changes are observed after annealing to 110°C. On the other hand, the band which seems to be the most sensitive to the first increase of the temperature, is the one at 1353.4 cm^{-1} ascribed to gg conformers. Its normalised absorbance has decreased by nearly 35% of its original value after annealing to 95°C. A further decrease up to 45% of its original value is observed after annealing to 110°C. A similar behaviour can be noticed for the band at 1341 cm^{-1} and, at least up to 95°C, for the one at 1363.8 cm^{-1}. Indeed, after annealing to 110°C, the normalised absorbance of this last band decreases only a little.

The remaining bands show a slightly different behaviour as a function of the annealing temperature. Indeed, the normalised absorbance of the bands at 1370.1 cm^{-1}, 1329.2 cm^{-1} and 1346.2 cm^{-1} decreases only by around 10% of their original value after the first increase of the temperature up to 95°C. The normalised absorbance of these bands decreases further after annealing to 110°C, respectively down to around 25% of their original value in the case of the first two and down to around 35% of its original value in the case of the last one.

The general decrease of the intensity of the bands ascribed to methylene groups involved in the vibration of specific conformers indicates a perfecting of the crystals. Also, the infrared band at 1346.2 cm^{-1} ascribed to the {110} fold is strongly affected. Changes in the conformation of the initial {110} fold may explain the changes observed in the normalised absorbance of this last band.

Some of the bands present in Table IV.15 (bold type) are shown in Figure IV.67 where their integrated absorbance (maximum value arbitrarily fixed to one) is plotted against the temperature from which the sample was cooled down.

Figure IV.67 : Scaled area of the major infrared bands present in the lower frequency part of the low temperature spectra as a function of annealing temperature

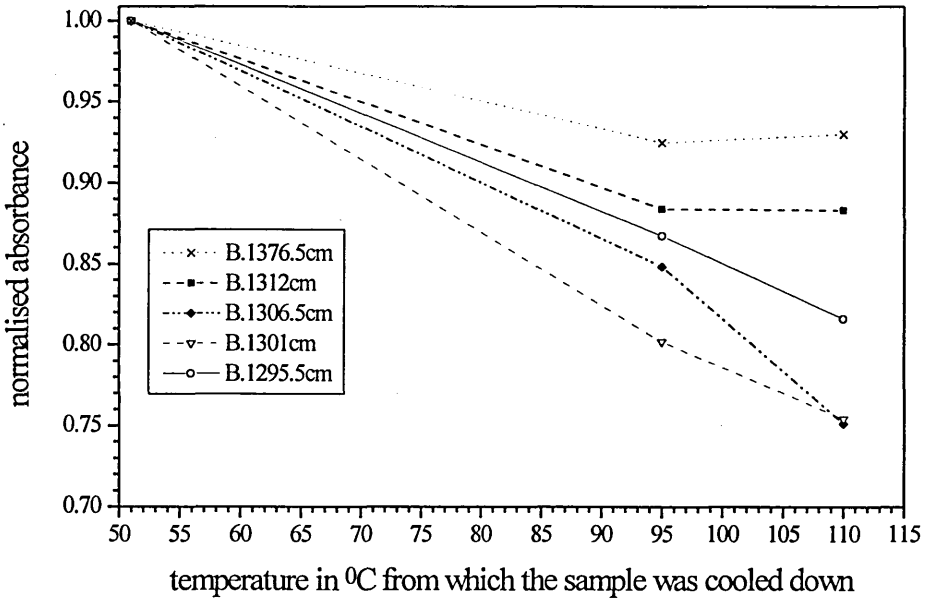

Bands at 1312 cm^{-1} (nearly resolved in the spectra), 1306.5 cm^{-1} and 1301 cm^{-1} ascribed to the gtg/gtg' defect conformations, and 1295.5 cm^{-1} (ascribed to the off zone centre methylene wagging mode) were used in the curve fitting procedures. The normalised absorbance of each band decreases with the increase of the temperature at which the sample was annealed. The normalised absorbance of the less sensitive band at 1312 cm^{-1} decreases by 12% of its original value after annealing to 95°C. It stays unchanged after annealing to 110°C. On the other hand, the normalised absorbance of the infrared bands at 1306.5 cm^{-1} and 1301 cm^{-1} decreases respectively by 15% and 20% after annealing to 95°C. A further decrease is observed, down to around 25% of their original value, after annealing to the highest temperature. Thus, contrary to the case of the high temperature spectra, the normalised absorbance of the different infrared bands assigned to gtg/gtg' conformers show here a similar behaviour as function of the temperature. Finally, a

linear decrease of the normalised absorbance of the 1295.5 cm^{-1} band is observed as function of the temperature.

Figure IV.68 shows the variation of the area of the infrared bands at 1376.5 cm^{-1}, 888 cm^{-1} and 1174 cm^{-1} ascribed respectively to the symmetric methyl bending, methyl rocking and methylene wagging modes of vibration.

Figure IV.68 : Scaled area of several infrared bands present in the low temperature spectra of sample (1) as a function of annealing temperature

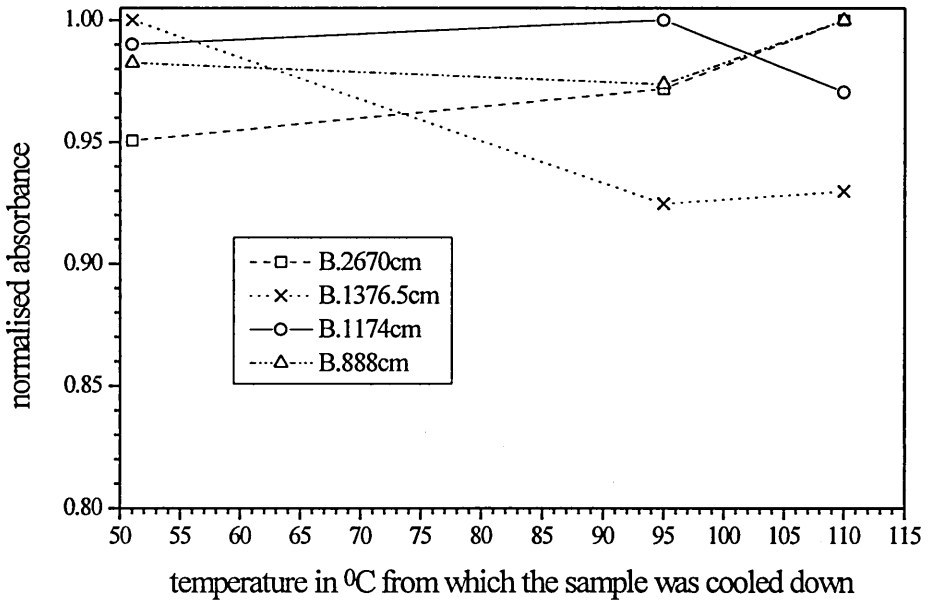

Also, the variation of the area of the broad infrared band present between 2690 cm^{-1} and 2558 cm^{-1} is shown. The normalised integrated absorbance of the three infrared bands, centred outside the wagging mode region of the infrared spectra, varies within 5% of their maximum values.

In Figure IV.69, the C-C stretching mode region of the low temperature infrared spectra of sample (1) is shown as a function of the annealing temperature.

Figure IV.69 : Low temperature infrared spectra of the C-C stretching mode region of sample (1)

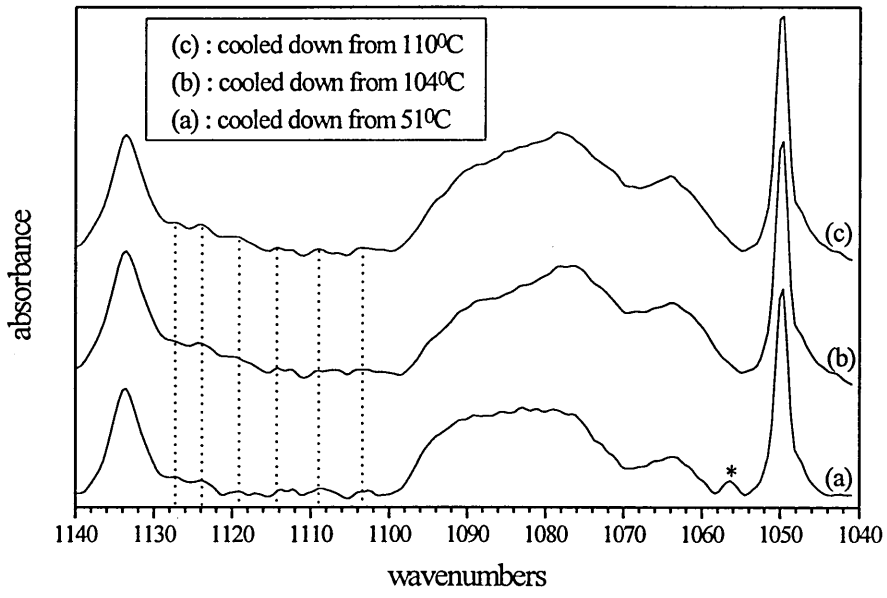

The band progression region is limited by two extreme bands at 1133 cm^{-1} and 1050 cm^{-1} ascribed[37] respectively to the in-phase stretching of all C-C bonds and the methylene twisting fundamental. Each one of the progression bands present in this region (crossed by a vertical dotted line) is ascribed to non-localised mode of vibration involving the motion of adjacent carbon atoms with the same phase difference along the n-alkane chain. The band marked by an asterisk at 1056 cm^{-1}, present in the spectrum of sample (1) cooled down from 51°C may be related to a distorted methylene twisting mode characteristic of imperfect crystal forms which may have been formed during the sample preparation (crystallisation from solution and pressure applied over the sample surface lower than 0.4 ton per cm^2). The disappearance of this band, in addition to a better resolution of the progression bands, may be seen as a perfecting of the once folded crystals inside which the concentration of remaining non-all trans conformers, which may be present in the extended part of the n-alkane chains, decreases. Finally, one can observe two different regions within the spectra. Above 1100 cm^{-1}, the progression bands are observed. Below this frequency, three broad bands at around 1089 cm^{-1}, 1078 cm^{-1} and 1064 cm^{-1} are observed. The bands at 1078 cm^{-1} and 1064 cm^{-1} were

ascribed by Krimm et al.[61] to C-C stretching modes, the first one being a fingerprint of gauche conformers present in the sample. Moreover, Wolf et al.[47] have calculated by the Green's function method the localised mode frequencies of a tight {110} fold in polyethylene. They assigned an infrared band at 1082.5 cm^{-1} to the {110} folds. Thus, in the lowest frequency part of the infrared spectra of sample (1) shown in Figure IV.69, some of the bands may be due to the presence of the {110} folds or some disorder at the ends of the chains.

Finally, we tried to identify each one of the progression bands present in this region. To achieve this, we used the frequency-phase curve for the C-C stretching modes of short chain n-alkanes from n-$C_{20}H_{42}$ to n-$C_{30}H_{62}$ determined by Snyder and Schachtschneider[39]. Then, from the frequency of each progression band present in the spectra of Figure IV.69 we were able to determine each phase difference. The phase difference φ_k, is related to the number of carbon atoms n_C, involved in the vibration of the chains and an integer k, characteristic of each progression band by the equation :

Equation IV.50

$$\varphi_k = \frac{k \times \pi}{n_c - 1}$$

Therefore, estimates for both the best series of k values and the number of carbon atoms involved in the extended part of the n-alkane chains were determined. To achieve this, we first chose an estimated number of carbon atoms present in the extended part of the n-alkane chains. In each case, we began with the highest possible number of carbon atoms (e.g. 99 for n-$C_{198}H_{398}$ in once folded form). Then, a series of k values is determined using Equation IV.50. We determined from this series the numbers of successive decreasing integers going from the highest k value to the lowest one. This completed the first step of the operation. Then, we went again through the full process using for an estimated number of carbon atoms, one less than the previous case (e.g. 98 for n-$C_{198}H_{398}$ in once folded form). A new series of k values was determined. The numbers of successive decreasing integers k was noted, completing the second step in the operation. On average, less than twenty steps are used. Once the best fit of frequencies was determined, we used the k values to determine using once again Equation IV.50, an average number of carbon atoms involved in the all-trans part of the

n-alkane chains. A $^{+}/_{-}$ 1 error bar is estimated for the values of the integers k. In the case of sample (1), the average number of carbon atoms involved in the extended part of the n-alkane chains was estimated to be equal to 90 $^{+}/_{-}$ 16. The frequency of each of these progression bands is plotted against the integer k, in Figure IV.70. Also, the frequency of each of these bands was fitted by a third order polynomial curve Y, shown by the black line.

Figure IV.70 : Frequency of the progression bands ascribed to the C-C stretching mode against k, integer, for sample (1) cooled down from 110^{0}C.

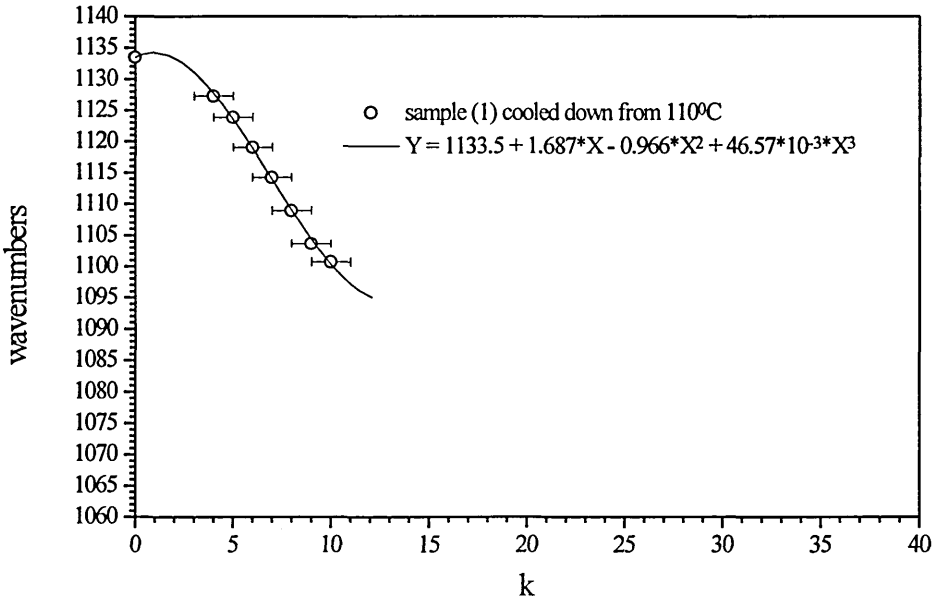

IV.3.1.4.a.5 Interpretation.

The tilting of the chains inside the crystals of sample (1) was expected to lead to an increase in the number of defects present in the n-alkane chains, and more especially at the chain ends.

In the low temperature spectra, a general decrease of the absorbance of all the bands present in the methylene wagging mode region was observed. Particularly, the normalised absorbance of the bands ascribed to the end gauche and gg conformers decreases by around 45% of their initial values through the heating process. Furthermore, the normalised absorbance of the band assigned to the {110} fold also

decreases by nearly 35% of its initial value. These results are opposite to the ones expected for thermally activated crystal defects.

On the other hand, in the high temperature spectra, the absorbance of the band ascribed to the end gauche conformers is found to increase by around 10% of its original value with the increase in temperature. This increase may be linked with the tilting of the n-alkane chains inside the crystal layers. Also, the absorbance of the bands ascribed to the gtg/gtg' conformers in the low frequency part of the spectra decreases by around 20% with the annealing temperature while the absorbance of the one at higher frequency increases by around 25%. This observation indicates the non equivalence of the high and low frequency bands both previously ascribed to the gtg/gtg' conformers. Nevertheless, a greater decrease of the normalised absorbance (35% of its initial value) is noted for the band ascribed to the {110} fold. This may be explained by a change in the conformation of the original {110} fold. Also, it may be explained by a partial transformation from folded to extended chain conformations due to the increase of the annealing temperature. Contrary to previous work[79], no increase of the tilt angle was observed with the increase of the annealing temperature. Differences in the sample preparations may explain this difference. Indeed, our samples are thin films produced by applying slight pressure to a mat formed after crystallisation from solution, whereas for previous studies no applied pressure was needed[79].

Nevertheless, all the above observations seem to indicate a perfecting process of the n-alkane crystals occurring at elevated temperatures This may predominate over the formation of chain end defects due to the chain tilting, masking the latter effect in the infrared data.

IV.3.1.4.b Tilting of n-alkane chains at 95^{0}C.

In a previous work[79], an n-$C_{198}H_{398}$ sample crystallised from solution in once folded form was heated from room temperature to the melting point at 5^{0}C per minute. Above 90^{0}C, the n-alkane chains were found to tilt from the crystal surfaces. Using S.A.X.S. measurements, the tilt angle was found to be around 3^0 at 90^{0}C. Moreover, by increasing further the temperature, the tilt angle was found to increase up to 24^0 at around 116^{0}C.

In order to observe by the means of vibrational spectroscopy conformational changes associated with the tilting of n-alkane chains from the crystal surfaces, we prepared a sample containing the lowest possible number of crystal defects. To achieve this, sample (1) was annealed at 85°C for 20 hours before cooling it down to -173°C. Doing so, we hoped to obtain crystals with the highest degree of perfection in the once folded form with the n-alkane chain axis still perpendicular to the surface of the crystal layers. Then, after heating this sample to 95°C for around 2 minutes, 10 minutes and 64 hours respectively, it was successively cooled down to -173°C. Doing so, we hoped to obtain tilted n-alkane chains in the once folded form. Therefore, changes observed in the infrared spectrum of sample (1) cooled down from the highest temperature could be assigned to differences in the concentration of rotational isomers due to the chain tilt rather than to changes in the concentration of crystallographic defects and non all-trans conformers due to the increase of the thermal population of rotational isomers with increasing the annealing temperature. For a similar sample heated at 95°C, Boda[79] found that the n-alkane chains were tilted from the crystal surfaces with an angle near to 7°.

IV.3.1.4.b.1 S.A.X.S. measurements.

Sample (1) was annealed at 95°C for 2 minutes, 10 minutes and 64 hours. The layer periodicities were found to be equal respectively to 124.3 $^{+}/_{-}$ 0.6 Å, 120.5 $^{+}/_{-}$ 1.7 Å and 120.5 $^{+}/_{-}$ 0.6 Å. After annealing at 85°C for 20 hours and cooling down to -173°C, sample (1) was believed to be in a once folded conformation with the chain axis perpendicular to the crystal surfaces, the fold in the middle of the chains and also, with the lowest possible concentration of crystallographic defects. After annealing at 95°C for around 2 minutes, no tilt angle was detected from S.A.X.S. measurements. After 10 minutes and 64 hours at 95°C, the n-alkane chains are still in the once folded form but they were now tilted from the crystal surfaces with an angle close to 14.9° with errors, respectively, of $^{+}/_{-}5^{0}$ and $^{+}/_{-}3^{0}$. Within the experimental errors, no differences in the tilt angle of the n-alkane chains were found after 10 minutes and 64 hours at 95°C.

IV.3.1.4.b.2 Infrared spectroscopy : low temperature spectra.

Infrared spectra were recorded at -173°C on cooling sample (1) after annealing at successively higher temperatures. After each stage, a part of sample (1) was taken away from the sample holder to perform S.A.X.S. experiments. Therefore, due to the displacement of the sample during this manipulation, the area sampled by the infrared beam will have changed. To be able to compare the intensity differences of the different infrared spectra we need to use a reference band which is not sensitive to changes in the chain conformation. We have not succeeded in finding such a band in the infrared spectra of n-paraffins. Nevertheless, we chose to use the integrated area of the broad band between 2689.9 cm^{-1} and 2557.8 cm^{-1} to normalise the different spectra of sample (1) recorded at -173°C. Indeed, in the infrared spectra recorded at -173°C, the area of this band has been found to vary by less than 5% over a range of samples and annealing process. This broad band is certainly one of the least sensitive infrared bands to changes in chain conformation and crystal structure. The methylene wagging mode region of these normalised spectra is shown in Figure IV.71 after baseline subtraction. A combination of linear baselines was used, with reference points of 1391 cm^{-1}, 1322 cm^{-1} and 1260.3 cm^{-1}.

Figure IV.71 : Low temperature F.T.I.R. spectra of sample (1) as a function of annealing temperature

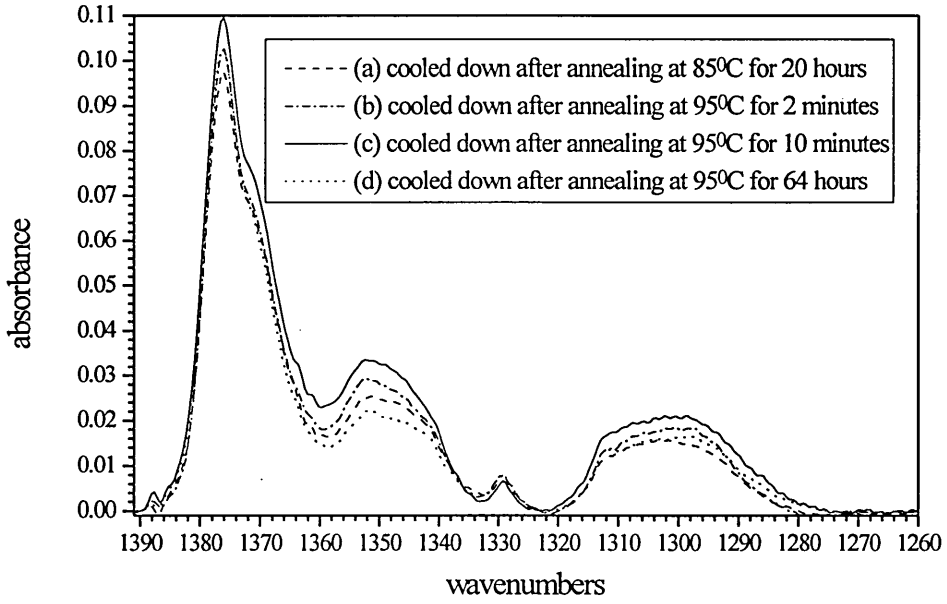

The absorbance of the different bands present in this region of the spectra increases with both the annealing temperature and the initial time spent at that temperature. Indeed, the overall absorbance in the wagging mode region is highest after annealing 10 minutes at 95°C. Nevertheless, a decrease of the overall intensity in this region is observed with increasing time spent at 95°C. After 64 hours annealing at 95°C, the overall absorbance of the spectrum of sample (1) has decreased and is now the lowest of the series. The increase followed by the decrease of the overall absorbance of the infrared spectra through the isothermal annealing process can be easily observed by looking at the absorbance of the bands at around 1353 cm^{-1}, 1347 cm^{-1} and 1341 cm^{-1}. Second derivatives, deconvolutions and curve fitting procedures were therefore monitored from 1391 cm^{-1} to 1322 cm^{-1} (Table IV.16) to determine with accuracy the frequency and area of all the different bands.

Table IV.16 : Curve fitting results performed on the infrared spectra of sample (1) recorded at -173°C

	area			
wavenumbers in cm^{-1}	cooled down from 85°C / 20 hours (a)	cooled down from 95°C / 2 minutes (b)	cooled down from 95°C / 10 minutes (c)	cooled down from 95°C / 64 hours (d)
(1) 1376.5	**0.64351**	**0.67672**	**0.73271**	**0.69335**
(2) 1370.2	**0.33528**	**0.33969**	**0.37576**	**0.31776**
(3) 1364.1	**0.20679**	**0.21863**	**0.2656**	**0.19443**
(4) 1353.7	**0.18245**	**0.21245**	**0.25077**	**0.15882**
(5) 1347.1	**0.14554**	**0.16952**	**0.19714**	**0.1222**
(6) 1340.9	**0.12389**	**0.11473**	**0.12772**	**0.10485**
1329.4	0.03795	0.04139	0.02747	0.04199

The bands present in Table IV.16 and identified by an arbitrary number in brackets are shown in Figure IV.72 where their integrated absorbance (maximum value arbitrarily fixed to one) is plotted as a function of both the time and the temperature. The indices (a), (b), (c) and (d) in Figure IV.72 refer to those in Table IV.16.

Figure IV.72 : Normalised area of the major infrared bands present in the low temperature spectra as a function of both annealing temperature and time.

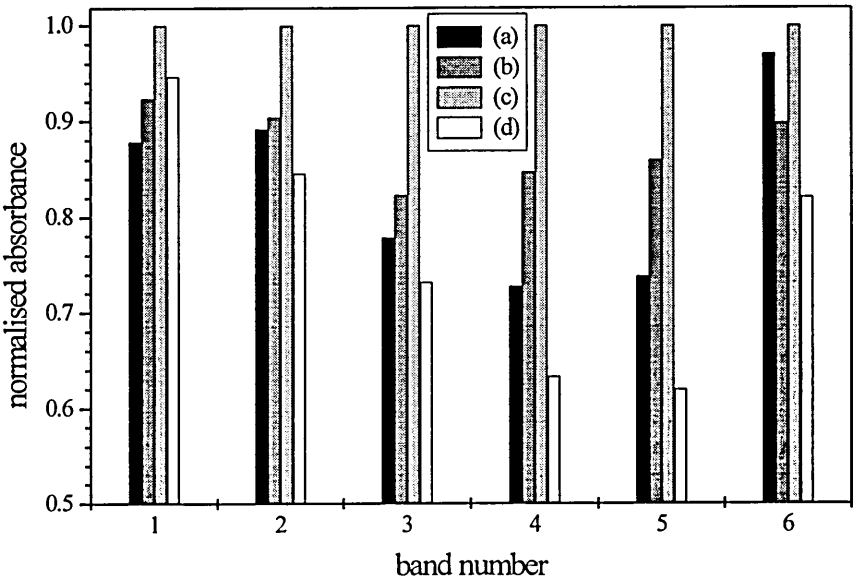

We can observe in Figure IV.72 that the increase of the annealing temperature from 85°C to 95°C (up to 10 minutes) is reflected in the infrared spectra (a), (b) and (c) by an increase of the integrated normalised absorbance of most the bands assigned to non all trans conformers and so, by an increase in their concentrations in sample (1). But, a small decrease of the absorbance (6%) of the 1341 cm^{-1} band assigned to the end gauche conformers is observed going from spectrum (a) to spectrum (b). Nevertheless, in all the cases, the highest value of the normalised absorbance is observed in the spectrum of the sample after annealing at 95°C for 10 minutes. Indeed, even in the case of the 1341 cm^{-1} band, the normalised absorbance increases by 2%. Then, as observed directly from the spectra of Figure IV.71, Figure IV.72 confirms that the normalised absorbance of the bands assigned to non all trans conformers is at its lowest value in the spectrum of the sample after annealing at 95°C for 64 hours. Thus, after annealing at the higher temperature and for the longest time, the concentration of non all-trans conformers has decreased below the initial concentration observed after annealing at 85°C for 20 hours. It is interesting to note that the normalised absorbance of the band ascribed to the symmetric methyl bending mode at 1376 cm^{-1} follows a similar pattern. Indeed, the normalised absorbance increases with both the increase of the annealing temperature and the time spent at this temperature. Nevertheless, there is a difference in behaviour, since in the spectrum (d) the normalised absorbance of this band decreases but does not reach its minimum value.

IV.3.1.4.b.3 Interpretation.

The increase in temperature from 85°C to 95°C for 2 minutes causes an increase of the absorbance of most of the bands present in the methylene wagging mode region of the infrared spectrum recorded at -173°C. S.A.X.S. experiments have shown that, at this point, the n-alkane chains are still perpendicular to the crystal surfaces. The increase we observe in the concentration of non all-trans conformers may be due to the increase of the thermal population of rotational isomers occurring at this higher temperature.

Leaving the sample at the same temperature (95°C) but for a longer time (10 minutes), a strong increase of the absorbance of all the bands is observed. From S.A.X.S. experiments we know that the n-alkane chains are now tilted form the crystal surfaces.

They are still in a once folded chain conformation. At least two explanations may be offered. First, the jump in the normalised absorbance of all the infrared bands may be linked to the tilting of the n-alkane chains in sample (1). In this way, tilting of the chains inside n-alkane crystals occurs through a disordering process which allows the formation of the tilt. This disorder does not preferentially affect the ends of the n-alkane chains. On the other hand, the previous annealing of sample (1) at 95^{0}C for 2 minutes may not have been long enough to allow thermal equilibrium to take place. Therefore, the increase in absorbance may be expected at this point, as thermal equilibrium is approached.

Leaving the sample at 95^{0}C for the longest time (64 hours), a general decrease of the absorbance is observed. Furthermore, at this point, the absorbance of each infrared band assigned to non all-trans conformers is at its lowest value for this sequence of measurements. From S.A.X.S. experiments, we know that the n-alkane chains are tilted from the crystal surfaces with the same angle as found for the previous annealing time. Also, the chains are still in the once folded chain conformation. This decrease can thus be explained, once again, by a perfecting of the n-alkane crystals in the last stage of this experiment. Therefore, the presence of tilted chains inside n-alkane crystals does not induce a higher concentration of non all-trans conformers, either inside or at the ends of the chains. On the other hand, the onset of tilted n-alkane chains occurs through a temporary increase of the concentration of these conformers.

Furthermore, this experiment shows that the structure of once folded n-alkane crystals inside which the chains are perpendicular to the crystal surfaces may have intrinsically higher probabilities for non all-trans conformers than once folded n-alkane crystals with the chains tilted from the crystal surfaces. Thus, the tilting of the chains inside n-alkane crystals may be seen as a process by which n-alkane chains tend to adopt a more perfect conformation, the nearest possible to the all-trans form. Finally, the tilting of the n-alkane chains from the crystal surfaces may change the conformation of the {110} fold present initially in the middle of the chains. This may explain the observed decrease of the absorbance of the infrared band ascribed to the {110} folds. As no low frequency Raman spectra were recorded for sample (1) after annealing at 95^{0}C for 64 hours, the number of carbon atoms composing the all-trans stems characteristic of the lamellar

crystals has not been determined. Changes in the lamellar thickness may also have occurred in the final annealing stage.

IV.3.1.4.c Conclusion.

We tried to observe conformational changes related to the tilting of the n-alkane chains inside the crystals of sample (1) using infrared spectroscopy. Infrared spectra were recorded at elevated temperatures and at -173^{0}C. Also, chain conformation and tilt angle were determined by low frequency Raman spectroscopy and S.A.X.S. measurements carried out at room temperature. Contrary to the results obtained in previous work, the value of the angle by which the n-alkane chains tilt from the crystal surfaces was not found to increase with increasing annealing temperature. A 15^0 tilt angle was found in all the cases. The degree of disorder in the n-alkane crystals was found to be dependent on the annealing temperature and on the period of time spend at this temperature. By successively increasing the annealing temperature and cooling down sample (1) to -173^{0}C, we observed a perfecting of the crystals which may predominate over the formation of non all-trans conformers due to the chain tilting. Therefore, we tried to obtain the most perfect crystals possible by annealing sample (1) at 85^{0}C for 20 hours. Then, we increased the annealing temperature up to 95^{0}C for different periods of time. At this temperature, tilting of the n-alkane chains was believed to occur. For the shorter period of time, no chain tilt was detected by a S.A.X.S. experiment but, nevertheless, an increase in the number of non all-trans conformers was observed by infrared spectroscopy. Then, after a longer time at the same temperature, a strong increase in the number of these conformations was detected and n-alkane chains were found to be tilted from the crystal surfaces by around 15^0. Finally, after the longest time spent at 95^{0}C, a general decrease in the number of non all-trans conformers was observed by infrared spectroscopy, S.A.X.S. measurements indicating that n-alkane chains were remaining tilted from the crystal surfaces by an angle of 15^0. Thus, the tilting of the n-alkane chains seems to occur in a two step process. First, an increase of the disorder is necessary to create tilted chains. Secondly, once the chains are tilted, they try to adopt a more stable conformation. By doing so, the concentration of defects present in the n-

alkane chains is reduced. Also, changes in the initial {110} fold conformations seem to occur.

IV.3.1.5 **Transition from n-$C_{198}H_{398}$ in once folded to extended form.**

After annealing sample (1) at 110^{0}C, n-alkane chains were found to tilt from the crystal surfaces with an angle near to 15^0. The transformation from folded to extended crystals is expected around 119^{0}C, followed by the formation of the tilted extended form. Previous works have shown that extended chains formed through this transition were tilted[20,25,79,91] from the crystal surfaces by an angle of approximately 35^0. Also, the melting point of the extended form crystals was determined[16] to be 126.7 $^+/_-$ 0.3 ^{0}C. In order to study this transition, we annealed sample (1) successively at 112^{0}C and 124^{0}C, in each case followed by cooling down to -173^{0}C.

IV.3.1.5.a S.A.X.S. experiments.

After annealing sample (1) at 112^{0}C, we believe that the n-alkane chains were in a tilted once folded conformation. After annealing at the highest temperature, 124^{0}C, we used S.A.X.S. measurements to determine the layer periodicity. It was found to be equal to 248.1 $^+/_-$ 1.3 Å. The alkane chains were thus in the extended form with the chain axis tilted from the crystal surfaces with an angle approximating 12 $^+/_-$ 3 ^{0}. Once again, the value of the tilt angle is smaller than the one expected, on the basis of previous work[79].

IV.3.1.5.b Infrared spectroscopy.

IV.3.1.5.b.1 Low temperature infrared spectra.

The methylene wagging mode region of the infrared spectra of sample (1) recorded at -173^{0}C is shown in Figure IV.73.

Figure IV.73 : Low temperature F.T.I.R. spectra of sample (1) cooled down from 112°C and 124°C

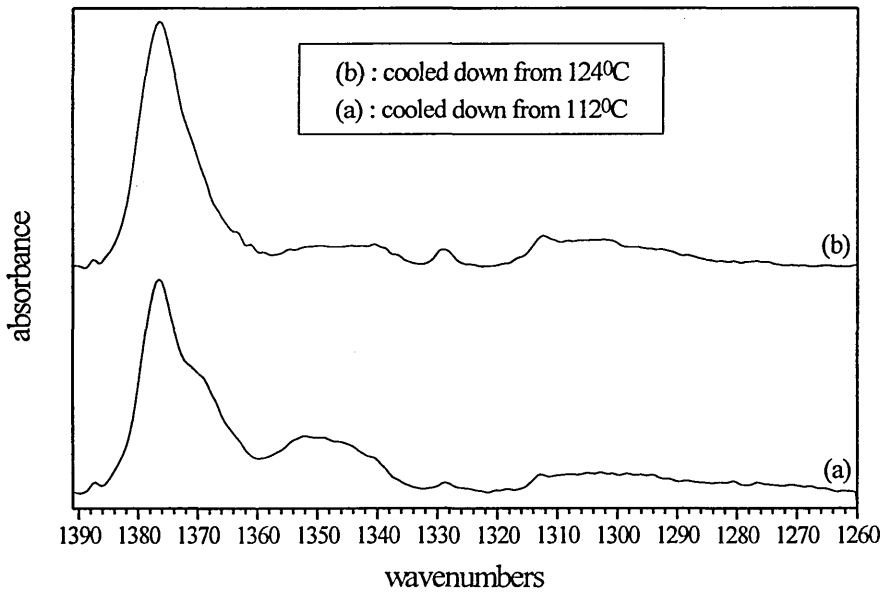

The low temperature infrared spectrum of sample (1) cooled down from 112°C is believed to be characteristic of n-$C_{198}H_{398}$ samples in tilted once folded form. The low temperature infrared spectrum of sample (1) cooled down from 124°C is believed to be characteristic of n-$C_{198}H_{398}$ samples in tilted extended form. In both cases, a strong band is present at 1376.5 cm^{-1} and is ascribed to the methyl symmetric bending mode. Also, two weak bands at 1329 cm^{-1} and 1312 cm^{-1} are present in both spectra. On the other hand, a clear difference in the intensity of the bands present in the spectra at around 1370 cm^{-1}, 1354 cm^{-1} and 1346 cm^{-1} can be observed. The intensity of these bands, assigned respectively to the gtg/gtg' conformers, gg conformers and {110} fold conformation, is greater in the spectrum of sample (1) cooled down from 112°C. Therefore, from the above observation it seems that the extended and once folded forms can be identified from their low temperature infrared spectra. A more precise comparison of the concentration of non all-trans conformers present in n-$C_{198}H_{398}$ extended and folded form crystals will be presented later in this chapter.

Due to the poor quality of the infrared spectrum below 1200 cm^{-1} of sample (1) cooled down from 112°C, we used in the following section the infrared spectrum of sample (1)

cooled down from 110°C, as determined previously during the study of the tilting of the n-alkane chains as a function of the annealing temperature. Thus, the C-C stretching mode region of the infrared spectra of sample (1) cooled down from 110°C and 124°C is shown in Figure IV.74. This region is limited by two infrared bands at 1133 cm^{-1} and 1050 cm^{-1} as noted earlier (see Figure IV.69).

Figure IV.74 : Low temperature C-C stretching mode region of the infrared spectra of sample (1)

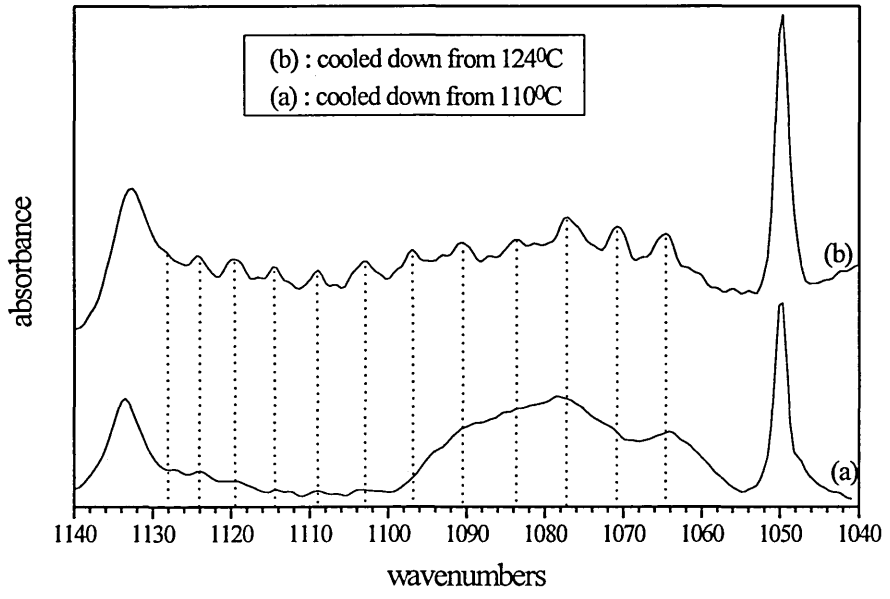

In the case of the infrared spectrum of sample (1) cooled down from 124°C additional bands present between these two previous bands are observed. They are, as noted earlier, progression bands. The presence of these progression bands through the full range of the C-C stretching mode region of the spectrum of sample (1) cooled down from 124°C is characteristic of the extended chain conformation in n-alkane crystals. Nevertheless, the weak intensity and poor regularity of some of these bands may be indicative of poor quality of these extended form crystals. In the case of sample (1) cooled down from 110°C where the n-alkane chains are in the once folded form, only the progression bands present above 1100 cm^{-1} were detected. Furthermore, their frequencies seem to correspond to the ones of the bands present in the spectrum of the extended form crystals. This observation may indicate that in the case of the once folded

form sample, the two all-trans parts of the chains going through the crystal layers and linked by the {110} folds correspond to the progression bands observed at the same frequencies in the case of the extended form sample. Indeed, in the infrared spectrum of n-$C_{198}H_{398}$ crystallised in extended form, where the number of carbon atoms present in the all-trans part of the chains going through the crystal layers is similar to the one present in n-$C_{198}H_{398}$ in once folded form, the value of the frequency shift between each successive progression band should be about twice the value found in the last case.

Finally, the virtual absence of the broad bands at around 1089 cm^{-1}, 1078 cm^{-1} and 1064 cm^{-1} in the spectrum of sample (1) cooled down from 124^{0}C seems to support the assignment of these bands to gauche conformers present at the crystal surfaces of the sample and, perhaps for some of them, more specifically to the {110} fold.

In the case of sample (1) cooled down from 124^{0}C, estimates of both the best series of k values and the number of carbon atoms involved in the extended part of the n-alkane chains were determined. A $^+/_-1$ error bar is estimated for the values of the integers k. The average number of carbon atoms involved in the extended part of the n-alkane chains was estimated to be equal to 191 $^+/_-$ 8. The frequency of each of these progression bands is plotted against k, integer, in Figure IV.75. Also, the frequency of each of these bands was fitted by a third order polynomial curve Y, shown by a black line.

Figure IV.75 : Frequency of the progression bands ascribed to the C-C stretching mode against k, integer, for sample (1) cooled down from 124°C.

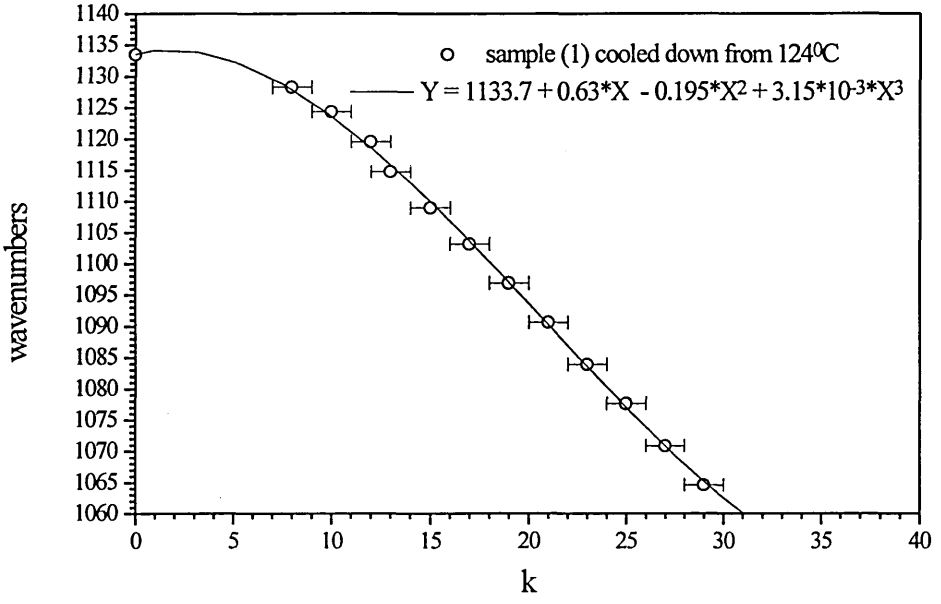

IV.3.1.5.b.2 Series of elevated temperature infrared spectra.

Sample (1) was annealed at 110°C for one hour. Then, it was heated up from 110.4°C to 121.6°C with a heating rate of 0.4°C/minute. A spectrum was recorded every four minutes (or every 1.6°C). It took a total of three minutes fifty five seconds to record the run. The full series of infrared spectra is shown in Figure IV.76.

Figure IV.76 : F.T.I.R. spectra of sample (1) heated up at 0.4°C.min^{-1} between 110.4°C and 121.6°C.

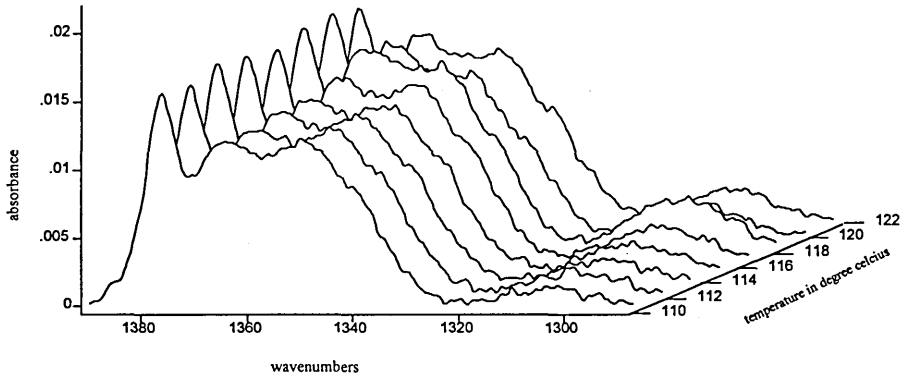

Apart from the band at 1377.4 cm^{-1} ascribed to the methyl symmetric bending mode, all the bands present in these infrared spectra are assigned to non all trans conformers. The broad band at around 1307 cm^{-1} with the one at 1365.4 cm^{-1} are assigned to the vibration of methylene groups involved in gtg/gtg' conformers. The band around 1351 cm^{-1} is assigned to the gg conformers. Finally, the one at 1341.3 cm^{-1} is assigned to end gauche conformers. Due to the poor quality of these spectra, we did not try to determine the exact area and frequency of these bands using deconvolution and curve fitting procedures. In fact, we simply determined the peak frequency for each band, as plotted against the temperature in Figure IV.77 (maximum value arbitrarily fixed to one).

Figure IV.77 : Normalised maximum intensity of the major bands present in the infrared spectra of sample (1) heated from 110.4°C to 121.6°C at 0.4°C/minute

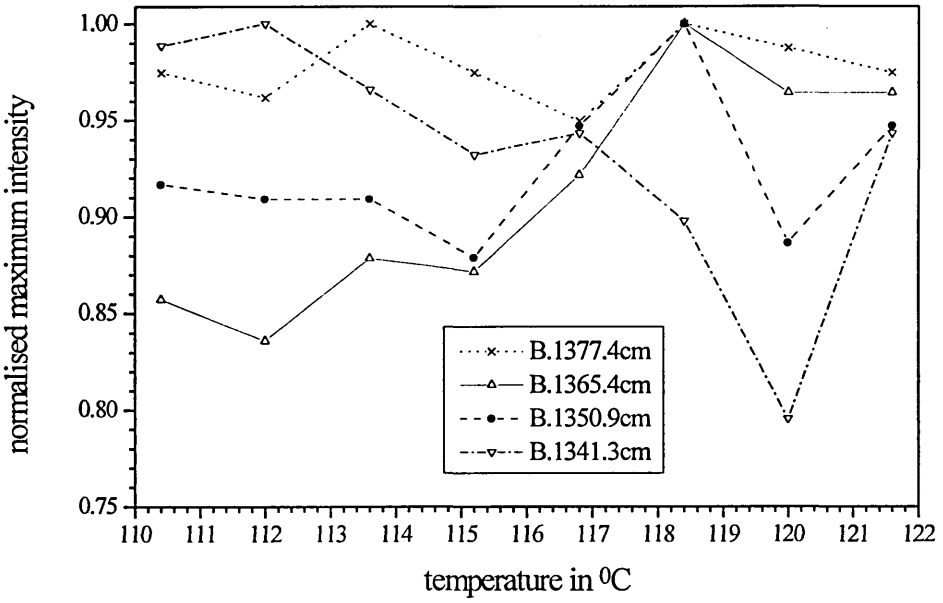

The normalised peak height of the 1377.4 cm^{-1} band varies within 5% of its maximum value over the temperature range used. In the wagging mode region, this infrared band is the least sensitive to the increase in temperature. At the same time, the normalised peak height of the band at 1350.9 cm^{-1} ascribed to the gg conformers increases by roughly 10% of its maximum value. Its maximum is reached at 118.4°C. Indeed, a further increase of the temperature above 118.4°C is followed by a decrease of its normalised intensity. The normalised peak height of the band at 1365.4 cm^{-1} ascribed to gtg/gtg' conformers increases by around 15% of its maximum value between 110.4°C and 121.6°C. Its maximum is reached at 118.4°C. In the case of the 1307 cm^{-1} band (not plotted in Figure IV.77 to improve the clarity of the figure) also ascribed to gtg/gtg' conformers, the normalised peak height was found to increase by more than 60% of its maximum value over the temperature range used. Its maximum is reached, once again, at 118.4°C. Above 118.4°C, a decrease of the peak height by around 50% of its maximum value is detected. On the other hand, the normalised peak height of the 1341.3 cm^{-1} band assigned to the end gauche conformers decreases by around 20% with

increasing temperature up to 120°C. In the last spectrum recorded at 121.6°C, its value finally increases by around 15%.

By increasing the temperature up to 119°C, the temperature at which the transition occurs, the number of the non all-trans conformers positioned in the interior of the n-alkane chains increases. The highest concentration of non all trans conformers is detected at the transition temperature. Within a few degrees above this transition, the concentration of these conformers is reduced. On the other hand, the concentration of end gauche conformers does not follow the same pattern. Indeed, a decrease in the concentration of end gauche conformers by nearly 20% of its maximum value is observed with the increase in temperature up to 120°C. Once again, this observation is contradictory to the results which were expected on the basis of thermally activated non all-trans conformers.

IV.3.1.5.c Conclusion

Using F.T.I.R spectroscopy we can identify, from the methylene wagging mode region of the low temperature spectra, once folded crystals from the extended form. Indeed, the absorbance of the infrared bands assigned to the methylene groups involved in non all-trans conformers is clearly lower in the case of the extended form crystals. Moreover, in the next section, we will use this region of the infrared spectra to estimate the disorder present in each of the different crystal forms. Also, in the wagging mode region of the infrared spectra recorded at elevated temperatures, the absorbances of the bands assigned to non all-trans conformers are found to be sensitive to the phase transition occurring between the two different crystal forms. At this transition, a maximum in the absorbance of the bands ascribed to non all-trans conformers placed in the interior of the n-alkane chains is observed. On the other hand, the absorbance of the band assigned to end gauche conformers decreases up to the transition. The transition from once folded to extended chain crystals thus occurs through a disordering process involving essentially the internal bonds of the n-alkane chains. Also, at the transition, the disorder reaches a local maximum.

By studying the C-C stretching mode region of the low temperature infrared spectra we can differentiate the once folded form crystals from the extended form. Indeed, the

presence of progression bands through the full region and the absence of infrared bands at around 1078 cm^{-1} and 1064 cm^{-1} are a fingerprint of the extended chain crystals. Also, from the identification of each one of these progression bands, we estimate the number of carbon atoms involved in the extended part of the n-alkane chains in both once folded and extended forms to be respectively 90 $^{+}/_{-}$ 16 and 191 $^{+}/_{-}$ 8. These numbers of carbon atoms can be compared with the ones determined from both low frequency Raman spectroscopy and S.A.X.S. measurements. In the case of the once folded crystals, the numbers of carbon atoms determined by S.A.X.S. measurements and Raman spectroscopy are respectively 97 $^{+}/_{-}$ 1 and 98 $^{+}/_{-}$ 2. In the case of the extended form crystals, the numbers of carbon atoms determined from the S.A.X.S. experiment is 194 $^{+}/_{-}$ 1. Thus, infrared spectroscopy, S.A.X.S. techniques and low frequency Raman spectroscopy give similar results for the number of carbon atoms present in the chain stem of both once folded and extended form crystals

IV.3.2 Sample (2) : n-$C_{198}H_{398}$ crystallised in extended form.

IV.3.2.1 S.A.X.S. measurements.

The calculated value of the crystal thickness for n-$C_{198}H_{398}$ in the extended chain conformation is 254 Å. The layer periodicity corresponding to sample (2) was found to be equal to 253.3 $^{+}/_{-}$ 1.3 Å. This value is in very good agreement with the calculated one. Within sample (2) crystals, n-alkane chains are in an extended form with the chain axis perpendicular to the crystal surfaces. We note that three orders of diffraction were observed on the S.A.X.S. patterns for an exposure time of 25 hours.

S.A.X.S. measurements were made on sample (2) annealed at 115^{0}C. The average layer periodicity was found to be equal to 253.7 $^{+}/_{-}$ 1.2 Å. This value is similar to the original one. At least up to 115^{0}C, n-alkane chains within the crystals of sample (2) are in the extended form with the chain axis perpendicular to the surface of the crystal layers. Up to nine orders of diffraction were observed on the S.A.X.S. patterns of this last sample for an exposure time of 24 hours. The higher number of orders of diffraction in the sample annealed at 115^{0}C could be explained by a more perfect crystal stacking. This

may indicate a higher regularity of crystals and amorphous layers which become more perfectly superposed after annealing at 115°C.

IV.3.2.2 **Raman Spectroscopy.**

The Raman spectrum of sample (2) recorded at room temperature between 1650 cm^{-1} and 850 cm^{-1} is shown in Figure IV.78.

Figure IV.78 : Raman spectrum of sample (2) recorded at room temperature

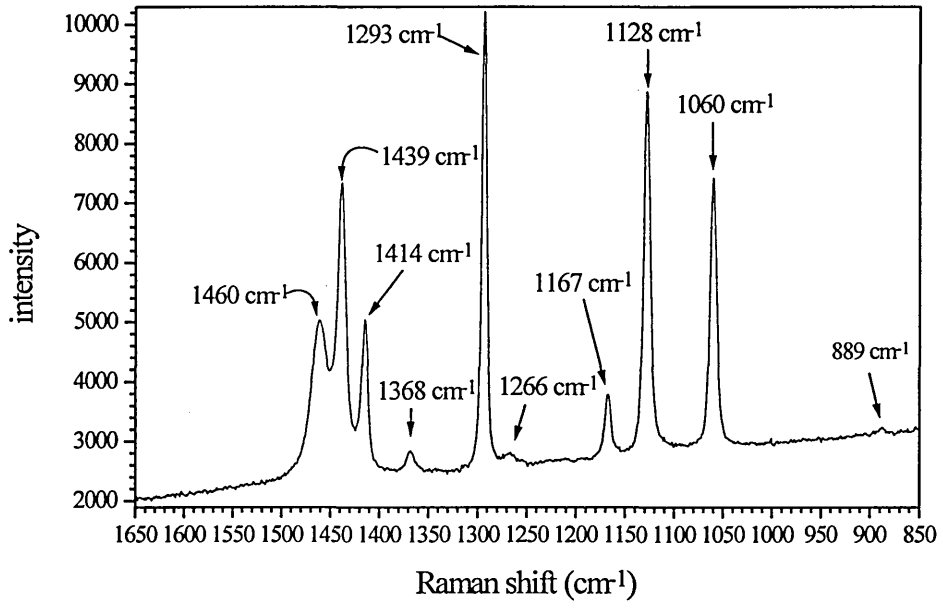

The Raman bands present in the spectrum of sample (2) shown in Figure IV.78 are assigned in Table IV.17.

Table IV.17 : Assignment of the Raman bands present in the spectrum of sample (2)

Raman shift (cm^{-1})	assignment
1460	methylene bending mode[84]
1439	methylene bending mode[84]
1414	methylene bending mode[84], characteristic of the orthorhombic subcell packing[85]
1368	methylene wagging mode[85]
1293	in-phase methylene twisting mode[40]
1167	out-of-phase methylene rocking mode[40]
1128	in-phase C-C stretching mode[85]
1060	out-of-phase C-C stretching mode [85]
889	methyl rocking mode[92]

The C-H stretching region of the Raman spectrum of sample (2) is shown in Figure IV.79.

Figure IV.79 : Raman spectrum of sample (2) recorded at room temperature between 3100 cm^{-1} and 2500 cm^{-1}

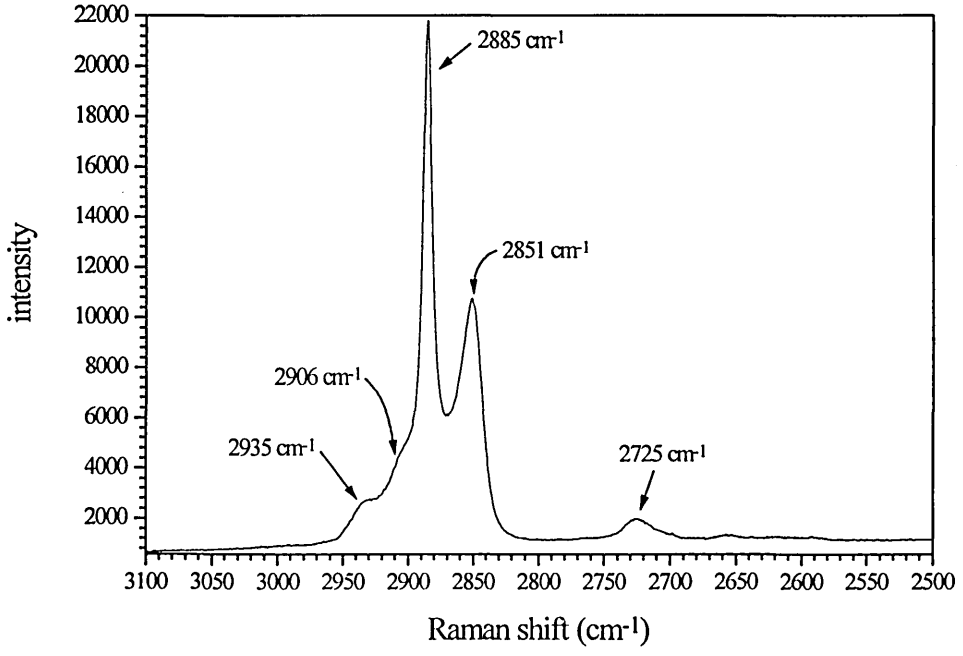

The Raman active bands at 2851 cm^{-1} and 2885 cm^{-1} are ascribed respectively to the symmetric and antisymmetric methylene C-H stretching modes. The bands present in the Raman spectrum at 2906 cm^{-1} and 2935 cm^{-1} are also associated to the symmetric and antisymmetric methylene C-H stretching modes but, in this case, are the result of Fermi resonance[86,87]. The Raman spectra of samples (1) and (2) recorded at room temperature are similar in the region above 850 cm^{-1}. Nevertheless, the low frequency region of the spectra can be used to differentiate them.

Figure IV.80 shows the low frequency Raman spectrum of sample (2) recorded at room temperature.

Figure IV.80 : Low frequency Raman spectrum of sample (2) recorded at room temperature

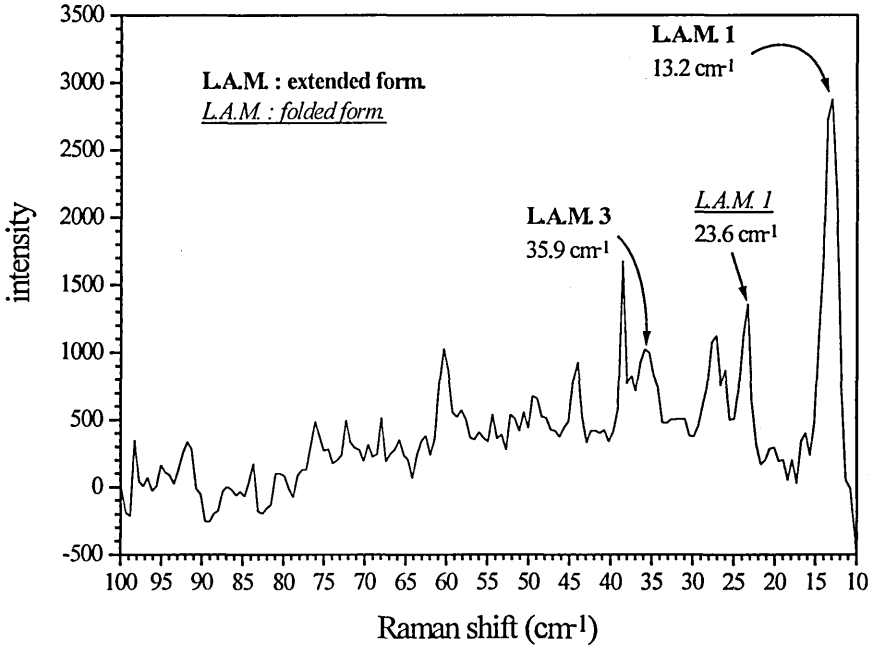

The first and third orders of the Longitudinal Acoustic Modes of vibration are found at respectively 13.2 cm^{-1} and 35.9 cm^{-1} and are ascribed to n-$C_{198}H_{398}$ chains in an extended form conformation. Nevertheless, we can observe the first order of the L.A.M. of vibration at 23.6 cm^{-1} ascribed to n-$C_{198}H_{398}$ chains in once folded form conformation. So, a minority of chains are in once folded form conformation inside the crystals of sample (2).

IV.3.2.3 **Infrared Spectroscopy.**

Originally crystallised in extended form with the chain axis perpendicular to the surface of the crystal layers, sample (2) was annealed successively at 35°C, 110°C, 120°C and 126°C, cooling down to -173°C after each step.

After annealing sample (2) up to 115°C, n-alkane chains within the crystals were found to be in extended form with the chain axis perpendicular to the surface of the crystal layers. The melting point of the n-$C_{198}H_{398}$ extended form crystals was found at 126.7°C. Annealing sample (2) up to 126 +/- 1 °C may thus have caused a partial melting of the sample.

IV.3.2.3.a Low temperature spectra.

The low temperature infrared spectra of sample (2) cooled down from 35°C, 110°C, 120°C and 126°C are shown in Figure IV.81 after baseline subtraction.

Figure IV.81 : Low temperature infrared spectra of sample (2) as a function of annealing temperature

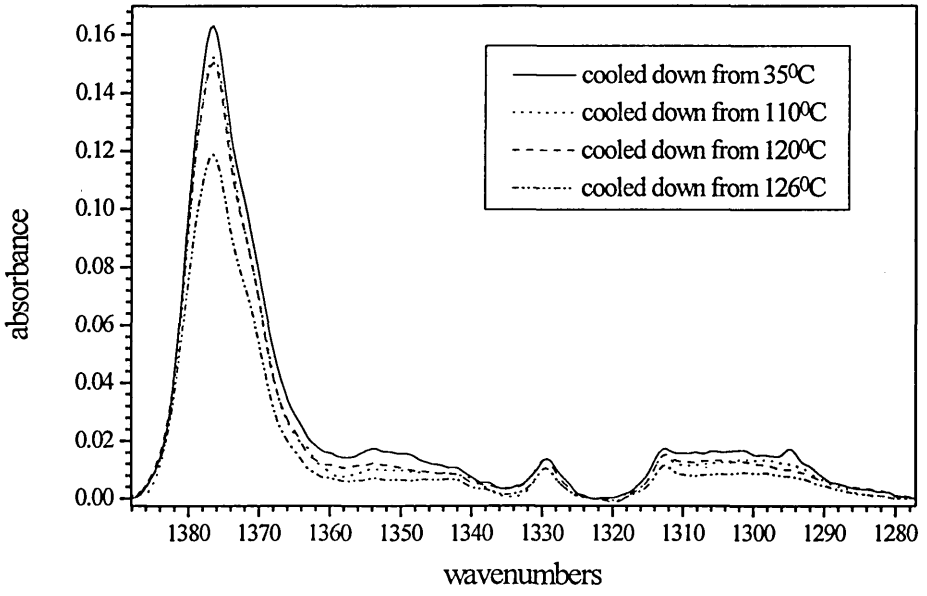

Again, a decrease of the total absorbance of the spectra with increasing annealing temperature is observed. The strongest band in this region is the one at 1377 cm^{-1} ascribed to the methyl symmetric bending mode. Also, two clear bands are present at

1329 cm^{-1} and 1312 cm^{-1}. Compared to the spectra of Figure IV.62, we notice here a weaker intensity of the bands ascribed to the non all-trans conformers. Second derivatives, deconvolutions and curve fitting procedures were used in the wagging mode region between 1388.1 cm^{-1} and 1323 cm^{-1} (Table IV.18) and between 1323 cm^{-1} and 1277.2 cm^{-1} (Table IV.19).

Table IV.18 : Frequency and area of the infrared bands determined by curve fitting procedures on low temperature spectra of sample (2)

	area			
wavenumbers cm^{-1}	cooled down from T=35°C	cooled down from T=110°C	cooled down from T=120°C	cooled down from T=126°C
1377	1.2405	1.1531	1.1556	0.9294
1370.7	0.3766	0.3741	0.3597	0.2867
1364.2	0.2174	0.1227	0.1429	0.0880
1353.7	0.1468	0.0936	0.1106	0.0636
1346	0.0651	0.0580	0.0459	0.0360
1341	0.0706	0.0387	0.0526	0.0365
1329.4	0.0710	0.0430	0.0671	0.0463

Table IV.19 : Frequency and area of the infrared bands determined by curve fitting procedures on low temperature spectra of sample (2)

	area			
wavenumbers cm^{-1}	cooled down from T=35°C	cooled down from T=110°C	cooled down from T=120°C	cooled down from T=126°C
1312.6	**0.0921**	**0.0660**	**0.0662**	**0.0491**
1308.5	**0.0469**	**0.0364**	**0.0412**	**0.0250**
1305.7	**0.0322**	**0.0232**	**0.0266**	**0.0208**
1302	**0.0950**	**0.0781**	**0.0751**	**0.0447**
1298.2	0.0321	0.0284	0.0105	0.0114
1294.9	**0.0586**	**0.0485**	**0.0656**	**0.0518**
1288.8	0.0297	0.0268	0.0327	0.0205
1283.1	0.0128	0.0223	0.0142	0.0308

The bands present in Table IV.18 are shown in Figure IV.82 and Figure IV.83 where their integrated absorbance (maximum value arbitrarily fixed to one) is plotted against the temperature from which the sample was cooled down.

Figure IV.82 : Scaled area of the infrared bands present in the low temperature spectra of sample (2) as a function of the annealing temperature

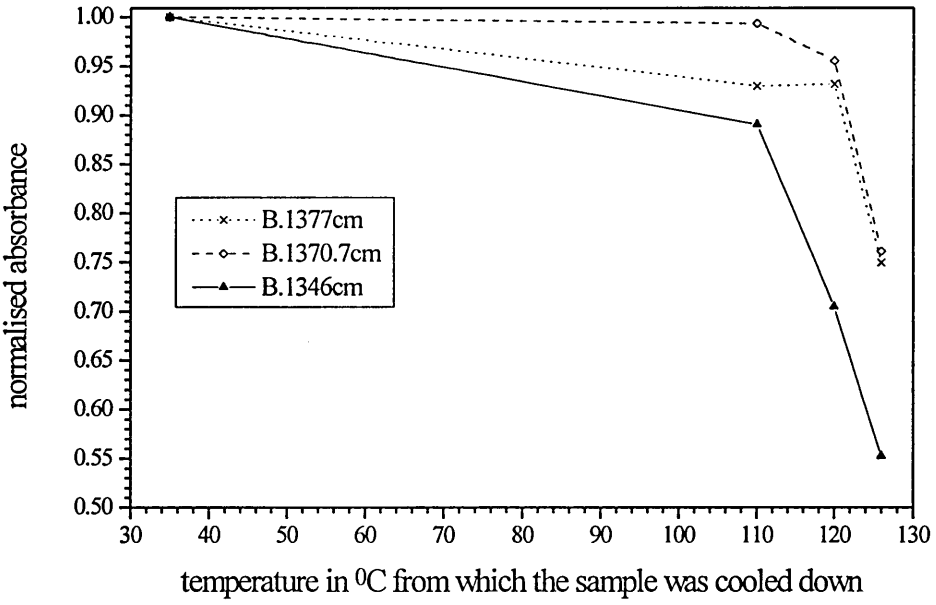

Thus, we observe in Figure IV.82 the normalised integrated absorbance of the bands at 1377 cm^{-1} (methyl deformation) and at 1370.7 cm^{-1} (ascribed to the gtg and gtg' defects) is nearly unchanged up to 120°C and decreases by around 20% of the original value, on annealing at 126°C. The large variation in absorbance of the methyl deformation band strongly suggests a change in the sample thickness after annealing to 126°C. Sample (2) is believed to have been at least partially melted. The presence in the spectra of sample (2) of the infrared band at 1346 cm^{-1} ascribed to the {110} fold conformation may be explained by a small proportion of folded chains originally formed during the crystallisation of sample (2) from solution. A strong decrease of the normalised absorbance of this band is observed after annealing sample (2) up to 120°C. Indeed, its normalised absorbance decreases by nearly 30% of its original value. The melting point of n-$C_{198}H_{398}$ folded crystals was found to be around 119°C. Therefore, the above observation is believed to be due to the premelting phase transition occurring between once folded and extended crystals at around 119°C. After annealing sample (2) at 126°C, the absorbance of the 1346 cm^{-1} band decreases by about 45% of its original value.

In Figure IV.83, the variation of the normalised integrated absorbance of the bands at 1364.2 cm^{-1}, 1353.7 cm^{-1}, 1341 cm^{-1} and 1329 cm^{-1} can be observed.

Figure IV.83 : Scaled area of the infrared bands present in the low temperature spectra of sample (2) as a function of the annealing temperature

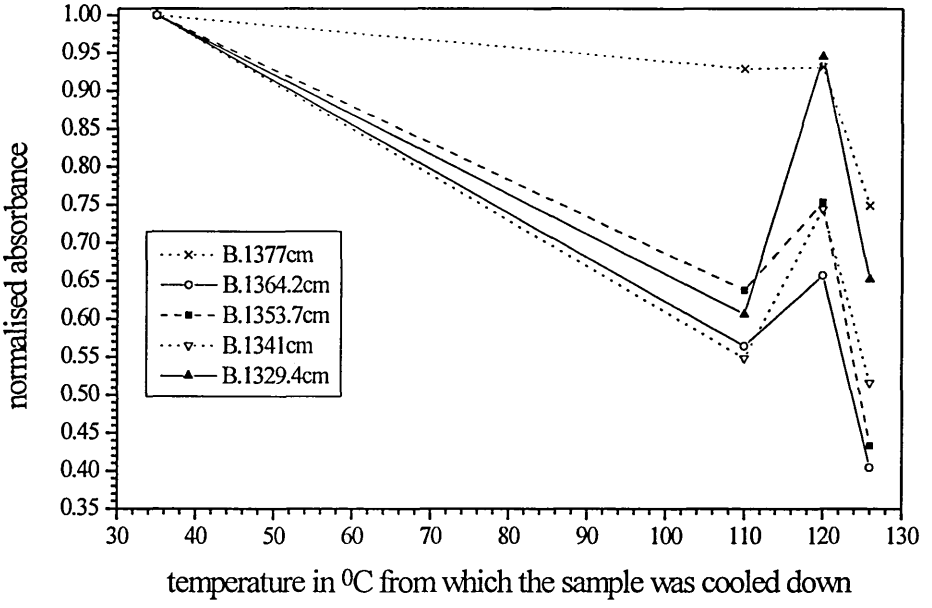

After annealing to 110°C, the area of each of these bands decreases by around 40% of their original values. Apart from the band at 1329 cm^{-1}, all the others are assigned to non all-trans conformers. Therefore, the strong decrease of the normalised absorbance indicates a decrease in the concentration of the conformers related to these bands within the n-alkane crystals. Furthermore, after annealing at 126°C, the absorbance of the bands at 1364.2 cm^{-1} and 1353.7 cm^{-1} decreases by nearly 60% of their original values. Through the annealing and cooling of sample (2), a perfecting of the n-alkane crystals occurs. Nevertheless, a clear increase in the absorbance of these four infrared bands is observed on annealing at 120°C. As explained earlier, a phase transition between once folded and extended form crystals occurs at around 119°C. Therefore, at this transition, the degree of disorder reaches a local maximum. Also, the sample requires some time at the temperature to reach thermal equilibrium. Therefore, the increase of the normalised absorbance of the bands present in Figure IV.83, may be caused by this premelting

phase transition. Also, this effect may be enhanced if the sample spent different times at the chosen temperatures.

Some of the bands present in Table IV.19 (bold type) are shown in Figure IV.84 and Figure IV.85 where their integrated absorbance (maximum value arbitrarily fixed to one) is plotted against the temperature from which the sample was cooled down.

Figure IV.84 : Scaled area of the infrared bands present in the low temperature spectra of sample (2) as a function of the annealing temperature

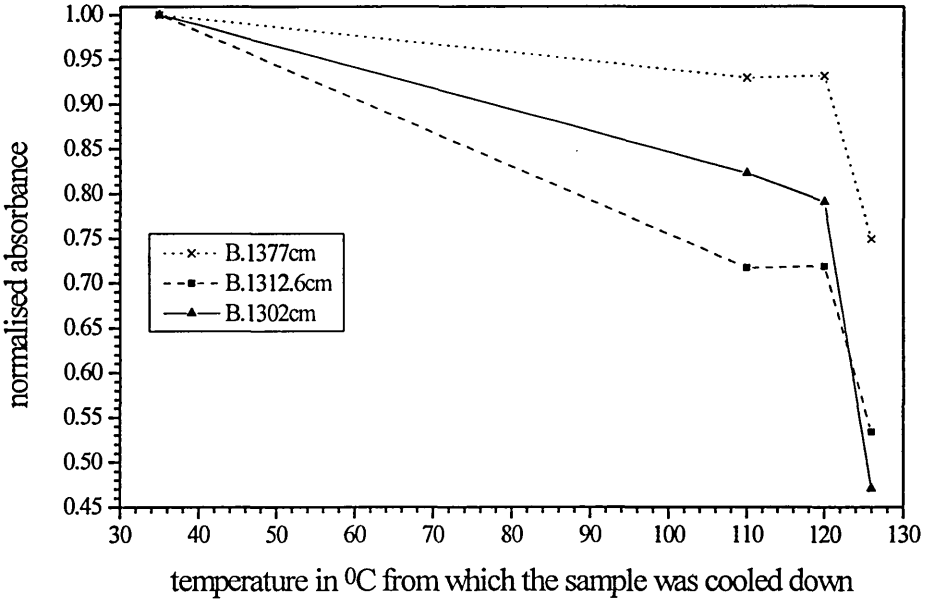

The scaled areas of the bands at 1312.6 cm^{-1} and 1302 cm^{-1} decreased by around 20% of their maximum values after annealing to 110°C. The largest decrease, nearly 50%, occurs after annealing to 126°C. Once again, this effect is believed to be linked to the thinning of the sample occurring through its partial melting.

Figure IV.85 : Scaled area of the infrared bands present in the low temperature spectra of sample (2) as a function of the annealing temperature

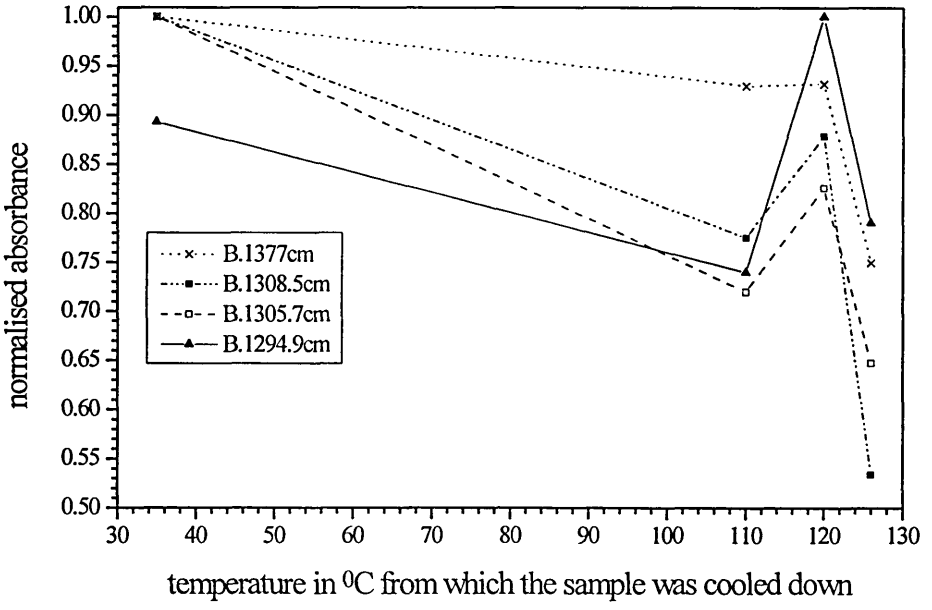

In Figure IV.85, a general decrease of the scaled areas of the bands at 1308.5 cm^{-1}, 1305.7 cm^{-1} and 1294.9 cm^{-1} can be observed with the increase of the annealing temperature. Nevertheless, after sample (2) was cooled down from 120^{0}C, a clear increase of the intensity of all the bands occurs.

Figure IV.86 : Scaled area of some infrared bands present in the low temperature spectra of sample (2) as a function of the annealing temperature

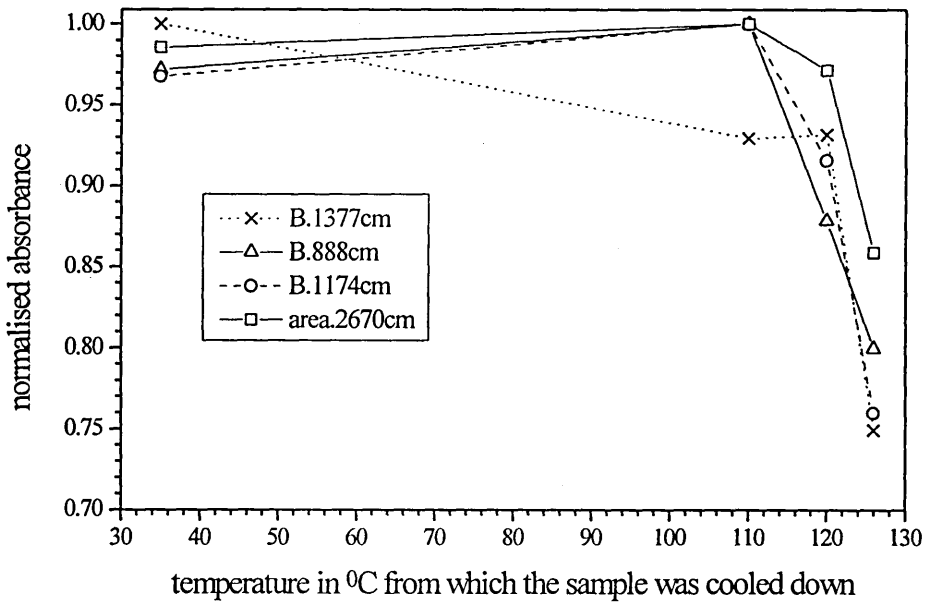

In the case of sample (2), no tilting of the n-alkane chains inside the crystal layers was expected with the increase in temperature below the melting point. No change in the original value of the average layer periodicity of sample (2) was observed after annealing up to 115^{0}C. The presence of the {110} fold band at 1346 cm^{-1} can be explained by the formation of a minority of folded chains during the initial crystallisation from solution. This is supported by the presence of the first order of the L.A. mode at 23.6 cm^{-1} in the low frequency Raman spectrum of sample (2) in Figure IV.80. The strong decrease of the absorbance of the 1346 cm^{-1} band after annealing to 120^{0}C may be explained by the melting, occurring around 119^{0}C, of crystals inside which the alkane chains were in a once folded form conformation. Also, an unexpected increase of the absorbance of the bands represented in Figure IV.83 and Figure IV.85 was observed, on cooling down from 120^{0}C. This too may be due to the folded chain premelting phase transition, possibly combined with the fact that the sample may not have spent the same times at the chosen temperatures.

Figure IV.86 shows the variation of the area of different infrared bands (maximum value arbitrarily fixed to one), as a function of the temperature at which the sample was

annealed. All but one is centred outside the wagging mode region of the infrared spectra. The infrared bands at 888 cm^{-1} and 1174 cm^{-1} are ascribed respectively to the methyl rocking and methylene wagging modes of vibration. The variation of the area of a broad band between 2690 cm^{-1} and 2558 cm^{-1} and centred around 2670 cm^{-1} is also plotted. The maximum area of each band was arbitrarily fixed equal to one. The area of each of these infrared bands decreases strongly after annealing to 126°C. Changes in the density or thickness of the sample may have occurred, through the partial melting, which was suggested earlier. In order to compensate for the thinning of the sample due to its partial melting, we decided to normalise the low temperature infrared spectra shown in Figure IV.81 using the area of the band which was the least sensitive to the annealing of sample (2). The broad band centred at 2670 cm^{-1} is the one chosen. Indeed, its normalised area varies within less than 5% of its original value, for low temperature data. The original spectra of sample (2) cooled down from 35°C, 110°C, 120°C and 126°C were thus multiplied respectively by 1.0144, 1, 1.0293 and 1.1647. The normalised low temperature infrared spectra of sample (2) are shown in Figure IV.87.

Figure IV.87 : Low temperature F.T.I.R. spectra of sample (2) normalised using the area of the 2670 cm^{-1} band.

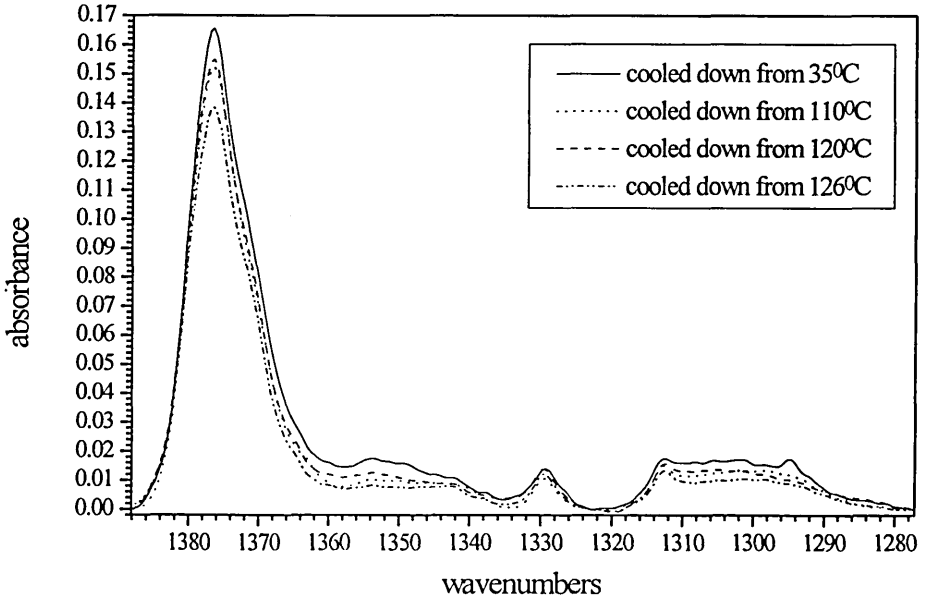

The previous observations made on the spectra shown in Figure IV.81 are still valid for Figure IV.87. Nevertheless, the clear decrease in intensity of the bands present in the spectrum of sample (2) cooled down from 126°C has been reduced.

In order to facilitate the observation of the variation of the normalised absorbance (its maximum is arbitrarily fixed to one) as a function of the temperature from which the sample (2) was cooled down, some of the bands present in the normalised spectra shown in Figure IV.87 are shown in Figure IV.88 and Figure IV.89.

Figure IV.88 : Variation of the area of some of the bands present in the normalised low temperature spectra of sample (2)

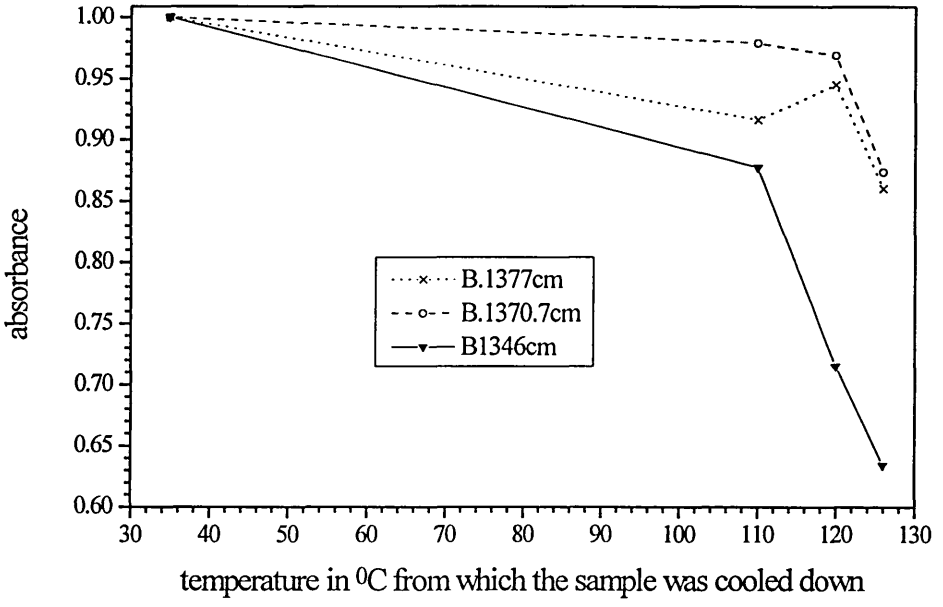

Over the annealing temperature range used, a decrease of the normalised integrated absorbance of the bands at 1377 cm^{-1} and 1370.7 cm^{-1} occurs within less than 15% of their maximum value. Also, the normalised absorbance of the band at 1346 cm^{-1} assigned to the {110} fold conformation decreases by nearly 30%, on cooling from 120°C. This effect can be explained by the phase transition occurring at 119°C between once folded to extended form crystals. A small further decrease of the normalised absorbance is observed, down to 35% of its original value, on cooling from 126°C.

Figure IV.89 : Variation of the area of some of the bands present in the normalised low temperature spectra of sample (2)

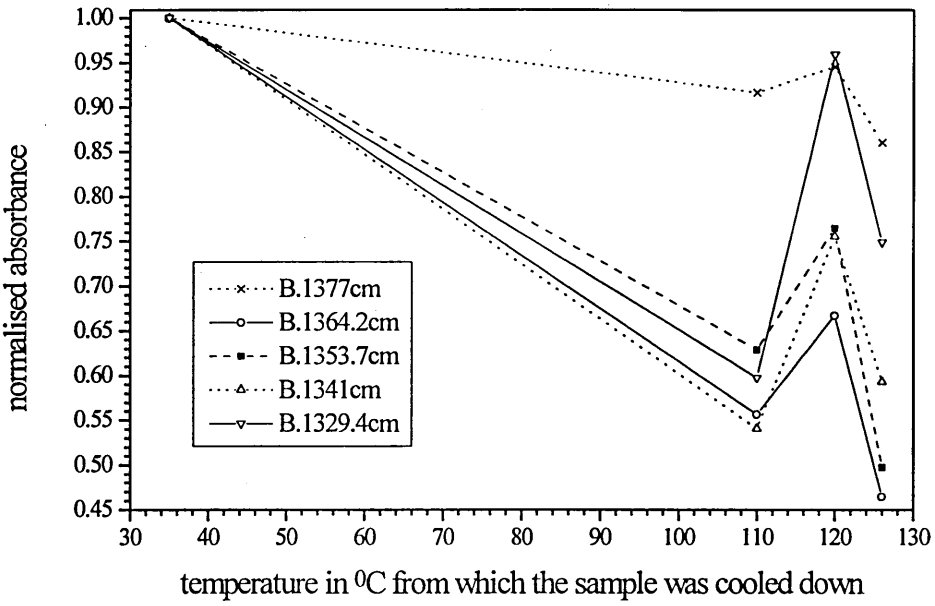

The observations made on the variation of the normalised integrated absorbance of the 1364.2 cm^{-1}, 1353.7 cm^{-1}, 1341 cm^{-1} and 1329.4 cm^{-1} bands shown in Figure IV.83 are still applicable to the Figure IV.89. Indeed, the normalised absorbance of all the bands shown here decreases by around 40% of their original value, for annealing at 110^{0}C. This indicates a perfecting of the crystals through the annealing process. A further decrease is observed for the bands at 1364.2 cm^{-1} and 1353.7 cm^{-1}, for cooling from 126^{0}C. At the same time, there is no significant change in the value of the absorbance obtained for the band at 1341 cm^{-1} assigned to the end gauche conformers. On the other hand, the normalised absorbance of the band at 1329.4 cm^{-1} increases, being 25% down from its original value. Also, a clear jump in the absorbance of these four infrared bands is observed, for annealing at 120^{0}C. As explained earlier, this increase in the normalised absorbance may be caused by the premelting phase transition occurring between once folded and extended form crystals. Also, this effect may be enhanced if the sample spent different times at the chosen temperatures.

The C-C stretching mode region of the infrared spectra of sample (2) successively annealed at 35°C, 110°C, 120°C and 126°C, and then cooled down to -173°C, is shown in Figure IV.90.

Figure IV.90 : Low temperature infrared spectra of the C-C stretching mode region of sample (2)

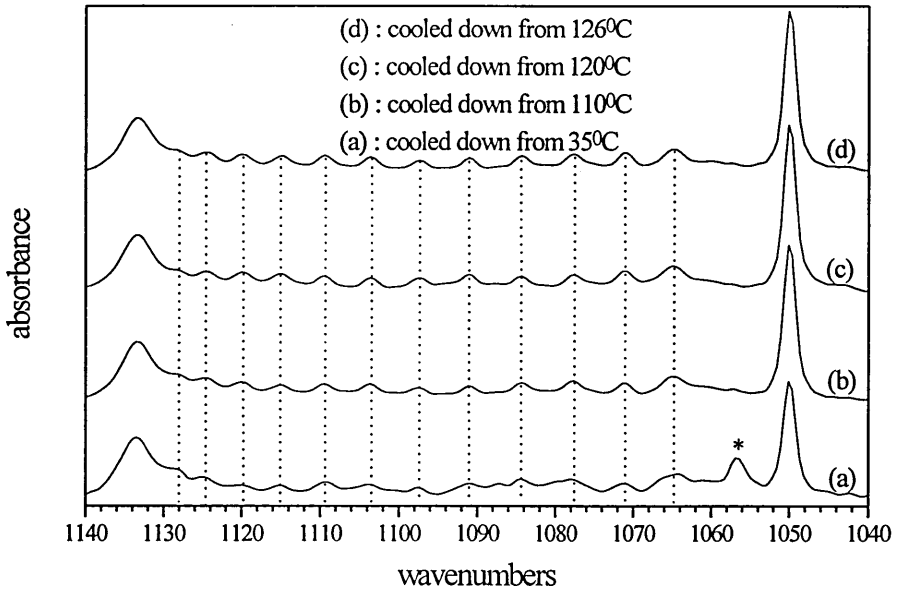

The band progression region is limited by two extreme bands at 1133 and 1050 cm^{-1}. Each one of the progression bands present in this region (crossed by a vertical dotted line) is ascribed to non-localised mode of vibration, as noted earlier. The disappearance of the 1056 cm^{-1} band noted earlier, in addition to both the higher regularity and better resolution of the progression bands, may be seen as evidence of a perfecting of the extended crystals inside which the concentration of remaining non all-trans conformers present, in particular near the crystal surfaces originally formed during the crystallisation of sample (2) from solution, decreases. Furthermore, the higher regularity and better resolution of the progression bands may be due to a narrower distribution of all-trans extended chain lengths with the increase of annealing temperature.

In the case of sample (2) cooled down from 126°C, estimates for both the best series of k values and the number of carbon atoms involved in the extended part of the n-alkane chains were determined. A $^{+}/_{-}1$ error bar is estimated on the values of the integers k. The

average number of carbon atoms involved in the extended part of the n-alkane chains is estimated to be equal to 192 +/- 12. The frequency of each of these progression bands is plotted against the integer k, in Figure IV.91. Also, the frequency of each of these bands was fitted by a third order polynomial curve Y, shown by a black line.

Figure IV.91 : Frequency of the progression bands ascribed to the C-C stretching mode against k, integer, for sample (2) cooled down from 126^{0}C.

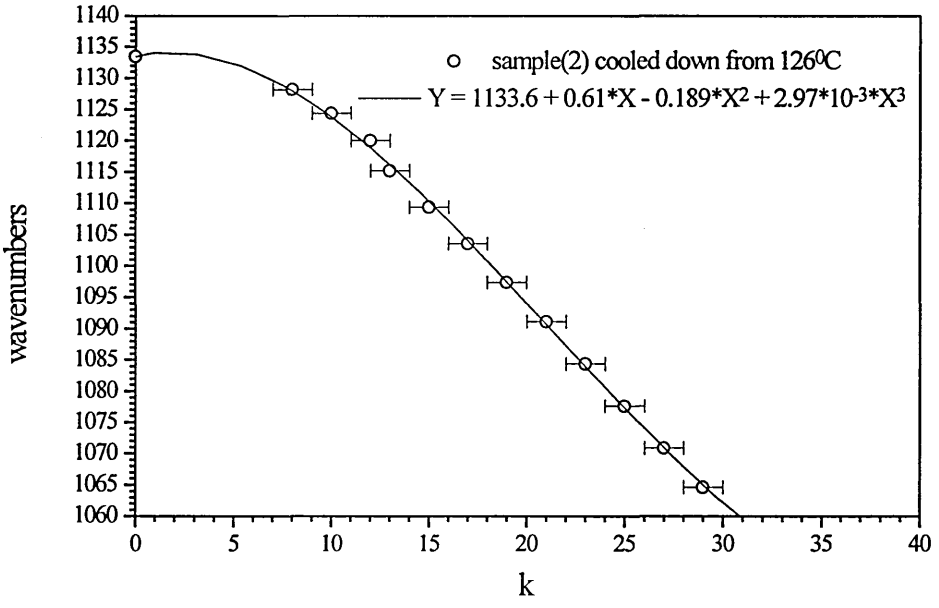

The frequency differences between each of these successive bands ($\bar{\nu}_k - \bar{\nu}_{k+2}$) is plotted against the integer k in Figure IV.92.

Figure IV.92 : Frequency differences between successive progression bands present in the C-C stretching mode region of the low temperature infrared spectra of sample (2)

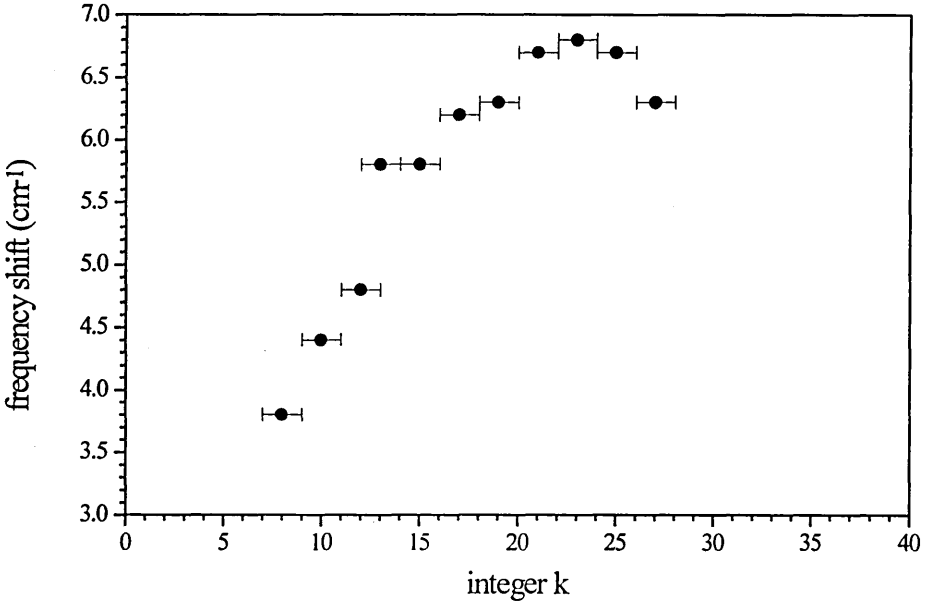

This frequency difference is found to go through a maximum which is centred on the band at 1084.3 cm^{-1}. The shape of this curve is similar to what can be found studying the infrared spectra of short chain n-alkane crystals[41]. Therefore, this may be indicative of a high degree of order within sample (2) crystals.

IV.3.2.3.b Elevated temperature spectra.

The infrared spectra of sample (2) were also recorded at 35°C, 110°C, 120°C and 126°C. We normalised the elevated temperature infrared spectra using the values of the area of the broad band at 2670 cm^{-1} determined in the spectra of sample (2) recorded at -173°C. These normalised infrared spectra are shown in Figure IV.93.

Figure IV.93 : F.T.I.R. spectra of sample (2) recorded at elevated temperature, after baseline subtraction and normalisation

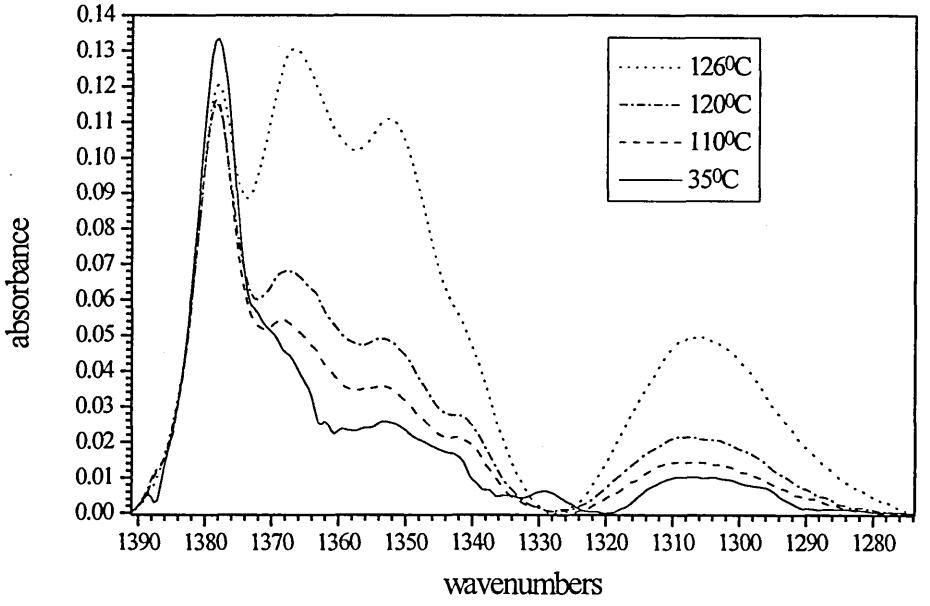

The absorbance of each infrared band present in the wagging mode region and assigned to the non all-trans conformers is increasing with the temperature at which the spectrum of sample (2) is recorded. This is the case for the bands at 1370 cm^{-1} and 1307 cm^{-1}, 1356 cm^{-1} and 1342 cm^{-1} respectively assigned to gtg/gtg', gg, and end gauche conformers. On the other hand, the absorbance of the band at 1378.4 cm^{-1} assigned to the methyl symmetric bending mode decreases with the increase in temperature up to 120°C. After annealing to 126°C, the absorbance of this band increases. Finally, the band present at 1329 cm^{-1} in the spectrum of sample (2) recorded at 35°C disappears after further increase of the temperature.

Second derivatives, deconvolutions and curve fitting procedures were used in the wagging mode region between 1391 cm^{-1} and 1324.8 cm^{-1}. The results of this work are shown in Table IV.20.

Table IV.20 : Frequency and area of the infrared bands determined by curve fitting procedures on elevated temperature spectra of sample (2)

	area			
wavenumbers cm^{-1}	T=35°C	T=110°C	T=120°C	T=126°C
1386	0.0391	0.0548	0.0664	0.0562
1378.4	**0.9737**	**0.883**	**0.8714**	**0.9085**
1370	**0.394**	**0.3636**	**0.4165**	**0.6153**
1364	**0.2061**	**0.2783**	**0.3921**	**0.7546**
1356	**0.1405**	**0.3558**	**0.4729**	**1.0239**
1349	**0.1942**	**0.1192**	**0.2337**	**0.6962**
1342	**0.0633**	**0.1678**	**0.1985**	**0.4067**
1336	**0.0312**	**0.0371**	**0.0418**	**0.1035**

Some of the bands present in Table IV.20 (bold type) are shown in Figure IV.94 and Figure IV.95 where their integrated absorbance (maximum value arbitrarily fixed to one) is plotted against the annealing temperature.

Figure IV.94 : Normalised area of the infrared bands present in the elevated temperature spectra of sample (2) as a function of the annealing temperature

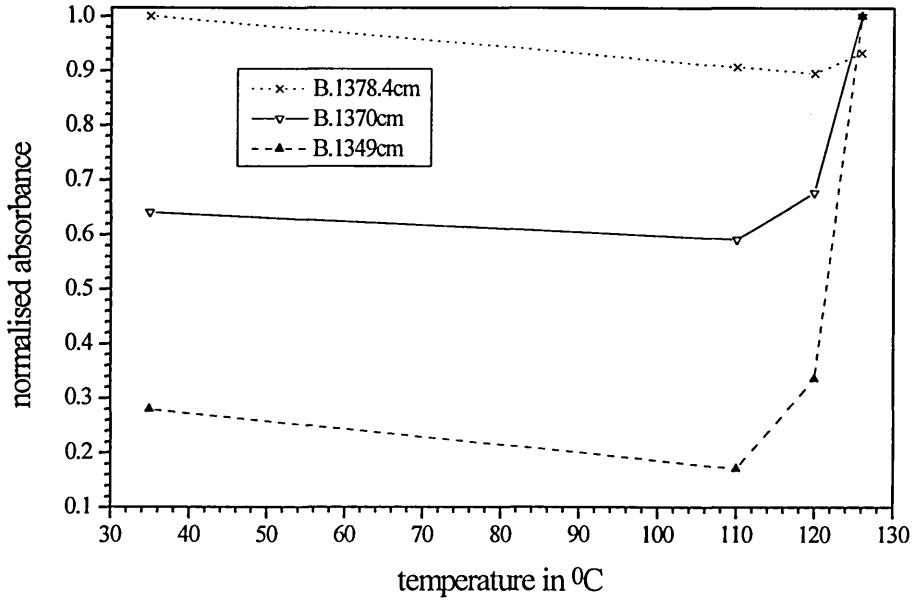

The normalised integrated absorbance of the band at 1378.4 cm^{-1} varies within 10% of its original value. As observed previously, after a decrease of its intensity up to 120°C, a

small increase is observed in the spectrum recorded at 126°C. In the case of the bands present at 1370 cm^{-1} and 1349 cm^{-1} assigned to the gtg/gtg' conformers and {110} fold conformation, a slight decrease of their normalised absorbance, less than 10% of their maximum value, is observed after the increase of the temperature up to 110°C. Then, an increase occurs after annealing at 120°C. Finally, the increase in temperature up to 126°C is followed by a large increase of the normalised absorbance, respectively by 35% and 60% of each of their maximum values. On the other hand, one can note the smaller variation of the normalised absorbance of the 1370 cm^{-1} band compared to the 1349 cm^{-1} band through the temperature range used. The same comments can be made comparing the variation of the 1370 cm^{-1} band with the infrared bands present in Figure IV.95. Thus, the low values of the normalised absorbance of most of the infrared bands below 126°C suggest that a partial melting of sample (2) crystals occurred at 126°C.

Figure IV.95 : Normalised area of the infrared bands present in the elevated temperature spectra of sample (2) as a function of the annealing temperature

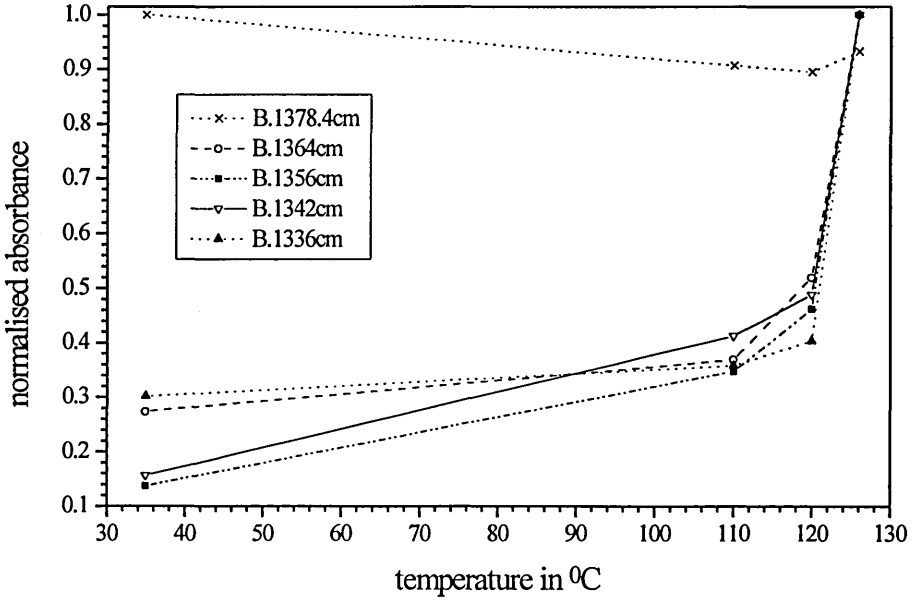

The normalised integrated absorbance of the infrared bands shown in Figure IV.95 increases rapidly with the increase of the annealing temperature. An increase of the normalised absorbance of all the bands by around 65% is observed after annealing to 126°C. This observation clearly indicates a major increase in the number of non all-trans

conformers present in the n-alkane chains and, therefore, may result from the partial melting of sample (2) at this temperature. This demonstrates the major difference in the concentration of non all-trans conformers in long n-alkane chains in the crystalline and liquid states.

IV.3.2.3.c Series of elevated temperature infrared spectra.

In order to compare properly the difference in the concentration of non all-trans conformers present in long chain n-alkanes in the crystalline and liquid states, sample (2) was heated up from 83.2°C to 131.2°C with a heating rate of 0.4°C/minute. A spectrum was recorded every four minutes (or every 1.6°C). It took a total of three minutes fifty five seconds to record the run. The full series of infrared spectra is shown in Figure IV.96.

Figure IV.96 : High temperature infrared spectra of sample (2) recorded between 83.2°C and 131.2°C, after baseline subtraction

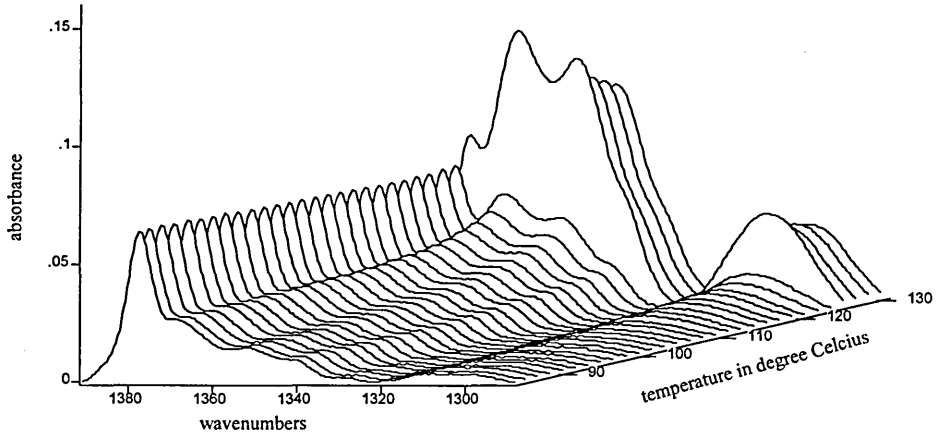

The peak height of each band present in each elevated temperature infrared spectra shown in Figure IV.96, was determined after baseline subtraction. Then, in Figure IV.97, the peak height of each band was plotted against the temperature. Also, in Figure IV.97, the maximum value of the peak height for each infrared band was arbitrarily fixed to one.

Figure IV.97 : Scaled peak height of each infrared band (maximum value arbitrarily fixed to one) as a function of the temperature, after baseline subtraction

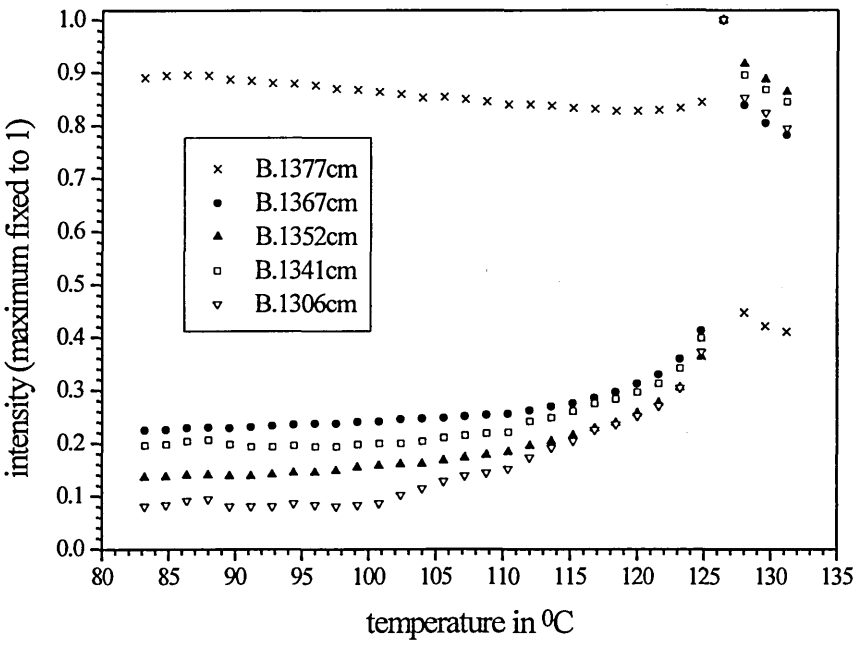

The scaled peak height of the infrared band present at 1377 cm^{-1} assigned to the methyl symmetric bending mode decreases progressively with the increase in temperature up to 120^{0}C. This effect may be due a thinning of the sample due to an increase in the pressure applied to the sample, related to the increase of the volume of the KBr plates and metal sample holder with the increase in temperature. From 121.6^{0}C, the peak height of the 1377 cm^{-1} band increases slightly and jumps by around 15% of its maximum value after annealing to 126.4^{0}C. The melting of extended form crystals is believed to take place at this temperature. Then, above this temperature, a huge decrease of this scaled intensity is observed. Once in the liquid state, the sample originally held between two KBr plates slowly leaks out of the cell. Thus, the sample volume in the infrared beam is reduced. In order to compare the concentrations of the different conformers present in sample (2) as a function of the temperature, we need to normalise the different infrared spectra. Thus, in Figure IV.98, we chose to use the area of the 1377 cm^{-1} band assigned to the methyl symmetric bending mode to normalise each spectrum. The Figure IV.98 shows the normalised peak height of each infrared band (maximum value arbitrarily fixed to one) plotted as a function of the temperature.

Figure IV.98 : Normalised peak height of each infrared band (maximum value arbitrarily fixed to one) as a function of the temperature, after baseline subtraction and normalisation using the area of the 1377 cm^{-1} band

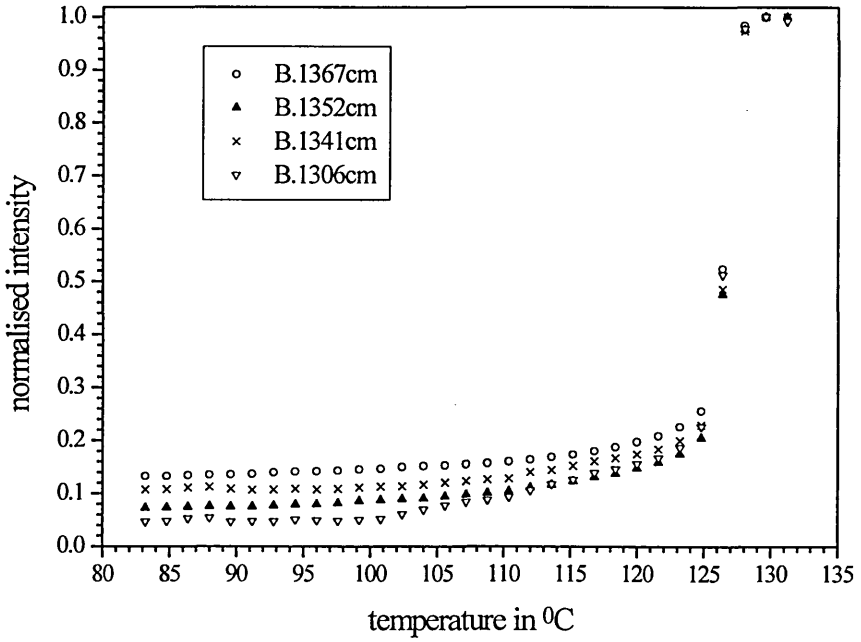

At a first approximation, we can say that the number of non all-trans conformers present in the extended chain crystals is one order of magnitude lower than for the liquid state. Also, differences in the normalised absorbances of the bands assigned to the specific conformers can be observed. Thus, the normalised absorbance of the band at 1367 cm^{-1} assigned to the gtg/**gtg'** conformers is greater below 110^{0}C than, in decreasing order, the normalised absorbances of the bands assigned respectively to the end gauche, gg and **gtg**/gtg' conformers. Also, the normalised absorbances of the bands assigned to the gtg/**gtg'**, end gauche and gg conformers seem to show the same behaviour as a function of the temperature, even if their initial values were different. Indeed, the normalised absorbance of the band at 1306 cm^{-1} assigned to the **gtg**/gtg' conformers is the lowest one. Nevertheless, a small jump in the normalised absorbance of this last band is observed around 105^{0}C. Above this temperature, its value overtakes that of the band assigned to gg conformers.

IV.3.2.4 **Conclusion.**

Low frequency Raman spectroscopic measurements on sample (2) indicate the presence of a minority of once folded crystals in addition to extended form ones. By successively annealing sample (2) at elevated temperatures, and then cooling it down to -173^{0}C, a more perfect crystal stacking takes place. Indeed, an increase of the number of orders of diffraction present on the S.A.X.S. patterns is observed. At the same time, a perfecting of the crystals takes place. This perfecting of the crystals can be observed in the wagging mode region of the low temperature infrared spectra of sample (2). Indeed, the absorbance of most of the infrared bands is found to decrease with increasing temperature. Nevertheless, after annealing at 120^{0}C, an increase in the absorbance of some of the infrared bands assigned to non all-trans conformers is observed and is believed to be due to the premelting phase transition occurring between the minority of once folded crystals formed during the crystallisation from solution to extended form crystals. Also, sample (2) may not have reached thermal equilibrium before cooling down from 126^{0}C. Therefore, the value of the absorbance of the different bands present in the wagging mode region of the spectra and assigned to non all-trans conformers may change as a function of the time spent at elevated temperature. On the other hand, the higher regularity of the band progression present in the C-C stretching mode region of the infrared spectra of sample (2) with the increase of annealing temperature also indicates a perfecting of the extended chain crystals. These results seem to relate the perfecting of the crystals with the more regular crystal surfaces (i.e. better crystal stacking). From the identification of each one of these progression bands, we estimate the number of carbon atoms involved in the extended part of the n-alkane chains in extended forms to be 192 $^+/_-$ 12. This number of carbon atoms can be compared with the ones determined from both low frequency Raman spectroscopy and S.A.X.S. measurements, which are respectively 198 $^+/_-$ 1 and 187 $^+/_-$ 2. After the partial melting of sample (2) annealed at 126^{0}C, changes in sample thickness occur. We then normalised the infrared spectra using the area of the band present in the low temperature spectra at around 2670 cm^{-1}, which is believed to give the most reliable result.

Finally, by studying a series of infrared spectra of sample (2) recorded between 83^{0}C and 132^{0}C, the degree of disorder present in extended form crystals a few degrees

Celsius below their melting point was found to be one order of magnitude smaller than in the liquid state. The different infrared spectra were normalised using the maximum intensity of the 1377 cm^{-1} band in this case.

IV.3.3 Number of specific conformers in n-$C_{198}H_{398}$ crystals.

In order to estimate the number of specific conformers per molecule in sample (1) cooled down from 51°C and sample (2) cooled down from 126°C, we used the values of the areas of the infrared bands assigned to the non all-trans conformers present in the infrared spectrum of liquid hexadecane, combined with the estimates of specific conformers, using the assumption of the Rotational Isomeric State statistics. Thus, the area of the 1377 cm^{-1} infrared band ascribed to the methyl symmetric bending mode was used to normalise the spectra of sample (1) and sample (2) recorded at -173°C.

Table IV.21 : Estimates of the numbers of specific conformers in once folded and extended n-$C_{198}H_{398}$ crystal forms at -173°C

Band Position / cm^{-1}		Assignment	Number of Conformations per Molecule.	
Folded	Extended		Folded	Extended
1376.5	1377	CH_3 Deformation	Normalising	
1370.1	1370.7	gtg / gtg' conformers	1.4	0.8
1363.8	1364.2	Strained gg ?	1.3	0.4
1353.4	1353.7	gg conformers	1.8	0.3
1346.4	1346	{110} Fold	0.8	0.2
1341	1341	End Gauche conformers / {110} Fold	0.7	0.2

Table IV.21 shows the number of each type of conformer per molecule. A larger number of conformers was found in the case of sample (1), where the n-alkane chains are in a perpendicular once folded form conformation. There is, in this case, approximately one conformer of each type per chain. Nevertheless, nearly two gg

conformers per chain are found in the once folded form crystals. On the other hand, in sample (2) crystals, where the n-alkane chains are in the extended form, the numbers of gg, end gauche and strained gg conformers as well as the number of {110} folds are at least three time smaller. Furthermore, in the case of the gg conformers, this ratio is six times smaller. As noticed previously, the remaining band at 1346 cm^{-1} which appears in the infrared spectrum of sample (2) cooled down from 126°C indicates that some crystals in the folded form may still be present in sample (2) which is essentially in extended form conformation.

IV.3.4 Spectral subtraction.

With the aim of determining the different conformations composing the fold in the n-$C_{198}H_{398}$ sample, we used a spectral subtraction technique. The result is shown in Figure IV.99 where the spectrum recorded at -173°C of sample (2) cooled down from 126°C was subtracted from the spectrum recorded at -173°C of sample (1) cooled down from 51°C. The choice of these two spectra was made to avoid observing any possible components in the subtracted spectrum due to the tilting of the alkane chains inside the crystal layers when sample (1) is annealed above 95°C. Linear baselines were used with reference points of 1388.1 cm^{-1}, 1323 cm^{-1} and 1260.3 cm^{-1}. In this case, the area of the broad band between 2690 cm^{-1} and 2558 cm^{-1} was determined by curve fitting and was used to normalise the two infrared spectra.

Figure IV.99 : Fold itself determined by spectral subtraction at -173°C

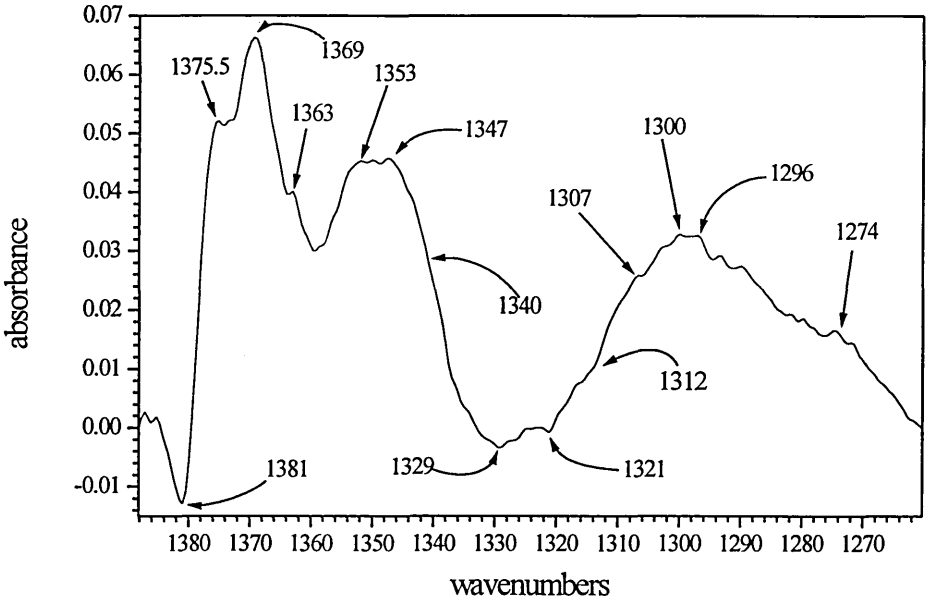

All the different bands of the wagging mode region known to be due to non all-trans conformers involving methylene groups are present in this spectrum. Thus, the bands at 1353 cm^{-1} (ascribed to gg), 1340 cm^{-1} (ascribed to end gauche), 1300 cm^{-1} and 1296 cm^{-1} (ascribed to the off zone centre methylene wagging mode) are shown in Figure IV.99. Also, the bands at 1363 cm^{-1} possibly ascribed to a strained gg conformer and 1307 cm^{-1} ascribed to the **gtg**/gtg' conformers are present in this spectrum. The strongest band of this region is the one at 1369 cm^{-1} ascribed to the gtg/**gtg'** conformers. As expected, the band at 1347 cm^{-1} ascribed to the {110} fold itself is there. Finally, another strong band is at 1375.5 cm^{-1}. This frequency is on the lower side of the commonly accepted frequency range for a methyl group involved in a symmetric bending mode of vibration and placed at the end of an alkane chain, the sample having an orthorhombic subcell. On the other hand, the negative band at 1381 cm^{-1} is on the higher side of this commonly accepted frequency range. The presence of these two last bands of opposite sign near the frequency of the methyl symmetric bending mode may indicate the non equivalence of the deformation of a methyl group placed at the end of an alkane chain in folded or extended chain conformations. Again, the general view which considers this band as

conformationally insensitive may be pointed out. Finally, two clear negative bands at 1329 cm^{-1} and 1321 cm^{-1} with, perhaps another one at 1312 cm^{-1} are present in the subtraction spectrum. These bands may be ascribed to a vibration involving the methyl end groups. Indeed, the bands at 1329 cm^{-1} and 1312 cm^{-1} are observed in the spectra of toluene and other long chain n-alkanes.

IV.3.5 Sample (3) : n-$C_{246}H_{494}$ crystallised in once folded form.

In order to observe both the possible tilting of the n-$C_{246}H_{494}$ once folded n-alkane chains from the crystal layers and the premelting phase transition occurring between the once folded to extended chain crystals at around 122.5 +/- 1.5 ^{0}C , we annealed sample (3) successively at 105^{0}C, 115^{0}C and 122^{0}C, cooling down to -173^{0}C after each stage. The melting point of n-$C_{246}H_{494}$ crystals in the extended form conformation was found[20] to be 128.6^{0}C. The melting point of n-$C_{246}H_{494}$ crystals in once folded form conformation was found[20] to be 122.5^{0}C.

IV.3.5.1 **S.A.X.S. measurements.**

The average layer periodicity of sample (3) determined by S.A.X.S. measurements was found to be equal to 158.6 +/- 1.7 Å. This value is similar to that calculated[60] for n-$C_{246}H_{494}$ in a once folded chain conformation, 158 Å.

After annealing to 105^{0}C, 115^{0}C and 122^{0}C, the average layer periodicity of crystals present in sample (3) was found to be respectively equal to 157.8 +/- 2 Å, 157.8 +/- 2 Å and 315.5 +/- 2 Å. Thus, after annealing to 122^{0}C, sample (3) originally crystallised in once folded form, was transformed to an extended chain conformation with the alkane chain axis perpendicular to the surface of the crystal layers. It should be noted that the annealing of sample (3) up to 115^{0}C did not significantly change the value of the average layer periodicity. Therefore, contrary to sample (1), the once folded n-alkane chains do not seem to tilt from the crystal surfaces with increasing annealing temperature.

IV.3.5.2 **Low frequency Raman spectroscopy.**

The low frequency Raman spectrum of sample (3) recorded at room temperature is shown in Figure IV.100. Notwithstanding the low signal to noise ratio of this Raman spectrum, we are able to determine the frequency of the first order of the longitudinal acoustic mode at 19.2 cm^{-1}.

Figure IV.100 : Low frequency Raman spectrum of sample (3) recorded at room temperature, after baseline subtraction

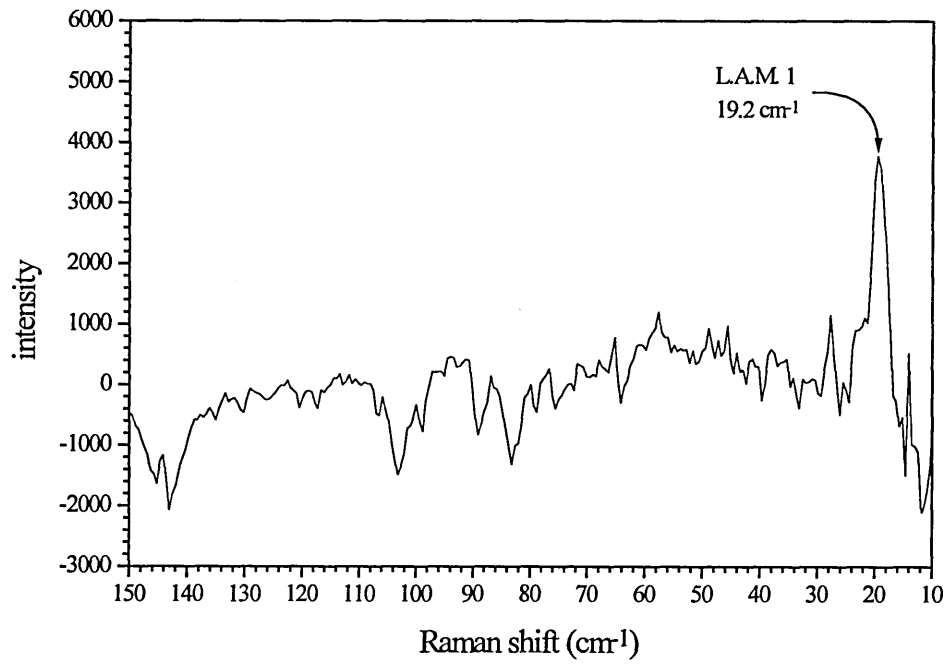

The number of carbon atoms involved in the all-trans stem characteristic of the lamellar crystals of sample (3) was determined using the value of the frequency of this Raman band and Equation IV.49. The number of carbon atoms was found to be equal to 128. Nearly exactly half the number of carbon atoms composing the n-$C_{246}H_{494}$ chains are involved in this L.A. mode. Therefore, the n-alkane chains are in the once folded conformation. This result confirms the one obtained by S.A.X.S. measurements.

IV.3.5.3 **Infrared spectroscopy.**

IV.3.5.3.a Methylene wagging mode region.

Sample (3) was annealed successively at 38°C, 105°C, 115°C and 122°C, in each case, followed by cooling down to -173°C. The wagging mode region of the infrared spectra of sample (3) recorded at -173°C is shown in Figure IV.101 after baseline subtraction.

Figure IV.101 : Low temperature F.T.I.R. spectra of sample (3) cooled down from 38°C, 105°C, 115°C and 122°C, after baseline subtraction

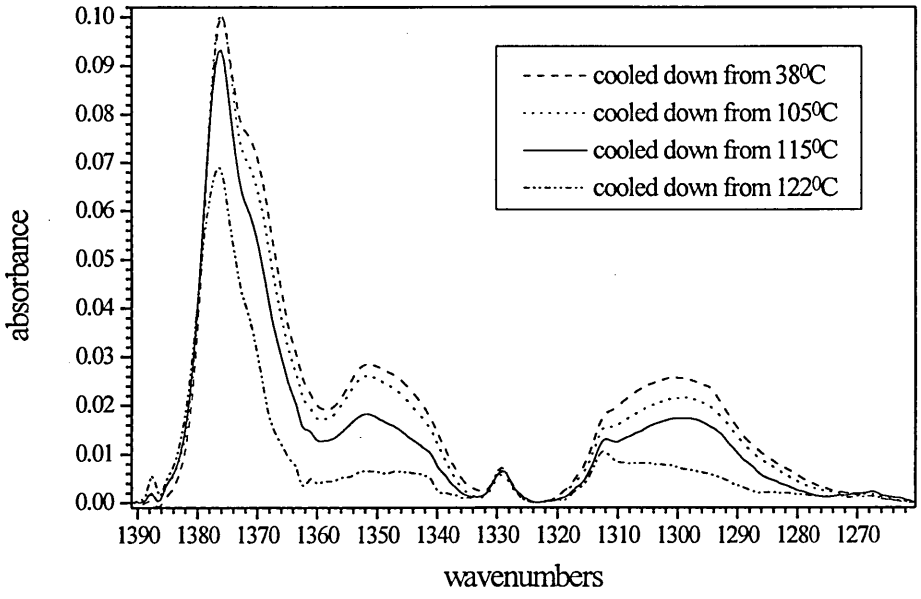

Again, a decrease of the absorbance of all the bands assigned to non all-trans conformers present in the spectra is observed with the increase of the annealing temperature. This effect is particularly pronounced between the spectra after cooling down from 115°C and 122°C.

The most intense band of this region is the one at around 1377 cm^{-1} ascribed to the methyl symmetric bending mode of vibration. Its observed intensity also decreases, with the increasing annealing temperature. Finally, a well resolved band present at 1329 cm^{-1} seems to be insensitive to the increase of the annealing temperature.

Second derivatives, deconvolutions and curve fitting procedures were used in the wagging mode region between 1391 cm^{-1} and 1323 cm^{-1} (see Table IV.22) and between 1323 cm^{-1} and 1260 cm^{-1} (see Table IV.23) to determine with accuracy the frequencies and areas of these different bands.

Table IV.22 : Curve fitting results performed on the higher frequency part of the infrared spectra of sample (3) recorded at -173°C

	area			
wavenumbers in cm^{-1}	cooled down from 38°C	cooled down from 105°C	cooled down from 115°C	cooled down from 122°C
1376.5	0.5521	0.5756	0.5494	0.5166
1370.5	0.4904	0.4269	0.3371	0.1684
1364	0.2243	0.1945	0.1505	0.0405
1353	0.2305	0.2175	0.1574	0.0695
1346	0.1836	0.1706	0.1097	0.0302
1341	0.0858	0.0561	0.0366	0.0271
1329.2	0.0273	0.0221	0.0275	0.0280

Table IV.23 : Curve fitting results performed on the lower frequency part of the infrared spectra of sample (3) recorded at -173°C

	area			
wavenumbers in cm^{-1}	cooled down from 38°C	cooled down from 105°C	cooled down from 115°C	cooled down from 122°C
1312.5	**0.1186**	**0.0716**	**0.0561**	**0.0398**
1307	**0.1169**	**0.1002**	**0.0788**	**0.0587**
1301	**0.1668**	**0.1578**	**0.1265**	**0.0435**
1295	**0.1103**	**0.0911**	**0.0765**	**0.0329**
1289	0.1246	0.1091	0.0793	0.0254

Some of the bands present in Table IV.22 and Table IV.23 (bold type) are shown respectively in Figure IV.102 and Figure IV.103 and in Figure IV.104 and Figure IV.105, where their integrated absorbance (maximum value arbitrarily fixed to one) is plotted against the temperature from which the sample was cooled down to -173°C.

Figure IV.102 : Scaled area of some of the infrared bands present in the higher frequency part of the spectra of sample (3) as a function of the temperature from which the sample was cooled down

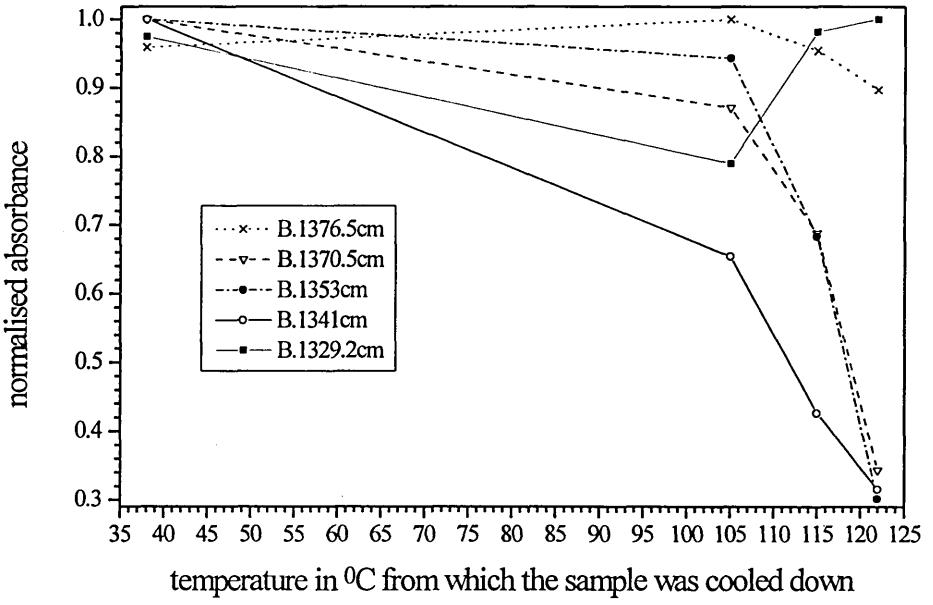

In Figure IV.102, the infrared band at 1376.5 cm^{-1} ascribed to the methyl symmetric bending mode of vibration is, in this wagging mode region of the spectra, the least sensitive band to conformational changes. Over the temperature range used in this experiment, the area of this last band decreases by only 10% of its maximum value when the area of most of the others decreases by more than 60%. Also, a small shift of this band towards higher wavenumbers was detected. Indeed, this band centred at 1376.5 cm^{-1} in the spectrum of sample (3) cooled down from 115°C is found at 1377.0 cm^{-1} in the spectrum of sample (3) cooled down from 122°C. In Figure IV.102, the area of the bands at 1370.5 cm^{-1} (ascribed to gtg and gtg' conformers), 1353 cm^{-1} (ascribed to gg conformers) and 1341 cm^{-1} (ascribed end gauche conformers) decrease by around 65% of their original value over the temperature range used. Most of this decrease occurs after annealing the sample above 105°C. One can notice the similar behaviour of the normalised absorbance of the bands assigned to the gtg/gtg' and gg conformers. Thus, the concentration of these non all-trans conformers has strongly decreased within the once folded form crystals of sample (3) annealed at 115°C. As in the case of sample

(1), by successively annealing sample (3) at a higher temperature and then, cooling down to -173°C, a perfecting of the n-alkane crystals is taking place. These observations also indicate that the lowest concentration of the non all-trans conformers is obtained within the extended chain crystals of sample (3) annealed at 122°C. On the other hand, we can notice that the normalised absorbance of the band at 1341 cm^{-1} ascribed to the end gauche conformers follows a different pattern from the one followed by the previous bands. Indeed, its normalised absorbance is far more affected by the increase of the temperature at 105°C and 115°C than by the increase of the temperature at 122°C. Therefore, the decrease of the concentration of end-gauche conformers with the increase of the temperature is not solely linked to the premelting phase transition occurring between the once folded and extended from crystals. Nevertheless, this decrease also indicates a perfecting of the n-alkane crystals. Finally, the variation of the normalised absorbance of the 1329.2 cm^{-1} band as a function of the temperature suggests that this band is not related to any mode of vibration involving non all trans conformers. Indeed, if the value indicated at 105°C is ignored, the normalised absorbance of this band varies within less than 3% over the temperature range used.

In Figure IV.103, the variation of the integrated absorbance (maximum value arbitrarily fixed to one) of the bands at 1364 cm^{-1} and 1346 cm^{-1} is plotted as a function of the temperature from which the sample was cooled down. The first band may be ascribed to a strained gg conformers. The second one is ascribed to the {110} fold itself.

Figure IV.103 : Scaled area of some of the infrared bands present in the higher frequency part of the spectra of sample (3) as a function of the temperature from which the sample was cooled down

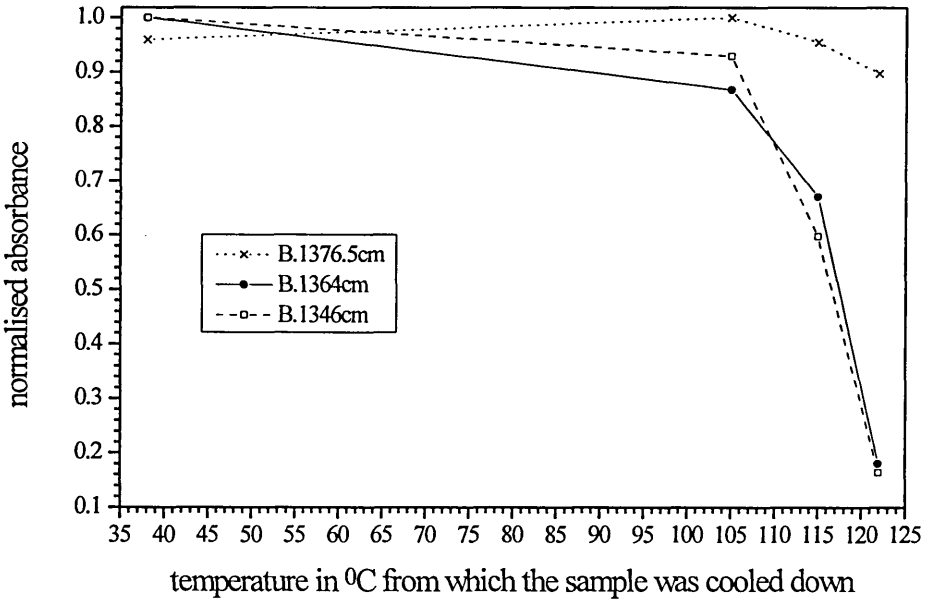

The normalised integrated absorbance of these two infrared bands has a very similar behaviour as a function of the temperature. After annealing at 115°C, the normalised absorbance of both bands decreases by around 35%. This decrease is believed to be due to the perfecting of once folded form crystals. Then, after annealing at 122°C, it decreases by nearly 85%. This effect is believed to be related to the premelting phase transition occurring between the once folded and extended form crystals at around 122°C.

The normalised absorbances of some of the bands present in the lower frequency range of the wagging mode region are shown Figure IV.104.

Figure IV.104 : Scaled area of some of the infrared bands present in the lower frequency part of the spectra of sample (3) as a function of the temperature from which the sample was cooled down

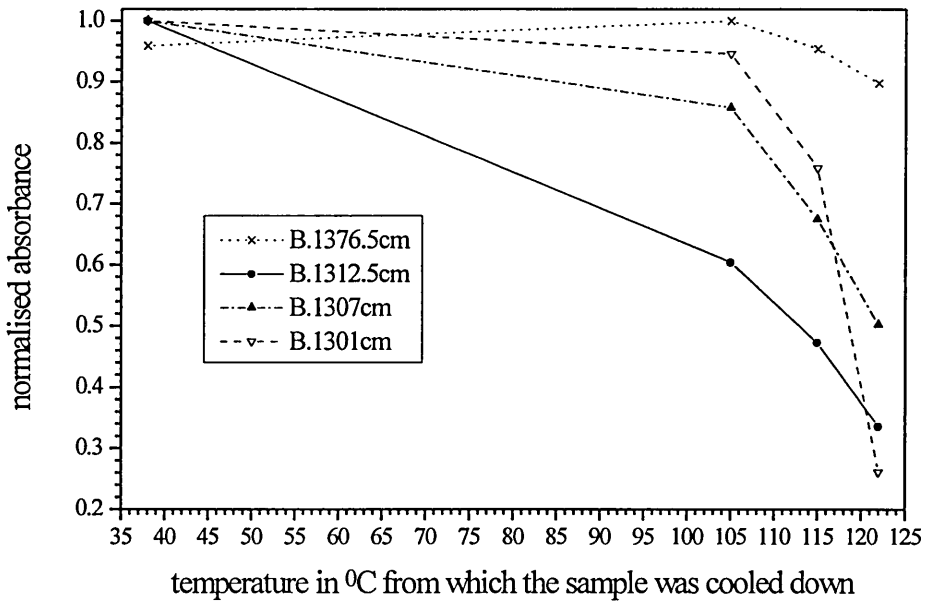

Maroncelli et al.[38] have shown, in the case of short chain n-alkanes, that the broad infrared band centred at around 1306 cm^{-1} is a sum of several components assigned to methylene wagging modes involved essentially in gtg' conformers placed at different sites along the n-alkane chains. Nevertheless, this band is also ascribed to methylene wagging modes involved in gtg conformers. Therefore, they deliberately neglected the presence of some gtg conformers in short chain n-alkane crystals. In particular, a band assigned to a methylene wagging mode approximately localised within the gtg' conformers was present at 1313 cm^{-1}. Therefore, in Figure IV.104, we ascribed the two bands at 1307 cm^{-1} and 1301 cm^{-1} to gtg/gtg' conformers. Their normalised absorbance is strongly affected by the increase of the annealing temperature at 115°C. Nevertheless, after annealing at 122°C, their absorbance decreases respectively by 50% and 75% of their initial values. These different values may indicate a different sensitivity of the gtg' conformers assigned to these two infrared bands, the ones related to the 1301 cm^{-1} band being more sensitive to the premelting phase transition than the ones related to the 1307 cm^{-1}. Finally, the band at 1312.5 cm^{-1} may also be assigned to the gtg' conformers. Its

normalised absorbance is already strongly affected after annealing sample (3) at 105°C, with a decrease of 40% of its original value. The gtg' conformers related to this infrared band may be more sensitive to the perfecting of the once folded form crystals than the ones ascribed to the 1301 cm^{-1} and 1307 cm^{-1} bands. Finally, over the temperature range used, its absorbance decreases by nearly 70%. Thus, the slightly different variations of the absorbance of these infrared bands with the increase of the temperature may indicate a different behaviour of the gtg' conformers placed at different sites along the n-alkane chains.

In Figure IV.105, the integrated absorbance (maximum value arbitrarily fixed to one) of the bands at 1295 cm^{-1} and 1289 cm^{-1} is plotted as a function of the temperature from which the sample was cooled down.

Figure IV.105 : Scaled area of some of the infrared bands present in the lower frequency part of the spectra of sample (3) as a function of the temperature from which the sample was cooled down

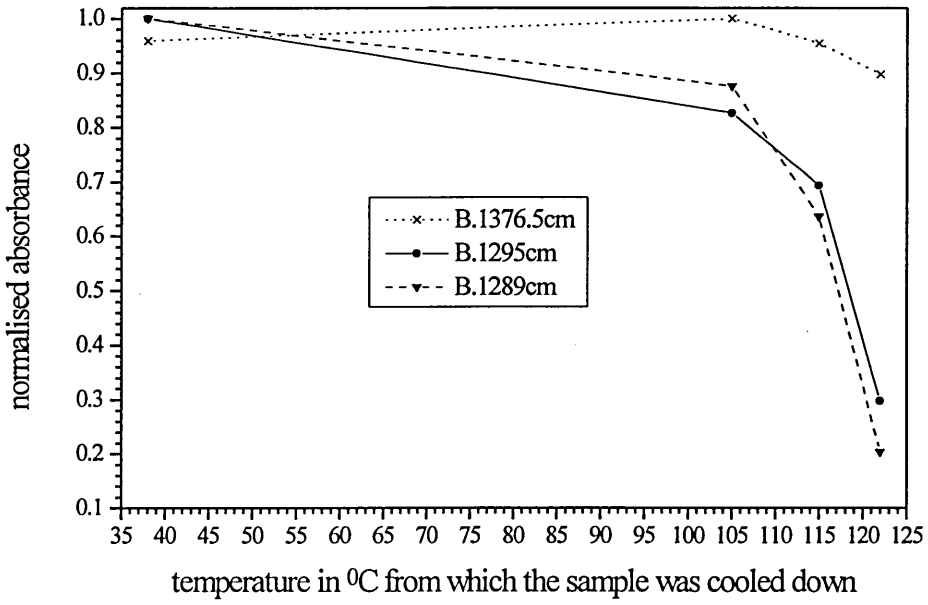

The variation of the normalised integrated absorbance of these two infrared bands as a function of the annealing temperature is very similar. After annealing sample (3) to 115°C, their normalised absorbance decreases by around 35%. This first decrease is believed to be linked to the perfecting of the once folded crystals. The major effect is

observed after annealing the sample to 122°C, their absorbance decreasing by around 75% of their initial values. Thus, this decrease is believed to be essentially related to the premelting phase transition occurring between the once folded and extended form crystals.

Figure IV.106 shows the variation of the area of the infrared bands at 1376.5 cm^{-1}, 888 cm^{-1} and 1174 cm^{-1} ascribed respectively to the symmetric methyl bending, methyl rocking and methylene wagging modes of vibration. Also, the variation of the integrated area of the broad infrared band present between 2690 cm^{-1} and 2558 cm^{-1} is shown.

Figure IV.106 : Normalised area of several infrared bands present in the low temperature spectra of sample (3) as a function of the temperature from which the sample was cooled down

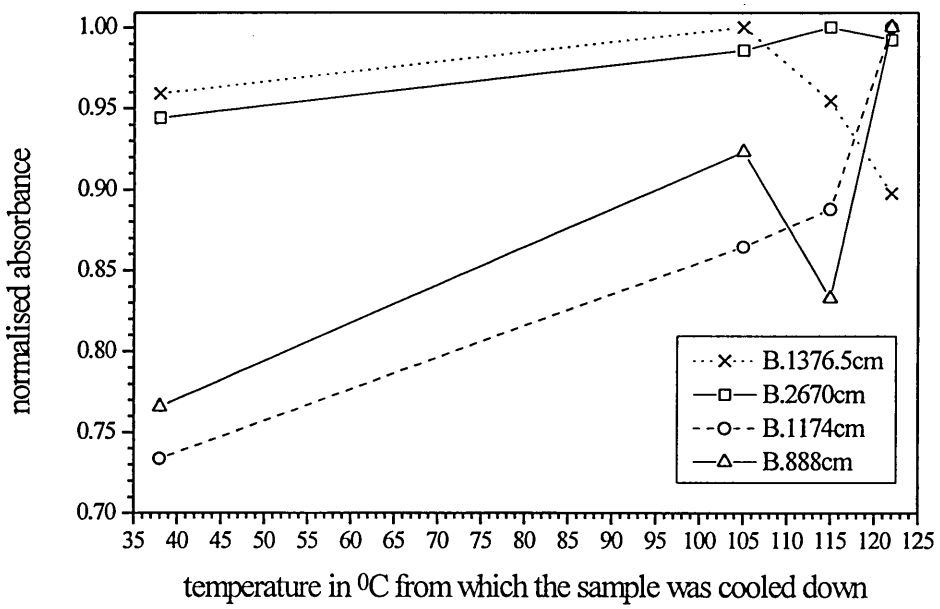

The normalised integrated absorbance of this last broad band, centred outside the wagging mode region of the infrared spectra, varies within 6% of its maximum value over the temperature range used. Also, a general increase of its intensity is observed as a function of annealing temperature. This observation contradicts the idea of a thinning of the sample through the annealing. Also, among the bands shown, this band at 2670 cm^{-1} is the least sensitive to the increase of the temperature. Therefore, this band may be preferred for normalising the infrared spectra recorded at low temperature.

IV.3.5.3.b C-C stretching mode region.

The C-C stretching mode region of the infrared spectra of sample (3) successively annealed at 38°C, 105°C, 115°C and 122°C, and in each case cooled down to -173°C, is shown in Figure IV.107.

Figure IV.107 : C-C stretching mode region of the low temperature infrared spectra of sample (3) cooled down from 38°C, 105°C, 115°C and 122°C

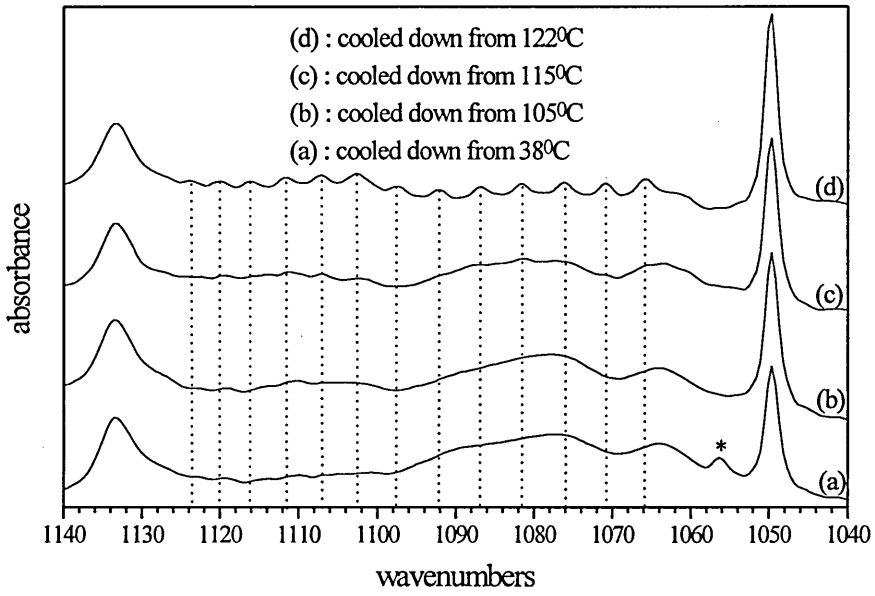

As seen previously, this region is limited by two extreme bands at 1133 cm^{-1} and 1050 cm^{-1}. The disappearance of the 1056 cm^{-1} band may be seen as a perfecting of the once folded crystals inside which the concentration of remaining non-all trans conformers, originally formed during the crystallisation from solution, decreases. A vertical dot line marks each progression band present in the spectrum of sample (3) cooled down from 122°C. These bands are ascribed to a non-localised mode of vibration involving the motion of adjacent carbon atoms with the same phase difference along the n-alkane chains. Also, some of the progression bands clearly present in the spectrum (d) can just be detected in the spectrum (c) and with great difficulty in the spectrum (b). Therefore, progression bands which are essentially a characteristic of the infrared spectra of sample

(3) in extended form can be partially observed in the spectra of sample (3) in once folded form after successively annealing and cooling down. This heating process produces a perfecting of the crystals. Also, some conversions to extended form crystals may have occurred before annealing at 122°C. Nevertheless, the absence of the broad bands at around 1089 cm^{-1}, 1078 cm^{-1} and 1064 cm^{-1} in the spectrum of sample (3) cooled down from 122°C indicates an absence of significant gauche conformers near to the crystal surfaces and {110} folds in the sample.

In the case of sample (3) cooled down from 122°C, estimates for both the best series of k values and the number of carbon atoms involved in the extended part of the n-alkane chains were determined. A $^{+}/_{-}1$ error is estimated for the values of the integers k. The average number of carbon atoms involved in the extended part of the n-alkane chains is estimated to be equal to 244 $^{+}/_{-}$ 13. The frequency of each of these progression bands is plotted against the integer k, in Figure IV.108. Also, the frequency of each of these bands was fitted by a third order polynomial curve shown by the black line.

Figure IV.108 : Frequency of the progression bands ascribed to the C-C stretching mode against k, integer, for sample (3) cooled down from 122°C.

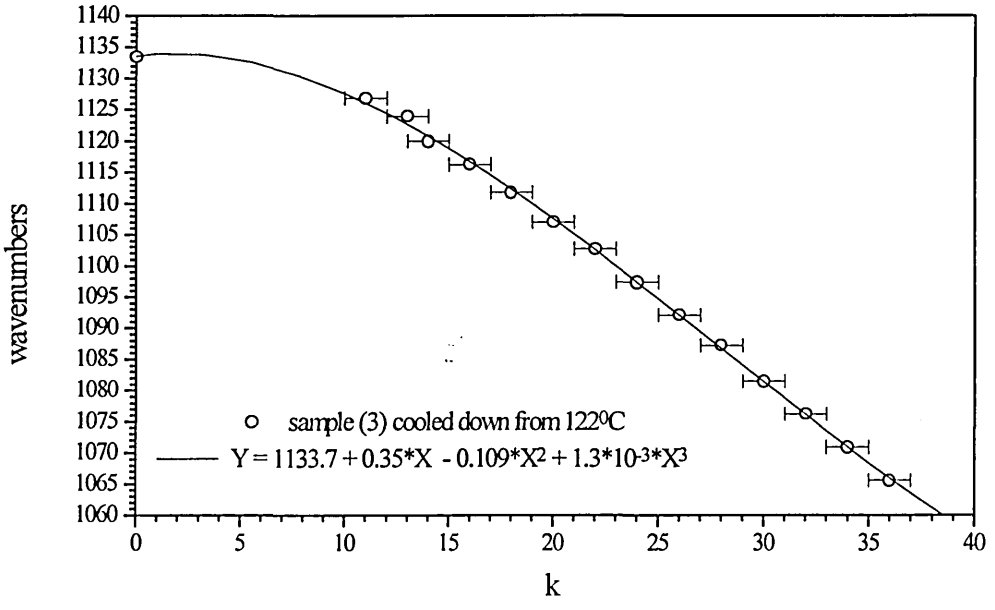

IV.3.5.3.c Conclusion.

As in the case of sample (1), we should expect the formation of tilted once folded form crystals within sample (3) with increasing annealing temperature. The values of the average layer periodicity determined by S.A.X.S. measurements on sample (3) have demonstrated the absence of these tilted structures. Up to 115^{0}C, the axes of the once folded n-alkane chains are perpendicular to the surface of the crystal layers. Also, a perfecting of the once folded form crystals is observed. After annealing up to 122^{0}C, sample (3) is no longer in a once folded crystal conformation, but in an extended one with the chain axis perpendicular to the crystal surfaces. This transition occurring between the two crystal forms is characterised by a strong decrease of all the bands ascribed to the modes of vibration of methylene groups involved in non-all trans conformers. Moreover, the band ascribed to the methyl symmetric bending mode is affected by this premelting transition too. Its area decreases by around 10% between 105^{0}C and 122^{0}C with a small shift in its position, going from 1376.5 cm^{-1} to 1377 cm^{-1}. Furthermore, the clear progression bands observed in the C-C stretching mode region of the spectrum of sample (3) cooled down from 122^{0}C confirm the occurrence of the transition between the two crystal forms.

Finally, the study of the methylene wagging mode region of the infrared spectra has shown the different sensitivities of the infrared bands present around 1307 cm^{-1} and assigned to gtg' conformers placed at different sites along the n-alkane chains as a function of the changes in the chain conformation within n-$C_{246}H_{494}$ crystals.

In pursuit of the least sensitive infrared band to chain conformational changes, the broad band between 2690 cm^{-1} and 2558 cm^{-1} present in the spectra recorded at -173^{0}C may be the one of greatest interest for use in band normalisation.

V BRANCHED AND MIXTURES OF LONG CHAIN N-ALKANES

V.1 Background.

As we have already seen, monodisperse long chain n-alkanes, are recognised to be an ideal model to study crystallisation and structure of polymers and paraffinic compounds. In the initial stages of their crystallisation from the melt, real-time S.A.X.S. measurements[20] have shown that their crystal thickness can be equal to a non integer fraction of the extended chain length. Then, through thickening or thinning, they transform respectively into extended or folded crystal forms. A long chain alkane with a methyl branch in the middle of the chain has shown similar behaviour : the crystallisation of $C_{96}H_{193}CH(CH_3)C_{94}H_{189}$, where the methyl group is present in the middle of the chain, has shown an initial formation of non integer form crystals[93]. Then, thinning occurs to produce once folded crystals. The once folded form seems to be a preferred conformation for this methyl branched long alkane sample when crystallised from both solution or melt. However, there is currently some concern as to whether the S.A.X.S. measurements unequivocally indicate the presence of folded chain crystals, since extended chain crystals might be expected to show a disordered layer including the methyl groups (Dr Goran Ungar, personal communication).

The study of melt crystallised mixtures of different monodisperse long chain n-alkane should improve the understanding of lamellar crystal structures and melting behaviour of polymers. With this aim, an appropriate binary mixture of monodisperse long chain n-alkanes was studied[50] by real-time S.A.X.S. measurements and D.S.C. experiments. In the case of the crystallisation from the melt of a 1:1 w/w binary mixture of the n-alkanes n-$C_{246}H_{494}$ and n-$C_{162}H_{326}$, a fully reversible transition was observed between low and high temperature phases around 90°C. The Fourier transform reconstruction of the density profiles obtained from the X-ray experiments indicates a triple layer crystal structure at the lowest temperatures where the n-alkane chains are in a tilted extended form. This triple layer crystal structure is composed of two crystal layers of the same thickness, 170 Å comprising a chain of 162 carbon atoms tilted by 35°, and one thinner crystal layer of 89 Å composed of a chain of 84 carbon atoms tilted by 35°. A phase

transition to the non integer form of the extended chain structure is observed with increasing temperature. In this case, there is only one crystal layer and an amorphous layer. The crystal layer is formed by 162 carbon atoms. The crystal structures expected at low and high temperatures are shown in Figure V.109 where the longest chains, namely n-$C_{246}H_{494}$, are represented in black and the shortest ones, namely n-$C_{162}H_{326}$, are represented in grey for clarity.

Figure V.109 : Different crystal structures observed in binary mixture of long chain n-alkanes.

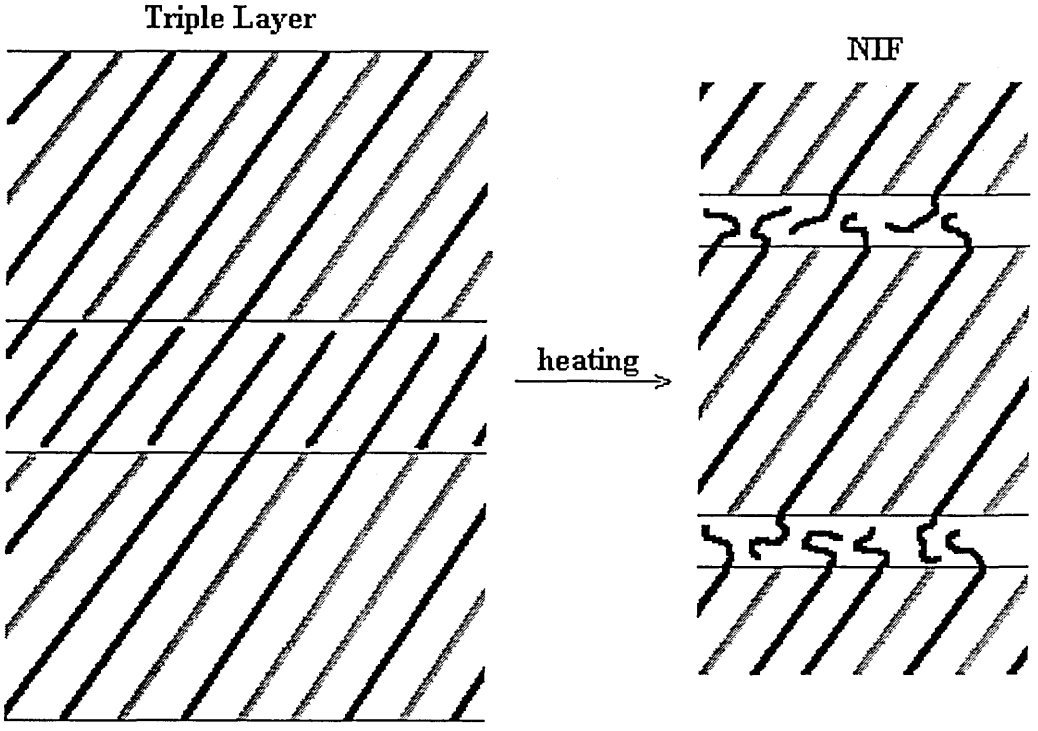

In this chapter, we will focus our discussion on the study of the disorder and fold structures within two branched monodisperse long chain n-alkane samples, namely $C_{96}H_{193}CH(CH_3)C_{94}H_{189}$ and $C_{96}H_{193}CH(CH_2\text{-}CH_2\text{-}CH_2\text{-}CH_3)C_{94}H_{189}$, using S.A.X.S. measurements, low frequency Raman spectroscopy and infrared spectroscopy techniques. We will compare the results obtained with a linear n-alkane sample of similar chain length, n-$C_{198}H_{398}$.

Finally we will try to observe, by means of infrared spectroscopy, the phase transition occurring between the triple layer and non integer form of the extended chain crystal structures within a 1:1 binary mixture of monodisperse long chain n-alkanes, n-$C_{246}H_{494}$ and n-$C_{162}H_{326}$.

V.2 Sample preparation.

Samples were synthesised by Brooke et al.[17] We crystallised the branched samples from solution in Aristar grade toluene and prepared as follows :

(4) $C_{96}H_{193}$-$CH(CH_3)$-$C_{94}H_{189}$ crystallised from 1.24% $^{w}/_{v}$ solution in toluene at 73.8 $^{+}/_{-}$ 0.4 ^{0}C for 90 minutes to obtain crystals in the once folded chain conformation, and then filtered. The resulting mat was allowed to dry before pressing (pressure applied over the sample surface lower than 0.4 ton per cm^2).

(5) $C_{96}H_{193}$-$CH(CH_2$-CH_2-CH_2-$CH_3)$-$C_{94}H_{189}$ crystallised from 1.18% $^{w}/_{v}$ solution in toluene at 74.2 $^{+}/_{-}$ 0.4 ^{0}C for 90 minutes to obtain crystals in the once folded chain conformation, and then filtered. The resulting mat was allowed to dry before pressing (pressure applied over the sample surface lower than 0.4 ton per cm^2).

A 1:1 binary mixture of n-$C_{246}H_{494}$ and n-$C_{162}H_{326}$ was prepared by X. Zeng (Sheffield University) and then :

(6) the 1:1 binary mixture of n-$C_{246}H_{494}$ and n-$C_{162}H_{326}$ was crystallised from the melt with a cooling rate of 2^{0}C per minute from 130^{0}C down to 80^{0}C, and left at 80^{0}C for 120 minutes before further cooling to room temperature. This process is expected to produce a crystal with a triple layer structure as shown in the left part of Figure V.109.

Using the S.A.X.S. technique, we determined the average layer periodicity of the samples (4) and (5), and hence the nature of the chain conformation. Using the relationship between carbon number and chain length reported by Broadhurst[60], values of the crystal thickness for both samples in once folded form were calculated and found to be equal to 122.5 Å. The S.A.X.S. layer periodicity for sample (4) was found to be 121.6 $^{+}/_{-}$ 1.5 Å. This value is in good agreement with the calculated one for a once folded structure. The S.A.X.S. layer periodicity corresponding to sample (5) was found to be 127.6 $^{+}/_{-}$ 2 Å. This value is in good agreement with the calculated one for a once folded structure, without taking in account the presence of the butyl branch groups within the amorphous layers. One should remark that a different crystal structure could also correspond to these average layer periodicities. Indeed, a structure where the alkane chains would be in extended form with the branch groups delimiting two crystal layers of thickness equal to half the chain length, will produce similar X-ray patterns.

Therefore, further X-ray scattering measurements to determine the electron density of the different crystal interfaces should enable us to choose between the extended and once folded models. Nevertheless, the once folded form model with the branch groups at the crystal surfaces must be preferred, pending these further experiments.

Finally, the way sample (6) was prepared is believed to have produced a sample in the low temperature phase characterised by a triple layer crystal structure where n-alkane chains from both chain lengths are in a tilted extended form (shown in the left side of Figure V.109).

V.3 Results.

V.3.1 Sample (4) : $C_{96}H_{193}$-$CH(CH_3)$-$C_{94}H_{189}$ crystallised in once folded form.

V.3.1.1 Low frequency Raman spectrum.

The low frequency Raman spectrum of sample (4) recorded at room temperature is shown in Figure V.110.

Figure V.110 : Low frequency Raman spectrum of sample (4) recorded at room temperature , after baseline subtraction.

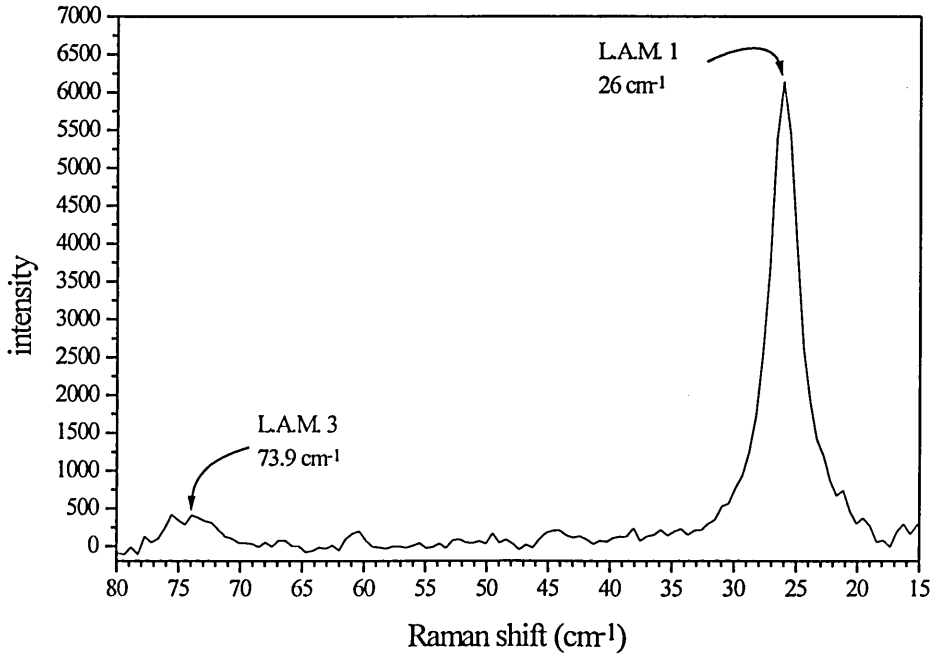

The first and third order of the Longitudinal Acoustic mode of vibration are present at 26 cm^{-1} and 73.9 cm^{-1}. The number of carbon atoms involved in the all-trans stem characteristic of the lamellar crystals of sample (4) was determined using the value of the frequency of the first order of the L.A. mode and equation IV.2. The number of carbon atoms was found to be equal to 94. Exactly half the number of carbon atoms composing the sample (4) chains are involved in this L.A. mode. Therefore, the n-alkane chains are in the once folded form conformation. This result confirms the one obtained by the previous S.A.X.S. measurements, although it is subject to the same reservation as noted earlier.

V.3.1.2 **S.A.X.S. measurements.**

Sample (4) is believed to crystallise from both solution or melt only in the once folded form. Previous measurements made on sample (4) crystallised from solution by means of S.A.X.S. techniques have tented to confirm this idea. We decided to melt sample (4) (melting point near to 117°C) by annealing it at 119°C and then cooling it down to -173°C to record an infrared spectrum. After cooling, S.A.X.S. measurements were carried out. The average layer periodicity was found to be equal to 100.6 $^{+}/_{-}$ 1.5 Å. This value is similar to 100.3 Å calculated for $C_{96}H_{193}$-$CH(CH_3)$-$C_{94}H_{189}$ in a tilted once folded chain conformation with a typical tilt angle of 35°. Thus, after annealing at 119°C and cooling to -173°C, sample (4) is in once folded form with the chain axis tilted from the crystal surfaces with an angle close to 35°.

V.3.1.3 **Infrared spectroscopy.**

V.3.1.3.a Methylene wagging mode region.

In sample (4), the methyl group is positioned nearly exactly in the middle of the alkane chain. Thus, in the case of sample (4) crystallised from solution, the alkane chains are probably in an once folded form conformation and the methyl group is attached to one of the carbon atoms composing the fold. Sample (4) was annealed successively at 35°C and 119°C, in both cases followed by cooling down to -173°C (with a cooling rate of around 10°C per minute), at which temperature the infrared spectra were recorded.

After annealing at 119°C, sample (4) was molten. Changes in the thickness of the sample after its melting required a normalisation procedure. To achieve this, as was done in the previous chapter we used as reference the integrated area of the broad band between 2690 cm^{-1} and 2558 cm^{-1}. The methylene wagging mode region of the infrared spectra of sample (4) recorded at -173°C is compared for the two annealing temperatures in Figure V.111. The signal to noise ratio of the spectrum of sample (4) cooled down from 35°C is greater than the one cooled down from 119°C.

Figure V.111 : Methylene wagging mode region of the low temperature F.T.I.R. spectra of sample (4) cooled down from 35°C and 119°C, after baseline subtraction and normalisation.

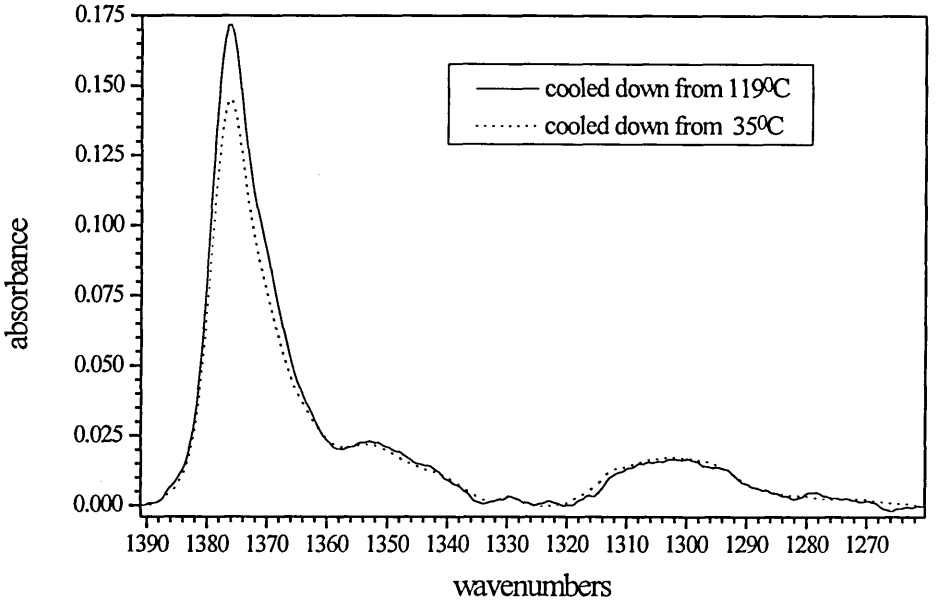

Several bands characteristic of the methylene wagging mode region are observed in these two infrared spectra. The major band of this region is assigned to the methyl symmetric bending mode at 1376.5 cm^{-1}. Then, a shoulder at around 1370 cm^{-1} is detected and is assigned to the gtg and gtg' conformers. At lower frequency, a broad band centred at 1306 cm^{-1} is also ascribed to gtg and gtg' conformers. A band at 1354 cm^{-1} is assigned to the gg conformers. The end-gauche conformers are observed at 1341 cm^{-1}. The {110} fold conformation is characterised by a band at around 1347 cm^{-1}. Two bands near 1330 cm^{-1} and 1312.5 cm^{-1} are detected and may be linked to the methylene

and methyl groups placed at the end of the alkane chains. A band present at 1295 cm^{-1} is ascribed to an off-zone centre methylene wagging mode.

Second derivatives, deconvolutions and curve fitting procedures were used for the region between 1391 cm^{-1} and 1322 cm^{-1} (Table V.24) and from 1322 cm^{-1} to 1260.3 cm^{-1} (Table V.25) to determine with accuracy the frequencies and areas of these different bands.

Table V.24 : Curve fitting results obtained for the infrared spectra of sample (4) recorded at -173°C.

	area	
wavenumbers cm^{-1}	cooled down from T=35°C	cooled down from T=119°C
1384.9	0.0283	0.0283
1376.4	**1.0591**	**1.2468**
1370.1	**0.3912**	**0.4666**
1363.8	0.2692	0.2850
1353.6	0.2246	0.2199
1347.2	**0.0554**	**0.0760**
1341	0.0906	0.0833
1329.7	0.0141	0.0133

Table V.25 : Curve fitting results obtained for the lower frequency part of the infrared spectra of sample (4) recorded at -173°C.

	area	
wavenumbers cm^{-1}	cooled down from T=35°C	cooled down from T=119°C
1312.4	**0.0846**	**0.0614**
1306.3	0.0962	0.0994
1301	0.0808	0.0723
1295.6	0.0904	0.0899
1289.2	0.0702	0.0666

From these results, we can observe that the major difference between the two infrared spectra of sample (4) recorded at -173°C is an increase of the integrated area of the band at 1347 cm^{-1} assigned to the {110} fold by nearly 25% of its original value. This

observation may be directly due to the tilting of the alkane chains from the crystal surfaces. Indeed, the tilting of the alkane chains may have changed the conformation of the {110} folds, and hence, the integrated absorbance of the band at 1347 cm^{-1}. At the same time, the integrated area of the band at 1312.4 cm^{-1} decreases by nearly 25% of its original value. In this case, two possibilities may be put forward. Firstly, due to the tilting of the alkane chains, changes in the direction of the dipole moment characteristic of this vibration may have occurred and so caused the decrease of its integrated area. Secondly, the number of specific conformers assigned to this band may have decreased with the tilting of the chains. Finally, as easily observed from Figure V.111, the integrated areas of the bands at 1376.4 cm^{-1} and 1370.1 cm^{-1} increase by about 15% of their original values. In both cases the tilting of the chains from the crystal surfaces may have changed the direction of the dipole moment linked to these modes of vibration, and thus the integrated intensity of the infrared bands assigned to them. Furthermore, in the case of the second band at 1370.1 cm^{-1} assigned to gtg and gtg' conformers, changes in the number of specific conformers may have occurred too and caused the increase of the integrated area of this band.

In the case of the other bands present in Table V.24 and Table V.25, their integrated absorbance has changed by less than 10% of their maximum value and the changes are not considered significant.

In order to compare the infrared spectra of sample (4) recorded at -173^{0}C, we decided to subtract the spectrum of sample (4) cooled down from 35^{0}C from the spectrum of sample (4) cooled down from 119^{0}C. The result of this subtraction is shown in Figure V.112.

Figure V.112 : Infrared spectrum of sample (4) cooled down from 35°C subtracted from the infrared spectrum of sample (4) cooled down from 119°C.

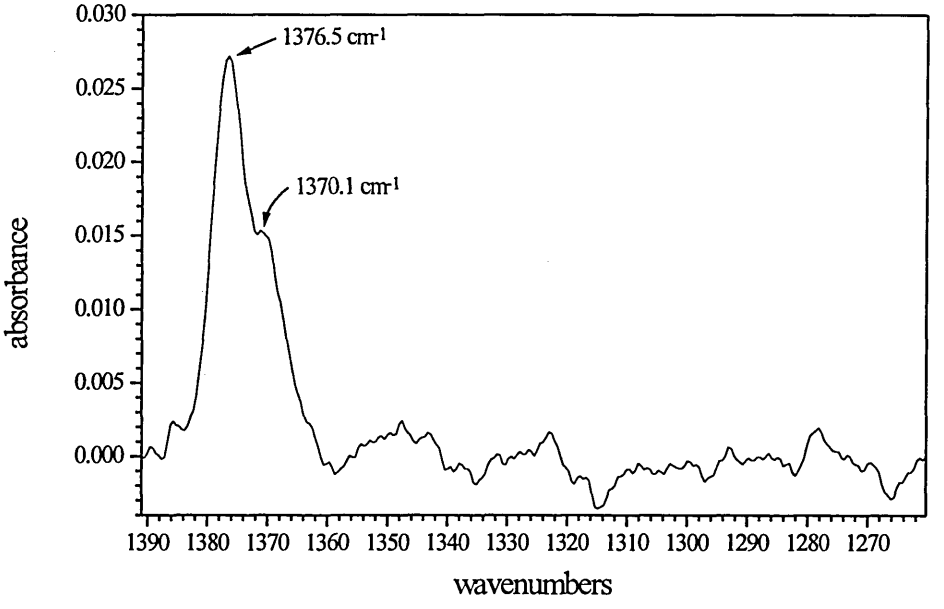

Only the bands with the greatest absorbance are clearly visible in this subtracted spectrum, at 1376.5 cm^{-1} and 1370.1 cm^{-1}. They are respectively ascribed to the methyl symmetric deformation and gtg and gtg' conformers. On the other hand, the changes of the absorbance of the bands at 1347 cm^{-1} and 1312.4 cm^{-1} are not detectable due to the weak absorbance of these bands in the original infrared spectra.

V.3.1.3.b Conclusion.

Changes in the infrared spectra of sample (4) cooled down from 35°C and 119°C were studied by the means of curve fitting and subtraction techniques. Both the increase of the integrated absorbance of the band at 1370.1 cm^{-1} and the decrease of the integrated absorbance of the band at 1312.4 cm^{-1} are probably due, at least in part, to the tilting of the alkane chains from the crystal layers. Changes in the direction of the dipole moments and/or in the number of conformers assigned to these modes of vibrations may both explain these observations. In the case of the bands at 1376.5 cm^{-1} and 1347 cm^{-1} assigned respectively to the methyl symmetric bending and {110} folds, the increase of their integrated absorbance may simply be due to a change in the dipole moment direction after the tilting of the chains. It is interesting to note that no significant

changes in the integrated absorbance of the 1341 cm^{-1} and 1353.6 cm^{-1} bands assigned respectively to the end-gauche and gg conformers were detected.

V.3.1.3.c C-C stretching mode region.

The C-C stretching mode region of the low temperature infrared spectra of sample (4) cooled down from 35°C and 119°C is shown in Figure V.113. The signal to noise ratio of the spectrum of sample (4) cooled down from 35°C is significantly greater than the one cooled down from 119°C.

Figure V.113 : C-C stretching mode region of the low temperature infrared spectra of sample (4) cooled down from 35°C and 119°C, after baseline subtraction and normalisation.

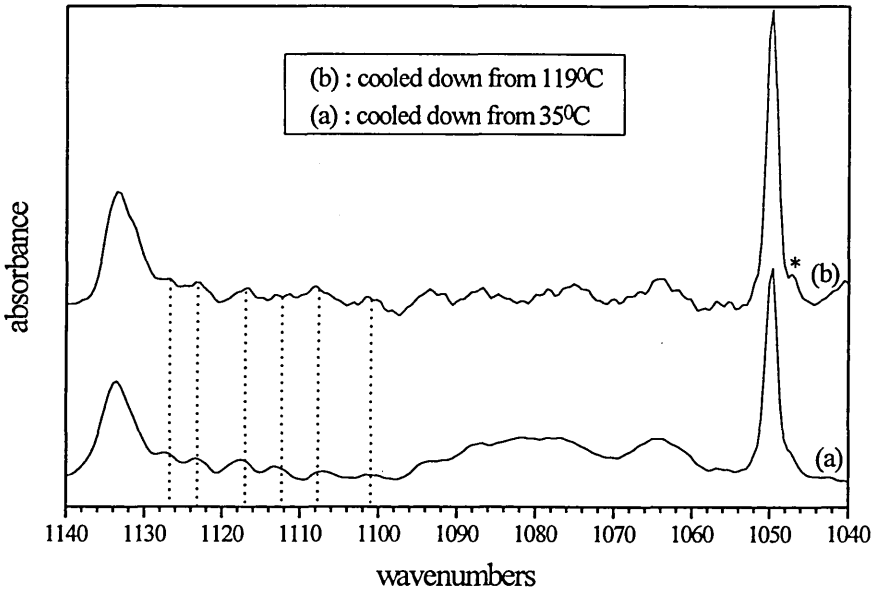

The band marked by an asterisk at 1047 cm^{-1}, present in the spectrum of sample (4) cooled down from 119°C may be related to a methylene twisting mode characteristic of non all-trans conformers formed during the crystallisation from the melt. Also, progression bands present in the spectra of sample (4) recorded at -173°C and crossed by a vertical dotted line are better resolved and slightly more regular in spectrum (a) than in spectrum (b). All these observations may indicate a more perfect crystal structure at

173^0C in the case of sample (4) crystallised from solution rather than the sample crystallised from the melt.

One can observe two distinct regions within the spectra (specially spectrum (a)). Above 1100 cm^{-1}, the progression bands are observed. Below this frequency, at least three broad bands at around 1089 cm^{-1}, 1078 cm^{-1} and 1064 cm^{-1} are observed. The bands at 1078 cm^{-1} and 1064 cm^{-1} were ascribed by Krimm et al.[61,94] to C-C stretching modes, the first one being characteristic of the presence of gauche conformers. Wolf et al.[47] have calculated by the Green's function method the defect frequencies of a tight {110} fold in polyethylene. They assigned an infrared band at 1082.5 cm^{-1} to the {110} folds. Thus, in the infrared spectra of sample (4), some of these bands may be due to the presence of the {110} folds or some disorder near the ends. Moreover, differences in this lower frequency part of spectra (a) and (b) may indicate differences in the conformation of the {110} folds present in sample (4) crystallised from both solution and melt.

Finally, we tried to identify each one of the progression bands present in this region. To achieve this, we used the frequency-phase curve for C-C stretching modes of short chain n-alkanes from n-$C_{20}H_{42}$ to n-$C_{30}H_{62}$ determined by Snyder and Schachtschneider[39] (for more details, see chapter IV). Estimates for both the best series of k values characteristic of each progression band and the number of carbon atoms involved in the extended part of the n-alkane chains were determined. A $^{+}/_{-}1$ error is estimated on the values of the integers k. The average number of carbon atoms involved in the extended part of the n-alkane chains is estimated to be equal to 101 $^{+}/_{-}$ 2. The frequency of each of these progression bands is plotted against the integer k, in Figure V.114. Also, the frequency of each of these bands was fitted to a third order polynomial curve shown by the black line.

Figure V.114 : Frequency of the progression bands ascribed to the C-C stretching mode against k, integer, for sample (4) cooled down from 122°C.

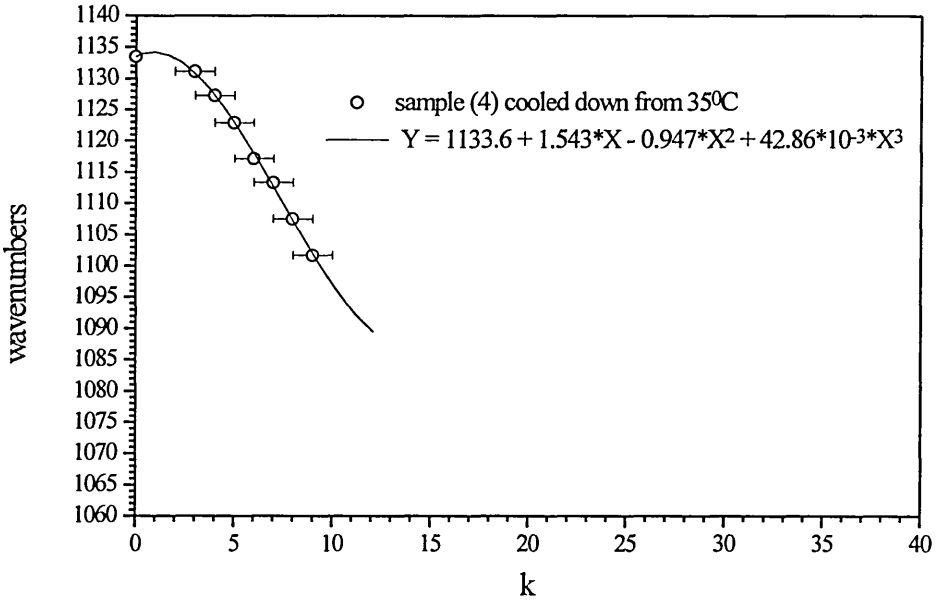

V.3.2 Comparison of the infrared spectra of samples (4) and (5).

With the aim of studying the effect of different branch groups placed nearly exactly in the middle of long chain alkanes crystallised from solution in once folded form, we recorded the infrared spectra of samples (4) and (5) cooled down from 35°C to -173°C.

V.3.2.1 Methylene wagging mode region.

In order to compare the methylene wagging mode region of the infrared spectra of samples (4) and (5) we normalised the spectra using as a reference the integrated absorbance of the broad band between 2690 cm^{-1} and 2558 cm^{-1}. The infrared spectra recorded at -173°C are shown in Figure V.115 after normalisation and baseline subtraction.

Figure V.115 : Methylene wagging mode region of the infrared spectra of samples (4) and (5) recorded at -173^{0}C after normalisation and baseline subtraction.

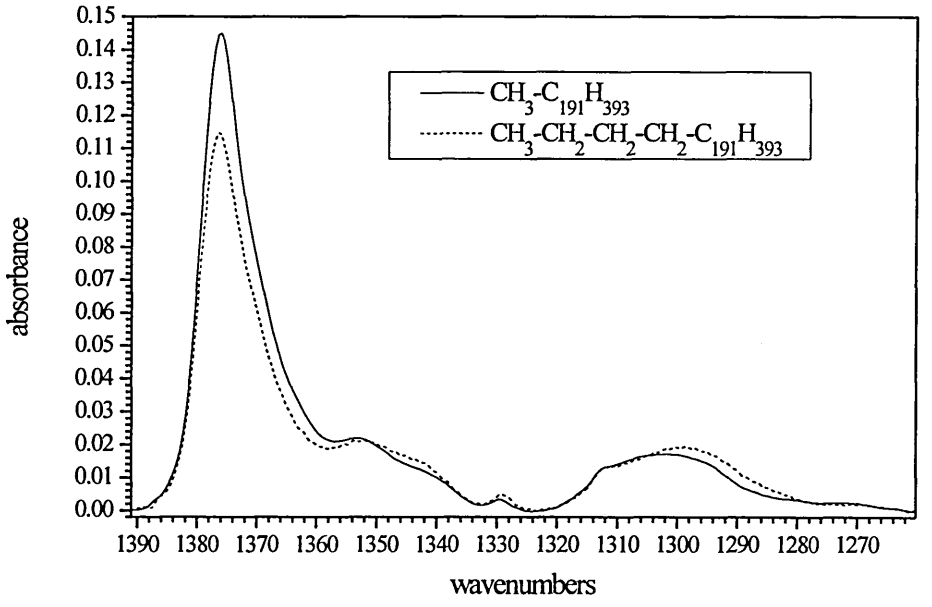

The usual infrared bands characteristic of the methylene wagging mode region of the infrared spectra of long chain alkanes at low temperature can be observed.

Second derivatives, deconvolutions and curve fitting procedures were used for the region between 1391 cm^{-1} and 1322 cm^{-1} (Table V.26) and from 1322 cm^{-1} to 1260.3 cm^{-1} (Table V.27) to determine with accuracy the frequencies and areas of these different bands.

Table V.26 : Curve fitting results obtained for the infrared spectra of samples (4) and (5) recorded at -173°C.

	area	
wavenumbers cm^{-1}	sample (4) cooled down from T=35°C	sample (5) cooled down from T=119°C
1384.9	0.0283	0.0139
1376.4	**1.0591**	**0.8692**
1370.1	**0.3912**	**0.3110**
1363.8	**0.2692**	**0.2042**
1353.6	0.2246	0.2127
1347.2	**0.0554**	**0.0712**
1341	**0.0906**	**0.1042**
1329.7	**0.0141**	**0.0210**

Table V.27 : Curve fitting results obtained for the lower frequency part of the infrared spectra of samples (4) and (5) recorded at -173°C.

	area	
wavenumbers cm^{-1}	sample (4) cooled down from T=35°C	sample (5) cooled down from T=35°C
1312.4	0.0846	0.0806
1306.3	0.0962	0.0912
1301	**0.0808**	**0.0913**
1295.6	**0.0904**	**0.1031**
1289.2	0.0702	0.1149

Going from the infrared spectrum of sample (4) to the spectrum of sample (5), a decrease of the integrated absorbance of the infrared bands at 1376.4 cm^{-1} and 1370.1 cm^{-1} by nearly 20% and of the 1363.8 cm^{-1} band by around 25% is observed. The number of methyl groups per chain is the same in both samples. So, changes in the integrated absorbance of 1376.4 cm^{-1} band assigned to the methyl symmetric bending mode may be explained by a difference in the orientation of the methyl groups at the crystal surfaces. Also, the deformation of the methyl group placed at the end of the butyl branched chain may have a slightly different fingerprint in an infrared spectrum

compared to the ones placed at the end of the long alkane chains. The decrease of the integrated absorbance of the 1370.1 cm^{-1} band assigned to the gtg and gtg' conformers seems to indicate a lower concentration of gtg and gtg' conformers within sample (5) crystals. The further decrease of the integrated absorbance of the 1363.8 cm^{-1} band in the spectrum of sample (5), which may be assigned to strained gtg and gtg' conformers, reinforces this idea. Moreover, the integrated absorbance of the bands at 1353.6 cm^{-1} assigned to gg conformers, 1306.3 cm^{-1} assigned to gtg and gtg' conformers and 1312.4 cm^{-1} varies within only 5% of their maximum value. Therefore, no major changes in the number of gg conformers were detected between the two branched samples. On the other hand, going from the infrared spectrum of sample (4) to the spectrum of sample (5), an increase of the integrated absorbance of the infrared bands at 1295.6 cm^{-1}, 1301 cm^{-1} and 1341 cm^{-1} by around 15% is observed. In the case of the 1341 cm^{-1} band assigned to end-gauche conformers, this result may indicate an increase in the number of these conformers within sample (5). This increase may be related to a higher concentration of end-gauche conformers in the butyl branch part of the chain than in the long alkane chains. The increase of the absorbance of the 1301 cm^{-1} band which can be ascribed to gtg and gtg' conformers may also be related to the branched part of the molecules. The integrated absorbance of the 1347.2 cm^{-1} band assigned to the {110} fold increases by nearly 25% going from the infrared spectrum of sample (4) to the spectrum of sample (5). Changes in the conformation of the {110} fold or a redistribution of the energy of vibration within the fold due to the butyl branched group may explain this observation. Finally, in the case of the bands at 1329.7 cm^{-1} and 1389.2 cm^{-1}, an increase of their integrated absorbance by respectively 35% and 40% of their maximum value is detected.

In order to compare the infrared spectra of samples (4) and (5) recorded at -173^{0}C, we also decided to subtract the spectrum of sample (5) cooled down from 35^{0}C from the spectrum of sample (4) cooled down from 35^{0}C. The result of this subtraction is shown in Figure V.116.

Figure V.116 : Infrared spectrum of sample (5) recorded at -173°C subtracted from the infrared spectrum of sample (4) recorded at -173°C, after baseline subtraction and normalisation.

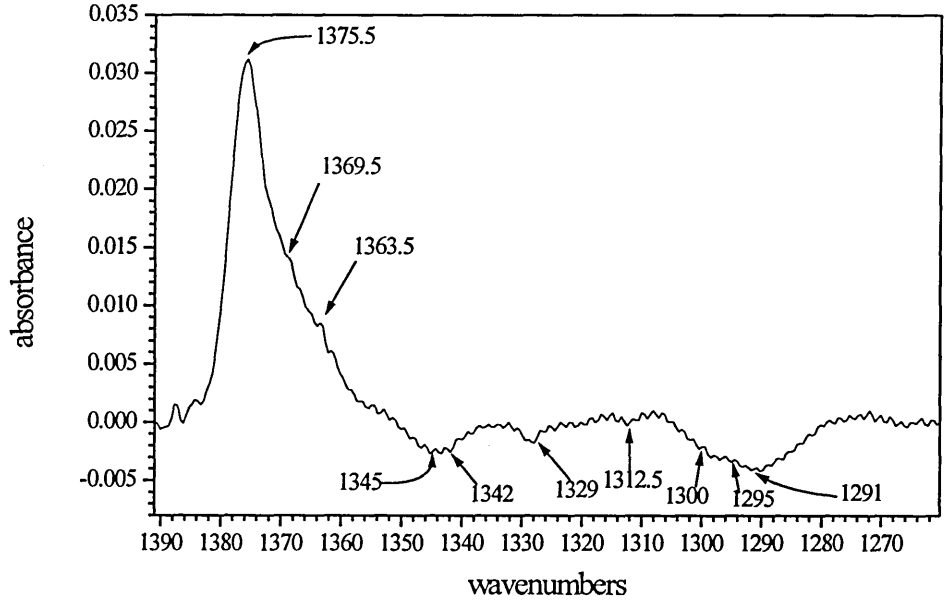

This spectrum confirms the result determined by the means of curve fitting techniques. The positive bands at 1375.5 cm^{-1}, 1369.5 cm^{-1} and 1363.5 cm^{-1} are the bands which have a greater integrated absorbance in the spectrum of sample (4) than in the spectrum of sample (5). Therefore, a higher number of gtg and gtg' conformers may be present in the chains of sample (4). The frequency of the band at 1375.5 cm^{-1} is slightly lower than the usual frequency of the methyl symmetric deformation. This may indicate a non-equivalence of some of the methyl groups present in the chains of samples (4) and (5). Most of the other bands are negative in this spectrum, since their integrated absorbance is greater in the spectrum of sample (5) than in the spectrum of sample (4) at -173°C. It is especially the case for the bands at 1345 cm^{-1} and 1291 cm^{-1}, the first of these being assigned to the {110} fold.

V.3.2.2 **C-C stretching mode region.**

The C-C stretching mode region of the low temperature infrared spectra of samples (4) and (5) cooled down from 35°C is shown in Figure V.117.

Figure V.117 : C-C stretching mode region of the infrared spectra of samples (4) and (5) recorded at -173^{0}C, after baseline subtraction.

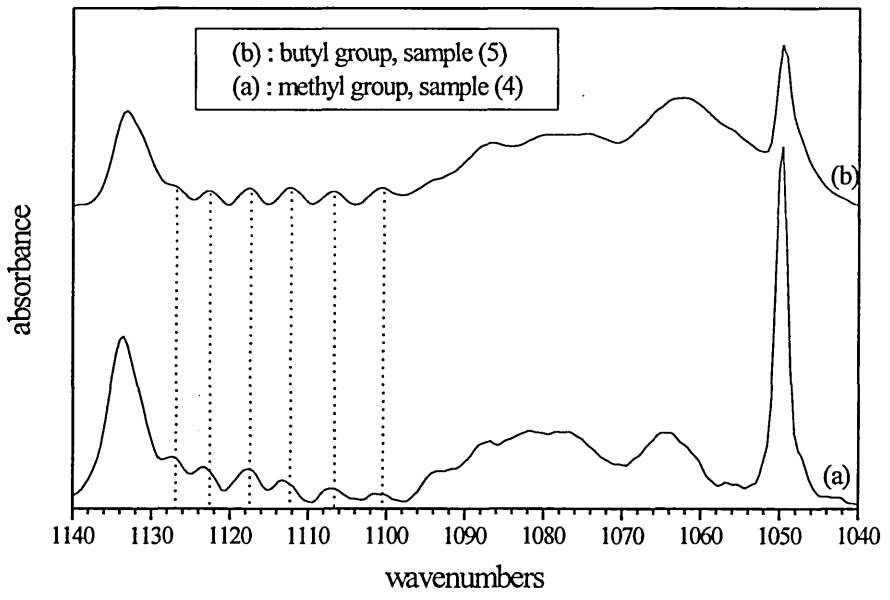

Each one of the progression bands present in the spectra (a) and (b) and crossed by a vertical dotted line has nearly the same frequency in both spectra. This observation seems to indicate that the average length of the all-trans sequences going through the crystal layers, which can be estimated from the frequency of each progression band, is approximately the same in both samples. Nevertheless, progression bands are slightly better resolved and more regular in spectrum (b) than in spectrum (a). These observations may indicate more perfect all-trans sequences in the case of sample (5) crystals. Perhaps a more likely explanation is that the distribution of chain lengths of the all-trans sequences within sample (5) crystals is narrower than the one within sample (4) crystals. In this case, the butyl branch group placed on one of the carbon atoms composing the fold seems to fix the number of carbon atoms involved in the all-trans sequences present in the crystal layers of sample (5).

The two distinct regions within the spectra are very clear. From 1100 cm^{-1} towards higher frequencies, the progression bands are observed. From 1100 cm^{-1} towards lower frequencies, at least three broad bands at around 1089 cm^{-1}, 1078 cm^{-1} and 1064 cm^{-1} are observed. Thus, in the infrared spectra of samples (4) and (5), some of these bands may

be due to the {110} folds or to the presence of some gauche conformers involved in the C-C stretching modes. In the case of sample (5), some non all-trans conformers present in the branched part of the chains may have a fingerprint in this region too. Therefore, the broader and more intense infrared bands present in this lower part of the C-C stretching mode region of the spectrum (b) may indicate a larger disorder at the crystal surfaces in the case of the butyl branch group. The average layer periodicity determined for sample (5) by S.A.X.S. measurements was equal to 127.6 $^{+}/_{-}$ 2 Å, around 6 Å larger than both the value determined for sample (4) and the calculated one which did not take into account the length of the butyl branch group. A larger amorphous layer formed partly by the butyl branched group may be present in sample (5) and explain partly the presence in spectrum (b) of this intense band at 1064 cm^{-1}. It may also account for differences in the conformation of the {110} folds present in both samples.

Finally, we tried to identify each one of the progression bands present in this region. To achieve this, we again used the frequency-phase curve reported for C-C stretching modes[39] (for more details, see chapter IV). Estimates for both the best series of k values characteristic of each progression band and the number of carbon atoms involved in the extended part of the n-alkane chains were determined. A $^{+}/_{-}$1 error is estimated on the values of the integers k. The average number of carbon atoms involved in the extended part of the n-alkane chains was estimated to be equal to 98 $^{+}/_{-}$ 2. The frequency of each of these progression bands is plotted against the integer k, in Figure V.114. Also, the frequency of each of these bands was fitted to a third order polynomial curve shown by the black line.

Figure V.118 : Frequency of the progression bands ascribed to the C-C stretching mode against k, integer, for sample (5) cooled down from 35^{0}C.

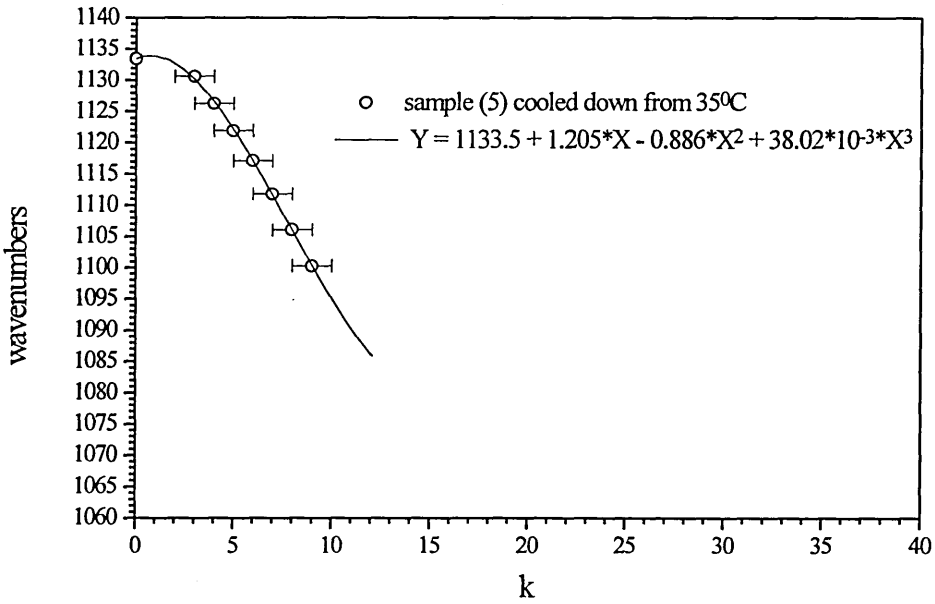

V.3.3 Comparison of the infrared spectra of samples (4) and (1).

In order to study the effect on the crystal structure of long chain n-alkanes of a small branch group placed in the middle of the chain, we compared the infrared spectra recorded at -173^{0}C of samples (1) and (4) crystallised from solution in once folded form.

V.3.3.1 Methylene wagging mode region.

In order to compare the methylene wagging mode region of the infrared spectra of samples (1) and (4), we normalised the spectra using as a reference the integrated absorbance of the broad band between 2690 cm^{-1} and 2558 cm^{-1}. The infrared spectra recorded at -173^{0}C are shown in Figure V.119 after normalisation and baseline subtraction.

Figure V.119 : Methylene wagging mode region of the infrared spectra of samples (1) and (4) recorded at -173°C after normalisation and baseline subtraction.

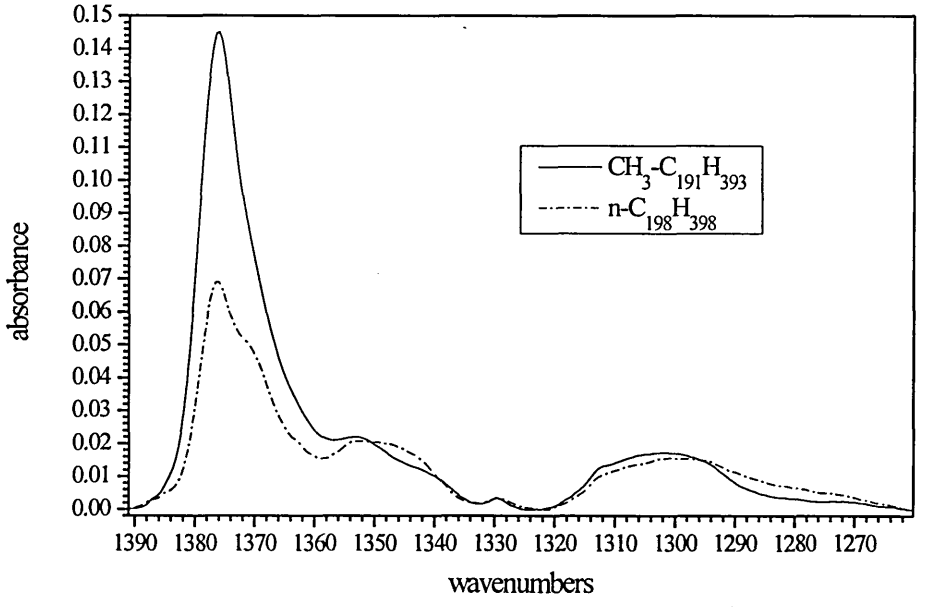

Second derivatives, deconvolutions and curve fitting techniques were monitored in the wagging mode region between 1391 cm^{-1} and 1322 cm^{-1} (Table V.28) and from 1322 cm^{-1} to 1260.3 cm^{-1} (Table V.29) to determine with accuracy the frequencies and areas of these different bands.

Table V.28 : Curve fitting results obtained for the higher frequency part of the infrared spectra of samples (1) and (4) recorded at -173°C.

	area	
wavenumbers cm^{-1}	sample (1) cooled down from T=51°C	sample (4) cooled down from T=35°C
1384.9	0.0255	0.0283
1376.4	**0.5110**	**1.0591**
1370.1	**0.2854**	**0.3912**
1363.8	**0.1706**	**0.2692**
1353.6	0.2243	0.2246
1347.2	**0.1002**	**0.0554**
1341	0.0895	0.0906
1329.7	**0.0201**	**0.0141**

Table V.29 : Curve fitting results obtained for the lower frequency part of the infrared spectra of samples (1) and (4) recorded at -173°C.

	area	
wavenumbers cm^{-1}	sample (1) cooled down from T=51°C	sample (4) cooled down from T=35°C
1312.4	**0.0686**	**0.0846**
1306.3	0.0905	0.0962
1301	0.0782	0.0808
1295.6	0.0915	0.0904
1289.2	**0.1090**	**0.0702**

Going from the infrared spectrum of sample (1) to the spectrum of sample (4), an increase of the integrated absorbance of the infrared bands at 1376.4 cm^{-1}, 1370.1 cm^{-1} and 1363.8 cm^{-1} by respectively nearly 50%, 35% and 25% is observed. The number of methyl groups per chain is not the same in both samples. Indeed, there are three methyl groups in the case of sample (4) and only two for sample (1). Therefore, an increase by around 30% of the integrated absorbance of the 1376.5 cm^{-1} band assigned to the methyl symmetric bending mode was expected in the spectrum of sample (4) assuming that the three methyl groups were equivalent. The observed increase of 50% was not expected. The 35% and 25% increase of the integrated absorbance of the 1370.1 cm^{-1} and 1363.8 cm^{-1} bands assigned respectively to regular and, maybe, strained gtg and gtg' conformers may indicate an increase of these specific non-all trans conformers within the alkane chains of sample (4) due to the presence of the additional methyl group on one of the carbon atoms composing the {110} fold. An increase by around 20% of the integrated area of the 1312.4 cm^{-1} band is observed. Also, the integrated absorbance of the bands at 1353.6 cm^{-1}, 1341 cm^{-1}, 1306.3 cm^{-1} and 1301 cm^{-1} assigned respectively to the gg, end-gauche and gtg and gtg' conformers varies within 5% of their maximum value. Therefore, the concentration of gg and end-gauche conformers seems to be of the same order in the alkane chains of both samples. On the other hand, the integrated absorbance of the bands at 1329 cm^{-1}, 1289 cm^{-1} and 1347.2 cm^{-1} decreases by respectively 30%, 35% and 45% going from the spectrum of sample (1) to the spectrum of sample (4). The last band is assigned to the {110} fold. This observation may be explained if one considers that the presence of the methyl group on one of the carbon

atoms composing the fold has changed the conformation of the fold or caused a redistribution of the energy of vibration within the fold.

In order to compare the infrared spectra of samples (1) and (4) recorded at -173°C, we also subtracted the spectrum of sample (1) cooled down from 51°C from the spectrum of sample (4) cooled down from 35°C. The two infrared spectra were normalised using the area of the band centred at 2670 cm^{-1}. The result of this subtraction is shown in Figure V.120.

Figure V.120 : infrared spectrum of sample (1) recorded at -173°C subtracted from the infrared spectrum of sample (4) recorded at -173°C, after baseline subtraction and normalisation.

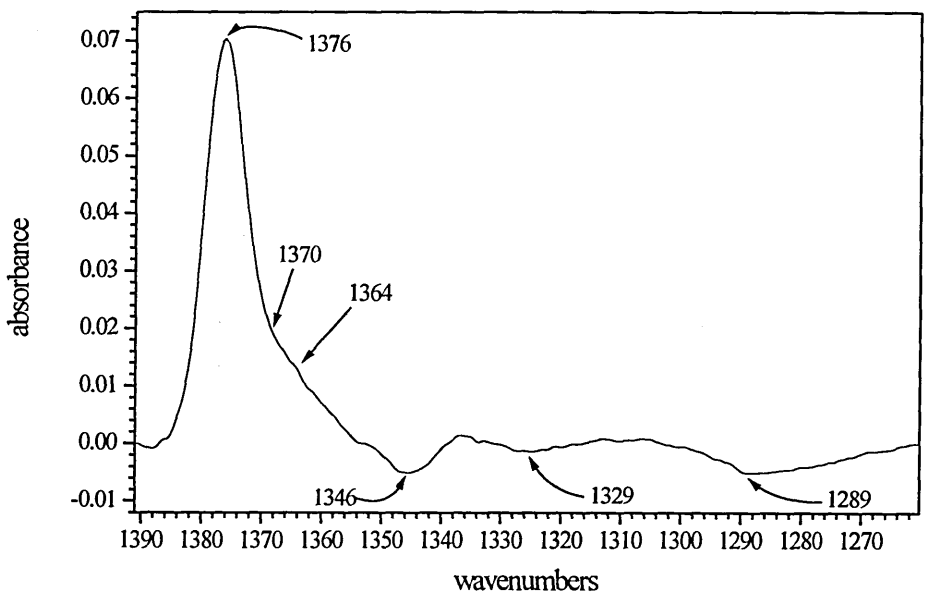

The positive bands at 1376 cm^{-1}, 1370 cm^{-1} and 1364 cm^{-1} are the bands which have a greater integrated absorbance in the spectrum of sample (4) than in the spectrum of sample (1). Therefore, a higher number of gtg and gtg' conformers may be present in the chains of sample (4). Most of the other bands are negative in this spectrum. Their integrated absorbance is greater in the spectrum of sample (1) than in the spectrum of sample (4) at -173°C. This is especially the case for the bands at 1346 cm^{-1}, 1329 cm^{-1} and 1289 cm^{-1}, the first one being assigned to the {110} fold.

V.3.3.2 **C-C stretching mode region.**

The C-C stretching mode region of the low temperature infrared spectra of samples (1) and (4) cooled down from respectively 51°C and 35°C is shown in Figure V.121.

Figure V.121 : C-C stretching mode region of the infrared spectra of samples (1) and (4) recorded at -173°C, after baseline subtraction.

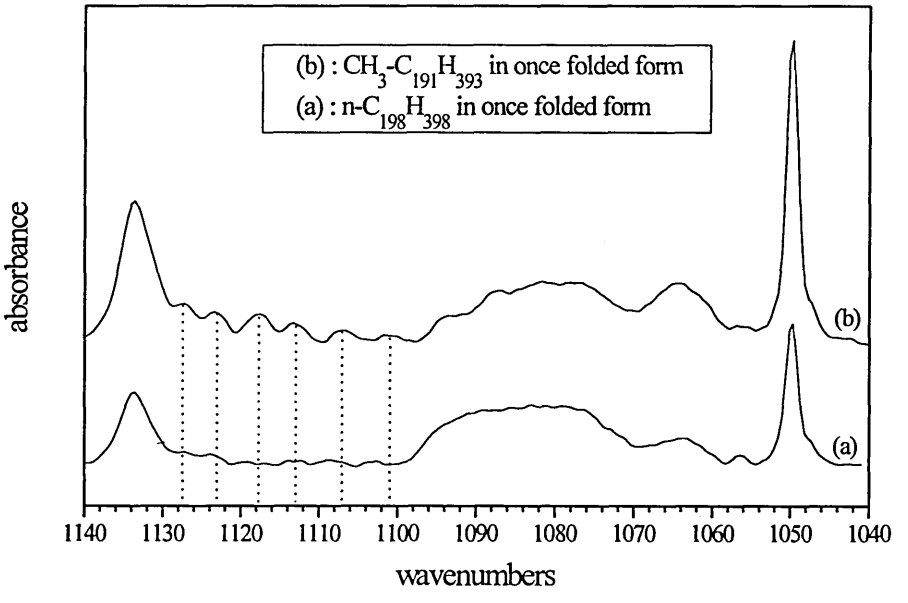

Some progression bands are present in the infrared spectra (a) and (b). The ones present in spectrum (b) are crossed by a vertical dotted line. Their frequencies differ slightly from those of spectrum (a). This observation seems to indicate that the average length of the all-trans sequences going through the crystal layers, which can be estimated from the frequency of each progression band, is different in samples (1) and (4). This result should be expected for samples having slightly different chain lengths. Also, progression bands are better resolved and more regular in spectrum (b). These observations seem to indicate that the distribution of chain lengths of the all-trans sequences within sample (4) crystals is narrower than that for sample (1) crystals. Therefore, the methyl branch group placed on one of the carbon atoms composing the fold seems to regulate the number of carbon atoms involved in the all-trans sequences going through the crystal layers.

Two distinct regions within the spectra are very clear. From 1100 cm^{-1} towards higher frequencies, the progression bands are observed. From 1100 cm^{-1} towards lower frequencies, at least three broad bands at around 1089 cm^{-1}, 1078 cm^{-1} and 1064 cm^{-1} are observed. In the infrared spectra of samples (1) and (4), some of these bands may be due to the {110} folds or to the presence of some disorder at the end parts of the chains. The broader and more intense infrared bands present in this lower part of the C-C stretching mode region of the spectrum (b) may indicate a higher disorder at the crystal surfaces in sample (4). It may also indicate differences in the conformation of the {110} folds present in both samples.

V.3.4 Comparison of the infrared spectra of samples (5) and (1).

In order to study the effect on the crystal structure of long chain n-alkanes of a bigger branched group placed in the middle of the chain, we compared the infrared spectra recorded at -173^{0}C of samples (1) and (5) crystallised from solution in once folded form.

V.3.4.1 **Methylene wagging mode region.**

In order to compare the methylene wagging mode region of the infrared spectra of samples (1) and (5), we normalised the spectra using as a reference the integrated absorbance of the broad band between 2690 cm^{-1} and 2558 cm^{-1}. The infrared spectra recorded at -173^{0}C are shown in Figure V.122 after normalisation and baseline subtraction.

Figure V.122 : Methylene wagging mode region of the infrared spectra of samples (1) and (5) recorded at -173°C after normalisation and baseline subtraction.

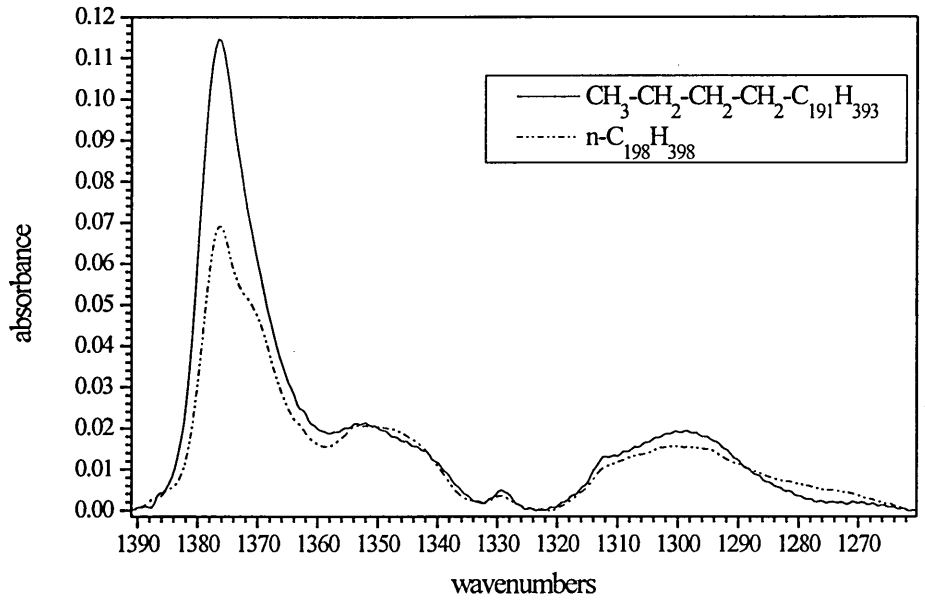

Second derivatives, deconvolutions and curve fitting techniques were monitored in the wagging mode region between 1391 cm^{-1} and 1322 cm^{-1} (Table V.30) and from 1322 cm^{-1} to 1260.3 cm^{-1} (Table V.31) to determine with accuracy the frequencies and areas of these different bands.

Table V.30 : Curve fitting results obtained from the higher frequency part of the infrared spectra of samples (1) and (5) recorded at -173°C.

	area	
wavenumbers cm^{-1}	sample (1) cooled down from T=51°C	sample (5) cooled down from T=35°C
1384.9	0.0255	0.0139
1376.4	**0.5110**	**0.8692**
1370.1	0.2854	0.3110
1363.8	**0.1706**	**0.2042**
1353.6	0.2243	0.2127
1347.2	**0.1002**	**0.0712**
1341	**0.0895**	**0.1042**
1329.7	0.0201	0.0210

Table V.31 : Curve fitting results obtained from the lower frequency part of the infrared spectra of samples (1) and (5) recorded at -173°C.

	area	
wavenumbers cm^{-1}	sample (1) cooled down from T=51°C	sample (5) cooled down from T=35°C
1312.4	**0.0686**	**0.0806**
1306.3	0.0905	0.0912
1301	**0.0782**	**0.0913**
1295.6	**0.0915**	**0.1031**
1289.2	0.1090	0.1149

Going from the infrared spectrum of sample (1) to the spectrum of sample (5), an increase of the integrated absorbance of the infrared bands at 1376.4 cm^{-1} by nearly 40% is observed. Due to the presence of three methyl groups per chain in sample (5) and assuming that they are equivalent, an increase by around 30% of the integrated absorbance of the 1376.5 cm^{-1} band assigned to the methyl symmetric bending mode was expected. The integrated absorbance of the bands at 1363.8 cm^{-1}, 1341m^{-1}, 1312.4 cm^{-1} and 1301 cm^{-1} increases by around 15% going from the spectrum of sample (1) to the spectrum of sample (5). The 1341 cm^{-1} and 1363.8 cm^{-1} bands are ascribed respectively to end-gauche and strained gtg and gtg' conformers. Their concentration may be higher in the sample (5) crystals. Some of these conformers may be located within the butyl branch groups. The integrated absorbance of the bands at 1370 cm^{-1} and 1306 cm^{-1} both assigned to gtg and gtg' conformers, 1353 cm^{-1} assigned to gg conformers, 1329 cm^{-1} and 1289 cm^{-1} varies within 10% of their maximum value. A similar concentration of gg, gtg and gtg' conformers seems to be present in both samples (1) and (5). Finally, the integrated absorbance of the 1347 cm^{-1} band assigned to the {110} fold decreases by around 30% going from the spectrum of sample (1) to the spectrum of sample (5). This observation may indicate a change in the conformation of {110} folds or a redistribution of the energy of vibration within the folds due to the presence of a butyl group on one of the carbon atoms composing the fold.

In order to compare the infrared spectra of samples (1) and (5) recorded at -173°C, we also subtracted the spectrum of sample (1) cooled down from 51°C from the spectrum of

sample (5) cooled down from 35°C. The result of this subtraction is shown in Figure V.123.

Figure V.123 : Infrared spectrum of sample (1) recorded at -173°C subtracted from the infrared spectrum of sample (5) recorded at -173°C, after baseline subtraction and normalisation.

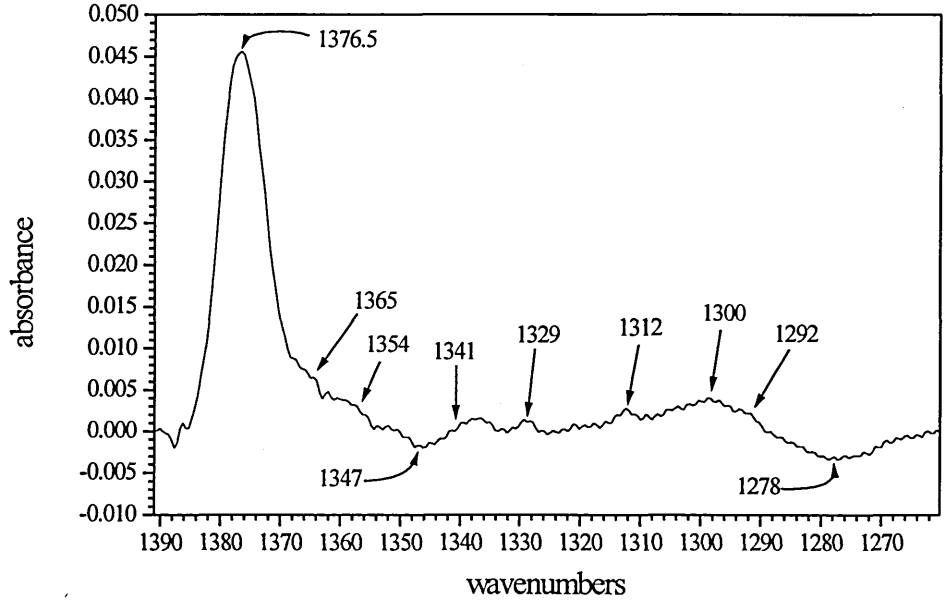

The positive band at 1376.5 cm^{-1} is the major band of the region. It is assigned to the methyl symmetric deformation. Due to the presence of three methyl groups per chain in sample (5) instead of two in sample (1), this band was expected to be observed. The other positive bands present in the spectrum at 1365 cm^{-1}, 1354 cm^{-1}, 1341 cm^{-1}, 1329 cm^{-1}, 1312 cm^{-1}, 1300 cm^{-1} and 1292 cm^{-1} are very much weaker and may indicate a higher concentration of gtg, gtg' and end-gauche conformers in the crystals of sample (5). Finally, two negative bands at 1278 cm^{-1} and 1347 cm^{-1} are detected. The last one assigned to the {110} folds may indicate some differences in the conformation of the {110} folds or a redistribution of the energy of vibration within the {110} folds due to the presence of the butyl groups on one of the carbon atoms composing the folds within sample (5) crystals.

V.3.4.2 **C-C stretching mode region.**

The C-C stretching mode region of the low temperature infrared spectra of samples (1) and (5) cooled down from respectively 51°C and 35°C is shown in Figure V.124.

Figure V.124 : C-C stretching mode region of the infrared spectra of samples (1) and (5) recorded at -173°C, after baseline subtraction.

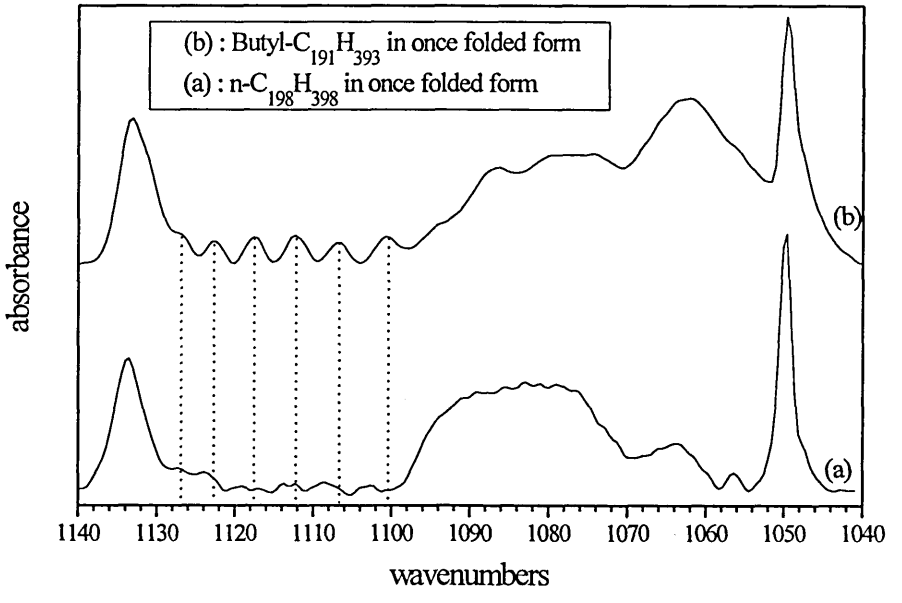

Some progression bands are present in the infrared spectra (a) and (b). The ones present in spectrum (b) are crossed by a vertical dotted line. Their frequencies differ slightly from those of spectrum (a). Similar observations made when we compared the spectra of sample (1) and (4) can be found here too. Indeed, the average length of the all-trans sequences going through the crystal layers, which can be estimated from the frequency of each progression band, is different in samples (1) and (5). Also, progression bands are very much better resolved and more regular in spectrum (b) than in spectrum (a). Therefore, the distribution of chain lengths of the all-trans sequences within sample (5) crystals appears to be narrower than the one within sample (1) crystals. Hence, the butyl branch group placed on one of the carbon atoms composing the fold seems to regulate the number of carbon atoms involved in the all-trans sequences going through the crystal layers.

As observed earlier, some of the bands present in the lower frequency part of this region may be due to the {110} folds or to the presence of some disorder at the end parts of the chains. They are much broader and more intense in the spectrum (b) which may indicate a higher disorder at the crystal surfaces in the case of sample (5). The average layer periodicity determined for sample (5) by S.A.X.S. measurements was equal to 127.6 +/- 2 Å, around 6 Å larger than the calculated value which did not take in account the length of the butyl branch group. A larger amorphous layer formed partly by the butyl branched group may be present in sample (5) and partly explain the presence in spectrum (b) of these broader bands. It may also indicate differences in the conformation of the {110} folds present in the two samples.

V.3.5 Conclusion.

From S.A.X.S. measurements, we determined the average layer periodicity of sample (4) crystallised in once folded form from both solution and melt. Crystallised from the melt, the alkane chains were found to be tilted from the crystal surfaces by an angle close to 35^0. Differences in the integrated area of the bands assigned to the {110} folds, methyl symmetric deformation and gtg and gtg' conformers present in the methylene wagging mode region as well as changes in the regularity and resolution of the progression bands present in the C-C stretching mode region of the infrared spectra recorded at -173^0C were discussed with regard to the tilting of the alkane chains.

Then, we studied the methylene wagging mode region of the infrared spectra recorded at -173^0C of methyl branched, butyl branched and unbranched long chain alkanes of similar chain lengths. We identified different specific conformers and compared their concentrations in each sample. Samples with a branch group in the middle of the chains were found to contain a higher concentration of non-all trans conformers. In the case of the butyl branched sample, some of these non all-trans conformers may be present within the branched part of the chains. Changes detected in the integrated absorbance of the 1347 cm^{-1} band assigned to the {110} fold conformation may indicate changes in the conformation of the fold in the different samples or a redistribution of the energy of vibration due to the different branched groups placed on one of the carbon atoms composing the folds.

From the higher frequency part of the C-C stretching mode region of the low temperature infrared spectra of the different samples, we compared the distribution and average chain lengths of the all-trans parts of the alkane chains going through the crystal layers. The lower frequency part of this region was taken to give an indication of the amount of disordered material for each of the different samples. Also, some of the bands present in this region may be related to several conformations of {110} folds. By increasing the size of the branches in the middle of the alkane chains, the distribution of the chain lengths for the all-trans parts of the chains going through the crystal layers seems to become narrower. At the same time, the amount of disordered material present in the different samples may increase.

V.3.6 Sample (6) : 1:1 binary mixture of n-$C_{246}H_{494}$ and n-$C_{162}H_{326}$.

V.3.6.1 Infrared spectrum of sample (6) recorded at -173^{0}C.

An infrared spectrum of sample (6) in the low temperature crystal structure was recorded at -173^{0}C. In this triple layer crystal structure, the n-alkane chains have been found to be in an extended tilted form by the means of S.A.X.S. measurements[50] (see Figure V.109). The wagging mode region of the spectrum is shown in Figure V.125 after baseline subtraction.

Figure V.125 : Methylene wagging mode region of the infrared spectrum recorded at -173^{0}C of sample (6) in a triple layer crystal form, after baseline subtraction.

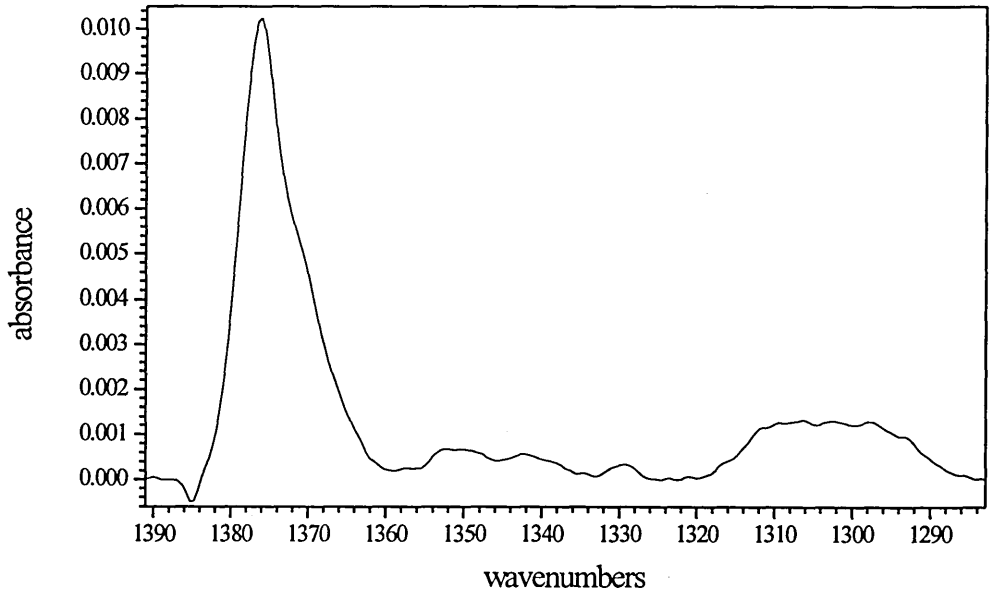

The maximum absorbance of the spectrum in this region is quite low (just over 0.01). This is due to the very small quantity of sample used. The major infrared bands of this region are assigned to the methyl symmetric deformation at 1376 cm^{-1} and to the gtg and gtg' conformers at 1370 cm^{-1}. It is interesting to note the weak intensity of the bands present at 1354 cm^{-1}, 1341 cm^{-1} and 1329 cm^{-1}. The first two are assigned respectively to the gg and end-gauche conformers. The absence of a significant band at 1347 cm^{-1}, in addition to the weak intensity of the previous bands, may indicate an absence of {110} fold in sample (6). In the lower frequency part of this spectrum, below 1320 cm^{-1}, a broad band is present. It has components at 1312 cm^{-1}, 1306 cm^{-1}, 1301 cm^{-1}, 1298 cm^{-1} and 1295 cm^{-1}. These bands are more intense than those at around 1350 cm^{-1}.

The C-C stretching mode region of the low temperature infrared spectra of sample (2) cooled down from 126^{0}C (n-$C_{198}H_{398}$ in extended form), sample (3) cooled down from 122^{0}C (n-$C_{246}H_{494}$ in extended form) and sample (6) cooled down from room temperature are shown in Figure V.126 after baseline subtraction.

Figure V.126 : C-C stretching mode region of the infrared spectra of samples (2), (3) and (6) recorded at -173^{0}C, after baseline subtraction.

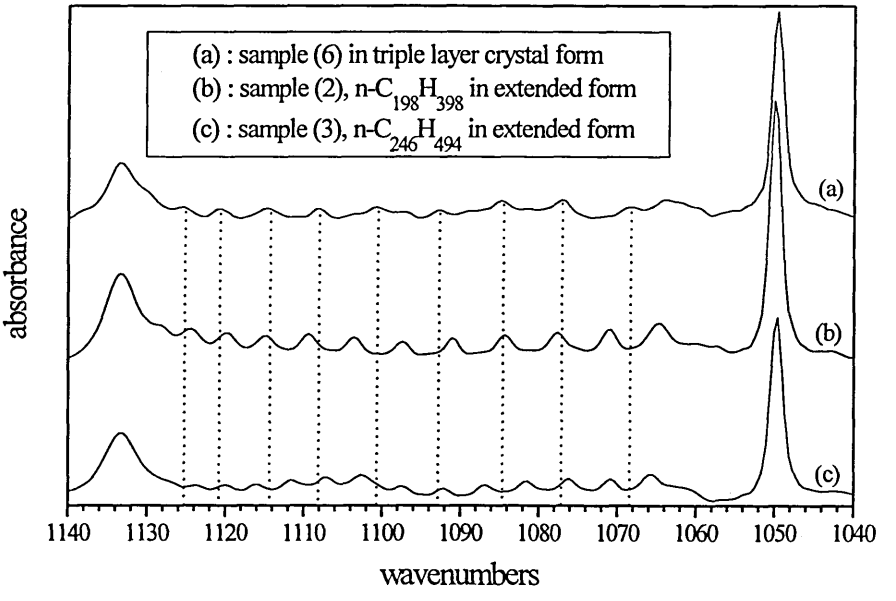

In the three spectra, progression bands are clearly detected throughout the C-C stretching mode region. There are no longer two clearly separable regions in the spectra. From this observation, we may assume that in sample (6) crystals, as in the case of samples (2) and (3), the n-alkane chains are primarily in an extended chain conformation. The more prominent progression bands present in spectrum (a) are crossed by a vertical dotted line. These bands are slightly less well resolved than in spectra (b) and (c). Also, their frequencies differ from those of spectra (b) and (c). The frequency shift between each successive progression band is much larger in the case of sample (6) than in the case of samples (2) and (3). It is also larger in the case of sample (2) than in the case of sample (3). Therefore, the average length of the all-trans sequences going through the crystal layers, which can be estimated from the frequency of each successive band, is different in samples (6), (2) and (3). Furthermore, we can conclude from these results that the average chain length in sample (6) is smaller than in sample (2) and also, that the average chain length is smaller in sample (3) than in sample (2).

The absence of any significant infrared bands at around 1089 cm^{-1}, 1078 cm^{-1} or 1064 cm^{-1} which may be linked to the {110} folds or to the presence of some disorder near the chain ends may indicate the absence of a significant amount of {110} fold conformation or disorder at the crystal surfaces in sample (6). Indeed, a similar amount of non purely all-trans conformers may be present in the three samples.

Finally, we tried to identify each one of the progression bands present in this region. Estimates for both the best series of k values characteristic of each progression band and the number of carbon atoms involved in the extended part of the n-alkane chains were determined. A $^{+}/_{-}1$ error is estimated for the values of the integers k. The average number of carbon atoms involved in the extended part of the n-alkane chains is estimated to be equal to 158 $^{+}/_{-}$ 15. The frequency of each of these progression bands is plotted against the integer k, in Figure V.114. Also, the frequency of each of these bands was fitted to a third order polynomial curve shown by the black line.

Figure V.127 : Frequency of the progression bands ascribed to the C-C stretching mode against k, integer, sample (6) cooled down from room temperature.

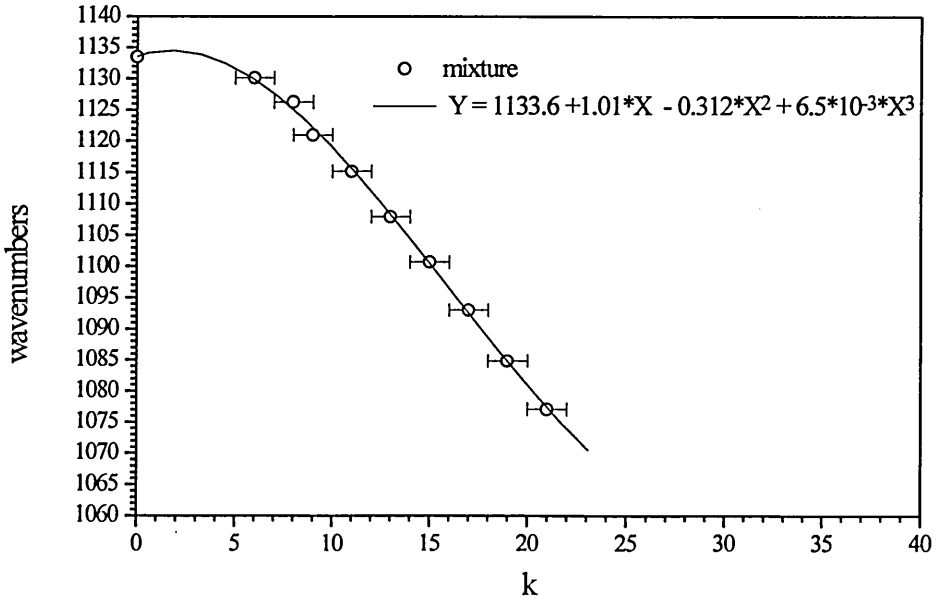

The study of the infrared spectrum of sample (6) recorded at -173°C indicates that no significant amount of {110} fold material is present in sample (6) crystals. Therefore, the n-alkane chains present in the sample are in an extended chain conformation. The

all-trans alkane chain length within the crystal layers is smaller in the 1:1 binary mixture than in the case of n-$C_{198}H_{398}$ crystals in extended form. The number of carbon atoms going through the crystal layers has been estimated to be 158 +/- 15. This value is very similar to 162 which is the number of carbon atoms composing the shortest chains of the mixture. Nevertheless, a similar amount of "amorphous" material is present in samples (2), (3) and (6). This implies that the longer alkane chains present in the 1:1 binary mixture, n-$C_{246}H_{494}$, are also in an extended conformation with few carbon atoms outside the crystal layers. Therefore, this is consistent with a triple layer structure as determined by Zeng and Ungar.

V.3.6.2 **Effects of heating at a variable rate.**

With the aim of observing the phase transition occurring within sample (6) between a triple layer crystal structure and a non integer form involving extended segments, we heated sample (6) from 70.4°C to 115.2°C. An infrared spectrum was recorded every 3.2°C between 70.4°C and 97°C, then every 0.8°C between 97°C and 108°C and at 112°C and 115.2°C. A baseline has been used with reference points at 1391 cm^{-1}, 1328 cm^{-1} and 1283 cm^{-1}. The infrared spectra recorded between 97°C and 115.2°C are shown in Figure V.128 after baseline subtraction.

Figure V.128 : Methylene wagging mode region of the infrared spectra of sample (6) recorded between 97°C and 115.2°C, after baseline subtraction.

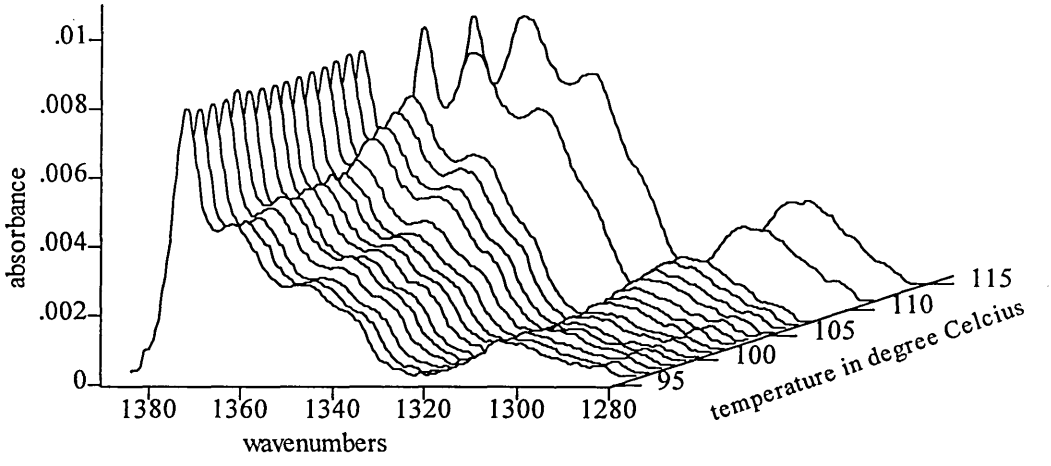

The major bands are found at 1376.5 cm^{-1}, assigned to the methyl symmetric deformation, 1368 cm^{-1} assigned to the gtg and gtg' conformers, 1353 cm^{-1} ascribed to the gg conformers, 1342 cm^{-1} ascribed to the end-gauche conformers and 1307 cm^{-1} assigned to the gtg and gtg' conformers. The first fifteen spectra were recorded every 0.8°C. At around 105°C a clear increase of the intensity of the bands assigned to the non all-trans conformers is observed. The phase transition between the the triple crystal layer and the N.I.F. structure may have occurred around this temperature. In order to verify this observation the intensity of each band present in each elevated temperature infrared spectrum recorded between 70.4°C and 115.2°C was determined after baseline subtraction. The peak intensity of each band was normalised using the intensity of the 1376.5 cm^{-1} band assigned to the methyl symmetric deformation. The normalised intensity of each band is plotted against the annealing temperature in Figure V.129.

Figure V.129 : Intensity of each band plotted as a function of the temperature, after baseline subtraction and normalisation using the 1376.5 cm^{-1} band as reference.

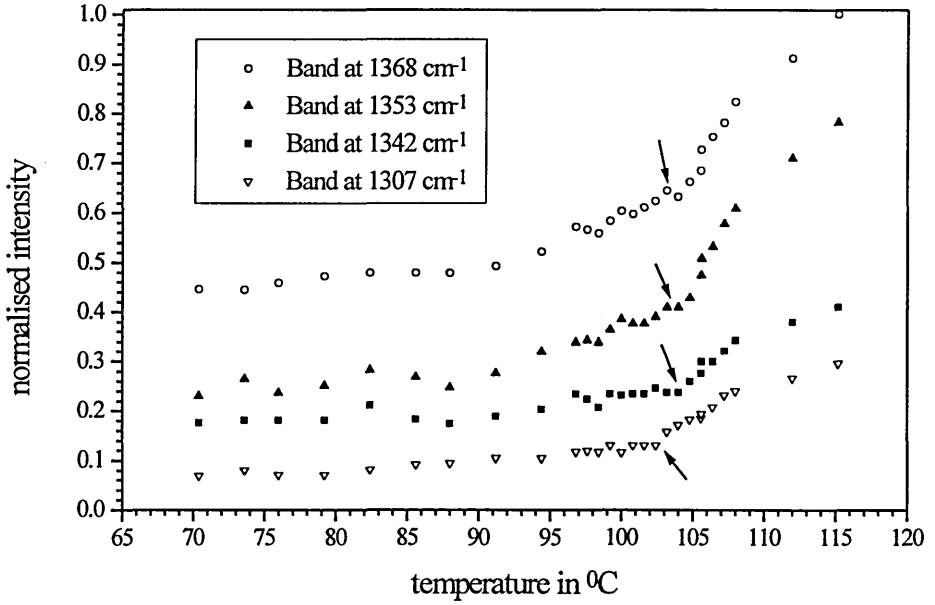

For each band ascribed to non all-trans conformers present in the spectra of sample (6) a change in the rate of increase of the normalised intensity as afunction of temperature is detected and marked by an arrow in Figure V.129. This jump in the normalised intensity occurs in each case at 104 $^{+}/_{-}$ 0.8 ^{0}C.

V.3.6.3 **Heating at constant rate.**

Sample (6) was recrystallised from the melt and cooled down at $2^{0}C$ per minute from $130^{0}C$ down to $80^{0}C$ and left at $80^{0}C$ for 120 minutes before further cooling to room temperature. Prepared in this way, sample (6) is believed to be in the triple layer crystal structure. Then, sample (6) was heated up from $76.5^{0}C$ to $139^{0}C$ with a heating rate of $0.4^{0}C$ per minute. A spectrum was recorded every four minutes (or every $1.6^{0}C$). A baseline has been subtracted between 1391 cm^{-1} and 1323 cm^{-1}. Then, the methylene wagging mode region of the full series of the infrared spectra is shown in Figure V.130 after baseline subtraction.

Figure V.130 : Methylene wagging mode region of the infrared spectra of sample (6) recorded between 76.5^{0}C and 139^{0}C, after baseline subtraction.

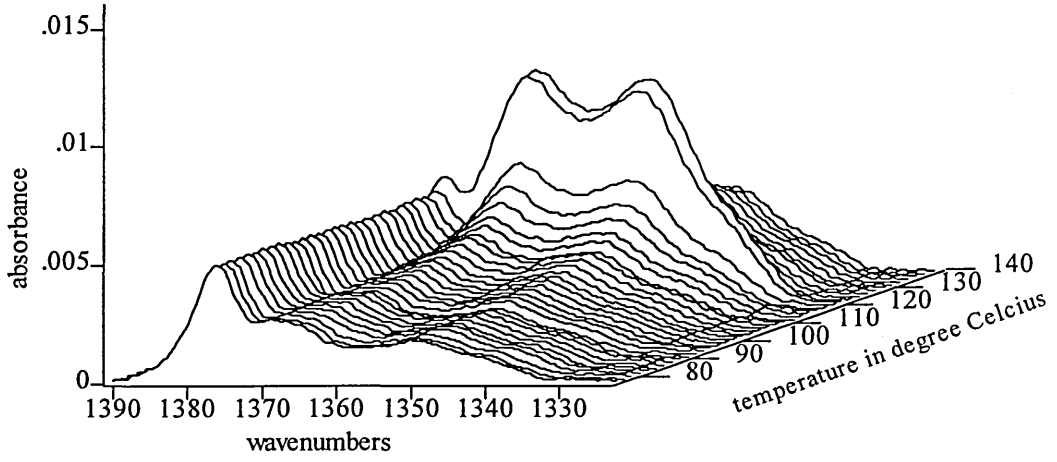

The major bands are as in the previous run. This time, a strong increase in the intensity of the infrared bands present in Figure V.130 is observed at around 122.8 $^+/_-$ 1.6 ^{0}C. The phase transition observed at this temperature is believed to be the melting of sample (6). Therefore, we did not observe directly from Figure V.130 the transition between the low temperature and high temperature phases. The intensity of each band was normalised using the intensity of the 1376.5 cm^{-1} band assigned to the methyl symmetric deformation. The normalised intensity of each band is plotted against the annealing temperature in Figure V.131.

Figure V.131 : Intensity of each band plotted as a function of the temperature, after baseline subtraction and normalisation using the 1376.5 cm^{-1} band as reference.

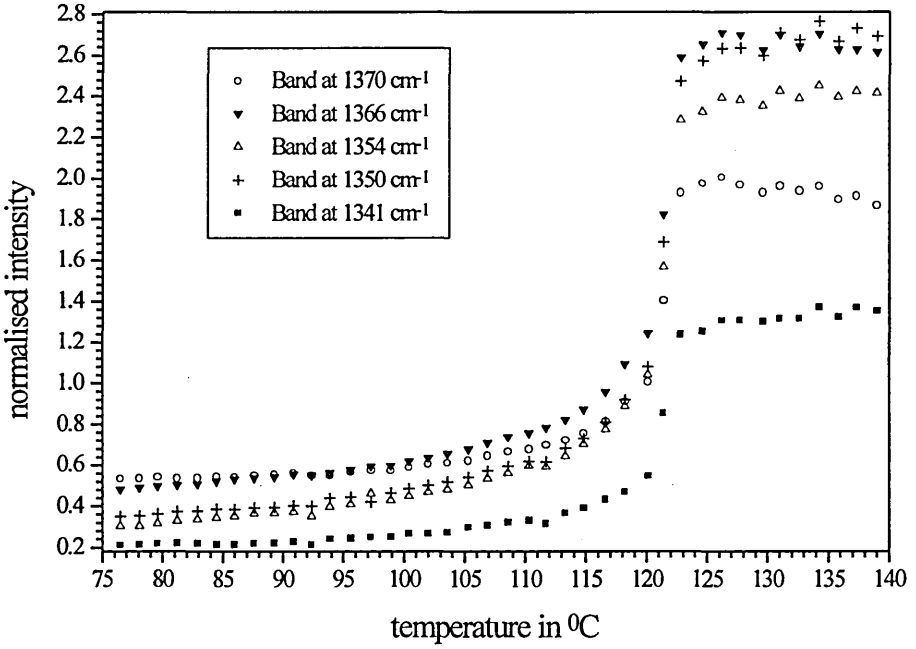

For each band ascribed to non all-trans conformers present in the spectra of sample (6) a change in the rate of increase with temperature of the normalised intensity is detected at 122.8 +/- 1.6 ^{0}C. Above this temperature, the sample is in the liquid state. No indication of a transition is observed around 105^{0}C.

In Figure V.132, the intensity of each infrared band present in the spectra has been normalised using the 1376.5 cm^{-1} band as reference and then, the maximum intensity of each band has arbitrarily been scaled to one.

Figure V.132 : Scaled intensity of each band plotted as a function of the temperature, after baseline subtraction, normalisation using the 1376.5 cm^{-1} band as reference and maximum intensity arbitrarily fixed to one.

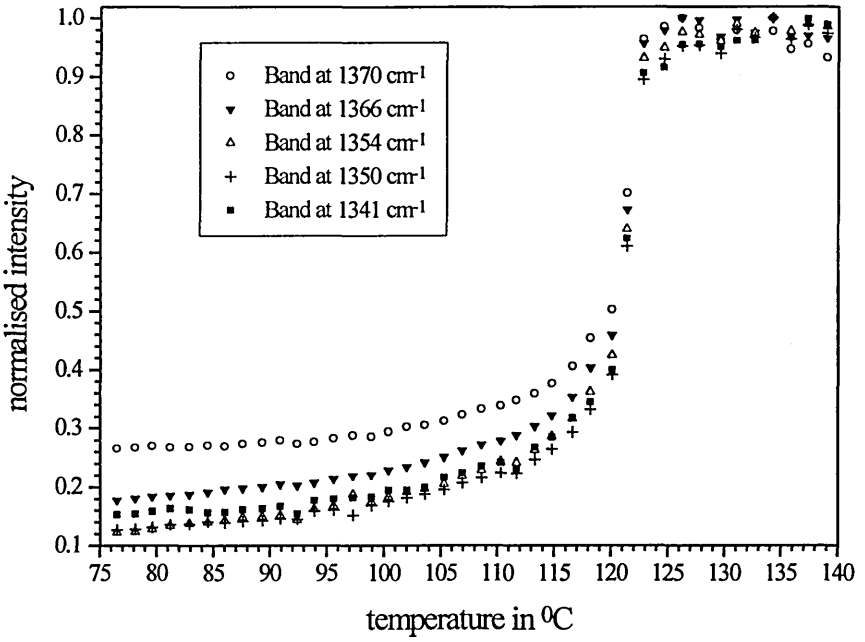

Apart from the melting of the sample, no other phase transition is observed. Nevertheless, we can remark that within sample (6) the number of the non all-trans conformers is approximately five times lower than in the liquid state. In the case of gtg and gtg' conformers, their number is roughly three times lower than in the liquid state. The absence of any indication of phase transition between the triple layer crystal form and the N.I.F. structure may be due to the choice of heating rate we used in this last experiment. Indeed, we may think that this transition may be detected by infrared spectroscopy only in the case of heating the samples using very low heating rate.

V.3.7 Conclusion.

The methylene wagging mode region of the low temperature infrared spectrum of sample (6) shows low intensity of the bands assigned to gg and end-gauche conformers and even lower intensity for the band ascribed to the {110} fold conformation. The C-C stretching mode region of the same spectrum indicates a similar amount of disorder within the 1:1 binary mixture in the triple layer crystal form to that observed in the n-

$C_{198}H_{398}$ and n-$C_{246}H_{494}$ extended forms. Moreover, from the frequency of the successive progression bands present in this last region, we were able to determine that the average number of carbon atoms involved in the all-trans chain length going through the crystal layers of sample (6) is lower than the one going through the crystal layers of n-$C_{198}H_{398}$ in extended form. The average values are respectively 158 $^{+}/_{-}$ 15 and 192 $^{+}/_{-}$ 12.

By annealing the sample between 70.4^{0}C and 115.2^{0}C with a variable heating rate, we observed a strong increase of the intensity of the infrared bands assigned to non all-trans conformers for spectra recorded at around 104 $^{+}/_{-}$ 0.8 ^{0}C. This is believed to be the temperature at which the phase transition between the two crystal structures occurs.

Sample (6) was crystallised once again from the melt and cooled down to obtain the triple layer crystal form. Then, sample (6) was annealed from 76.5^{0}C to 139^{0}C with a constant heating rate of 0.4^{0}C per minute. The study of the intensity of the bands present in the wagging mode region of the infrared spectra assigned to non all-trans conformers as a function of temperature does not show any transition apart from the melting occurring at 122.8 $^{+}/_{-}$ 1.6 ^{0}C. Therefore, the observation of the phase transition occuring between the triple layer crystal form and the N.I.F. structure by the means of infrared spectroscopy may be affected by the heating rate used during the experiment.

VI CONCLUSION.

Purely monodisperse long chain n-alkanes are an ideal model to study crystallisation and disorder within polymers in general and polyethylene in particular. Indeed, similarly to polyethylene, these molecules are highly flexible, mobile, they do not involve any specific inter-molecular interactions and do not have large side groups. Disorder is an important parameter which can affect the mechanical and physical properties of polymers. For example, the diffusion of a solvent within a polymer film will be highly affected by the crystallinity and by the concentration of non all-trans conformers present along the polymer chains. The main objective of this thesis was to study the degree of disorder within these highly ordered materials which are purely monodisperse long chain n-alkanes. To achieve this, the use of infrared spectroscopy was essential. Indeed, spectroscopic techniques, sensitive to molecular details, are the only ones able to characterise specific types of disorder in both quantitative and qualitative ways. In order to get a complete structural picture of these monodisperse long chain alkane crystals, the results obtained from D.S.C., X-ray scattering techniques and Raman spectroscopy were combined with those obtained from infrared spectroscopy. The experimental part of this thesis covered by the chapters III, IV and V follows a pattern along which the potential degree of disorder within the different samples increases. The starting point of this thesis is a structural study of a short member of the n-alkane family, namely n-$C_{44}H_{90}$, which does not have the ability to crystallise by chain folding. Then, in chapter IV, we concentrate our attention on two pure long chain n-alkanes, namely n-$C_{198}H_{398}$ and n-$C_{246}H_{494}$. The disorder within these samples crystallised in different chain conformations was studied using the same spectroscopic techniques and characterisation as previously. Finally, the study of crystals prepared from branched long chain alkanes and mixtures of long chain n-alkanes gave some indications of structural features likely in polymers arising from branching and polydispersity.

In the first experimental chapter of this thesis, chapter III, the different crystal structures (namely monoclinic {011}, monoclinic {101}, orthorhombic I and triclinic forms) of the short chain n-alkane, n-$C_{44}H_{90}$, crystallised from solution were identified and transitions were characterised by a combination of D.S.C. and X-ray scattering

measurements. N-$C_{44}H_{90}$ samples with different crystal structures were studied using infrared and low frequency Raman spectroscopy. Each one of the infrared bands assigned to a methyl vibration has shown a great sensitivity, in both frequency and intensity, to the crystal structure. In particular, the frequencies of the infrared bands present in the spectra recorded at -173^{0}C and ascribed to the symmetric methyl bending mode have been found to vary as a function of the crystal structure between 1385 cm^{-1} and 1368 cm^{-1}. On the other hand, a single band at 1378 cm^{-1} was observed in the spectrum of n-$C_{44}H_{90}$ in the liquid state. We note that the symmetric methyl bending mode is not the only methyl mode sensitive to the crystal structure. Indeed, as a function of the crystal structure the frequency of the out-of-plane methyl rocking mode is found between 885 cm^{-1} and 893 cm^{-1}, the asymmetric methyl bending mode is found between 1440 cm^{-1} and 1468 cm^{-1} and finally, the in-plane and out-of-plane asymmetric methyl C-H stretching modes are found between 2950 cm^{-1} and 2962 cm^{-1}. These results confirm the close relationship between the packing of the methyl groups at the crystal surfaces and the crystal structure in the case of the short chain n-alkanes. Also, this highlighted the difficulty in using the band assigned to the symmetric methyl bending mode for normalisation purposes, certainly in the case of short chain n-alkanes, and possibly also in the case of longer chain n-alkanes (i.e. n-alkanes able to crystallise by chain folding). At the phase transition between different monoclinic forms, an abrupt increase in the integrated intensity of the 1342 cm^{-1} infrared band assigned to end-gauche conformers is observed. In all the infrared spectra of n-$C_{44}H_{90}$ recorded at -173^{0}C, none of the bands present in the methylene wagging mode region and assigned to non all-trans conformers were strong enough to be detected. At this low temperature, the alkane chains are essentially in an all-trans conformation. The identification of the band progressions present in the low temperature infrared spectra and assigned to the different methylene modes of vibration can be used to estimate the number of carbon atoms present in the alkane chain. This estimate can be compared with the ones derived directly from the value of the average layer periodicity determined by S.A.X.S. measurements and from the frequency of the first order of the longitudinal acoustic mode determined by low frequency Raman spectroscopy. We have also shown that the frequency of the first order of the longitudinal acoustic mode present in the low frequency Raman spectra was sensitive to the crystal structure. Indeed, the presence of

crystals in the orthorhombic II form was identified by an infrared band at 1385 cm^{-1} assigned to the methyl symmetric bending mode and by the frequency of the first order of the L.A.M. at 60.3 cm^{-1}. Crystals in the monoclinic {011} form were assigned to a Raman band at 58.1 cm^{-1}.

In the last experimental chapters of this thesis, chapters IV and V, respectively dedicated to two purely monodisperse long chain n-alkanes (namely n-$C_{198}H_{398}$ and n-$C_{246}H_{494}$) and to the potentially more disordered branched long chain alkanes and binary mixtures of long chain n-alkanes, we identified different chain conformations and phase transitions using S.A.X.S. techniques, Raman and infrared spectroscopy. We have shown that the low frequency Raman spectra could be used to identify several chain conformations present within the same sample. For example, in the case of sample (2), n-$C_{198}H_{398}$ crystallised from solution in essentially extended form, a Raman band at 35.9 cm^{-1} was observed in addition to a strong band at 13.2 cm^{-1}. The first Raman band is ascribed to the first order L.A.M. of the once folded crystal form whereas the second one is ascribed to the first order L.A.M. of the extended crystal form.

In view of the infrared results obtained from the previous experimental chapter, the use of the broad infrared band at about 2670 cm^{-1} for spectral normalisation has been preferred to the use of the band assigned to the symmetric methyl bending mode found at 1377 cm^{-1} in the low temperature spectra of the long chain n-alkanes. The methylene wagging mode region of the infrared spectra confined between 1400 cm^{-1} and 1260 cm^{-1} is rich in information related to specific non all-trans conformers which may be present in the n-alkane chains. Indeed, the gtg and gtg', gg and end-gauche conformers are assigned to the infrared bands present at respectively 1370 cm^{-1} and 1308 cm^{-1}, 1354 cm^{-1} and 1341 cm^{-1}. These infrared bands were used to identify those of these conformers present in the long chain alkane crystals in different forms. Also, a spectral subtraction technique was used to determine the different conformers characteristic of the fold itself in the case of n-$C_{198}H_{398}$ crystals studied at the lowest temperature. The subtraction spectrum showed a strong positive band present at 1375.5 cm^{-1} with a smaller negative one at 1381 cm^{-1}. This is believed to indicate the non-equivalence of the deformation of the methyl groups placed at the end of an n-alkane chain in folded or extended chain conformations. We were able to estimate the numbers of each specific conformer per n-alkane chain from the integrated area of the bands present in this region

of the infrared spectra. There are at least three times more non all-trans conformers per chain within the once folded form crystals than within the extended form crystals. Also, we observed that the branched alkane crystals contained a higher concentration of these conformers than the unbranched samples. One can note that in the case of the butyl branch samples, one of these conformers could be present within the branched part of the chains. Also, in the infrared spectra of the branched and unbranched long chain alkanes, differences observed in the integrated absorbance of the band at 1347 cm^{-1} may be due to changes in the conformation of the {110} fold or to a redistribution of the energy of vibration due to the branch groups on one of the carbon atoms composing the fold. Finally, for the linear n-alkanes the concentration of non all-trans conformers in the liquid state was found to be one order of magnitude higher than in the crystalline state near to their melting points.

We observed that the successive increases of temperature at which the different monodisperse long chain n-alkane crystals were heated prior to cooling to -173^0C produced progressively more perfect crystals. This perfecting of the long chain n-alkane crystals was indicated by the decrease of the integrated absorbance of most of the bands assigned to the non all-trans conformers present in the wagging mode region of the infrared spectra. Several progression bands are present in the C-C stretching mode region of the lowest temperature infrared spectra of the different samples confined between 1130 cm^{-1} and 1050 cm^{-1}. From the identification of each one of these bands, we were able to estimate the number of carbon atoms involved in the all-trans parts of the alkane chains. For example, by identifying the progression bands present in this region of the infrared spectra of the binary mixture of long chain n-alkanes recorded at -173^0C, we estimate that the crystal layers were composed of 158 carbon atoms. This result seems to correspond to the thickness of the larger crystal layers present in the triple layer crystal form proposed by Ungar and Zeng. In the case of the monodisperse long chain n-alkanes, the perfecting of the different crystals as a function of the annealing temperature induced a better regularity and resolution of the progression bands. The regularity of these bands is related to both the perfection of the all-trans part of the alkane chains (i.e. absence of gauche conformers within the internal bonds of the chains) and the length distribution of the parts of the chains in the all-trans conformation (i.e. the number of contiguous methylene groups involved in the all-trans bonds for each

chain). Finally, the increase of the number of orders of diffraction on the S.A.X.S. patterns of the annealed extended form crystals indicates a better stacking of the crystals due to more regular crystal surfaces. At the phase transition between long chain n-alkane crystals in the once folded and extended forms, the disorder was found to reach a local maximum characterised by an increase of the integrated area of the bands present in the wagging mode region of the infrared spectra and ascribed to the non all-trans conformers present within the internal bonds of the chains. In the case of the binary mixtures of long chain n-alkanes, we observed from a study of the wagging mode region of the spectra a similar behaviour of the concentration of non all-trans conformers at the phase transition between the triple layer structure and the non-integer form involving extended segments.

In the case of the long chain n-alkanes, the values of the frequency differences between the progression bands present in the C-C stretching mode region of the spectra of once folded form crystals were expected to be equal to roughly twice the values obtained from the spectra of the extended form crystals. Indeed, this would have been due to the presence of the fold in the first case which splits the chains into two all-trans stems of similar chain length. Nevertheless, in both cases we observed similar values of the frequency differences between the progression bands. Furthermore, the frequency of each progression band was identical in the spectra of both crystal forms. This unexpected result may be due to the molecular symmetry, related to the high regularity of the fold conformation in crystals of monodisperse long chain n-alkanes. It also suggests that the disordered chain sections in once folded and extended form crystals are of similar length. Nevertheless, in the first case, the weaker intensity of these bands may suggest that for symmetry reasons only the more regular chains participate to the C-C stretching mode of vibration.

At a phase transition between two crystal forms, changes are observed within this region. Indeed, the bands present at around 1089 cm^{-1}, 1078 cm^{-1} and 1064 cm^{-1} were detected only in the spectra of the once folded form crystals. These bands are assigned to non all-trans conformers. Some of those may be related to the fold itself. This region of the infrared spectra of the butyl branched sample has shown how useful infrared spectroscopy could be for the study of the conformation of paraffinic chains. Indeed, in the particular case of the butyl branched alkane, the identification of the highly regular

and well resolved progression bands present in the higher frequency part of this region indicated that 98 carbon atoms were involved in the extended part of the chains. Several broad bands were found in the lower frequency part of the region at around 1089 cm^{-1}, 1078 cm^{-1} and 1064 cm^{-1} suggesting the presence of some non all-trans conformers and folds. Therefore, a general picture of this sample could be drawn from these observations : the butyl branched sample is in the once folded form with the fold nearly exactly in the middle of the chains. The two stems passing through the crystal layers are highly regular (mostly all-trans conformation) and are of similar chain length. Some non all-trans conformers are present near the crystal surfaces and within the branch part of the chains. We have also shown that by increasing the size of the branch groups (from a methyl to a butyl group) the distribution of chain lengths in the all-trans conformation seems to get narrower. At the same time, the amount of non all-trans conformers near the crystal surfaces may have increased.

In the case of spectra of extended form crystals, the progression bands are found over the full frequency region. In the spectrum recorded at -173^{0}C of the crystals of the binary mixture of n-alkanes, the absence of the broad bands in the lower frequency part of this region indicates an absence of folded chains and a low concentration of non all-trans conformers. This is confirmed by studying the wagging mode region of the same spectrum.

In the case of the monodisperse long chain n-alkanes, tilting of the chains from the crystal surfaces can be induced by heating. The tilt angle can be determined from S.A.X.S. measurements after initial identification of the crystal form by low frequency Raman spectroscopy. The tilting of the chains inside the crystals was expected to lead to an increase in the number of non all-trans conformers present in the alkane chains, and more especially at the chain ends. The methylene wagging mode region of the infrared spectra of a sample successively heated up at different increasing temperatures, and then cooled down to –173^{0}C, was studied. We observed an unexpected decrease of the integrated absorbance of most of the bands assigned to non all-trans conformers present in the n-alkane chains with the increase of annealing temperature. This is explained by a perfecting of the crystals. The perfecting of the crystals may predominate over the formation of non all-trans conformers at the chain ends due to the chain tilting, masking the latter effect in the infrared data. In order to separate these two effects, n-$C_{198}H_{398}$

were prepared with the lowest possible concentration of non all-trans conformers. We then studied the wagging mode region of its infrared spectra as a function of the time spent at a fixed temperature at which the tilting was known to occur. At the shortest time, this region indicated that the tilting of the n-alkane chains occurred through a disordering process which does not preferentially affect the chain ends. Then, at the longest annealing time, the tilted chains adopt a more stable conformation where the number of non all-trans conformers is reduced. Also, due to changes in the intensity of the 1346 cm^{-1} band, we believe that the conformation of the initial {110} fold may have changed. All these results indicate that the concentration of non all-trans conformers is not only temperature dependent but also time dependent.

The identification of all the progression bands present in the infrared spectra recorded at -173^{0}C of the different monodisperse long chain alkanes studied in their different chain conformations is shown in Figure VI.133. Sample (1) corresponds to n-$C_{198}H_{398}$ crystallised from solution in once folded form. Sample (1) ext. corresponds to n-$C_{198}H_{398}$ crystallised from solution in once folded form and transformed to the extended form by heating. Sample (2) corresponds to n-$C_{198}H_{398}$ crystallised from solution in the extended form. Sample (3) corresponds to n-$C_{246}H_{494}$ crystallised from solution in once folded form. Sample (3) ext. corresponds to n-$C_{246}H_{494}$ crystallised from solution in once folded form and transformed to the extended form by heating. Sample (4) corresponds to $C_{96}H_{193}CHCH_3C_{94}H_{189}$ crystallised from solution in once folded form. Sample (5) corresponds to $C_{96}H_{193}CH(CH_2)_3CH_3C_{94}H_{189}$ crystallised from solution in once folded form. Finally, sample (6) corresponds to the binary mixture of n-$C_{162}H_{326}$ and n-$C_{246}H_{494}$ in the triple layer crystal form.

Figure VI.133 : Frequency of the progression bands ascribed to the C-C stretching mode against k, integer, for samples (1), (2), (3), (4), (5) and (6).

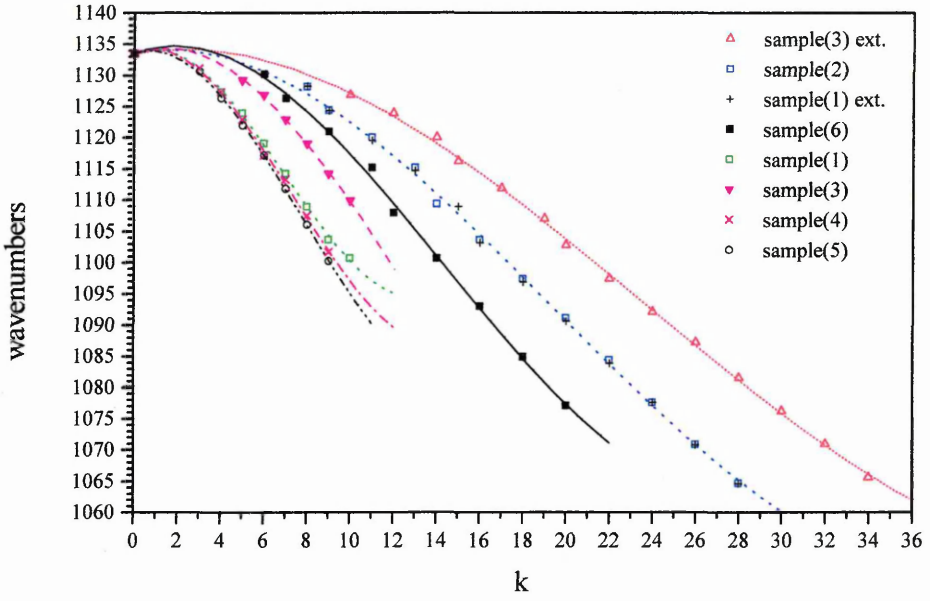

Estimates of the numbers of carbon atoms present in the extended part of the monodisperse alkane chains determined by S.A.X.S. measurements, low frequency Raman spectroscopy and by studying the C-C stretching mode region of the infrared spectra recorded at -173^{0}C are presented in Table VI.32.

Table VI.32 : Estimates of the numbers of carbon atoms determined by S.A.X.S. measurements, low frequency Raman spectroscopy and infrared spectroscopy.

	Number of carbon atoms within the extended part of alkane chains		
	S.A.X.S.	L.A.M.	C-C stretching mode
sample (1)	$97^{+}/.1$	$98^{+}/.2$	$90^{+}/.16$
sample (1) ext.	$194^{+}/.1$	?	$191^{+}/.8$
sample (2)	$198^{+}/.1$	$187^{+}/.2$	$192^{+}/.12$
sample (3)	$123^{+}/.1$	$128^{+}/.2$	?
sample (3) ext.	$247^{+}/.2$	?	$244^{+}/.13$
sample (4)	$94^{+}/.1$	$94^{+}/.2$	$101^{+}/.2$
sample (5)	$99^{+}/.2$	?	$98^{+}/.2$
sample (6)	?	?	$158^{+}/.15$

It can be observed that the number of carbon atoms present in the extended part of the alkane chains determined from the study of the C-C stretching mode region of the infrared spectra is usually smaller than the one determined by S.A.X.S. measurements or Raman spectroscopy. Also, the uncertainty for each value is usually larger in the case of the use of the C-C stretching mode region. Finally, we should note that estimates of the number of carbon atoms using the C-C stretching mode region are made for crystals at -173^0C rather than room temperature as in the case of the two other methods. Hence, S.A.X.S. and Raman measurements are carried out on more disordered crystals. The conditions applicable for the observation of the C-C stretching progression appear to be more stringent than those for observing a S.A.X.S. peak or a Raman LA mode. This suggests that the requirement of an all-trans chain is more rigorous in the first case.
Finally, a summary of the full information which can be obtained from the study of the infrared spectra of these monodisperse long chain n-alkanes is presented in Table VI.33.

Table VI.33 : Information obtained from the different spectral regions of the infrared spectra of paraffins.

Modes of Vibrations	Frequency range (cm^{-1})	Information
Methyl C-H stretching	2965-2950	Crystal structure, surface disorder
Methylene C-H stretching	2920-2840	crystal disorder
Asymmetric methyl bending	1468-1440	crystal structure
Methylene bending	around 1470	crystal disorder
Methyl symmetric bending	1385-1368	crystal structure, surface disorder
Methylene wagging	1400-1300	qualitative and quantitative study of the surface and crystal disorders, fold conformation, phase transition
Methylene twisting	1300-1175	crystal disorder
C-C stretching	1150-950	gauche conformers, fold structure, estimates of the crystal layer thickness, phase transition
Methyl rocking	893-885	Crystal structure, surface disorder
Methylene rocking	1050-720	Crystal structure, estimates of the crystal layer thickness, gauche conformers

Future work :

The different studies carried out on the monodisperse long chain n-alkanes provide essential information for the understanding of the mechanism of crystallisation by chain folding and, more generally, for the crystallisation of polymers. The combination of the different techniques used in this thesis should provide the means for testing structures having high degrees of disorder and new more complex layered phases expected to occur in the mixtures of monodisperse long chain n-alkanes and in the branched long

chain alkanes. Complex multilayered crystals also present in the subsequent transformation of these long chain n-alkanes from primary forms present in the initial stages of crystallisation could be studied. The use of infrared spectroscopy and especially the C-C stretching mode region of the spectra (the importance of which has been revealed in this thesis) should definitively provide the additional structural information needed. The full range of monodisperse long chain n-alkanes which are now available from n-$C_{98}H_{198}$ to n-$C_{390}H_{782}$ should be studied by the combination of these techniques. Changes in the fold conformation as a function of the chain length could be investigated. For polymers, it is almost certain that some folds are not adjacent. This might occur in the long chain n-alkanes for a larger number of folds. Therefore, the study of the fold conformation as a function of the number of folds per chain could be carried out. Mixtures of different monodisperse long chain n-alkanes provide the opportunity to study new lamellar structures. The controlled polydispersity within these samples provides a well defined model for polymer crystallisation. New synthesis of different branched long chain alkanes such as a star-shaped samples, should lead to new forms of chain organisation within crystals. These could be studied using the same combination of techniques : indeed, infrared spectroscopy is the best method to estimate the degree of disorder within such crystals. Finally, newly synthesised monodisperse long chain n-alkanes with deuterated end caps are also available. In addition to the previous techniques used, neutron scattering should provide new structural information. Also, the study of these deuterated long chain n-alkanes may help to assign some of the infrared bands present in the spectra. It should give the opportunity to differentiate non all-trans conformers present at different positions along the alkane chains.

References

1 G. R. Strobl, The Physics of Polymers, 2nd Ed., Springer-Verlag Berlin Heidelberg (1997)
2 P. J. Flory, Statistical Mechanics of Chain Molecules, John Willey & sons. Inc. (1969)
3 R. J. Young and P. A. Lovell, Introduction to Polymers, 2nd Ed., Chapman & Hall (1991)
4 W. O. Statton and P. H. Geil, J. Appl. Polym. Sci., **3**, 357 (1960)
5 A. Keller, Phil. Mag., **2**, 1171 (1957)
6 A. Peterlin, J. Appl. Phys., **31**, 1934 (1960)
7 D. M. Sadler, **24**, 1401 (1983)
8 D. M. Sadler, **28**, 1440 (1987)
9 J. I. Jr Lauritzen and J. D. Hoffman, J. Res. Nat. Bur. Stds, **64A**, 73 (1960)
10 L. A. Wood, Scientific Progress in the Field of Rubber and Synthetic Elastomers, **2**, 57, Interscience, New York (1946)
11 P. J. Barham, R. A. Chivers, A. Keller, J. Martinez-Salazar and S. J. Organ, J. Mater. Sci., **20**, 1625 (1985)
12 W. M. Leung, R. St. John Manley and A. R. Panaras, Macromolecules, **18**, 746-771 (1985)
13 A. J. Kovacs, C. Straupe and A. Gonthier, J. Polym. Sci., Polym. Symp. Ed., **59**, 31 (1977).
14 J. P. Arlie, P. Spegt and A. Skoulios, Makromol. Chem., **104**, 212 (1967)
15 I. Bidd and M. C. Whiting, J. Chem. Soc., Chem. Commun, 543 (1985)
16 G. Ungar, J. Stejny, A. Keller, I. Bidd and M. C. Whiting, Science, **229**, 386 (1985)
17 G. M. Brooke, S. Burnett, S. Mohammed, D. Proctor and M. C. Whiting, J. Chem. Soc., Perkin Trans. 1, 1635 (1996)
18 G. Ungar, S. J. Organ, A. Keller, J. Polym. Sci., Polym. Lett. Ed., **26**, 259 (1988)
19 J. K. Hobbs, M. J. Hill, A. Keller and P. J. Barham, J. Polym. Sci. Part B, Polym. Phys., **37**, 3188 (1999)
20 G. Ungar and A. Keller, Polymer, **27**, 1835 (1986)
21 X. Zeng and G. Ungar, Polymer, **39**, *19*, 4523 (1998)
22 X. Zeng, G. Ungar and S.J. Spells, Abstract of Papers of the American Chemical Society, **128**, *2*, 98 (1999)
23 G. Ungar, A. Keller, Polymer, **28**, 1899 (1987)
24 S. J. Organ, A. Keller, M. Hikosaka and G. Ungar , Polymer, **37**, *12*, 2517 (1996)
25 E. Boda, G. Ungar, G. M. Brooke, S. Burnet, S. Mohammed, D. Proctor and M. C. Whiting, Macromolecules, **30**, *16*, 4674 (1997)
26 S. J.Organ, G. Ungar and A. Keller, Macromolecules, **22**, 1995 (1989)
27 S. J. Organ, G. Ungar and A. Keller, J. Polym. Sci., Polym. Phys., **28B**, 2365 (1990)
28 P. G. Higgs and G. Ungar, J. Chem. Phys., **100**, *1*, 640 (1994)
29 J. D. Hoffman, Polymer, **32**, 2828 (1992)
30 J. D. Hoffman and R. L. Miller, Polymer, **38**, *13*, 3151 (1997)
31 S. J. Organ and A. Keller, J. Polym. Sci., Polym. Phys. Ed., **25**, 2409 (1987)
32 D. C. Bassett, R. H. Olley, S. J. Sutton and A. S. Vaughan, Macromolecules, **29**, 1852 (1996)

33 D. C. Bassett, R. H. Olley, S. J. Sutton and A. S. Vaughan, Polymer, **37**, *22*, 4993 (1996)
34 S. J. Sutton, A. S. Vaughan and D. C. Bassett, Polymer, **37**, *25*, 5735 (1996)
35 S. P. Chum, G. W. Knight, J. M. Ruiz and P. J. Phillips, Macromolecules, **27**, 656 (1994)
36 R. Patil and D. H. Reneker, Polymer, **35**, *9*, 1909 (1994)
37 R. G. Snyder, J. Chem. Phys., **47**, *4*, 1316 (1967)
38 M. Maroncelli, S. P. Qi, H. L. Strauss and R. G. Snyder, J. Am. Chem. Soc., **104**, 6237 (1982)
39 R. G. Snyder and J. H. Schachtschneider, Spectrochim. Acta, **19**, 85 (1963)
40 R. G. Snyder and J. H. Schachtschneider, Spectrochim. Acta, **19**, 117 (1963)
41 G. Zerbi, Pure Appli. Chem., **26**, 499 (1971)
42 G. Zerbi, L. Piseri, F. Cabassi, Mol. Phys., **22**, *2*, 241 (1971)
43 P. C. Painter, J. Havens, W. W. Hart and J. L. Koenig, J. Polym. Sci., Polym. Phys. Ed., **15**, 1223 (1977)
44 P. C. Painter, J. Havens, W. W. Hart and J. L. Koenig, J. Polym. Sci., Polym. Phys. Ed., **15**, 1237 (1977)
45 S. J. Spells, S. J. Organ, A. Keller and G. Zerbi, Polymer, **28**, 697 (1987)
46 G. Ungar and S. J. Organ, Polym. Commun., **28**, 232 (1987)
47 S. Wolf, C. Schmid, P. C. Hägele, Polymer, **31**, 1222 (1990)
48 S. Wolf, P. C. Hägele and C. Schimd, Colloid Polym. Sci., **269**, 364 (1991)
49 M. Maroncelli, H. L. Strauss and R. G. Snyder, J. Chem. Phys., **82**, *6*, 2811 (1985)
50 X. Zeng and G. Ungar, to be published.
51 J. L. McHale, Molecular spectroscopy, First Edition, Prentice-Hall, Inc., (1999)
52 S. I. Mizushima and T. Shimanouchi, J. Am. Chem. Soc., **71**, 1320 (1949)
53 R. F. Schaufele and T. Shimanouchi, J. Chem. Phys., **47**, 9 (1967)
54 G. V. Fraser, Indian J. Pure Appl. Phys., **16**, 344 (1978)
55 H. G. Olf, A. Peterlin, W. L. Peticolas, J. Polym. Sci., Polym. Phys. Ed., **12**, 359 (1974)
56 F. Khoury, B. Fanconi, J.D. Barnes and L.H. Bolz, J. Chem. Phys., **59**, 11, 5849 (1973)
57 G.R. Strobl and R. Eckel, J. Polym. Sci., Polym. Phys. Ed., **14**, 913 (1976)
58 R. G. Snyder, H. L. Strauss, R. Alamo and L. Mandelkern, J. Chem. Phys., **100**, 5422 (1994)
59 J. W. Cooley and J. Tukey, Math. Comp., **19**, 297 (1965)
60 M. G. Broadhurst, J. Res. Nat. Bur.Stand., **66A**, 241 (1962)
61 S Krimm, C.Y. Liang and G.B.B.M. Sutherland, J. Chem. Phys., **25**, *3*, 549 (1956)
62 R.B. Richards, J. Appl. Chem. (London), **1**, 370 (1951)
63 I.I. Novak and E.S. Slouev, Optika y Spektroskopya, **2**, *1*, 62 (1957)
64 R.A. Oetjen and H.M. Randall, Reviews of Modern Physics, **16**, *3/4*, 260 (1944)
65 J.R. Nielsen and R.F. Holland, J. Mol. Spectroscopy, **4**, 488 (1960)
66 R.G. Snyder, J. Mol. Spectroscopy, **4**, 411 (1960)
67 R.G. Snyder, J. Mol. Spectroscopy, **7**, 116 (1961)
68 R.F. Holland and J.R. Nielsen, J. Mol. Spectroscopy, **8**, 383 (1962)
69 M. Kobayashi, T. Kobayashi, Y. Itoh, Y. Chatani and H. Tadokoro, J. Chem. Phys., **72**, 2024 (1980)

70 R.A. MacPhail, R.G. Snyder and H.L. Strauss, J. Chem. Phys., **77**, 1118 (1982)
71 R.A. MacPhail, H.L. Strauss, R.G. Snyder and C.A. Elliger, J. Phys. Chem., **88**, 334 (1984)
72 R.G. Snyder, J. Chem. Phys., **71**, *8*, 6391 (1979)
73 B.G. Rånby, F.F. Morehead and N.M. Walter, J. Polym. Sci., **44**, 349 (1960)
74 S.C. Nyburg and J.A. Potworowski, Acta Cryst., **B29**, 347 (1973)
75 R. Boistelle, B. Simon and G. Pepe, Acta Cryst., **B32**, 1240 (1976)
76 S.R. Craig, G.P. Hastie, K.J. Roberts and J.N. Sherwood, J. Mater. Chem., **4**, 977 (1994)
77 S. Ishikawa, H. Kurosu and I. Ando, J. Mol. Structure, **248**, 361 (1991)
78 I. Bidd and M. C. Whiting, J. Chem. Soc., Chem. Commun, 543 (1985)
79 E. Boda, Thesis of Master of Philosophy, The University of Sheffield, (1997)
80 G. L. Liang, D. W. Noid, B. G. Sumpter and B. Wunderlich, J. Phys. Chem., **98**, 11739, (1994)
81 F. C. Frank, Faraday Discuss. Chem. Soc., **68**, 7 (1979)
82 P. J. Flory, Faraday Discuss. Chem. Soc., **68**, 14 (1979)
83 D. C. Bassett, "Principles of Polymer Morphology", Cambridge University Press, (1981)
84 D. I. Bower, W. F. Maddams, "The vibrational spectroscopy of polymers", Cambridge University press (1992)
85 J. C. Rodriguez-Cabello, J. Martin-Monge, J. M. Lagaron and J. M. Pastor, Macromol. Chem. Phys., **199**, 2767 (1998)
86 R. G. Snyder, H. L. Strauss, C. A. Elliger, J. Phys. Chem., **86**, 5145 (1982)
87 R. G. Snyder, S. L. Hsu, S. Krimm, Spectrochim. Acta, **34A**, 395 (1978)
88 D. C. Basset and B Turner, Nature (London), Phys. Sci., **240**, 146 (1972)
89 J. Tsau and D. F. R. Gilson, J. Phys. Chem., **72**, 4082 (1968)
90 J. K. Wilmshurst and H. J. Bernstein, Can. J. Chem., **35**, 911 (1957)
91 W. Piesczek, G.R. Strobl and K. Malzahn, Acta Cryst., **B30**, 1278 (1974)
92 Y. Kim, H. L. Strauss, R. G. Snyder, J. Phys. Chem., **93**, 485, (1989)
93 G. Ungar, X.B. Zeng, G.M. Brooke and S. Mohammed, Macromolecules, **31**, *6*, 1875 (1998)
94 S. Krimm, Advances in Polymer Science (1960)